Transcranial stimulation to enhance cortical plasticity in the healthy and stroke-affected motor system

Submitted toward the degree of Doctor of Philosophy by

Ugwechi Amadi

St. John's College
University of Oxford
Michaelmas Term 2012

Transcranial stimulation to enhance cortical plasticity in the healthy and stroke-affected motor system

Ugwechi Amadi

Michaelmas Term 2012 St. John's College

A thesis submitted in partial fulfilment of the requirements for the degree of Doctor of Philosophy in Clinical Neurology at the University of Oxford

Abstract

This thesis investigated transcranial direct current stimulation (tDCS) as applied to the motor system, and its ability to modulate underlying cortical processes and resultant motor behaviours. Functional magnetic resonance imaging (fMRI) and transcranial magnetic stimulation (TMS) were employed to assess the extent to which tDCS induces quantifiable changes in neural structure and function in controls and stroke patients.

Modifications in the connectivity of intrinsic functional networks following tDCS application were examined using resting state fMRI. Polarity-specific changes were found: cathodal (inhibitory) tDCS increased the strength of the default mode network and increased functional coupling between major nodes within the motor network. No significant effects were found following anodal (excitatory) tDCS.

Although anodal tDCS elicited only subtle changes in resting activity, it is known to produce robust modifications of behaviour. Single and paired-pulse TMS were used to investigate the neurophysiological underpinnings of these changes. Consistent with the theory of homeostatic plasticity, anodal tDCS applied prior to task performance increased $GABA_A$-mediated cortical inhibition and worsened behaviour. The specificity of these changes suggests a central role for the mechanism of surround inhibition.

A longitudinal clinical trial in chronic stroke patients was conducted to determine the utility of tDCS as an adjunct in motor rehabilitation. Serial MRI scans revealed that, when combined with motor training, anodal tDCS increased functional activity and grey matter in primarily ipsilesional motor areas. These brain changes were correlated with behavioural improvements in the stroke-affected upper limb.

The laterality of connectivity at baseline, as measured by resting state activity and corticospinal tract integrity, was predictive of response to the rehabilitation program, particularly in those stroke patients who received tDCS. Asymmetry favouring the contralesional hemisphere predicted greater behavioural gains. Such results underscore the importance of re-normalisation of structure and functional activity toward the lesioned hemisphere in stroke rehabilitation.

This thesis contains approximately 48,000 words.

TABLE OF CONTENTS

i. Abbreviations

ADM	Abductor Digiti Minimi
AMT	Active Motor Threshold
APB	Abductor Pollicis Brevis
ANOVA	Analysis of Variance
ARAT	Action Research Arm Test
BA	Brodmann Area
BCM	Bienenstock-Cooper-Munro
BEDPOSTX	Bayesian Estimation of Diffusion Parameters Obtained using Sampling Techniques
BET	Brain Extraction Tool
BOLD	Blood Oxygen Dependent Level
BBR	Boundary Based Registration
COPE	Contrast of Parameter Estimates
CST	Corticospinal Tract
DMN	Default Mode Network
DTI	Diffusion Tensor Imaging
DWI	Diffusion Weighted Image
EMG	Electromyograph
EPI	Echo Planar Imaging
FA	Fractional Anisotropy
FDI	First Dorsal Interosseous
FDT	FMRIB Diffusion Toolbox
FEAT	FMRI Expert Analysis Tool
FLIRT	FMRIB Linear Registration Tool

fMRI	Functional Magnetic Resonance Imaging
FNIRT	FMRIB Nonlinear Registration Tool
FSL	FMRIB Software Library
GABA	γ-Amino Butyric Acid
GLM	General Linear Model
ICA	Independent Component Analysis
LTD	Long Term Depression
LTP	Long Term Potentiation
M1	Primary Motor Cortex
MD	Mean Diffusivity
MELODIC	Multivariate Exploratory Linear Optimized Decomposition into Independent Components
MEP	Motor Evoked Potential
MRI	Magnetic Resonance Imaging
PMC	Premotor Cortex
PMd	Dorsal Premotor Cortex
PMv	Ventral Premotor Cortex
PROBTRACKX	Probabilistic Tracking with Crossing Fibres
RMT	Resting Motor Threshold
ROI	Region of Interest
RSN	Resting State Network
RT	Reaction Time
rTMS	Repetitive Transcranial Magnetic Stimulation
SEM	Standard Error of the Mean
SICI	Short Interval Intracortical Inhibition

SMA	Supplementary Motor Area
tDCS	Transcranial Direct Current Stimulation
TE	Echo Time
TR	Repetition Time
TMS	Transcranial Magnetic Stimulation
UE-FM	Upper Extremity Fugl-Meyer
VBM	Voxel Based Morphometry

ii. List of figures

iii. List of tables

iv. Acknowledgements

This thesis could not have been without the support and help of a great number of people, including the entire team at FMRIB. Special thanks are due to the following, for going above and beyond the call of duty:

The volunteers who took time out of their daily lives to participate in this research. In particular, to the patients who inspired me with their joviality and youthful spirits; and to the controls, my dear friends, for being such good sports and showing an interest in my work, all in the name of camaraderie.

My sincerest gratitude goes to Heidi Johansen-Berg and Charlie Stagg, the best co-supervisors a DPhil student could ask for. I could not have done this without their neverending support, enthusiasm, understanding, and seemingly limitless supply of innovative ideas. Thank you both for being such stellar examples of what it should mean to be a woman in science.

Claire Allman for recruiting and scheduling the stroke patients, and performing the motor training. And, perhaps most importantly, for dealing with the eternal headache that is taxi companies. To Leigh Wilkins who carried on the torch after her. To Andrei Ilie, for collecting the resting state scans in Chapter 4.

Adam Thomas for patiently teaching me how to do the VBM analysis presented in Chapter 6, modifying the scripts to accommodate my data set, and not hiding every time I began a sentence with, “Adam, I have a question…”.

The Rhodes Trust for providing my funding, and giving me the opportunity to come to Oxford in the first place. Specifically, to the Warden Don Markwell for his inspired suggestion that I “keep an ace in my back pocket.”

And to my family, my personal cheerleaders, for their trans-Atlantic love.

Chapter 1: Plasticity in the Human Motor System

This foundational chapter explains the organization of the motor system, including its anatomy and connectivity. Though comprised of functionally distinct regions, the motor system is interconnected in structure, and tampering with one area will have downstream effects on others. These modifications are rooted in the concept of plasticity, the ability of external influences to induce persistent changes in the brain via alterations in synaptic strength. Such mechanisms govern normal learning processes in the healthy brain, as well as adaptive responses in the stroke-affected brain, both immediately following the infarct and during recovery.

1.1 Organization of the Motor System

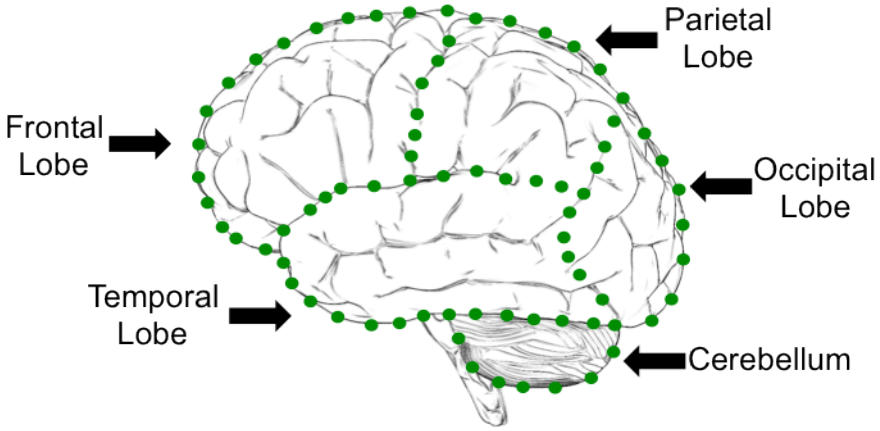

Figure 1.1: Illustration of the lateral view of the brain, depicting the four lobes of the neocortex and the cerebellum.

At a gross level, the cerebral cortex is divided into four lobes (Figure 1.1). Though this classification was originally based on location relative to anatomical landmarks of sulci and gyri, the distinct functional significance of each lobe was later noted. Attempts at partitioning the brain into finer cortical divisions have been made for over a century, beginning with the work of Meynert in the mid-1800's

(Kötter & Wanke, 2005). The early 20th century brought a wealth of proposals for the classification of subdivisions of the cortex using cytoarchitecture. The most broadly used of those maps today is that introduced by neuroanatomist Korbinian Brodmann. The 47 different subdivisions within this map, named Brodmann areas (BA), are delineated according to their varying cytoarchitectural composition, with each BA possessing a distinct functional role (Figure 1.2).

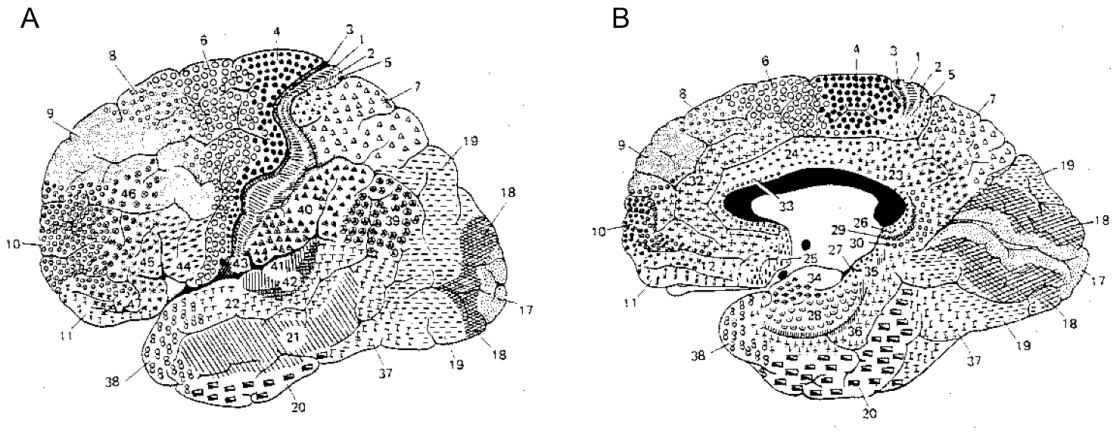

Figure 1.2: Brodmann's map. Lateral (A) and medial (B) views of the brain, depicting the cytoarchitecturally and functionally distinct brain regions known as Brodmann Areas (BA). Of note are BA 4 and BA 6, the primary and premotor cortices, respectively. Figure originally from Brodmann, 1909.

1.1.1 CORTICAL MOTOR REGIONS

The major cortical areas responsible for motor control are located primarily within the frontal lobe, anterior to the central gyrus. This region corresponds to BA 4 and 6, consisting of precentral and intermediate precentral cortex. The classification of BA 4 has remained relatively consistent over the years, and is termed the primary motor cortex (M1). BA 6, however, has undergone multiple iterations of further fractionation. Based on results from lesion studies, Fulton proposed that the lateral portion of BA 6 be deemed the premotor cortex (PMC) (Fulton & Sheehan, 1935). More recently, the PMC was found to be composed of

functionally distinct dorsal and ventral components (Kötter & Wanke, 2005; Tomassini et al., 2007; Zilles et al., 2004). The medial portion of BA 6 is now referred to as the supplementary motor area (SMA) (Woolsey et al., 1952). Figure 1.3 provides a visual reference of these motor areas, which are discussed in more detail in the following sections.

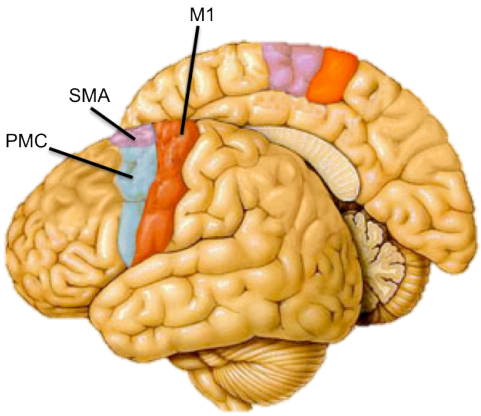

Figure 1.3: Lateral and medial aspects showing the major cortical motor regions: primary motor cortex (M1), supplementary motor area (SMA), premotor cortex (PMC). Figure adapted from thebrain.mcgill.ca.

1.1.1.1 Primary Motor Cortex (M1, BA 4)

As suggested by its name, the primary motor cortex (M1) forms the core of the cortical areas involved in movement. Located on the precentral gyrus, M1 is bound by the precentral sulcus anteriorly, and the central sulcus posteriorly. It is histologically agranular, with an indistinguishable cortical layer IV. M1 has numerous pyramidal cells of varying sizes, and is the originating locus of 40% of all pyramidal tract neurons (Leonard, 1997). In 1937, neurosurgeon Wilder Penfield found that electrical stimulation of particular points within M1 elicited reproducible movement of specific body parts. This led to the concept of motor somatotopy, which posited that cortical control of areas of the body were distributed in strict form within M1 (Penfield & Boldrey, 1937). This homunculus, as it came to be

known, is an exaggerated representation of the human body, with increased cortical area devoted to dexterous body parts, such as the hand (Figure 1.4).

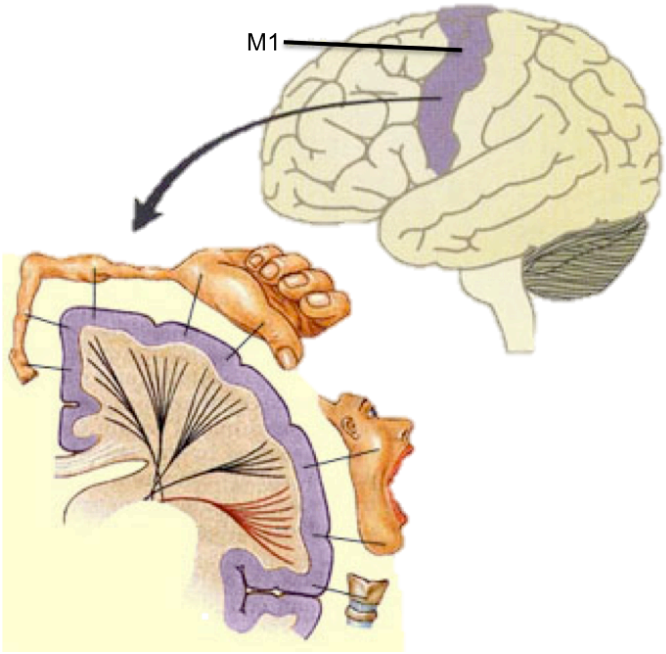

Figure 1.4: Penfield's motor homunculus. (Top) Schematic image depicting the location of M1, which contains a somatotopic representation of the body (Bottom). Figure adapted from thebrain.mcgill.ca.

Although neuroimaging studies support the existence of a motor homunculus (Cheyne, et al., 1991; Rao et al., 1995), the strict view of 1:1 somatotopy is simplistic, as Penfield himself cautioned. Motor somatotopy is applicable when differentiating *between* body parts, but not necessarily *within* a body part. For example, the representation of the arm is indeed separate from those of the leg or head; however, there exist multiple, overlapping representations of particular arm muscles and movements, not just one (Sanes & Schieber, 2001). Indeed, results from stimulation studies in primates suggest that regions of M1 represent functional muscle groups, not individual muscles (Donoghue et al.,, 1992). It is possible, then, that these intracortical connections provide the physical basis for plasticity (discussed further in section 1.2.2).

M1 exerts primarily contralateral influence over movements: the left M1 controls the movement of the right side of the body, and vice versa. There is, however, substantial communication between the left and right M1, via predominately inhibitory interhemispheric connections (Ferbert et al., 1992). Alterations to this hemispheric balance play a prominent role in disease pathology, particular in stroke (Murase et al., 2004) (see section 1.3). Damage to M1 itself results in muscle paresis and spasticity, including loss of precision and complex multi-joint movements (Leonard, 1997).

1.1.1.2 Premotor Cortex (PMC, lateral BA 6)

The premotor cortex, lateral BA 6, is located on the precentral gyrus, immediately anterior to M1. It is involved in the higher aspects of movement, and damage to this area often causes deficits in motor planning abilities (Leonard, 1997). The PMC has direct connections to the spinal cord, though less numerous than those arising from M1. The PMC is, however, more widely connected to non-motor cortical regions than M1, and uses information from these areas to influence M1 and coordinate movement (Dum & Strick, 1991). In line with the functional neuroanatomy of non-human primates (Barbas & Pandya, 1987), recent imaging studies have demonstrated that the PMC can be divided into dorsal (PMd) and ventral (PMv) components (Mayka et al., 2006; Tomassini et al., 2007).

Dorsal Premotor Cortex (PMd). The PMd integrates visual and spatial information with motor output (Chouinard & Paus, 2006). It is strongly connected to the contralateral PMd and M1 (Bestmann et al., 2008). Patients with surgical excisions of the PMd have difficulty associating arbitrary cues such as coloured lights, with predefined motor movements (Petrides, 1997). Indeed, cortical

recordings in monkeys have shown that PMd neurons fire after the presentation of a cue to perform a certain movement (Kurata & Hoffman, 1994). PMd neurons remain active during the execution of the movement, in a similar manner to M1 neurons (Lee & van Donkelaar, 2006).

Ventral Premotor Cortex (PMv). The PMv is heavily involved in the grasping and manipulation of objects (Chouinard & Paus, 2006). In monkeys, PMv firing is modulated by the strength of grip force (Hepp-Reymond et al., 1994; Hepp-Reymond et al., 1999); neuroimaging studies in humans have yielded similar results (Ehrsson et al., 2001). The PMv facilitates the planning and execution of arm movements requiring both distal and proximal muscles, and the coordination of such movements with visual and geometric inputs (Hoshi & Tanji, 2007). The PMv is also thought to be the location of mirror neurons, which activate not only when performing a task, but also upon watching another individual perform the task (Rizzolatti & Luppino, 2001).

1.1.1.3 Supplementary Motor Area (SMA, medial BA 6)

The SMA is located in the dorsomedial prefrontal cortex, anterior to the leg representation in M1 (Nachev et al., 2008). In monkeys, approximately ten percent of all CST neurons originate here (Wise, 1996). The SMA can be divided into three regions based on cytoarchitecture, connectivity, and function: the SMA proper, the pre-SMA, and the supplementary eye field (SEF). Stimulation studies have confirmed that the SMA proper—and to a lesser extent the pre-SMA, is somatotopically arranged (Fried et al., 1991). Similar to the PMC, the SMA is involved in movement planning and preparation (Brinkman & Porter, 1979; Tanji & Kurata, 1982). However, while the PMC plays a key role in externally-triggered

movements, human neuroimaging studies have shown that the SMA is more actively involved in self-initiated, sequential movements. This is particularly true of the pre-SMA (Jenkins, Jahanshahi, Jueptner, Passingham, & Brooks, 2000). Deficits resulting from damage to the SMA span a diverse range of motor impairments, including, for example, involuntary grasping of objects and the inability to make spontaneous movements (Nachev et al., 2008). Patients may also experience Parkinsonian-like movements, potentially due to damage to the connections between the SMA and basal ganglia (Akkal et al., 2007).

1.1.2 Subcortical Motor Regions

Beneath the cortex lie additional brain regions that have been implicated in motor behaviours. These subcortical structures often integrate diverse modalities beyond the motor domain. Three such structures, the basal ganglia, cerebellum, and thalamus, are discussed below (Figure 1.5).

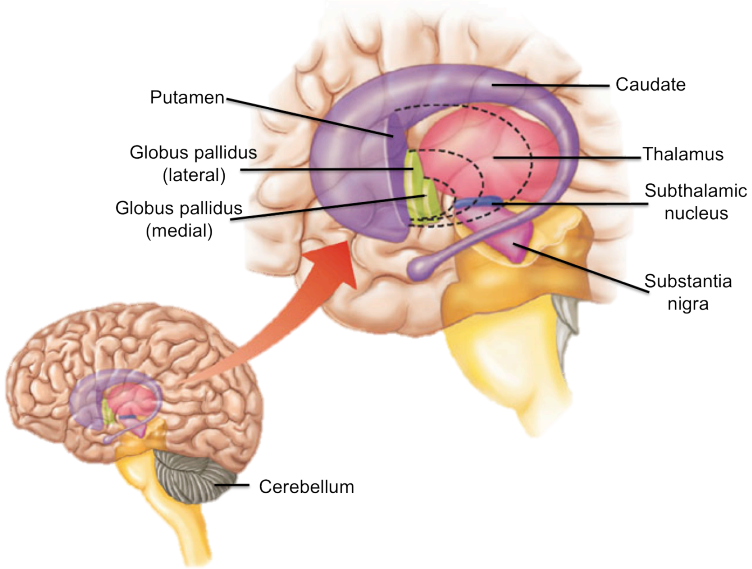

Figure 1.5: Subcortical motor structures. (Bottom left) Lateral view of the brain, indicating the locations of the thalamus, basal ganglia, and cerebellum. (Top right) Enlarged view of the thalamus and subdivisions of the basal ganglia. Figure adapted from cti.itc.virginia.edu.

1.1.2.1 Basal Ganglia

The basal ganglia consist of the caudate, putamen, globus pallidus, substantia nigra, and the subthalamic nucleus bilaterally. Based on similar histology and functional connectivity patterns, the caudate and putamen together are said to comprise the striatum. The basal ganglia are important for both voluntary and involuntary motor processes, but have no direct projections to the spinal cord. Rather, they exert their influence via projections to and from the cortex, and relay information through the corticospinal, rubrospinal, and reticulospinal tracts (Leonard, 1997). Most inputs to the basal ganglia arrive in the striatum, while most basal gangliar outputs are relayed from the globus pallidus and substantia nigra, the majority of which project to thalamic nuclei (Nolte, 2008). Damage to the basal ganglia results in lack of control over both voluntary and involuntary movements, resulting in symptoms such as tremor (Leonard, 1997).

1.1.2.2 Cerebellum

The cerebellum is widely connected to the rest of the brain, receiving inputs from cortical and subcortical motor systems (Leonard, 1997). Like the brain itself, the cerebellum (literally meaning “little brain”) is composed of an outer cortical layer and an inner white matter region. The cerebellar cortex consists of an outer molecular layer, an intermediate Purkinje cell layer, and an inner granular layer. The cortical layer is divided into the spinocerebellum, cerebrocerebellum, and vestibulocerebellum. The spinocerebellum receives sensory input from the spinal cord, and is primarily involved in motor execution and control of posture. The cerebrocerebellum receives direct input from the cerebral cortex, and is responsible for motor planning. The vestibulocerebellum, the oldest of the cortical layers,

maintains balance (J. Martin, 2003). The cerebellar white matter contains nuclei that relay information between the cerebellar cortical layers, and to and from the thalamus (Nolte, 2008). Damage to the cerebellum results in postural instability, and loss of timing and coordination of movements (Leonard, 1997).

1.1.2.3 Thalamus

Nestled between the cerebral cortices, the thalamus is a major hub of all sensory pathways excluding olfaction, and contains the primary motor relay nuclei for the cortex. It is also an integral component of the anatomical circuits of the basal ganglia and cerebellum (J. Martin, 2003). The thalamus is comprised of three divisions: anterior, medial, and lateral, which contain the principal nuclei. The two nuclei most relevant to motor behaviour are located in the lateral division: the ventral anterior (VA) and ventrolateral (VL) nuclei. The VA receives the majority of the basal ganglia inputs; the VL receives many cerebellar inputs (Nolte, 2008). Both nuclei project to the motor and premotor cortices (Leonard, 1997). Due to its involvement in an array of sensory processes, damage to the thalamus may produce both sensory and motor deficits (Leonard, 1997).

1.1.3 DESCENDING MOTOR PATHWAYS

Cortical and subcortical areas influence motor behaviours through axonal projections to the spinal cord. The corticospinal and corticobulbal tracts original from layer V of the cerebral cortex, and are collectively referred to as the pyramidal tracts. The reticulospinal, vestibulospinal, tectospinal, and rubrospinal tracts originate from brainstem nuclei. The following sections briefly examine these descending motor pathways (Figure 1.6).

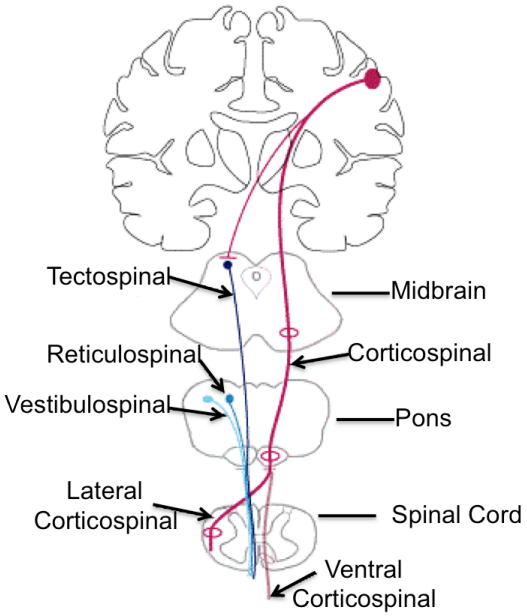

Figure 1.6: Schematic of descending motor tracts. Figure adapted from bioon.com.

1.1.3.1 Cortical Tracts

Corticospinal Tract. Axons of the corticospinal tract originate primarily in the frontal lobe, continue through the posterior limb of the internal capsule, the midbrain, pons, and to the medullary pyramids (Nolte, 2008). Here, the corticospinal tract divides into lateral and ventral components. The lateral corticospinal tract crosses at the pyramidal decussation and terminates in the lateral spinal column. The majority of its axons originate in M1, but many also arise from other sensorimotor areas. Its primary function is voluntary movement of the limb muscles (J. Martin, 2003). Damage to this tract results in chronic impairments in limb use, such as loss of movement fractionation (Leonard, 1997). The ventral corticospinal tract is uncrossed, and ends in the ventral spinal column. Its axons are primarily from M1 and the PMC. It regulates voluntary movement of axial muscles (J. Martin, 2003).

Corticobulbar Tract. The corticobulbar tract originates in the sensorimotor areas of the frontal lobe. It contains both crossed and uncrossed fibres, and

terminates in the brain stem. It primarily controls voluntary movement of the cranial muscles. Upper facial muscles are bilaterally innervated, while lower facial muscles are contralaterally controlled (J. Martin, 2003).

1.1.3.2 Brain Stem Tracts

Reticulospinal Tracts. In addition to the pyramidal tracts, the reticulospinal tracts are the major alternative route for the control of voluntary movements. Its axons arise from the pontine and medullary reticular formation, and terminate in the medial and lateral portions of the spinal cord, respectively (Nolte, 2008).

Vestibulospinal Tracts. The vestibulospinal tracts are responsible for postural adjustments and head movements. Fibres of the lateral vestibulospinal tract descend uncrossed from the lateral vestibular nucleus in the pons, and terminate in the spinal cord to compensate for shifts in body orientation. The medial vestibulospinal tract begins in the medial vestibular nucleus and maintains head position (Nolte, 2008).

Tectospinal Tract. Composed of axons from the superior colliculus, the tectospinal tract crosses the midbrain at the dorsal tegmental decussation and terminates at the cervical level of the spinal cord. It mediates reflex turning in response to sensory stimuli (Nolte, 2008).

Rubrospinal Tract. The smallest of the brain stem tracts, the rubrospinal tract originates in the red nucleus of the rostral midbrain, where it receives inputs from the motor cortex and cerebellum. It decussates in the ventral tegmental area, and descends to the lateral anterior horn of the spinal cord. Like the lateral corticospinal tract, the rubrospinal tract primarily influences distal muscles (Nolte, 2008).

1.2 MOTOR LEARNING AND PLASTICITY

Motor learning is defined as the modification of a movement behaviour by experience. It can be categorised as either explicit or implicit on the basis of whether the behaviour is actively or passively acquired. Rather than being a static entity, motor learning progresses through a series of phases characterised by the gradual lessening of effortfulness and increasing of proficiency. These various stages of motor learning recruit the primary and secondary motor areas described in sections 1.1.1 and 1.1.2, as well as association areas such as the prefrontal cortex. Within these regions, the mechanisms of neuroplasticity subserve the changes that allow such learning to occur.

1.2.1 MOTOR LEARNING

1.2.1.1 Types of Motor Learning

Explicit motor learning involves the conscious, declarative recollection of previous motor actions. Implicit motor learning is an unintentional form of learning that is often characterized by behavioural improvements (Halsband & Lange, 2006). In some instances, the use of explicit processes on an implicit task may lead to impaired learning (Fletcher et al., 2005; Fulton & Sheehan, 1935). Though helpful, the distinction between explicit and implicit motor tasks is not absolute. The execution of many motor behaviours begins explicitly, then transitions to an implicit process as learning progresses (Forkstam & Petersson, 2005). An additional classification system differentiates between general motor learning that requires the association of a stimulus and motor reflex response, and motor *skill* learning, which refers to the learning of more complex movements, such as riding a bicycle

(Luft & Buitrago, 2005). Motor skill learning, as compared to other forms of motor learning, occurs slowly over several sessions, and is typically retained over extended periods of time (Luft & Buitrago, 2005).

Learning of both skilled and general motor tasks may occur through three broad processes: error-based, reinforcement, and use-dependent learning. Both error-based and reinforcement learning use outcome information to shape motor behaviours toward the desired goal. Use-dependent learning relies on the repetition of movements to cause modifications in the level of motor performance (Wolpert et al., 2011). Error-based and use-dependent learning have been shown to work in parallel, with learning accrued via the latter process exhibiting the greatest longevity (Diedrichsen et al., 2010).

1.2.1.2 Phases of Motor Learning

The acquisition of a motor behaviour is defined as motor learning. The execution of that behaviour is motor performance, and the retention of that behaviour is a motor memory (Leonard, 1997). The interplay between motor learning, performance, and memory normally proceeds through three distinct phases: early, intermediate, and late. Early learning is the phase in which the movement is initially acquired, creating a novel association between sensory cues and the appropriate motor output (Halsband & Lange, 2006). Early learning is also referred to as the cognitive phase, as performance of the task requires mental concentration and constant monitoring via verbal processing of the motor goal (Leonard, 1997). The intermediate phase consists of trial and error learning. Different strategies to perform the motor task are sampled, and results compared (Leonard, 1997). Critically, the intermediate phase marks the beginning of the

establishment of a sensorimotor map detailing the movement (Halsband & Lange, 2006). There is a "fast learning" that occurs during active practice, and a slower learning that occurs between sessions (Luft & Buitrago, 2005). This is the stage in which the majority of consolidation occurs, both through sleep (Walker et al., 2003) and mental rehearsal of the movement (Mulder et al., 2004). Practice and consolidation lead to a progressive increase in motor execution speed and fluidity (Penhune & Steele, 2012). In the late stage of motor learning, the movement has become automatic and skilful. The behaviour can be performed proficiently without consciously attending to the action (Halsband & Lange, 2006). It is in the late stage and beyond that a motor skill may progress to a long-lasting motor memory (Penhune & Steele, 2012).

1.2.1.3 Involvement of Brain Regions in motor learning

As detailed above, motor learning can be divided into multiple phases, during which time specific processes occur. Figure 1.7 depicts the various components of motor learning, and summarizes the general functions and contributions of particular brain regions.

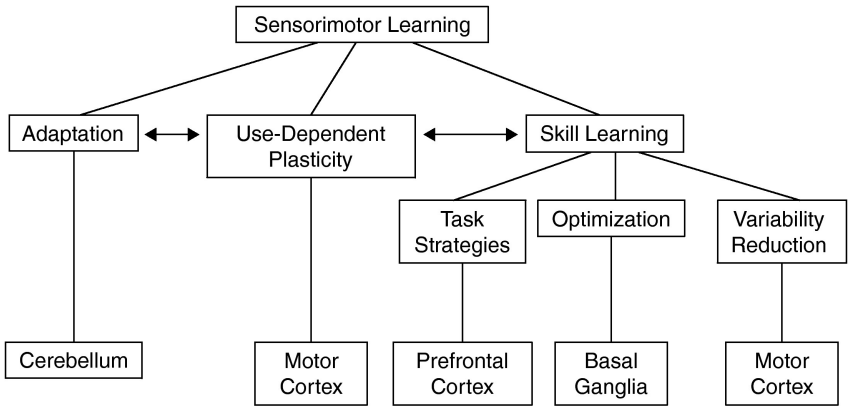

Figure 1.7: A proposed structure for the function of motor-related brain regions. From Krakauer (2011).

Cortical Motor Areas. Training on implicit motor tasks such as implicit sequence learning leads to increased and enlarged activation within M1 (Karni et al., 1995). If the task is practiced for several weeks, these changes can persist for several months. Similarly, during skill learning, motor representations within M1 transition from representing a single muscle to a group of muscles responsible for the skill itself. Indeed, TMS applied to the M1 of skilled musicians found an expanded representation of task-relevant muscle combinations (Gentner et al., 2010). Explicit motor learning tasks can evoke increased contralateral M1 activation within minutes of task onset (Halsband & Lange, 2006). The SMA exhibits both implicit and explicit practice-related increases, particularly in response to sequential movements that rely heavily on timing (Halsband & Lange, 2006). The PMC is active during the early stages of motor learning, likely forming an internal representation between spatial cues and motor commands (Deiber et al., 1997).

Subcortical Motor Areas. The striatum is critical for the consolidation and automatization of implicit motor learning tasks, especially those involving learned sequences (Doyon et al., 2009). The caudate in particular is activated during the early phase of skill acquisition, and is involved in the long-term storage of motor memories during the late phase (Halsband & Lange, 2006). Motor adaptation relies heavily on the cerebellum, which generates prediction errors in response to past performance (Synofzik et al., 2008). The basal ganglia and cerebellum may also form the basis of two distinct, yet complementary, cortico-subcortical loops. It has been suggested that the cortico-basal ganglia loop reinforces movements based on their reward value and likelihood, while the cortico-cerebellar loop is primarily concerned with sensorimotor accuracy (Hikosaka et al., 2002).

Associated Brain Areas. The early stages of explicit motor learning involve the prefrontal cortex. The Dorso-lateral prefrontal cortex (DLPFC) helps mediate trial-error and motor learning by associating movements with sensory cues using working memory processes (Halsband & Lange, 2006). During the early stages of motor skill learning, increased activity is seen in the right inferior parietal cortex, which may work to integrate sensory information and feedback processing (Kawashima et al., 2000). As the motor skill becomes more automatic, recruitment of such frontal areas decreases, and activation shifts towards the subcortical areas discussed above (Wu et al., 2008).

1.2.1.4 Stroke Recovery as Motor Learning

Though the extent to which stroke-induced movement impairments result in motor learning deficits is debated, many recovery processes in the stroke patient share similarities with motor learning in the healthy adult (Krakauer, 2006a). The modification of sensorimotor maps that occurs post-stroke parallels the alteration of motor cortical representations following learning, potentially drawing on the same or similar underlying mechanisms (Hosp & Luft, 2011a). Together with use-dependent learning, motor adaptation via error-based learning may be central in rehabilitative strategies following stroke. Such extrinsic feedback mechanisms become more essential because normally occurring intrinsic somatic feedback processes may have been damaged by the stroke (Subramanian at al., 2010). During the early stages of recovery, motor learning is best buoyed by general feedback regarding the overall sequence of movements; as rehabilitation progresses, increasingly precise feedback becomes more beneficial (van Vliet & Wulf, 2006). An

extended overview of stroke recovery and rehabilitation is presented in section 1.3.3.

1.2.2 Overview of Synaptic Plasticity

Plasticity is a persistent change in properties of the brain, both morphological and functional, in response to environmental change and experience. Though once believed to be a feature unique to the developing brain, we now know that plasticity processes also take place in the adult brain. Occurring at both the synaptic and network level, plastic alterations in the brain can cause behavioural modifications over time (Hummel & Cohen, 2005).

1.2.2.1 Hebbian Synaptic Plasticity

Early work by William James (1890) conjectured that external forces could cause changes in the brain, in an analogous manner to the way in which physical materials alter their shape when subjected to external pressure (Warraich & Kleim, 2010). The substrate for such changes was discovered nearly two decades later, when Ramon y Cajal and others found that the nervous system was composed of synapses (Warraich & Kleim, 2010). A synapse is the point of interaction between neurons, with the axon of the presynaptic neuron associating with a dendrite of the postsynaptic neuron. When the presynaptic cell is depolarized, it releases neurotransmitters into the synaptic cleft. Here, the neurotransmitters bind to receptors on the postsynaptic element. These receptors then modulate changes in the postsynaptic neuron that may alter its activity and firing pattern (Warraich & Kleim, 2010). If such temporally correlated activity between neurons occurs

repeatedly and persistently, processes may occur that strengthen or weaken the association between the two neurons.

This idea forms the basis of Hebbian (or use-dependant) synaptic plasticity, which proposes that synapses that are most effective at evoking a post-synaptic neuronal response should become stronger (Hebb, 1949). Hebbian plasticity progresses through two broad stages: the rapid reinforcement of pre-existing pathways, and the slower establishment of new pathways (Pascual-Leone et al., 2005). Though originally conceived as a process by which connections are strengthened, plasticity now encompasses processes that weaken associations. The two mechanisms that are mainly responsible for the mediation of Hebbian synaptic plasticity are long term potentiation (LTP) and depression (LTD).

1.2.2.2 Long Term Potentiation and Depression

Long term potentiation (LTP) refers to the neuronal process by which existing synapses become more effective; that is, presynaptic stimulation becomes increasingly likely to evoke a post-synaptic response. As such, there is an increase in excitatory synaptic potential (Siegelbaum & Kandel, 1991). Correspondingly, long term depression (LTD) results in sustained inhibition of synaptic transmission. As their names suggest, the effects of these phenomena can be long-term, persisting for hours or days (Siegelbaum & Kandel, 1991). LTP and LTD were originally studied in the hippocampus and cerebellum (Bliss & Lomo, 1973; Ito, 1989), and thus it is within these brain regions that their mechanisms are best characterized, though very closely related processes have subsequently been demonstrated elsewhere (Malenka & Bear, 2004). Pertinent to this thesis, both LTP-like (Hess & Donoghue, 1994) and LTD-like (Hess & Donoghue, 1996) processes have been documented in

the rat motor cortex. Generalizing across the multiple forms of LTP (Raymond, 2007) and LTD (Massey & Bashir, 2007), it is thought that glutamatergic LTP and LTD are primarily induced postsynaptically, for example by changes in receptor density, and maintained by presynaptic mechanisms such as modifications in neurotransmitter release.

1.2.2.3 Plasticity Underlying Motor Learning

The effects of neuronal plasticity can be quantified by measuring changes in the structure and function of individual neurons and populations of neurons. In this way, the interaction between motor learning and plasticity can be divided into four categories: individual-structural, individual-functional, population-structural, population-functional (Table 1.1). For example, plastic alterations in the structure of individual neurons can be measured by changes in spine density and number of synapses, changes in their function can be assessed by recording neuronal activity. Such studies necessarily have to be performed in non-human animals. For example, experimental studies at the level of individual neurons in rodents help to provide a robust characterization of the interaction between motor learning and mechanisms of plasticity as rodents have advanced motor systems that can be probed with a variety of electrophysiological and histological measures. Studies of population of neurons can be carried out in humans as well as in animals: Structural changes of populations of neurons can be determined by examining grey matter density, while the function of neuronal populations can be investigated with sensorimotor mapping (Warraich & Kleim, 2010).

	Individual Neurons	Populations of Neurons
Structural	Dendritic arbor Spine density Synapse number	Grey matter density Structure thickness
Functional	Neural activity Intrinsic excitability	Motor maps fMRI

Table 1.1: Measurements of neuronal plasticity in response to motor learning. Four categories of plasticity can be defined on the basis of whether it is observed via modification of the structure or function of individual or populations of neurons. Adapted from Warraich (2010).

Individual-Structural. Plastic alterations in the structure of individual neurons have been probed in rodents trained on a skilled forelimb reaching task. As early as one hour into skill acquisition, mice showed increased postsynaptic dendritic spine formation in the contralateral motor cortex. These spines were stabilised and maintained after training ended (Xu et al., 2009). An analogous study in rats demonstrated that such changes were specific to muscles involved in forelimb reaching and grasping, and not those controlling proximal muscles (Wang et al., 2011). These results suggest that during the early stages of learning, increased dendritic branching may occur.

Individual-Functional. In addition to the structural changes in individual neurons, similar rodent studies provide insight into the functional changes that are occurring, particularly through LTP and LTD processes. Rat studies found increased LTP-like plasticity within the M1 forelimb representation during training on a reaching task; these strengthened connections were maintained for weeks after training ended (Rioult-Pedotti et al., 2007). In humans, TMS studies documenting changes in the stimulation intensity required to elicit motor activation is perhaps the closest approximation of learning-induced plasticity changes in the function of individual (or small groups of) neurons. Following training on a five finger piano

sequence, the TMS intensity needed to activate the involved muscles significantly decreased, suggesting an increase in neuronal excitability (Pascual-Leone et al., 1995).

Population-Structural. Subjects trained on a juggling task showed increased grey matter in the occipito-temporal cortex, an area relevant to the processing of complex visual motion, as early as 7 days following the beginning of training (Draganski et al., 2004; Driemeyer at al., 2008; Scholz et al., 2009). A VBM study by Hamzei and colleagues found that five days of training on a signing motor task caused increased grey matter bilaterally in the PMd, ipsilaterally in the SMA, and contralaterally in the inferior parietal lobule (IPL). These changes were correlated with motor skill performance (Hamzei et al., 2012). Taken together, findings such as these suggest that motor skill learning and produce anatomical changes in the cortex.

Population-Functional. Functional changes at the level of the individual neuron may be responsible for the functional changes seen in populations of neurons. During the late phase of learning on the skilled forelimb reaching task, animals trained to reach had larger distal forelimb representations than control animals (Kleim et al., 2004). Such enlarged representations co-localize with areas of enhanced synaptogenesis (Kleim et al., 2002). Similar cortical reorganization following motor learning has been documented in humans. Long-term performance on a sequence learning task results in an increased area of activation in M1 to the learned sequence versus an unpractised sequence, a result which persists for several months (Karni et al., 1995). Training subjects on a 5-finger piano sequence resulted in TMS pulses to a broader area of scalp being able to elicit activation, also indicative of an expanded motor map (Pascual-Leone et al., 1995).

1.2.2.4 Homeostatic Plasticity

If left unchecked, repeated modification of cortical excitability by LTP and LTD carries the possibility of permanently altering the properties of neuronal networks. That is, persistent induction of LTP or LTD would bring synapses to their maximum and minimum, respectively. Neuronal signalling at such synapses would become saturated, the synapses themselves unusable, and further information processing precluded (Kim & Linden, 2007). As such situations are not normally observed in the healthy nervous system, there must exist a mechanism that prevents such a state from occurring. The Bienenstock-Cooper-Munro (BCM) theory of synaptic modification proposes such a model, suggesting that neuronal activity is stabilized by raising or lowering the "modification threshold" (θ_m) for LTP and LTD induction, based on the previous, time-averaged history of post-synaptic firing rates (Bienenstock, Cooper, & Munro, 1982) (Figure 1.8).

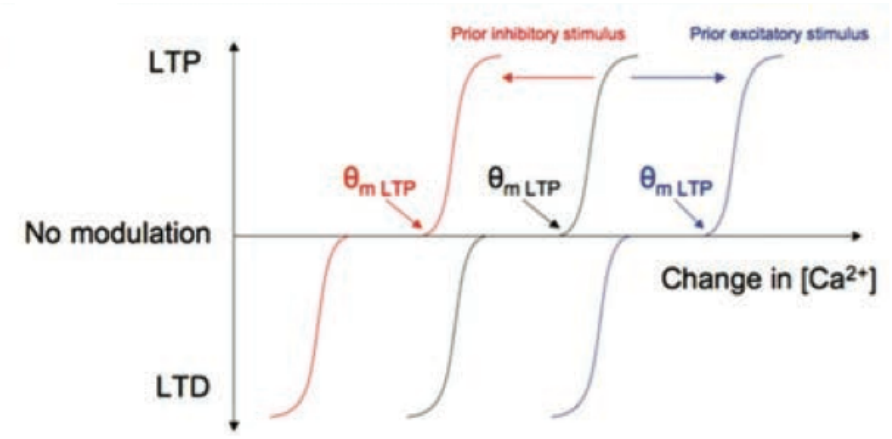

Figure 1.8: BCM theory of synaptic modification. A history of high post-synaptic firing shifts θ_m from baseline levels (in black) to the right (in blue), favouring LTD induction. Low levels of post-synaptic firing lower θ_m, favouring LTP (in red). Figure from Stagg, 2011.

In this way, a history of low post-synaptic activity would raise the modification threshold, favouring depolarization and the induction of LTP, and vice-versa. Such altering of thresholds ensures that an optimal mean firing rate is maintained within a particular target range, and forms the basis of homeostatic plasticity. In neuronal cultures, treatments that block spiking such as tetrodotoxin increase synapse size and neurotransmitter release. Such changes effectively lower the firing threshold, thereby promoting increased firing frequency (Turrigiano, 1999). Complementary results are found for treatments that increase spike firing.

Using paired transcranial stimulation methods, it has been found that the excitability of the human motor cortex may behave in a homeostatic manner. Stimulation paradigms that produce an LTD-like decrease in excitability boost the effects of subsequent LTP-like stimulation. Similarly, an initial application of LTP-like stimulation attenuates the effects of a second application LTP-like stimulation (Müller et al., 2007). Such experiments help illuminate the substrates that underlie the homeostatic behavioural results observed in the motor domain: prior learning of a motor task impedes the acquisition of a novel task that relies on the same effectors (Shadmehr & Brashers-Krug, 1997). Moreover, the inability to respond to acute increases in corticospinal excitability via homeostatic mechanisms is thought to partially underlie the pathophysiology of writer's cramp (Kang et al., 2011; Quartarone et al., 2005).

1.3 MOTOR FUNCTION AFTER STROKE

Each year, over fifteen million people will have a stroke in the world, with only ten percent experiencing a full recovery. The majority of stroke survivors are left with disabilities that can span the motor, sensory, and cognitive domains.

Various therapies are available to target these impairments, ranging from simple exercise regimes to non-invasive brain stimulation. As the proportion of the elderly in our population continues to rise, so too does the incidence of stroke. Because of this, a greater understanding of rehabilitative efforts aimed toward improving stroke recovery is becoming increasingly relevant.

1.3.1 Overview of Stroke

Stroke is the second most common cause of mortality per year in the developed world: over 5.5 million people die due to stroke and stroke-related complications annually (Strong et al.,2007). Moreover, stroke is the leading cause of adult disability, with nearly half of all survivors requiring continued care and a substantial number rating their quality of life as very poor (Chen et al., 2010). Several risk factors for stroke have been identified, including non-modifiable factors like gender and age, and modifiable lifestyle choices. Stroke occurs more often in men than in women, in the elderly than in the young, and in blacks than Hispanics or whites (Goldstein et al., 2006). Major modifiable risk factors include hypertension, smoking, and Type 2 diabetes. Combined, these preventable factors account for over half of the population attributable risk (Goldstein, 2009). Treating hypertension alone was found to result in a 38% reduction in risk of stroke. Cessation of smoking led to a 50% reduction after one year, and a return to baseline after five (Goldstein et al., 2006).

1.3.1.1 Classification

Stroke is a clinical syndrome that leads to loss of cerebral function lasting more than 24 hours, with no apparent cause other than a vascular origin (Warlow et

al., 2001). There are two main categories of stroke: ischaemic and haemorrhagic. The majority of strokes are ischaemic in nature, composing 80% of all cases. The remaining 20% of strokes fall into the subtypes of haemorrhagic stroke: intracerebral and subarachnoid. They account for 10 and 5 percent of strokes, respectively. Five percent of strokes are of an unknown haemorrhagic origin (Warlow et al., 2001). The initiating events for strokes are varied, with 50% of ischaemic strokes being caused by arterial wall disorders, 25% by intracranial small vessel disease, 20% due to an embolism from the heart, and the remaining 5% due to rare causes. The division is less clear for haemorrhagic strokes, which are more often caused by a combination of factors, rather than a single initiating event (excluding trauma) (Warlow et al., 2001).

The Oxfordshire Community Stroke Project (OCSP) has developed a system employed to classify strokes based on the symptoms and signs the patient presents with in the clinic. They note four subtypes of cerebral infarct. (Figure 1.9 depicts cerebral blood flow anatomy.) Total anterior circulation infracts (TACI) are those which result in higher level cerebral dysfunction and ipsilateral sensorimotor deficits, while partial anterior circulation infarcts (PACI) result in similar deficits that are less severe and confined to one body part. Posterior circulation infarcts (POCI) result in contralateral sensorimotor deficits or visual problems, and lacunar infarcts (LACI) tend to present in one modality, i.e. purely motor or purely sensory. TACI and PACI tend result from cortical lesions, and POCI from brainstem lesions. The aetiology of LACI is less clear, but its lesions often occur in deep subcortical nuclei. Of these, TACI patients have the poorest functional outcomes (Dewey et al., 2003).

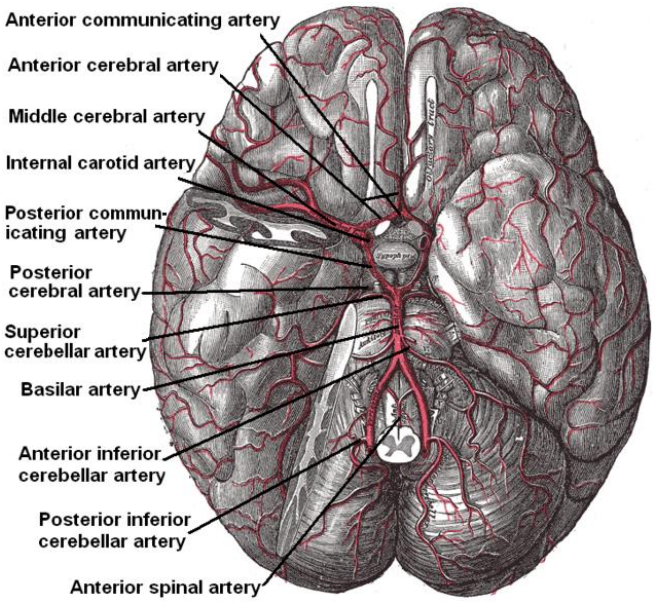

Figure 1.9: Cerebral blood supply. TACI and PACI affect anterior circulation, POCI affects posterior circulation, and LACI affects circulation to deep brain structures. Figure adapted from Gray (2000).

1.3.1.2 Metabolic Changes During Stroke Onset

In the healthy brain, the rate of blood flow is dependent on the brain's level of neuronal activity. As neuronal activity relies on aerobic glucose metabolism, cerebral blood flow (CBF) and oxygen use are linked (Warlow et al., 2001). During a stroke, arterial occlusion results in reduced CBF to the brain area that the blocked vessel serves. In an attempt to maintain normal levels of oxygen delivery in spite of reduced blood flow, the vessels dilate, a natural process known as autoregulation (Powers, 1991). If the occlusion remains and cerebral perfusion continues to fall, the brain's autoregulative ability to maintain oxygen demands will be exceeded. Cells will then increase the amount of oxygen extracted from the blood (the oxygen extraction ration, OER), leading to a state known as misery perfusion (Bornstein & Brown, 1991). Once the OER has reached its limit, oxygen delivery again falls, ultimately leading to neuronal damage and death (Bornstein & Brown, 1991). The extent to which this oxygen-deprived state exists and persists determines whether

the tissue becomes part of the central ischemic zone or the peripheral ischemic penumbra, an area that is functionally inactive but structurally intact (Davis et al., 2003).

1.3.1.3 Cognitive and Behavioral Sequelae

Because our population is rapidly aging, and advanced age is a significant risk factor for stroke, it is likely that the incidence of stroke will climb in the coming years (Strong et al., 2007). Moreover, as interventions become more effective and post stroke mortality declines, an increasing number of patients are surviving strokes, albeit with impairments. Fully half of all stroke survivors are left with cognitive or physical impairments of varying severity levels and presentation (Di Carlo, 2008). Cognitive changes following stroke include dementia, personality changes, and language impairments, each of which can influence and be influenced by depression (Kalaria & Ballard, 2001). Such cognitive changes are important when creating a motor rehabilitation regime, as they will affect the patient's ability to participate in and adhere to the program.

1.3.2 STROKE-INDUCED PLASTICITY

1.3.2.1 Perilesional Cortex

Adjacent to the ischemic core, there are two types of tissue to consider: that of the ischemic penumbra and the remaining peri-infarct cortex. As noted above, tissue in the penumbra is functionally inactive but maintains its structural integrity. The latter characteristic raises the possibility that this tissue can be converted to viable cortex. Indeed, studies in animals have demonstrated that, following a stroke, this area exhibits the greatest level of growth-related molecular changes (Cramer,

2008a). In humans, Furlan and colleagues have shown that reperfusion of penumbral tissue is critical in promoting early stroke recovery (Furlan et al., 1996). Recovery of function in the penumbra and peri-infarct cortex may be mediated by axonal sprouting, increased dendritic remodelling, and synaptogenesis (Hosp & Luft, 2011).

Slightly farther afield than the penumbra, tissue that remains both structurally and functionally intact may assume functions once performed by the damaged tissue. Specifically, somatotopic representations of the body may shift toward undamaged cortical areas. Such reorganization following brain injury was first documented in non-human primates (Nudo & Milliken, 1996), but may occur in stroke patients as well. Multiple studies have demonstrated a posterior shift in sensorimotor activation following stroke, as seen on task-activated fMRI scans (Calautti et al., 2003; Pineiro et al., 2001). In patients with isolated primary motor cortex stroke, a longitudinal study documented increasingly dorsal shifts in finger representations within M1 over a two year period (Jaillard et al., 2005). While these somatotopic shifts are presumably beneficial, increased perilesional activation following stroke has not been reliably shown to directly correlate with improved motor recovery (Cramer et al., 2006).

1.3.2.2 Lesioned Hemisphere

During the acute phase of stroke there is substantial oedema and modifications of cerebral blood flow occur. Such relatively transient effects may mask the activity of brain regions that are essentially unaffected, in a process termed diaschisis (Bornstein & Brown, 1991). The gradual resolution of this pathology may be partially responsible for early recovery. Moreover, in the weeks

and months following stroke, areas distant from but connected to the infarct may assume the functions of the damaged tissue to counteract the loss of input (Cramer, 2008a). After trauma resulting in reduction of signals from M1 to the corticospinal tract, secondary motor areas begin a compensatory process in which spared regions of M1, SMA, and PMC show increased activity (Ward & Cohen, 2004; Webster et al., 2006). Indeed, increased activity in the ipsilesional SMA is correlated with improved hand performance, and is predictive of better recovery (Loubinoux et al., 2003). Likewise, disruption of the ipsilesional PMd with TMS increases motor reaction times in patients but not controls (Fridman et al., 2004). Taken together, studies such as these argue for the beneficial nature of enhanced involvement of ipsilesional secondary motor areas following stroke.

1.3.2.3 Intact Hemisphere

Following stroke, there is a shift in movement-related activation towards the contralesional hemisphere, documented as a decrease in the laterality index of motor movements (Feydy et al., 2002). One view explains this phenomenon as the contralesional equivalent of the enhanced recruitment shown by ipsilesional motor areas (Cramer, 2008a). A second interpretation is that the shift in activity is a passive change brought about by reduced inhibition originating from the lesioned cortex (Dancause & Nudo, 2011). The increasingly active unlesioned motor cortex then further inhibits the lesioned motor cortex, as evidenced by TMS studies of interhemispheric inhibition (Murase et al., 2004). The resulting inhibition of the lesioned motor cortex may prove detrimental to long term recovery prospects. Stroke patients who are well recovered thirty days after stroke continue to show increased intracortical inhibition in the lesioned hemisphere, but have returned to

normal on the unaffected side (Manganotti et al., 2002). Poor recovery was associated with continued abnormal inhibition within both hemispheres (Manganotti et al., 2002). This suggests that increased inhibition emanating from the intact hemisphere is more deleterious than reduced inhibition from the lesioned hemisphere.

However, particularly during the chronic stage, such increased activity in the unaffected hemisphere may actually be beneficial. In healthy subjects, the ipsilateral SM1 is recruited during performance of complex or difficult motor tasks. After stroke, it may be that even apparently simple tasks become demanding, and so recruit the SM1 of the ipsilateral, SM1 (Calautti et al., 2003). It is possible that the intact hemisphere undergoes adaptive plasticity to become more involved in control of the impaired limb (Schaechter & Perdue, 2008). Data on this theory are conflicting, as TMS stimulation of the intact M1 does not usually result in muscle activity in the ipsilateral, affected limb (Palmer et al., 1992).

1.3.3 MOTOR RECOVERY FOLLOWING STROKE

Motor deficits following stroke vary from complete hemiplegia, to the loss of fine motor movement, to spasticity, defined as the inability to make smooth, fluid motor movements (Olvey, Armstrong, & Grizzle, 2010). Overall, 10% of stroke survivors achieve nearly full recovery, 25% have minor impairments, 10% require care in a long-term facility, and the remainder have moderate to severe motor deficits (Goldstein, 2009). To compensate for these impairments, patients often modify the way in which they perform motor tasks. Such behavioural compensation can be seen during gross movements, in which patients recruit muscles of the trunk to perform actions that would normally be performed solely by the arm (Cirstea &

Levin, 2000), and also in fine motor movements, such as object grasping (Raghavan et al., 2010). While beneficial in performing activities of daily life, such compensatory techniques should not be confused with actual recovery that returns both brain and behaviour to normal baseline functioning.

1.3.3.1 Predictors of Recovery

Some degree of spontaneous recovery is apparent in the weeks and months following a stroke, with the most dramatic improvements occurring within the first 30 days. In cases of severe impairment, rapid improvements may continue for up to 90 days before tapering off (Cramer, 2008a). This acute phase of recovery plateaus three to six months after the stroke (Studenski et al., 2001). Spontaneous recovery is associated with shifts in maps present in the cortex surrounding the infarct, increased activation in secondary areas that are normally connected to the injured zone, and a shift in interhemispheric lateralization toward the contralesional hemisphere (Cramer, 2008a). While such compensatory mechanisms are beneficial in the short term, they may become detrimental if they persist into the chronic phase (Ward et al., 2003).

Behavioural and anatomical characteristics of the stroke, as well as the level of preserved CNS function, can also aide in predicting the extent and rate at which recovery occurs during the chronic stage. Behaviourally, less severe impairments carry a better prognosis for recovery (Kwakkel et al.,1996), with the degree of motor deficits providing the most reliable predictions of motor recovery, followed by sensory and visual deficits (Stinear, 2010). Within the motor domain, the timecourse of recovery varies depending on whether the impairment primarily affected the upper or lower extremities. Following discharge, the rate of recovery in

the lower extremities drops, while that of the upper extremities remains constant (Desrosiers et al., 2003).

Information about the lesion itself can also be employed to predict the possible degree of recovery. Such neuroimaging results may prove more useful than behavioural measures (Milot & Cramer, 2008). Larger infarct volume is associated with more modest benefits from rehabilitation and poorer outcomes overall (Saver et al., 1999). A decrease in the fractional anisotropy in diffusion weighted MRI images is associated with poor recovery (Stinear, 2010), while the integrity of the corticospinal tract (CST) predicts responsiveness to rehabilitation (Riley et al., 2011). Relatedly, the presence of motor evoked potentials (MEPs), a measure of CST and nervous system function, is also highly predictive of motor recovery (Hendricks et al., 2002).

1.3.3.2 Motor Rehabilitation

Additional steps can be taken to improve recovery after stroke above and beyond naturally occurring processes. Hemiparetic patients exhibit elevated daily energy requirements, yet their maximum aerobic ability is lower than in healthy controls (Ivey et al., 2006). To address this incongruity, aerobic exercise programs aimed at increasing cardiovascular fitness have been used to provide patients with the energy necessary to support activities of daily living (Ivey et al., 2006). A broad and diverse group of rehabilitation regimens focuses on task specific training, utilizing goal directed practice, repetition, and feedback (Hubbard et al., 2009). Such rehabilitation programs are based on the assumption that patients' levels of functioning can improve with practice. Thus, the theories underlying many of these therapies overlap with the foundations of motor learning (see section 1.2.1.4)

(Krakauer, 2006). These types of programs are often geared toward the patient's specific deficit, emphasizing functional tasks rather than motor strengthening (Cramer, 2008b).

One such form of task-oriented training is Arm Ability Training. This program uses repetitive tasks, and varies their difficulty and training schedule, thus taking advantage of the advances made in motor learning (Krakauer, 2006). For patients with mild hemiparesis, this form of rehabilitation has been shown to improve performance of motor skills such as hand grip and aimed reaching (Platz et al., 2001). There are also several therapy programs available for patients with more moderate to severe impairments. In constraint-induced movement therapy (CIMT), the unaffected arm is physically restrained for up to 90% of the patient's waking hours. For patients in the acute phase, CIMT aims to prevent the development of compensatory behaviours that may hinder proper recovery. For patients in the chronic phase, CIMT helps to overcome learned non-use (Krakauer, 2006b). Following CIMT, increased fMRI activation in the ipsilesional SM1 is correlated with improved motor performance (Könönen et al., 2012).

Two additional rehabilitation programs that rely on machine assistance have gained increasing prominence. The first of which employs an augmented virtual reality. While receiving task-oriented therapies, patients are given visual feedback on their motor performance that is more selective and salient than in the real world (Deutsch et al., 2004), for example, on the exact positioning of their hand or on the velocity of their finger movements. In interactive robotic therapy, movements are performed within varying force fields that the patient must adapt to. This requires continual updating of the patient's internal representation of their movements, making this therapy more similar to conventional motor learning (Krakauer, 2006).

Interactive robotic therapy has proven useful in both the acute and chronic stroke phase, with improvements above and beyond those seen in conventional therapy (Fasoli et al., 2003; Lum et al., 2002; Volpe et al., 2000).

With each of these rehabilitation programs, it is important to assess the extent to which gains generalize to untrained tasks, and whether rehabilitation induced gains persist after treatment ceases.

1.3.3.3 Non-invasive Stimulation

Non-invasive stimulation, either peripheral or cortical, can be used in conjunction with motor training programs to produce more robust behavioural gains (Bolognini et al., 2009). Peripheral Sensory Stimulation (PSS) provides external somatosensory input during the execution of motor tasks, aiming to reinforce the sensorimotor feedback loop (Conforto et al., 2010). Single sessions of PSS result in transient improvements in pinch force for both acute (Klaiput & Kitisomprayoonkul, 2009) and chronic patients (Celnik et al., 2007). Another non-invasive form of peripheral stimulation, EMG Triggered Neuromuscular Stimulation, seeks to recruit spared motor areas during task performance. When muscle activity during motor performance reaches a predefined threshold as measured by EMG activity, an assistive electrical stimulus is given to facilitate completion of the movement (Krakauer, 2006). This system has been shown to improve motor performance in the subacute, acute, and chronic phases of stroke (Bolton, Cauraugh, & Hausenblas, 2004).

When used as an aide in stroke rehabilitation, a central goal of non-invasive cortical stimulation is to rectify overcompensation in the contralesional hemisphere that often accompanies spontaneous recovery. Specifically, repetitive transcranial

magnetic stimulation (rTMS) and transcranial direct current stimulation (tDCS) aim to restore the balance of inhibition between hemispheres. (The mechanisms of TMS and tDCS are discussed in detail in sections 2.1 and 2.2, respectively.) High frequency rTMS or anodal tDCS to the ipsilesional M1 are used to enhance excitability of the damaged cortex. Low frequency rTMS or cathodal tDCS applied to the contralesional M1 seek to suppress excitability of the unaffected cortex (Bolognini et al., 2009). rTMS protocols, when combined with motor training, have been shown effective in acute (Khedr et al., 2005) and chronic (Kim et al., 2006) stroke patients. Motor performance is also improved following either form of tDCS (Fregni et al., 2005; Hummel, 2005), including bilateral stimulation to simultaneously excite the lesioned hemisphere and suppress the unlesioned hemisphere (Lindenberg et al., 2010). The degree of such improvements following anodal tDCS to the ipsilesional M1 is correlated with increased task-related fMRI activity in the region (Stagg et al., 2012).

1.4 SUMMARY

This chapter has provided an overview of the human motor system, exploring its anatomy and physiology, as well its behavioural relevance in healthy adults and stroke patients. The overarching theme of this thesis is the way in which brain stimulation affects motor cortical physiology, and how this interaction can best be harnessed to improve motor recovery in stroke patients. Chapter 2 contains a summary of the stimulation methods used (tDCS and TMS), and Chapter 3 details the imaging techniques employed to capture the ensuing changes. The general aims of this thesis are to probe:

(a) how tDCS affects the functional connectivity of the brain as a whole,

(b) neurophysiological changes in intrinsic cortical networks within M1,

(c) the feasibility of tDCS as an adjunct in stroke rehabilitation.

Chapter 4 uses resting state imaging to examine wide-scale changes within functional networks of the brain, comparing the results produced by two different polarities of tDCS. Chapter 5 then focuses on the modulatory effects of tDCS within M1, investigating how the temporal relationship between stimulation and task performance affects subsequent behaviour and neurophysiology. The remaining two chapters explore how tDCS can be used to improve motor recovery in chronic stroke patients. In particular, Chapter 6 details the functional and structural changes that occur following a combined motor therapy and tDCS rehabilitation program. Chapter 7 presents baseline imaging measures that are predictive of response to said program.

REFERENCES

Akkal, D., Dum, R. P., & Strick, P. L. (2007). Supplementary motor area and presupplementary motor area: targets of basal ganglia and cerebellar output. *Journal of Neuroscience*, *27*(40), 10659–10673.

Barbas, H., & Pandya, D. N. (1987). Architecture and frontal cortical connections of the premotor cortex (area 6) in the rhesus monkey. *The Journal of comparative neurology*, *256*(2), 211–228.

Bestmann, S., Swayne, O., Blankenburg, F., Ruff, C. C., Haggard, P., Weiskopf, N., Josephs, O., et al. (2008). Dorsal premotor cortex exerts state-dependent causal influences on activity in contralateral primary motor and dorsal premotor cortex. *Cerebral cortex (New York, N.Y. : 1991)*, *18*(6), 1281–1291.

Bolognini, N., Pascual-Leone, A., & Fregni, F. (2009). Using non-invasive brain stimulation to augment motor training-induced plasticity. *Journal of NeuroEngineering and Rehabilitation*, *6*(1), 8.

Bolton, D. A. E., Cauraugh, J. H., & Hausenblas, H. A. (2004). Electromyogram-triggered neuromuscular stimulation and stroke motor recovery of arm/hand functions: a meta-analysis., *223*(2), 121–127.

Bornstein, R. A., & Brown, G. G. (1991). *Neurobehavioral aspects of cerebrovascular disease* (p. 367). Oxford University Press, USA.

Brinkman, C., & Porter, R. (1979). Supplementary motor area in the monkey: activity of neurons during performance of a learned motor task. *Journal of Neurophysiology*, *42*(3), 681–709.

Calautti, C., Leroy, F., Guincestre, J.-Y., & Baron, J.-C. (2003). Displacement of primary sensorimotor cortex activation after subcortical stroke: a longitudinal PET study with clinical correlation., *19*(4), 1650–1654.

Carota, A., Staub, F., & Bogousslavsky, J. (2002). Emotions, behaviours and mood changes in stroke. *Current opinion in neurology*, *15*(1), 57–69.

Celnik, P., Hummel, F., Harris-Love, M., Wolk, R., & Cohen, L. G. (2007). Somatosensory stimulation enhances the effects of training functional hand tasks in patients with chronic stroke., *88*(11), 1369–1376.

Cheyne, D., Kristeva, R., & Deecke, L. (1991). Homuncular organization of human motor cortex as indicated by neuromagnetic recordings. *Neuroscience letters*,

122(1), 17–20.

Chouinard, P. A., & Paus, T. (2006). The primary motor and premotor areas of the human cerebral cortex. *The Neuroscientist : a review journal bringing neurobiology, neurology and psychiatry*, *12*(2), 143–152.

Cirstea, M. C., & Levin, M. F. (2000). Compensatory strategies for reaching in stroke., *123 (Pt 5)*, 940–953.

Conforto, A. B., Ferreiro, K. N., Tomasi, C., Santos, dos, R. L., Moreira, V. L., Marie, S. K. N., Baltieri, S. C., et al. (2010). Effects of somatosensory stimulation on motor function after subacute stroke., *24*(3), 263–272.

Cramer, S. C. (2008a). Repairing the human brain after stroke: I. Mechanisms of spontaneous recovery. *Annals of Neurology*, *63*(3), 272–287.

Cramer, S. C. (2008b). Repairing the human brain after stroke. II. Restorative therapies. *Annals of Neurology*, *63*(5), 549–560.

Cramer, S. C., Shah, R., Juranek, J., Crafton, K. R., & Le, V. (2006). Activity in the peri-infarct rim in relation to recovery from stroke., *37*(1), 111–115.

Dafer, R. M., Rao, M., Shareef, A., & Sharma, A. (2008). Poststroke depression. *Topics in stroke rehabilitation*, *15*(1), 13–21

Dancause, N., & Nudo, R. J. (2011). Shaping plasticity to enhance recovery after injury., *192*, 273–295.

Davis, S., Fisher, M., & Warach, S. (Eds.). (2003). *Magnetic Resonance Imaging in Stroke* (1st ed. p. 280). Cambridge University Press.

Deiber, M. P., Wise, S. P., Honda, M., Catalan, M. J., Grafman, J., & Hallett, M. (1997). Frontal and parietal networks for conditional motor learning: a positron emission tomography study. *Journal of Neurophysiology*, *78*(2), 977–991.

Desrosiers, J., Malouin, F., Richards, C., Bourbonnais, D., Rochette, A., & Bravo, G. (2003). Comparison of changes in upper and lower extremity impairments and disabilities after stroke. *International journal of rehabilitation research. Internationale Zeitschrift für Rehabilitationsforschung. Revue internationale de recherches de réadaptation*, *26*(2), 109–116.

Deutsch, J. E., Merians, A. S., Adamovich, S., Poizner, H., & Burdea, G. C. (2004). Development and application of virtual reality technology to improve hand use and gait of individuals post-stroke., *22*(3-5), 371–386.

Di Carlo, A. (2008). Human and economic burden of stroke. *Age and Ageing*, *38*(1),

4–5.

Diedrichsen, J., White, O., Newman, D., & Lally, N. (2010). Use-dependent and error-based learning of motor behaviors. *Journal of Neuroscience*, *30*(15), 5159–5166.

Donoghue, J. P., Leibovic, S., & Sanes, J. N. (1992). Organization of the forelimb area in squirrel monkey motor cortex: representation of digit, wrist, and elbow muscles. *Experimental Brain Research*, *89*(1), 1–19.

Doyon, J., Bellec, P., Amsel, R., Penhune, V., Monchi, O., Carrier, J., Lehéricy, S., et al. (2009). Contributions of the basal ganglia and functionally related brain structures to motor learning. *Behavioural brain research*, *199*(1), 61–75.

Draganski, B., Gaser, C., Busch, V., Schuierer, G., Bogdahn, U., & May, A. (2004). Neuroplasticity: changes in grey matter induced by training. *Nature*, *427*(6972), 311–312.

Driemeyer, J., Boyke, J., Gaser, C., Büchel, C., & May, A. (2008). Changes in gray matter induced by learning--revisited. *PloS one*, *3*(7), e2669.

Dum, R. P., & Strick, P. L. (1991). The origin of corticospinal projections from the premotor areas in the frontal lobe. *The Journal of neuroscience : the official journal of the Society for Neuroscience*, *11*(3), 667–689.

Ehrsson, H. H., Fagergren, E., & Forssberg, H. (2001). Differential fronto-parietal activation depending on force used in a precision grip task: an fMRI study. *Journal of Neurophysiology*, *85*(6), 2613–2623.

Fasoli, S. E., Krebs, H. I., Stein, J., Frontera, W. R., & Hogan, N. (2003). Effects of robotic therapy on motor impairment and recovery in chronic stroke., *84*(4), 477–482.

Ferbert, A., Priori, A., Rothwell, J. C., Day, B. L., Colebatch, J. G., & Marsden, C. D. (1992). Interhemispheric inhibition of the human motor cortex. *The Journal of Physiology*, *453*, 525–546.

Feydy, A., Carlier, R., Roby-Brami, A., Bussel, B., Cazalis, F., Pierot, L., Burnod, Y., et al. (2002). Longitudinal study of motor recovery after stroke: recruitment and focusing of brain activation., *33*(6), 1610–1617.

Fletcher, P. C., Zafiris, O., Frith, C. D., Honey, R. A. E., Corlett, P. R., Zilles, K., & Fink, G. R. (2005). On the benefits of not trying: brain activity and connectivity reflecting the interactions of explicit and implicit sequence learning. *Cerebral cortex (New York, N.Y. : 1991)*, *15*(7), 1002–1015.

Forkstam, C., & Petersson, K. M. (2005). Towards an explicit account of implicit learning. *Current opinion in neurology*, *18*(4), 435–441.

Fregni, F., Boggio, P. S., Mansur, C. G., Wagner, T., Ferreira, M. J. L., Lima, M. C., Rigonatti, S. P., et al. (2005). Transcranial direct current stimulation of the unaffected hemisphere in stroke patients. *Neuroreport*, *16*(14), 1551–1555.

Fridman, E. A., Hanakawa, T., Chung, M., Hummel, F., Leiguarda, R. C., & Cohen, L. G. (2004). Reorganization of the human ipsilesional premotor cortex after stroke., *127*(Pt 4), 747–758.

Fried, I., Katz, A., McCarthy, G., Sass, K. J., Williamson, P., Spencer, S. S., & Spencer, D. D. (1991). Functional organization of human supplementary motor cortex studied by electrical stimulation. *The Journal of neuroscience : the official journal of the Society for Neuroscience*, *11*(11), 3656–3666.

Fulton, J. F., & Sheehan, D. (1935). The Uncrossed Lateral Pyramidal Tract in Higher Primates. *Journal of anatomy*, *69*(Pt 2), 181–187.

Furlan, M., Marchal, G., Viader, F., Derlon, J. M., & Baron, J. C. (1996). Spontaneous neurological recovery after stroke and the fate of the ischemic penumbra., *40*(2), 216–226. d

Gentner, R., Gorges, S., Weise, D., aufm Kampe, K., Buttmann, M., & Classen, J. (2010). Encoding of motor skill in the corticomuscular system of musicians. *Current biology : CB*, *20*(20), 1869–1874.

Ghika-Schmid, F., & Bogousslavsky, J. (2000). The acute behavioral syndrome of anterior thalamic infarction: a prospective study of 12 cases. *Annals of Neurology*, *48*(2), 220–227.

Goldstein, L. B. (Ed.). (2009). *A Primer on Stroke Prevention and Treatment: An overview based on AHA/ASA Guidelines* (1st ed. p. 280). Wiley-Blackwell.

Halsband, U., & Lange, R. K. (2006). Motor learning in man: a review of functional and clinical studies. *Journal of physiology, Paris*, *99*(4-6), 414–424.

Hendricks, H. T., van Limbeek, J., Geurts, A. C., & Zwarts, M. J. (2002). Motor recovery after stroke: a systematic review of the literature. *Archives of physical medicine and rehabilitation*, *83*(11), 1629–1637.

Hepp-Reymond, M. C., Hüsler, E. J., Maier, M. A., & Ql, H. X. (1994). Force-related neuronal activity in two regions of the primate ventral premotor cortex. *Canadian journal of physiology and pharmacology*, *72*(5), 571–579.

Hepp-Reymond, M., Kirkpatrick-Tanner, M., Gabernet, L., Qi, H. X., & Weber, B. (1999). Context-dependent force coding in motor and premotor cortical areas. *Experimental Brain Research*, *128*(1-2), 123–133.

Hoshi, E., & Tanji, J. (2007). Distinctions between dorsal and ventral premotor areas: anatomical connectivity and functional properties. *Current opinion in neurobiology*, *17*(2), 234–242.

Hosp, J. A., & Luft, A. R. (2011). Cortical plasticity during motor learning and recovery after ischemic stroke., *2011*, 871296.

Hubbard, I. J., Parsons, M. W., Neilson, C., & Carey, L. M. (2009). Task-specific training: evidence for and translation to clinical practice., *16*(3-4), 175–189.

Hummel, F. (2005). Effects of non-invasive cortical stimulation on skilled motor function in chronic stroke. *Brain*, *128*(3), 490–499.

Ivey, F. M., Hafer-Macko, C. E., & Macko, R. F. (2006). Exercise rehabilitation after stroke., *3*(4), 439–450.

Jaillard, A., Martin, C. D., Garambois, K., Lebas, J. F., & Hommel, M. (2005). Vicarious function within the human primary motor cortex? A longitudinal fMRI stroke study., *128*(Pt 5), 1122–1138.

Jenkins, I. H., Jahanshahi, M., Jueptner, M., Passingham, R. E., & Brooks, D. J. (2000). Self-initiated versus externally triggered movements. II. The effect of movement predictability on regional cerebral blood flow. *Brain*, *123 (Pt 6)*, 1216–1228.

Kalaria, R. N., & Ballard, C. (2001). Stroke and cognition. *Current Atherosclerosis Reports*, *3*(4), 334–339.

Karni, A., Meyer, G., Jezzard, P., Adams, M. M., Turner, R., & Ungerleider, L. G. (1995). Functional MRI evidence for adult motor cortex plasticity during motor skill learning. *Nature*, *377*(6545), 155–158.

Kauhanen, M., Korpelainen, J. T., Hiltunen, P., Brusin, E., Mononen, H., Määttä, R., Nieminen, P., et al. (1999). Poststroke depression correlates with cognitive impairment and neurological deficits. *Stroke*, *30*(9), 1875–1880.

Khedr, E. M., Ahmed, M. A., Fathy, N., & Rothwell, J. C. (2005). Therapeutic trial of repetitive transcranial magnetic stimulation after acute ischemic stroke., *65*(3), 466–468.

Kim, Y.-H., You, S. H., Ko, M.-H., Park, J.-W., Lee, K. H., Jang, S. H., Yoo, W.-K., et al. (2006). Repetitive transcranial magnetic stimulation-induced corticomotor

excitability and associated motor skill acquisition in chronic stroke., *37*(6), 1471–1476.

Klaiput, A., & Kitisomprayoonkul, W. (2009). Increased pinch strength in acute and subacute stroke patients after simultaneous median and ulnar sensory stimulation., *23*(4), 351–356.

Könönen, M., Tarkka, I. M., Niskanen, E., Pihlajamäki, M., Mervaala, E., Pitkänen, K., & Vanninen, R. (2012). Functional MRI and motor behavioral changes obtained with constraint-induced movement therapy in chronic stroke., *19*(4), 578–586.

Kötter, R., & Wanke, E. (2005). Mapping brains without coordinates. *Philosophical transactions of the Royal Society of London. Series B, Biological sciences*, *360*(1456), 751–766.

Krakauer, J. W. (2006). Motor learning: its relevance to stroke recovery and neurorehabilitation., *19*(1), 84–90.

Kurata, K., & Hoffman, D. S. (1994). Differential effects of muscimol microinjection into dorsal and ventral aspects of the premotor cortex of monkeys. *Journal of Neurophysiology*, *71*(3), 1151–1164.

Kwakkel, G., Wagenaar, R. C., Kollen, B. J., & Lankhorst, G. J. (1996). Predicting disability in stroke--a critical review of the literature. *Age and Ageing*, *25*(6), 479–489.

Lee, J.-H., & van Donkelaar, P. (2006). The human dorsal premotor cortex generates on-line error corrections during sensorimotor adaptation. *Journal of Neuroscience*, *26*(12), 3330–3334.

Leonard, C. T. (1997). *The Neuroscience Of Human Movement, 1e*. (M. Sasser, Ed.) (1st ed. p. 272). Mosby.

Leys, D., Hénon, H., Mackowiak-Cordoliani, M.-A., & Pasquier, F. (2005). Poststroke dementia. *Lancet neurology*, *4*(11), 752–759.

Lindenberg, R., Renga, V., Zhu, L. L., Nair, D., & Schlaug, G. (2010). Bihemispheric brain stimulation facilitates motor recovery in chronic stroke patients. *Neurology*, *75*(24), 2176–2184.

Loubinoux, I., Carel, C., Pariente, J., Dechaumont, S., Albucher, J.-F., Marque, P., Manelfe, C., et al. (2003). Correlation between cerebral reorganization and motor recovery after subcortical infarcts., *20*(4), 2166–2180.

Luft, A. R., & Buitrago, M. M. (2005). Stages of motor skill learning. *Molecular*

neurobiology, *32*(3), 205–216.

Lum, P. S., Burgar, C. G., Shor, P. C., Majmundar, M., & Van der Loos, M. (2002). Robot-assisted movement training compared with conventional therapy techniques for the rehabilitation of upper-limb motor function after stroke., *83*(7), 952–959.

Manganotti, P., Patuzzo, S., Cortese, F., Palermo, A., Smania, N., & Fiaschi, A. (2002). Motor disinhibition in affected and unaffected hemisphere in the early period of recovery after stroke., *Clinical Neurophysiology, 113*(6), 936–943.

Martin, J. (2003). *Neuroanatomy: Text and Atlas* (3rd ed. p. 532). McGraw-Hill Medical.

Mayka, M. A., Corcos, D. M., Leurgans, S. E., & Vaillancourt, D. E. (2006). Three-dimensional locations and boundaries of motor and premotor cortices as defined by functional brain imaging: a meta-analysis. *NeuroImage*, *31*(4), 1453–1474.

Milot, M.-H., & Cramer, S. C. (2008). Biomarkers of recovery after stroke., *21*(6), 654–659.

Mulder, T., Zijlstra, S., Zijlstra, W., & Hochstenbach, J. (2004). The role of motor imagery in learning a totally novel movement. *Experimental Brain Research*, *154*(2), 211–217.

Murase, N., Duque, J., Mazzocchio, R., & Cohen, L. G. (2004). Influence of interhemispheric interactions on motor function in chronic stroke. *Annals of Neurology*, *55*(3), 400–409.

Nachev, P., Kennard, C., & Husain, M. (2008). Functional role of the supplementary and pre-supplementary motor areas. *Nature Reviews Neuroscience*, *9*(11), 856–869.

Nolte, J. (2008). *The Human Brain: An Introduction to its Functional Anatomy* (6th ed. p. 736). Mosby.

Nudo, R. J., & Milliken, G. W. (1996). Reorganization of movement representations in primary motor cortex following focal ischemic infarcts in adult squirrel monkeys., *75*(5), 2144–2149.

Olvey, E. L., Armstrong, E. P., & Grizzle, A. J. (2010). Contemporary pharmacologic treatments for spasticity of the upper limb after stroke: a systematic review. *Clinical therapeutics*, *32*(14), 2282–2303.

Palmer, E., Ashby, P., & Hajek, V. E. (1992). Ipsilateral fast corticospinal pathways do not account for recovery in stroke., *32*(4), 519–525.

Penfield, W., & Boldrey, E. (1937). Somatic motor and sensory representation in the cerebral cortex of man as studied by electrical stimulation. *Brain*.

Penhune, V. B., & Steele, C. J. (2012). Parallel contributions of cerebellar, striatal and M1 mechanisms to motor sequence learning. *Behavioural brain research*, *226*(2), 579–591.

Petrides, M. (1997). Visuo-motor conditional associative learning after frontal and temporal lesions in the human brain. *Neuropsychologia*, *35*(7), 989–997.

Pineiro, R., Pendlebury, S., Johansen-Berg, H., & Matthews, P. M. (2001). Functional MRI detects posterior shifts in primary sensorimotor cortex activation after stroke: evidence of local adaptive reorganization?, *32*(5), 1134–1139.

Platz, T., Winter, T., Müller, N., Pinkowski, C., Eickhof, C., & Mauritz, K. H. (2001). Arm ability training for stroke and traumatic brain injury patients with mild arm paresis: a single-blind, randomized, controlled trial., *82*(7), 961–968.

Powers, W. J. (1991). Cerebral hemodynamics in ischemic cerebrovascular disease., *29*(3), 231–240.

Raghavan, P., Santello, M., Gordon, A. M., & Krakauer, J. W. (2010). Compensatory motor control after stroke: an alternative joint strategy for object-dependent shaping of hand posture., *103*(6), 3034–3043.

Rao, S. M., Binder, J. R., Hammeke, T. A., Bandettini, P. A., Bobholz, J. A., Frost, J. A., Myklebust, B. M., et al. (1995). Somatotopic mapping of the human primary motor cortex with functional magnetic resonance imaging. *Neurology*, *45*(5), 919–924.

Riley, J. D., Le, V., Der-Yeghiaian, L., See, J., Newton, J. M., Ward, N. S., & Cramer, S. C. (2011). Anatomy of Stroke Injury Predicts Gains From Therapy. *Stroke*, *42*(2), 421–426.

Rizzolatti, G., & Luppino, G. (2001). The cortical motor system. *Neuron*, *31*(6), 889–901.

Sanes, J. N., & Schieber, M. H. (2001). Orderly somatotopy in primary motor cortex: does it exist? *NeuroImage*, *13*(6 Pt 1), 968–974.

Saver, J. L., Johnston, K. C., Homer, D., Wityk, R., Koroshetz, W., Truskowski, L. L., & Haley, E. C. (1999). Infarct volume as a surrogate or auxiliary outcome measure

in ischemic stroke clinical trials. The RANTTAS Investigators., *30*(2), 293–298.

Schaechter, J. D., & Perdue, K. L. (2008). Enhanced cortical activation in the contralesional hemisphere of chronic stroke patients in response to motor skill challenge., *18*(3), 638–647.

Scholz, J., Klein, M. C., Behrens, T. E. J., & Johansen-Berg, H. (2009). Training induces changes in white-matter architecture. *Nature neuroscience*, *12*(11), 1370–1371.

Stagg, C. J., Bachtiar, V., O'Shea, J., Allman, C., Bosnell, R. A., Kischka, U., Matthews, P. M., et al. (2012). Cortical activation changes underlying stimulation-induced behavioural gains in chronic stroke., *135*(Pt 1), 276–284.

Stinear, C. (2010). Prediction of recovery of motor function after stroke. *Lancet neurology*, *9*(12), 1228–1232.

Strong, K., Mathers, C., & Bonita, R. (2007). Preventing stroke: saving lives around the world., *6*(2), 182–187.

Studenski, S. A., Wallace, D., Duncan, P. W., Rymer, M., & Lai, S. M. (2001). Predicting stroke recovery: three- and six-month rates of patient-centered functional outcomes based on the orpington prognostic scale. *Journal of the American Geriatrics Society*, *49*(3), 308–312.

Tanji, J., & Kurata, K. (1982). Comparison of movement-related activity in two cortical motor areas of primates. *Journal of Neurophysiology*, *48*(3), 633–653.

Tomassini, V., Jbabdi, S., Klein, J. C., Behrens, T. E. J., Pozzilli, C., Matthews, P. M., Rushworth, M. F. S., et al. (2007). Diffusion-weighted imaging tractography-based parcellation of the human lateral premotor cortex identifies dorsal and ventral subregions with anatomical and functional specializations. *Journal of Neuroscience*, *27*(38), 10259–10269.

Volpe, B. T., Krebs, H. I., Hogan, N., Edelstein OTR, L., Diels, C., & Aisen, M. (2000). A novel approach to stroke rehabilitation: robot-aided sensorimotor stimulation., *54*(10), 1938–1944.

Walker, M. P., Brakefield, T., Hobson, J. A., & Stickgold, R. (2003). Dissociable stages of human memory consolidation and reconsolidation. *Nature*, *425*(6958), 616–620.

Ward, N. S., & Cohen, L. G. (2004). Mechanisms underlying recovery of motor function after stroke., *61*(12), 1844–1848.

Ward, N. S., Brown, M. M., Thompson, A. J., & Frackowiak, R. S. J. (2003). Neural

correlates of motor recovery after stroke: a longitudinal fMRI study., *126*(Pt 11), 2476–2496.

Warlow, C. P., Dennis, M. S., van Gijn, J., Hankey, G. J., Sandercock, P. A. G., Bamford, J. M., & Wardlaw, J. M. (2001). *Stroke: A practical guide to management* (2nd ed. p. 804). Wiley-Blackwell.

Webster, B. R., Celnik, P. A., & Cohen, L. G. (2006). Noninvasive brain stimulation in stroke rehabilitation., *3*(4), 474–481.

Wise, S. P. (1996). Corticospinal efferents of the supplementary sensorimotor area in relation to the primary motor area. *Advances in neurology*, *70*, 57–69.

Wolpert, D. M., Diedrichsen, J., & Flanagan, J. R. (2011). Principles of sensorimotor learning. *Nature Reviews Neuroscience*, *12*(12), 739–751.

WOOLSEY, C. N., SETTLAGE, P. H., MEYER, D. R., SENCER, W., PINTO HAMUY, T., & TRAVIS, A. M. (1952). Patterns of localization in precentral and "supplementary" motor areas and their relation to the concept of a premotor area. *Research publications - Association for Research in Nervous and Mental Disease*, *30*, 238–264.

Zilles, K., Palomero-Gallagher, N., & Schleicher, A. (2004). Transmitter receptors and functional anatomy of the cerebral cortex. *Journal of anatomy*, *205*(6), 417–432.

Chapter 2: Methods for Stimulating the Motor System

Noninvasive stimulation is a powerful tool, able to both modify and measure motor cortical processes. Transcranial direct current stimulation (tDCS) is heavily used in each of the experiments in this thesis to modulate underlying neuronal activity. To measure these modifications in cortical excitability, an additional stimulation technique, transcranial magnetic stimulation (TMS), is employed. In the second experiment (Chapter 5), TMS is administered before and after twenty minutes of tDCS to quantify the resulting changes in neuromuscular output. Figure 2.1 illustrates the setup for TMS and tDCS administration. This chapter describes these two techniques, highlighting their synergistic use and providing an overview of their history, implementation, and mechanisms as relevant to this thesis.

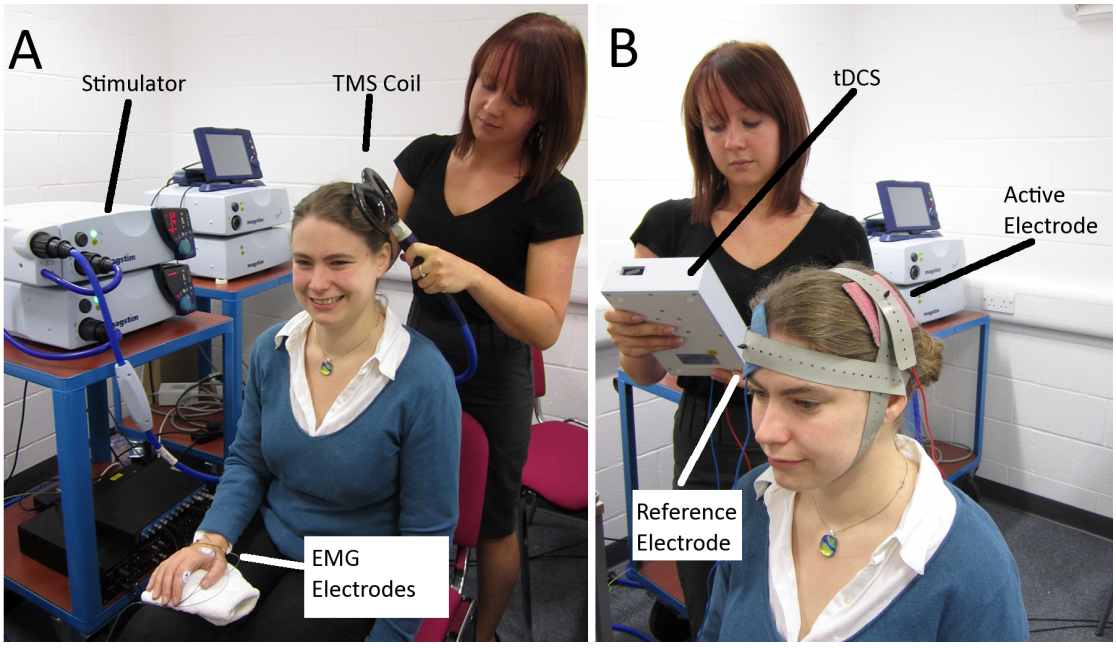

Figure 2.1: Setup for TMS and tDCS administration. A) The TMS coil stimulates the hand area of M1, while EMG electrodes affixed to the contralateral hand measure motor output. B) During tDCS, the active electrode is centered over M1, and the reference electrode is placed over the contralateral supraorbital ridge.

2.1 TRANSCRANIAL MAGNETIC STIMULATION

Transcranial magnetic stimulation (TMS) is a method by which neurophysiology, particularly that of the corticospinal tract, can be probed and monitored. Since its introduction over two decades ago, TMS has been used to investigate brain plasticity in a variety of domains. More recently, it has been explored as a diagnostic tool.

2.1.1 PRINCIPLES OF TMS

In 1980, Merton and Morton proposed a technique that used a brief, intense electric shock to stimulate the neurons within the motor cortex (Merton & Morton, 1980). One significant drawback of this method, transcranial electric stimulation (TES), was that it also activated pain fibers of the scalp, and thus was a painful process. Five years later, Barker introduced an alternative to TES, transcranial magnetic stimulation (Barker et al., 1985). Like TES, TMS is also able to activate neurons within the motor cortex and peripheral nerves through the scalp, but can do so with little or no pain.

TMS is based on Faraday's law of electromagnetic induction, which states that a moving electric current will induce a magnetic field. In TMS experiments, a coil of wire is placed parallel the scalp over the area of interest. A brief, high-current pulse of electricity is created within the wire. This produces a magnetic field of up to 2 Tesla perpendicular to the coil. The field itself is transient and lasts for only about 100 μs (Hallett, 2007). This magnetic field induces a secondary electric field, which is parallel to the scalp. Current flows in loops antiparallel to the coil and brain surface (Hallett, 2000) (Figure 2.2).

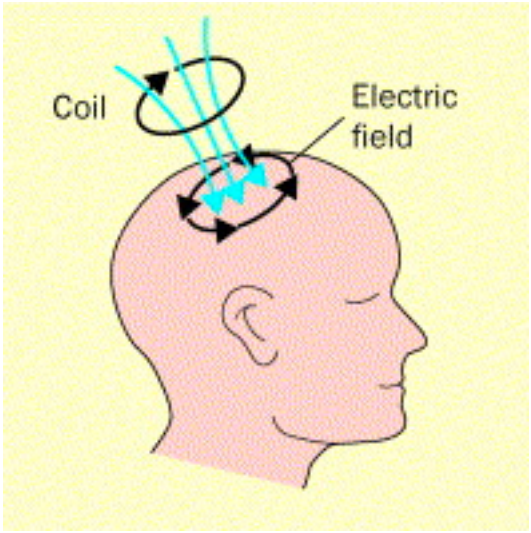

Figure 2.2: Current flow in the TMS coil and the induced electric field in the brain. A high pulse of current in the TMS coil produces a transient magnetic field (blue). The magnetic field induces an electric field antiparallel to the brain surface. Figure from Kobayashi (2003).

The intensity of the current in the coil can be modulated, thus systematically increasing or decreasing the induced magnetic field and secondary electric field. Critically, the frequency and pattern of the pulses can be modified, which dramatically alters the physiological effects that TMS produces (Kobayashi & Pascual-Leone, 2003). (See Section 2.1.2) Currently, the uses for TMS are many and varied. It can assist in clinical diagnosis and detecting pathophysiologies, measure brain plasticity in various sensory and cognitive modalities, create virtual lesions, or aide in therapeutic treatments (Rossini & Rossi, 2007).

2.1.2 Methodological Overview

Different protocols can be used to either measure or modify cortical activity. Paradigms that measure activity do so by eliciting neuroelectrical signals from the spinal cord and peripheral muscles. This activity is termed a motor evoked potential (MEP), and reflects the integrity of the corticospinal system (Rossini & Rossi, 2007).

Single TMS pulses are used to generate such MEPs. The amplitude of these MEPs can be modulated by the presence of an additional, subthreshold pulse given milliseconds prior to the main pulse. MEPs elicited by single and paired pulse TMS procedures are thought to depend on distinct underlying processes. In general, however, creation of an MEP involves three sequential steps: synapses onto corticospinal neurons, synapses onto motor neurons in the spinal cord, and finally neuromuscular synapses whose potentials are recorded as the MEPs by EMG electrodes (Huerta & Volpe, 2009).

TMS protocols that modify cortical activity differ in the number and frequency of pulses, and in the overall duration of pulse trains. For example, theta burst TMS and repetitive TMS, which deliver trains of pulses at different frequencies, can be used to increase or decrease cortical activity. When employed to dampen activity, they are often referred to as "virtual lesion" techniques, as they can transiently disrupt processing in targeted brain areas by increasing noise in the surrounding brain tissue. The experiments in this thesis employ single and paired pulse, but not repetitive, TMS. The remainder of this section focuses on such single and paired pulse measures, as summarized in Table 2.1.

TMS Measure	Pulse Type	Neurons Stimulated	Application
Motor Threshold (MT)	Single	Pyramidal neurons of the corticospinal tract (CST)	Intensity required to elicit an MEP of a desired size.
Input/Output Curve (I/O Curve)	Single	CST neurons; intracortical neurons beyond the hotspot	Slope reflects the ease with which neurons are excited.
Short Intracortical Inhibition (SICI)	Paired	$GABA_A$ergic interneurons	Measures suppression of cortical excitability
Intracortical Facilitation (ICF)	Paired	Glutamatergic interneurons; some GABAergic influence	Measures enhancement of cortical excitability

Table 2.1: Summary of Selected TMS Measures.

2.1.2.1 Single Pulse Measures

MOTOR THRESHOLDS. The excitability of the motor cortex can be assessed by calculating a 'motor threshold'. Motor thresholds (MT) are of two kinds: resting and active. The resting motor threshold (rMT) is the intensity of the TMS machine required to evoke an MEP of 50μV in 5 out of 10 trials during muscle relaxation. Similarly, the rMT_{1mV} can be defined as the intensity required to evoke an MEP of 1mV during muscle relaxation. The active motor threshold (aMT) is determined during a slight, voluntary muscle contraction of approximately 20% of maximal contraction, and is the lowest intensity required to obtain an MEP in 5 out of 10 trials. Both rMT and aMT reflect the excitability of a confined, spatially localized group of neurons. While rMT primarily reflects the activity of slow propagating pyramidal neurons, aMT may reflect fast-propagating neurons as well (Rossini & Rossi, 2007). MTs determined at the beginning of an experiment can be re-tested after an intervention to assess changes in excitability due to the intervention.

INPUT/OUTPUT CURVES. Input output curves (I/O) relate the intensity of the administered TMS pulse (the "input") to the magnitude of the elicited MEP (the "output"). As stimulation intensities are increased, the magnitude of the MEP tends to increase as well. This is due in part to the recruitment of a larger number of neurons than those recruited from the hotspot at the rMT, and also because less excitable neurons may also be recruited at these higher intensities (Hallett, 2007). The slope of the I/O curve is a measure of how easily surrounding neurons are recruited and excited, with steeper slopes reflecting greater excitability.

2.1.2.2 Paired Pulse Measures

SHORT INTRACORTICAL INHIBITION. Short intracortical inhibition (SICI) occurs when a conditioning sub-threshold pulse is delivered prior to a test pulse at or above the MT. This typically results in a diminution of the resulting MEP amplitude. The conditioning pulse is given with an interstimulus interval (ISI) of 1 to 5 ms with respect to the test pulse (Rossini & Rossi, 2007). At an ISI of 2.5 ms, this process reflects the activity of $GABA_A$ergic interneurons. The mechanisms mediating SICI at shorter ISIs are not well understood. While SICI at 1 ms ISI is not $GABA_A$ dependant, it may rely on extrasynaptic GABAergic activity (Stagg et al., 2011a) or on other synaptic processes (Reis et al., 2008). In the motor domain, reductions in SICI may mean that cortical representations of the intended muscle have been made less prone to inhibition, thus becoming more excitable and able to perform the desired task (Chen, 2004).

INTRACORTICAL FACILITATION. Related to SICI, intracortical facilitation (ICF) occurs when a subthreshold conditioning pulse increases the MEP that results from the test pulse. Here, the ISI is longer, on the order of 6 to 20 ms (Rossini & Rossi,

2007). ICF primarily reflects glutamatergic interneurons, though GABAergic effects are present as well (Stagg & Nitsche, 2011).

2.1.3 TECHNICAL CONSIDERATIONS

2.1.3.1 MEP Composition

When stimulating the motor cortex and obtaining EMG recordings from the muscles of the hand, MEPs are observed 20-30 ms after application of the TMS pulse. Deviations from this interval are indicative of motor dysfunction (Rossini & Rossi, 1998). Though often thought of as a single entity, MEPs actually consist of multiple components: direct waves (D-waves) and indirect waves (I-waves). D-waves result from direct depolarization of the corticospinal axon, and are elicited by high intensity pulses, such as those generated by TES (Reis et al., 2008). Most TMS measures influence I-waves which can be produced by lower intensities. There are multiple types of I-waves, which occur serially at 1.5ms intervals after the initial D-wave. Longer latencies are indicative of increasing distances from the initial corticospinal axon. That is, I_1-waves synapse directly onto the axon, whereas I_2 and later waves are evoked via multiple synapses (Reis et al., 2008). Motor thresholds probably primarily reflect I_1 waves, whereas SICI and I/O curves reflect the influence of I_2 and later waves (Hallett, 2007; Reis et al., 2008).

2.1.3.2 Coil Designs and Spatial Distribution

TMS coils vary in design, and the preferred shape for an experiment is largely dependent on how specific an area one wishes to target, and how deep that location is. The first coil developed was a simple circular coil. It produces a fairly widespread electric field, and is ideal for bihemispheric stimulation (Kobayashi &

Pascual-Leone, 2003). Presently, the most commonly used coil is the figure of 8 design. It consists of two intersecting circular coils, and provides more focal stimulation that occurs where the two circles intersect (Figure 2.3). This coil is ideal if attempting to stimulate a fairly localized area directly underneath the intersection of the two coils (Cohen et al., 1990).

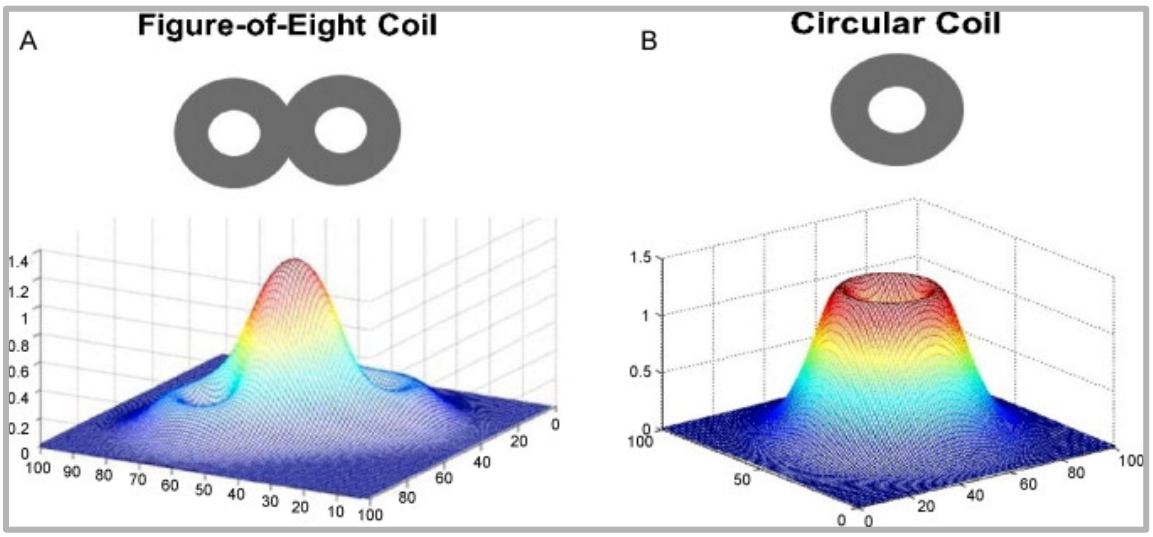

Figure 2.3: Magnetic field generated by two TMS coil designs. A) In a figure of 8 coil, the peak field is located at the intersection of the two coils. B) In a circular coil, the maximum field strength is located along the coil's perimeter. Figure from Giordano (2011).

A modification of the figure of 8 coil, the double-cone coil, has two intersecting coils that meet at an angle, further increasing its output's intensity and focality. Specialized coils have also been developed for stimulating deeper areas within the brain. One such coil is the Hesed coil, or H-coil. This allows for a penetrating current at much lower intensities than a standard figure of 8 coil, reducing participant discomfort (Zangen et al., 2005).

Regardless of the type of coil used, it must be properly oriented on the scalp to ensure optimal neuronal recruitment. In the motor cortex, there are networks of corticospinal axons that run in the horizontal plane at right angles to the precentral

gyrus. Consequently, to optimally stimulate the motor cortex, the induced TMS currents should also occur at a right angle to the precentral gyrus (Terao & Ugawa, 2002). To achieve such an orientation of the currents, the coil should be positioned approximately 50 degrees from the parasagittal plane, with the handle pointing backward (Mills et al., 1992). This positioning preferentially evokes I-waves, rather than D-waves.

2.1.3.3 Safety

Common side effects of TMS are tingling at the stimulation site and transient, mild headaches (Anand & Hotson, 2002). The most serious safety concern when administering TMS is the possibility of triggering a seizure. Though more prevalent with repetitive TMS, single and paired-pulse TMS have been shown to provoke seizures in subjects with epilepsy or other neurological conditions (Schrader et al., 2004). In healthy participants, a study by Chokroverty in 1995 reported no adverse effects following single pulses of TMS, including changes in blood pressure, heart rate, EEG measures, serum prolactin and cortisol levels, and various psychometric tests (Chokroverty et al., 1995).

In 2008, The Safety of TMS Consensus Group convened a session to update safety guidelines regarding the administration of TMS in research and clinical settings. Based on their findings, they determined that over 1800 single pulses could be administered at rMT without adverse effects (Rossi et al., 2009). The Consensus Group also established that, when recruiting participants, the only absolute exclusion criteria is "the presence of metallic hardware in close contact" to the TMS coil (Rossi et al., 2009). Other conditions, such as pregnancy, a history of epilepsy, or the presence of a pacemaker are not absolute contraindications, but are

generally used to screen individuals prior to inclusion in a study. Even when adhering to these guidelines, there has been a report of a seizure in a healthy individual during the establishment of motor thresholds (Kratz et al., 2011). Thus, it is important to continually monitor subjects taking part in TMS studies.

2.2 TRANSCRANIAL DIRECT CURRENT STIMULATION

In its earliest forms, the application of electric currents to the scalp can be traced back almost two millennia. Since then, transcranial direct current stimulation (tDCS) has gained widespread use in studies investigating a variety of neural and behavioural processes in both healthy and clinical populations. What follows is a general perspective on tDCS, providing an overview of its current usage and the physical principles behind its modulatory effects.

2.2.1 HISTORY

In the first century AD, Scrobinus Largus reported that applying a torpedo fish to the scalp of patients afflicted with headache caused transient relief of their pain (Utz et al., 2010). This and other such anecdotal findings spawned closer examination of these so-called "electric fish" by Walsh in 1773, and eventually led to a more scientifically rigorous investigation into the principles behind their electric properties (Kellaway, 1946). Volta and Galvani found that the behavioural effects elicited by applying such electric currents could be modulated by varying the intensity and duration of the stimulation. Armed with this cursory knowledge of direct currents—also referred to as galvanic currents, after the Italian scientist-clinicians began using transcranial electric stimulation to treat patients suffering from melancholia (Parent, 2004). The use of DC currents to treat psychiatric

disorders continued throughout the 1800s, but began to wane at the turn of the century due in part to inconsistent results (Lolas, 1977). In the 1930s, electroconvulsive therapy (ECT) became the gold standard to treat severe cases of depression, and low-intensity DC currents were all but discarded. Decades later, the introduction of effective drugs eclipsed both DC currents and ECT alike (Priori, 2003).

Though the scientific community's interest in DC currents has experienced peaks and troughs over the years, transcranial electric stimulation is currently experiencing a renaissance. Both basic scientists and clinicians have adapted tDCS for use in their studies. Today, it is used as an investigative tool to modulate motor performance (Nitsche et al., 2003b), assess the involvement of cortical areas in visual processing (Antal et al., 2003), and probe cognitive processes such as emotion (Ferrucci et al., 2011). It is also being wielded as a clinical device to boost recovery from stroke (Hummel, 2005), provide relief from chronic pain (Valle et al., 2009), and reduce the behavioural symptoms of neurodegenerative conditions like Alzheimer's disease (Boggio et al., 2009b). True to its beginnings, tDCS continues to be explored as a potential tool to treat depression (Merton & Morton, 1980; Palm et al., 2011). As the relevance of tDCS continues to grow, an emerging field of research studies the mechanisms of tDCS itself (Barker et al., 1985; Miranda et al., 2006). Although the applications of tDCS are quite broad, and its methodology tailored for each purpose, in principle tDCS is used to perform two basic functions: to enhance or diminish cortical excitability.

2.2.2 METHODOLOGICAL OVERVIEW

2.2.2.1 Administration

As its name suggests, tDCS is a technique used to deliver direct currents to the brain across the scalp. These direct currents are electric charges that flow in a constant direction and, for experimental purposes, are relatively small (1-2mA). The components of a tDCS setup are few: a battery operated DC device that generates the steady direct current, and electrodes used to deliver the current to the scalp. Current stimulators can be programmed to administer a current of a predefined amplitude for a specified amount of time. There is generally a fade-in and fade-out period at the beginning and end of the stimulation, during which time the current gradually increases to the desired intensity, and then gradually decreases to zero. Typically, two electrodes of opposite polarities are connected to the DC stimulator. The positive electrode is the anode; the negative electrode is the cathode. The electrodes are inserted into saline-soaked sponge sheaths, and attached to the scalp with non-conductive material, typically rubber straps. When the DC stimulator is turned on, a circuit is formed and the resultant current flows from the anode to the cathode, passing through the cranium to the underlying brain tissue, where it then exerts its excitability modulating effects.

2.2.2.2 Electrode Placement and Size

The electrode that is placed over the area of interest is termed the stimulating or active electrode, while the second electrode is deemed the reference electrode. When the anode is the stimulating electrode, tDCS is said to be delivering anodal stimulation, and current flows away from the area of interest. Conversely, when the cathode is the stimulating electrode, cathodal stimulation is occurring,

and current flows towards the area of interest. The ideal location for the stimulating electrode can be found using anatomical landmarks (Hallett, 2007; Stagg & Nitsche, 2011), functional localization via TMS (Hallett, 2000; Nitsche & Paulus, 2000), or neuroimaging (Baker et al., 2010; Kobayashi & Pascual-Leone, 2003). The reference electrode is generally placed over an area that is thought to be functionally decoupled from the process under investigation. In studies concerning the effects of tDCS to the visual cortex, for example, this may be the vertex (Antal et al., 2006; Rossini & Rossi, 2007). In many motor studies, this is the contralateral supraorbital ridge (Nitsche et al., 2008; Rossini & Rossi, 2007). In choosing a location for the reference electrode, it is important to bear in mind that, under typical conditions, this electrode is not functionally inert. That is, the reference electrode administers stimulation of the opposite polarity as the active electrode. This may confound the ability to accurately interpret results.

To circumvent this problem, some studies place reference electrodes further away from brain areas, for example on the mastoids (Huerta & Volpe, 2009; Marshall et al., 2004),chin (Priori et al., 1998; Rossini & Rossi, 2007), base of the neck (Accornero et al., 2007; Hallett, 2007), or completely extracephalically, like the deltoids (Monti et al., 2008; Rossini & Rossi, 2007). Such montages have the advantage over traditional electrode montages of not providing stimulation to other brain regions, but may produce qualitatively different excitability effects. Although it is typical to use two electrodes of opposing polarities, one each of an anode and a cathode, triplets of electrodes have been used as well when it proves beneficial for the study design. In order to deliver simultaneous stimulation to both motor cortices, two anodes have been used in conjunction with one reference cathode (DaSilva et al., 2011; Reis et al., 2008). One anode paired with two cathodes were

used in a potential treatment for Parkinson's disease (Chen, 2004; Miranda et al., 2006). By simultaneously employing two DC stimulators, multiple studies have used two pairs of anodes and cathodes (Ferrucci et al., 2008; Rossini & Rossi, 2007), (Priori et al., 2008; Stagg & Nitsche, 2011).

An ongoing field of work examines the ways in which the size of the electrodes modulates their current application. At the most basic level, the size of electrode determines the area that it covers. Standard electrodes range from 25-35cm^2. For studies targeting relatively small locations like the hand area, this is often several times larger than the intended area (Rossini & Rossi, 1998; Yousry et al., 1997). To solve this problem, smaller active electrodes may be used. A much larger reference electrode, on the order of 100cm^2, may be preferable when any possibility of the reference electrode exerting stimulating effects needs to be discounted (Boggio et al., 2009a; Reis et al., 2008), (Elmer at al., 2009; Reis et al., 2008). The potential stimulating effects of a reference electrode of this size are negligible (Kobayashi & Pascual-Leone, 2003; Nitsche et al., 2007). More than just determining the extent of the area being stimulated, the size of the electrodes influences the current delivered itself, by affecting current density. The smaller the surface area of the electrodes, the greater the delivered current density (Cohen et al., 1990; Nitsche et al., 2008). It should be noted, however, that smaller electrodes carry a greater risk of painful stimulation. (See Section 2.2.2.4 for a discussion of safety issues related to tDCS.)

2.2.2.3 Stimulation Types

There are three types of tDCS: anodal, cathodal, and sham. As stated above, anodal stimulation occurs when the positive anode is placed over the area of

interest, and cathodal stimulation is when the cathode is placed over the area of interest. In general, anodal stimulation tends to increase cortical excitability, whereas cathodal stimulation decreases it, as measured by recorded MEPs (Nitsche & Paulus, 2000; Zangen et al., 2005). This distinction tends to be most clear in the motor domain: the ability of cathodal stimulation to inhibit cortical activity is not consistently seen in the cognitive realm, particularly in language (Jacobson et al, 2011; Terao & Ugawa, 2002). In addition to these opposing effects on the neuronal populations, the behavioural changes induced by anodal and cathodal stimulation are often opposing as well. In studies concerning motor learning, anodal tDCS to the contralateral hemisphere improves performance, while cathodal tDCS has no effect, or may even worsen performance (Nitsche et al., 2003b; Stagg et al., 2011b). Similarly, anodal stimulation to the left dorsolateral prefrontal cortex increases verbal memory, while cathodal stimulation worsens it (Javadi et al., 2011; Mills et al., 1992). Though anodal and cathodal stimulation often yield opposing behavioural effects when administered in the same manner to the same location, both types of stimulation can be used to produce beneficial results. Anodal stimulation to the lesioned hemisphere (Anand & Hotson, 2002; Hummel, 2005) or cathodal stimulation to the intact hemisphere (Fregni et al., 2005; Schrader et al., 2004) can both improve the effect of physiotherapy after stroke.

The third type of tDCS administration is the sham or placebo condition, often used as a study's control. During sham stimulation, the current is ramped up in an identical manner as it would be for anodal or cathodal stimulation. However, rather than the constant current persisting for several minutes after this initial period, the DC stimulator is switched off. Because the sensory side effects that would alert a participant as to whether he or she was receiving real or sham tDCS predominantly

occur during this ramp-up period, sham tDCS is virtually indistinguishable from real tDCS (Chokroverty et al., 1995; Gandiga, Hummel, & Cohen, 2006). Though the rates of sensations such as tingling and itching are statistically higher in sessions where participants are receiving active versus sham stimulation, only 17% of subjects report feeling a difference between the three types of tDCS (Kessler et al., 2011; Rossi et al., 2009), (Poreisz et al., 2007; Rossi et al., 2009). Thus, while sham tDCS is not a perfect control condition, it is unlikely that study participants would consciously and actively know whether they were receiving real or sham stimulation to a degree that would impact their performance.

2.2.2.4 Safety

Transcranial direct current stimulation is generally well tolerated, with the most commonly experienced side effect being an itching under the electrode, particularly at its edges (Kratz et al., 2011; Poreisz et al., 2007). Covering the electrodes with saline-soaked pads helps reduce the intensity of this sensation, and also prevents the possibility of toxic compounds forming at the electrode-scalp interface (Nitsche et al., 2003a; Utz et al., 2010). Care should be taken to use saline solutions of concentrations between 15 and 140mM, as subjects found that this range produced the least discomfort (Dundas et al., 2007; Kellaway, 1946). Moreover, lower salinity is ideal for minimizing the accumulation of current around the electrode's edges (Minhas et al., 2011; Parent, 2004). However, ridding electrodes of their edges altogether by employing circular electrodes does not change participants' perceptions of skin itching (Ambrus et al., 2011; Lolas, 1977). The most probable cause of this itching sensation is the excitation of peripheral nerves (Minhas et al., 2011; Priori, 2003).

Other reported side effects of tDCS are generally innocuous: moderate fatigue, slight pain, and dizziness are commonly felt during or immediately following a stimulation session (Nitsche et al., 2003b; Poreisz et al., 2007). Nevertheless, serious adverse effects have also been reported. Administering repeated sessions of tDCS over the same areas has been shown to cause skin lesions (Antal et al., 2003; Palm et al., 2008), though in rare instances, a single session has been sufficient to cause a burn. Lagopoulous and Degabriele reported a case in which a single session of 1mA tDCS for twenty minutes resulted in first degree skin burns at the stimulation site (Ferrucci et al., 2011; Lagopoulos & Degabriele, 2008). They posited that this was because, prior to stimulation, the skin had been vigorously cleansed with an alcohol wipe, leading to uneven abrasion of the skin. Subsequent experiments without this step did not result in burns, even when participants received multiple, consecutive tDCS sessions over the same site (Hummel, 2005; Loo et al., 2011).

Though unique ways in which tDCS may elicit adverse effects are still being discovered on a case by case basis, there are guidelines in place that, in general, provide for the safe administration of tDCS. An early study by Agney and McCreery reported that the likelihood of tissue damage is determined by charge density per phase and current density. Such values depend on current intensity and duration, and electrode size (Agnew & McCreery, 1987; Valle et al., 2009). Based in part on a study in cats showing that direct stimulation of the cortex begins to cause tissue damage in the range of 40-400 $\mu C/cm^2$ (Boggio et al., 2009b; Yuen et al., 1981), they proposed a maximum charge density of 40 $\mu C/cm^2$. Because this value was extrapolated from direct cortical stimulation, it is unclear how appropriate it is for transcranial studies. In determining safety limits for tDCS, McCreery suggests that

the most appropriate value to consider is overall current density (Nitsche et al., 2003b). At current densities under 25 mA/cm^2, no damage to brain tissue occurs (McCreery et al., 1990). Presently, standard procedures fall well below this limit. For most experimental purposes, currents are held below 2mA and administered for less than 20 minutes, with average electrode sizes of 25-35 cm^2. At most, such parameters produce a current density of 0.08 mA/cm^2 (Nitsche et al., 2003a).

Administration of such protocols has been shown to be safe, as long as subjects pass a set of exclusion criteria. Participants should be free from metal implants near the location to be stimulated, and have no personal or family history of epilepsy (Nitsche et al., 2008). Within these guidelines, tDCS can be applied to healthy and patient populations alike. Compared to healthy volunteers, patients tolerate stimulation equally well, though they do report a higher incidence of headaches, and a lower prevalence of tingling around the electrode (Poreisz et al., 2007). A range of assessments has been used to demonstrate that tDCS does not impart negative physiological or psychological effects. After a session of tDCS, there was no increase in serum concentrations of neuron-specific enolase, a marker of neuronal damage (Nitsche & Paulus, 2001), nor did MRI scans show any signs of oedema (Nitsche et al., 2004d). Moreover, EEG recordings taken after tDCS contained no abnormalities, and psychometric behavioural testing found no impairment of cognitive function (Iyer et al., 2005).

2.2.3 Temporal and Spatial Characteristics

2.2.3.1 Temporal Resolution and Duration

Neuronal changes due to tDCS occur both during its application, and after stimulation has ceased. In the motor system, the online effects of tDCS begin a few

seconds after stimulation onset, and continue until stimulation is terminated (Priori et al., 1998). To produce aftereffects after five minutes of tDCS, the stimulation intensity must be at least 0.6 mA. Relatedly, at the standard intensity of 1 mA, aftereffects are induced after three minutes of stimulation (Nitsche & Paulus, 2000). The duration of this aftereffect period is highly dependent on the length and intensity of the stimulation (Figure 2.4). In general, longer stimulation periods and higher intensities produce more persistent aftereffects: anodal tDCS applied for 13 minutes results in aftereffects of over an hour (Nitsche & Paulus, 2001).

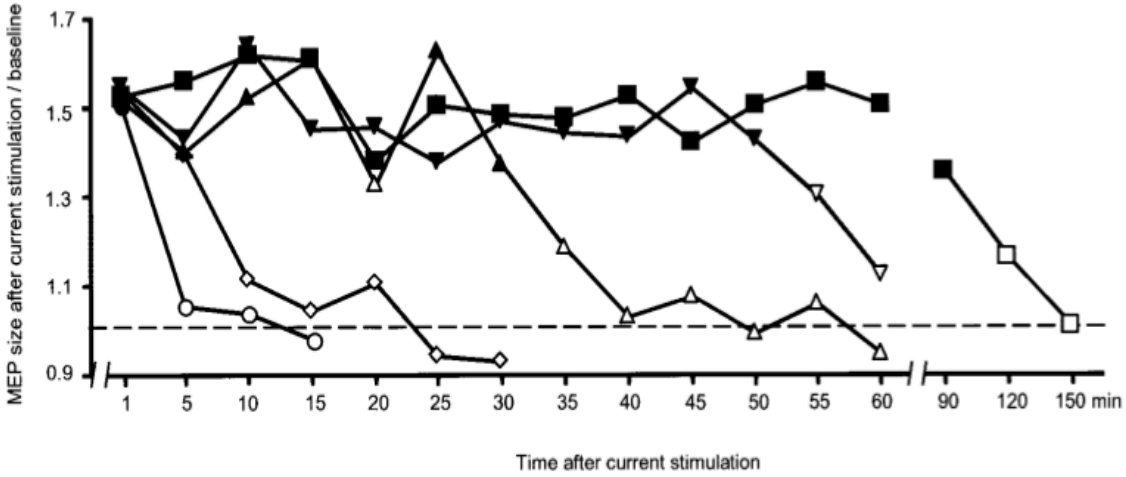

Figure 2.4: Aftereffects of varying durations of anodal tDCS on motor cortical excitability. Duration of anodal tDCS: circles (5 minutes), diamonds (7 minutes), upward-pointing triangles (9 minutes), downward-pointing triangles (11 minutes), squares (13 minutes). Figure from Nitsche (2001).

If longer aftereffects are desired, it is preferable to lengthen the duration of tDCS application, rather than increase its intensity, as the possibility of painful adverse reactions increases at higher intensities (Bikson et al., 2009). However, stimulation periods longer than 20 minutes are not generally used, as their safety has not been well investigated. Thus, it is unclear if longer sessions of tDCS could produce even more stable aftereffects, or if there is a ceiling effect. Rather, if tDCS effects are to be investigated in a long term way, multiple short sessions are given

daily, resulting in a cumulative effect (Reis et al., 2009). The induction of aftereffects may also be dependent on the area to which stimulation is applied. For example, stimulation to the visual system appears to produce aftereffects shorter than those elicited from the motor cortex (Antal et al., 2004), though they are still dependent on the length of stimulation given (Accornero et al., 2007).

That a comparatively short stimulation period can be manipulated to produce stable, long-lasting aftereffects allows researchers more freedom in the type of behaviours they can investigate. Yet it may be more difficult to perform studies that need rapid, fine temporal resolution. Since applying tDCS for even a few minutes results in aftereffects, if one wishes to reliably prevent the influence of tDCS on measures taken following stimulation, there must be a temporal gap between stimulation termination and task performance. Even if the stimulation duration is not long enough to produce recordable aftereffects, a waiting period of ten seconds is still recommended (Nitsche & Paulus, 2000). For ten minutes of stimulation, a waiting period of an hour is suggested; for tDCS durations that result in long lasting aftereffects of over an hour, most studies wait two days to a week as a precaution.

2.2.3.2 Spatial Focality

As previously mentioned, electrode size affects the current density delivered by tDCS. This can be used to increase the focality of tDCS application in one of two ways. First, increasing the size of the reference electrode reduces the possibility of the reference electrode stimulating unintended areas. This is due to the current density under the reference electrode being substantially decreased. Alternatively, the size of the active electrode may be altered. If the current density is held constant,

the size of the active electrode can be decreased. This focuses the stimulation on a smaller area while still delivering the same amount of stimulation. Reducing the active electrode to a tenth of its size yields comparable results when compared to standard-sized electrodes, albeit focused on a smaller location. Increasing the size of the reference electrode by a factor of three rendered it functionally inactive (Nitsche et al., 2007). In practice, reducing the size of the active electrode may result in lower stimulation than intended to deeper brain regions due to skull shunting and edge effects (Miranda et al., 2009). However, some studies have successfully increased the size of the reference electrode to 100 cm^2 to administer essentially unipolar stimulation (Knoch et al., 2008), (Boggio et al., 2009c).

Although the tDCS current is initially applied to an area the size of the stimulating electrode, it does not remain confined to that specific area. Computer simulations have been used to model this current flow, and have increased in sophistication with time. Early studies modelled the head as three concentric spheres representing the scalp, skull, and brain; the electrodes were represented by points (Rush & Driscoll, 1968; Ferdjallah et al., 1996). More recent studies have taken electrode size and shape into consideration, and used MRI guided finite head models that assign different electrical properties based on tissue characteristics. These differentiate between grey and white matter, CSF, and even tissue anisotropy (Oostendorp, 2008; Suh, et al., 2009). Studies employing such realistic head models have demonstrated that the highest current density is located around the perimeter of the electrode, and that half of the current may be shunted through the scalp (Miranda et al., 2006) (Figure 2.5).

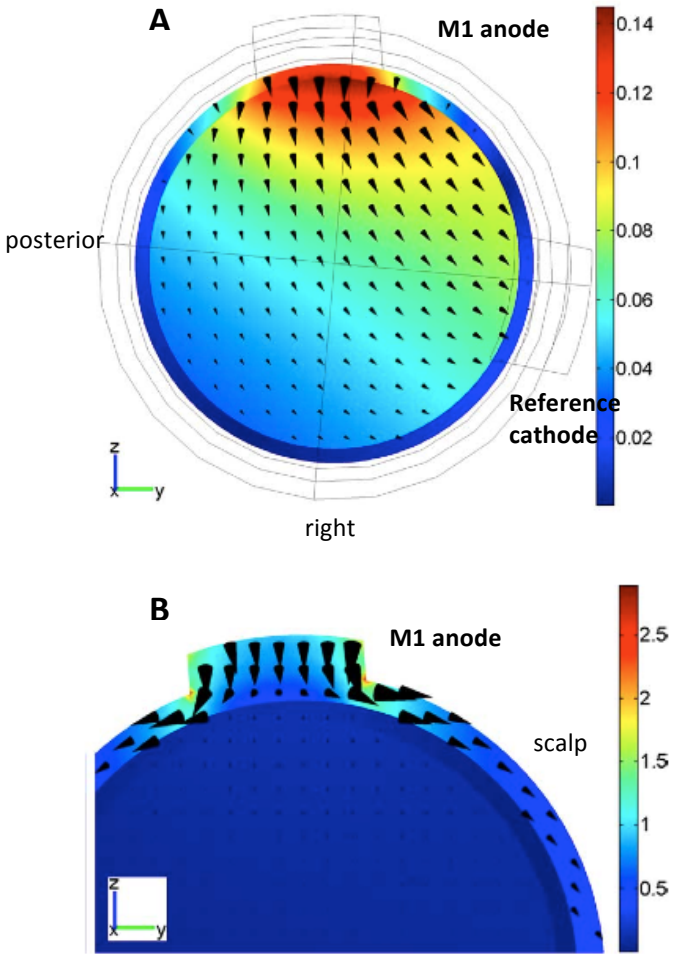

Figure 2.5: Current density of 2mA anodal tDCS applied via anode over M1 and cathode over contralateral supraorbital ridge. Magnitude is indicated by colour and direction by arrows. A) Current distribution across the scalp. Note that the arrows have a significant latero-mesial component (out of the paper). B) Close-up of the current density in the anode and scalp, illustrating the substantial shunting that occurs across the scalp. Figures adapted from Miranda (2006).

An ultra-realistic model considering additional variables such as blood, sclera, fat, and cartilage revealed that, within the brain, the highest current densities were found underneath the electrodes, but comparable densities were also found in distant regions (Sadleir et al., 2010). However, because the site of electrode placement varied among these studies, it is unclear whether their results can be directly compared.

In addition to electrode size, electrode shape can also affect current distribution. Concentric circular electrodes have a more focal current density peak than traditional, rectangular arrangements (Datta et al., 2008). Moreover, this singular peak is located directly under the electrode, and is thus not as widely dispersed across the brain as those generated by standard montages (Datta et al., 2009). Studies modelling tDCS current flow within the brain may also be extended to pathological cases: Wagner showed that cortical strokes increase the size of current density maximums, and often move their locations to the edge of the lesion site (Wagner et al., 2007).

2.2.4 Physiological Methods of Action

Though behavioural results had long suggested that transcranial currents can affect behaviour, decades would pass until actual evidence surfaced that tDCS currents do indeed penetrate the skull to affect the brain. It was posited from work in cats that anodal stimulation depolarizes cells, while cathodal stimulation hyperpolarizes them (Purpura & McMurty, 1965). This hypothesis was investigated in a pioneering study by Priori that combined tDCS with transcranial magnetic stimulation (TMS) to quantitatively measure changes in cortical excitability (Priori et al., 1998). By using tDCS protocols that either do or do not produce aftereffects, the actions of tDCS during versus following stimulation can be dissociated. The majority of studies employing this method have been performed on the motor cortex, and thus it is within this domain that the physiological underpinnings of tDCS are best understood.

When performed in conjunction with tDCS to the motor system, TMS is often used to elicit motor evoked potentials (MEPs). MEPs generated by different TMS

procedures are thought to depend on distinct underlying processes (described in more detail in Section 2.1.2). In brief, motor thresholds (MT) rely primarily on corticospinal tract (CST) neurons. Input output (I/O) curves depend on CST and intracortical neurons. Short interval intracortical inhibition (SICI) reflects the activity of $GABA_A$ergic interneurons, while intracortical facilitation (ICF) primarily stimulates glutamatergic interneurons (Stagg & Nitsche, 2011). Changes in these TMS measures provide a framework from which we can postulate the neurochemicals involved in tDCS. Pharmacological drugs can then be used to selectively enhance or diminish levels of these neurochemicals, providing the initial steps towards confirmation of their involvement. A summary of the following two sections is presented in Table 2.2.

	Anodal tDCS		**Cathodal tDCS**	
	During	After	During	After
MT	--	--	--	--
I/O Curve	Trend toward increase	Increase	Increase	Decrease
SICI	--	Decrease	--	Increase
ICF	--	Increase	Decrease	Decrease
Na^+/Ca^{2+} channels	Involved	Involved	--	--
NMDA receptors	--	Involved	--	Involved
D2 receptors	--	--	--	Involved

Table 2.2: Summary of the tDCS-induced alterations that occur during and following stimulation. Table shows whether MT, I/O curves, SICI, and ICF are modified by tDCS, and if the effects of tDCS are blocked by modification of Na^+, Ca^{2+}, NMDA, and dopamine.

2.2.4.1 During Stimulation

Neither anodal nor cathodal tDCS modulate motor thresholds during their stimulation periods. This demonstrates that, regardless of polarity, tDCS depends primarily on interneurons, and not the pyramidal neurons of the corticospinal tract (Nitsche et al., 2005). Anodal stimulation shows a trend toward increasing the slope of I/O curves, but this result does not reach significance. Only cathodal tDCS significantly modulates I/O curves by decreasing their slope (Nitsche et al., 2005). Because I/O curves depend on a broad intracortical neuronal population, this result suggests that cathodal tDCS effects a larger region of interneurons than anodal tDCS (Chen, 2000). Within the subtypes of cortical interneurons, anodal and cathodal stimulation affect differing populations. Neither cathodal nor anodal stimulation affect measures of SICI, implying that during stimulation, tDCS does not strongly affect $GABA_A$ergic interneurons. ICF, however, is decreased by cathodal stimulation which suggests that cathodal tDCS does exert effects on excitatory glutamatergic interneurons, potentially in addition to GABAergic interneurons (Nitsche et al., 2005). Taken together, these results indicate that, in terms of the neuronal populations they target, anodal tDCS is confined to a comparatively smaller network of cortical interneurons during stimulation, whereas cathodal tDCS affects a wider range of such neurons, primarily glutamatergic subtypes.

The intrastimulation effects of tDCS are not affected by NMDA-receptor antagonists (dextromethorphane, DMO) or $GABA_A$-receptor agonists (lorazepam, LOR) (Nitsche, 2003), (Nitsche et al., 2004a), (Nitsche et al., 2004c). This provides further evidence that neither anodal nor cathodal tDCS modulate GABAergic interneurons to a significant extent. However, it is likely that both anodal and cathodal stimulation affect membrane potential. In fact, this may be anodal tDCS's

primary method of action during stimulation. Blocking calcium channels with flunarzine (FLU) reduces the effects of anodal tDCS, and blocking sodium channels with carbamezipine (CBZ) completely eliminates them (Nitsche, 2003). Although FLU and CBZ did not affect cathodal stimulation, this result does not eliminate the possibility that cathodal tDCS relies on membrane potential. Rather, it is consistent with the model that cathodal stimulation hyperpolarizes neurons. Cathodal tDCS would have already inactivated calcium and sodium channels, thereby rendering any added effect of FLU or CBZ negligible (Nitsche, 2003). Moreover, cathodal stimulation modulates I/O curves, which themselves reflect membrane excitability (Nitsche et al., 2005).

2.2.4.2 After Stimulation

Anodal tDCS increases the slope of the I/O curve, increases ICF, and decreases SICI, while cathodal tDCS has the opposite effects (Nitsche et al., 2005). Moreover, anodal stimulation is known to increase MEPs, while cathodal tDCS decreases them (Nitsche & Paulus, 2000). The changes in these measures but not in MT suggest that the effects of both types of stimulation after termination depend on intracortical neurons. While the effects of tDCS during stimulation are primarily confined to effects on membrane potential, aftereffects depend both on membrane potential and changes in synaptic plasticity. Blocking sodium channels with CBZ or calcium channels with FLU eliminated the effects of anodal tDCS, but had no effects on cathodal tDCS (Liebetanz et al., 2002). This shows that the aftereffects of anodal tDCS are dependent on the modulation of subthreshold membrane potentials.

Both types of stimulation appear to be strongly dependent on NMDA receptors, which implies that the aftereffects of anodal and cathodal tDCS may be

explained by NMDA receptor dependant LTP and LTD, respectively (Nitsche, 2003). Indeed, blocking NMDA receptor activity with NMDA-receptor antagonist DMO abolishes the aftereffects of both cathodal and anodal tDCS (Liebetanz et al., 2002). Similarly, the addition of partial NMDA agonist D-cycloserine (CYC) prolongs the aftereffects of anodal tDCS (Nitsche et al., 2004b). Anodal tDCS aftereffects can also be prolonged by administering AMP, a catecholaminergic reuptake inhibitor (Nitsche et al., 2004a). This effect is blocked by DMO, further supporting the crucial role of NMDA receptors. Their activity likely depends on adrenergic receptors, as the aftereffects of anodal tDCS can be shortened with the beta-adrenergic antagonist propanalol (Nitsche et al., 2004a).

Cathodal tDCS appears to be strongly dependant on dopamine levels. Blockading dopaminergic D2 receptors prohibits the induction of cathodal aftereffects; increasing the activation of these receptors can prolong such aftereffects for up to 24 hours (Nitsche et al., 2006). Indeed, increasing dopaminergic tone with L-DOPA reversed the aftereffects of anodal tDCS and elicited cathodal-like behaviour (Kuo et al., 2008). However, anodal tDCS may depend on dopamine as well: if dopamine levels are decreased but not abolished completely, cathodal tDCS results in anodal-like facilitation (Kuo et al., 2008). In addition to dopamine, other neuromodulators affect anodal and cathodal tDCS. Boosting levels of serotonin increases both the duration and magnitude of the excitability enhancing effects seen after anodal tDCS. Likewise, a decrease in tonic serotonin increases the duration, but not magnitude, of cathodal tDCS (Nitsche et al., 2009). Moreover, increasing cholinergic tone abolishes anodal tDCS, whereas it facilitates cathodal tDCS by lengthening its duration (Kuo et al., 2007).

REFERENCES

Accornero, N., Li Voti, P., La Riccia, M., & Gregori, B. (2007). Visual evoked potentials modulation during direct current cortical polarization. *Experimental Brain Research*, *178*(2), 261–266.

Agnew, W. F., & McCreery, D. B. (1987). Considerations for safety in the use of extracranial stimulation for motor evoked potentials. *Neurosurgery*, *20*(1), 143–147.

Ambrus, G. G., Antal, A., & Paulus, W. (2011). Comparing cutaneous perception induced by electrical stimulation using rectangular and round shaped electrodes. *Clinical neurophysiology : official journal of the International Federation of Clinical Neurophysiology*, *122*(4), 803–807.

Anand, S., & Hotson, J. (2002). Transcranial magnetic stimulation: neurophysiological applications and safety. *Brain and cognition*, *50*(3), 366–386.

Antal, A., Kincses, T. Z., Nitsche, M. A., & Paulus, W. (2003). Modulation of moving phosphene thresholds by transcranial direct current stimulation of V1 in human. *Neuropsychologia*, *41*(13), 1802–1807.

Antal, A., Kincses, T. Z., Nitsche, M. A., Bartfai, O., & Paulus, W. (2004). Excitability changes induced in the human primary visual cortex by transcranial direct current stimulation: direct electrophysiological evidence. *Investigative ophthalmology & visual science*, *45*(2), 702–707.

Antal, A., Nitsche, M. A., & Paulus, W. (2006). Transcranial direct current stimulation and the visual cortex. *Brain research bulletin*, *68*(6), 459–463.

Baker, J. M., Rorden, C., & Fridriksson, J. (2010). Using transcranial direct-current stimulation to treat stroke patients with aphasia. *Stroke*, *41*(6), 1229–1236.

Barker, A. T., Jalinous, R., & Freeston, I. L. (1985). Non-invasive magnetic stimulation of human motor cortex. *The Lancet*, *325*(8437), 1106–1107.

Bikson, M., Datta, A., & Elwassif, M. (2009). Establishing safety limits for transcranial direct current stimulation. *Clinical neurophysiology : official journal of the International Federation of Clinical Neurophysiology*, *120*(6), 1033–1034.

Boggio, P. S., Fregni, F., Valasek, C., Ellwood, S., Chi, R., Gallate, J., Pascual-Leone, A., & Snyder, A. (2009a). Temporal lobe cortical electrical stimulation during the encoding and retrieval phase reduces false memories. *PloS one*, *4*(3), e4959.

Boggio, P. S., Khoury, L. P., Martins, D. C. S., Martins, O. E. M. S., de Macedo, E. C., & Fregni, F. (2009b). Temporal cortex direct current stimulation enhances performance on a visual recognition memory task in Alzheimer disease. *Journal of neurology, neurosurgery, and psychiatry*, *80*(4), 444–447.

Boggio, P. S., Liguori, P., Sultani, N., Rezende, L., Fecteau, S., & Fregni, F. (2009c). Cumulative priming effects of cortical stimulation on smoking cue-induced craving. *Neuroscience letters*, *463*(1), 82–86.

Chen, R. (2000). Studies of human motor physiology with transcranial magnetic stimulation. *Muscle & nerve. Supplement*, *9*, S26–32.

Chen, R. (2004). Interactions between inhibitory and excitatory circuits in the human motor cortex. *Experimental Brain Research*, *154*(1), 1–10.

Chokroverty, S., Hening, W., Wright, D., Walczak, T., Goldberg, J., Burger, R., Belsh, J., et al. (1995). Magnetic brain stimulation: safety studies. *Electroencephalography and clinical neurophysiology*, *97*(1), 36–42.

Cohen, L. G., Roth, B. J., Nilsson, J., Dang, N., Panizza, M., Bandinelli, S., Friauf, W., et al. (1990). Effects of coil design on delivery of focal magnetic stimulation. Technical considerations. *Electroencephalography and clinical neurophysiology*, *75*(4), 350–357.

DaSilva, A. F., Volz, M. S., Bikson, M., & Fregni, F. (2011). Electrode Positioning and Montage in Transcranial Direct Current Stimulation. *Journal of Visualized Experiments*, (51).

Datta, A., Bansal, V., Diaz, J., Patel, J., Reato, D., & Bikson, M. (2009). Gyri -precise head model of transcranial DC stimulation: Improved spatial focality using a ring electrode versus conventional rectangular pad. *Brain Stimulation*, *2*(4), 201–207.

Datta, A., Elwassif, M., Battaglia, F., & Bikson, M. (2008). Transcranial current stimulation focality using disc and ring electrode configurations: FEM analysis. *Journal of neural engineering*, *5*(2), 163–174.

Dundas, J. E., Thickbroom, G. W., & Mastaglia, F. L. (2007). Perception of comfort during transcranial DC stimulation: effect of NaCl solution concentration applied to sponge electrodes. *Clinical neurophysiology : official journal of the International Federation of Clinical Neurophysiology*, *118*(5), 1166–1170.

Elmer, S., Burkard, M., Renz, B., Meyer, M., & Jancke, L. (2009). Direct current

induced short-term modulation of the left dorsolateral prefrontal cortex while learning auditory presented nouns. *Behavioral and brain functions : BBF*, *5*, 29.

Ferdjallah, M., Bostick, F. X., & Barr, R. E. (1996). Potential and current density distributions of cranial electrotherapy stimulation (CES) in a four-concentric-spheres model. *IEEE transactions on bio-medical engineering*, *43*(9), 939–943.

Ferrucci, R., Giannicola, G., Rosa, M., Fumagalli, M., Boggio, P. S., Hallett, M., Zago, S., et al. (2011). Cerebellum and processing of negative facial emotions: Cerebellar transcranial DC stimulation specifically enhances the emotional recognition of facial anger and sadness. *Cognition & emotion*.

Ferrucci, R., Mameli, F., Guidi, I., Mrakic-Sposta, S., Vergari, M., Marceglia, S., Cogiamanian, F., et al. (2008). Transcranial direct current stimulation improves recognition memory in Alzheimer disease. *Neurology*, *71*(7), 493–498.

Fregni, F., Boggio, P. S., Mansur, C. G., Wagner, T., Ferreira, M. J. L., Lima, M. C., Rigonatti, S. P., et al. (2005). Transcranial direct current stimulation of the unaffected hemisphere in stroke patients. *Neuroreport*, *16*(14), 1551–1555.

Gandiga, P. C., Hummel, F. C., & Cohen, L. G. (2006). Transcranial DC stimulation (tDCS): a tool for double-blind sham-controlled clinical studies in brain stimulation. *Clinical neurophysiology : official journal of the International Federation of Clinical Neurophysiology*, *117*(4), 845–850.

Giordano, D., Kavasidis, I., Spampinato, C., Bella, R., Pennisi, G., & Pennisi, M. (2011). An integrated computer-controlled system for assisting researchers in cortical excitability studies by using transcranial magnetic stimulation. *Computer methods and programs in biomedicine*.

Hallett, M. (2000). Transcranial magnetic stimulation and the human brain. *Nature*, *406*(6792), 147–150.

Hallett, M. (2007). Transcranial magnetic stimulation: a primer. *Neuron*, *55*(2), 187–199.

Huerta, P. T., & Volpe, B. T. (2009). Transcranial magnetic stimulation, synaptic plasticity and network oscillations. *Journal of NeuroEngineering and Rehabilitation*, *6*, 7.

Hummel, F. (2005). Effects of non-invasive cortical stimulation on skilled motor function in chronic stroke. *Brain*, *128*(3), 490–499.

Iyer, M. B., Mattu, U., Grafman, J., Lomarev, M., Sato, S., & Wassermann, E. M. (2005).

Safety and cognitive effect of frontal DC brain polarization in healthy individuals. *Neurology*, *64*(5), 872–875.

Jacobson, L., Koslowsky, M., & Lavidor, M. (2011). tDCS polarity effects in motor and cognitive domains: a meta-analytical review. *Experimental Brain Research*.

Javadi, A. H., Cheng, P., & Walsh, V. (2011). Short duration transcranial direct current stimulation (tDCS) modulates verbal memory. *Brain Stimulation*.

Kellaway, P. (1946). *The part played by electric fish in the early history of bioelectricity and electrotherapy*.

Kessler, S. K., Turkeltaub, P. E., Benson, J. G., & Hamilton, R. H. (2011). Differences in the experience of active and sham transcranial direct current stimulation. *Brain Stimulation*.

Knoch, D., Nitsche, M. A., Fischbacher, U., Eisenegger, C., Pascual-Leone, A., & Fehr, E. (2008). Studying the neurobiology of social interaction with transcranial direct current stimulation--the example of punishing unfairness. *Cerebral cortex (New York, N.Y. : 1991)*, *18*(9), 1987–1990.

Kobayashi, M., & Pascual-Leone, A. (2003). Transcranial magnetic stimulation in neurology. *Lancet neurology*, *2*(3), 145–156.

Kratz, O., Studer, P., Barth, W., Wangler, S., Hoegl, T., Heinrich, H., & Moll, G. H. (2011). Seizure in a nonpredisposed individual induced by single-pulse transcranial magnetic stimulation. *The journal of ECT*, *27*(1), 48–50.

Kuo, M.-F., Grosch, J., Fregni, F., Paulus, W., & Nitsche, M. A. (2007). Focusing effect of acetylcholine on neuroplasticity in the human motor cortex. *Journal of Neuroscience*, *27*(52), 14442–14447.

Kuo, M.-F., Paulus, W., & Nitsche, M. A. (2008). Boosting focally-induced brain plasticity by dopamine. *Cerebral cortex (New York, N.Y. : 1991)*, *18*(3), 648–651.

Lagopoulos, J., & Degabriele, R. (2008). Feeling the heat: the electrode–skin interface during DCS. *Acta Neuropsychiatrica*, *20*(2), 98–100.

Liebetanz, D., Nitsche, M. A., Tergau, F., & Paulus, W. (2002). Pharmacological approach to the mechanisms of transcranial DC-stimulation-induced after-effects of human motor cortex excitability. *Brain*, *125*(Pt 10), 2238–2247.

Lolas, F. (1977). Brain polarization: behavioral and therapeutic effects. *Biological Psychiatry*, *12*(1), 37–47.

Loo, C. K., Martin, D. M., Alonzo, A., Gandevia, S., Mitchell, P. B., & Sachdev, P. (2011).

Avoiding skin burns with transcranial direct current stimulation: preliminary considerations. *The international journal of neuropsychopharmacology / official scientific journal of the Collegium Internationale Neuropsychopharmacologicum (CINP)*, *14*(3), 425–426.

Marshall, L., Mölle, M., Hallschmid, M., & Born, J. (2004). Transcranial direct current stimulation during sleep improves declarative memory. *Journal of Neuroscience*, *24*(44), 9985–9992.

McCreery, D. B., Agnew, W. F., Yuen, T. G., & Bullara, L. (1990). Charge density and charge per phase as cofactors in neural injury induced by electrical stimulation. *IEEE transactions on bio-medical engineering*, *37*(10), 996–1001.

Merton, P. A., & Morton, H. B. (1980). Stimulation of the cerebral cortex in the intact human subject. *Nature*, *285*(5762), 227–227.

Mills, K. R., Boniface, S. J., & Schubert, M. (1992). Magnetic brain stimulation with a double coil: the importance of coil orientation. *Electroencephalography and clinical neurophysiology*, *85*(1), 17–21.

Minhas, P., Datta, A., & Bikson, M. (2011). Cutaneous perception during tDCS: role of electrode shape and sponge salinity. *Clinical neurophysiology : official journal of the International Federation of Clinical Neurophysiology*, *122*(4), 637–638.

Miranda, P. C., Faria, P., & Hallett, M. (2009). What does the ratio of injected current to electrode area tell us about current density in the brain during tDCS? *Clinical neurophysiology : official journal of the International Federation of Clinical Neurophysiology*, *120*(6), 1183–1187.

Miranda, P. C., Lomarev, M., & Hallett, M. (2006). Modeling the current distribution during transcranial direct current stimulation. *Clinical neurophysiology : official journal of the International Federation of Clinical Neurophysiology*, *117*(7), 1623–1629.

Monti, A., Cogiamanian, F., Marceglia, S., Ferrucci, R., Mameli, F., Mrakic-Sposta, S., Vergari, M., et al. (2008). Improved naming after transcranial direct current stimulation in aphasia. *Journal of neurology, neurosurgery, and psychiatry*, *79*(4), 451–453.

Nitsche, M. A. (2003). Pharmacological modulation of cortical excitability shifts induced by transcranial direct current stimulation in humans. *The Journal of Physiology*, *553*(1), 293–301.

Nitsche, M. A., & Paulus, W. (2000). Excitability changes induced in the human motor cortex by weak transcranial direct current stimulation. *The Journal of Physiology*, *527 Pt 3*, 633–639.

Nitsche, M. A., & Paulus, W. (2001). Sustained excitability elevations induced by transcranial DC motor cortex stimulation in humans. *Neurology*, *57*(10), 1899–1901.

Nitsche, M. A., Cohen, L. G., Wassermann, E. M., Priori, A., Lang, N., Antal, A., Paulus, W., et al. (2008). Transcranial direct current stimulation: State of the art 2008. *Brain Stimulation*, *1*(3), 206–223.

Nitsche, M. A., Doemkes, S., Karakose, T., Antal, A., Liebetanz, D., Lang, N., Tergau, F., et al. (2007). Shaping the Effects of Transcranial Direct Current Stimulation of the Human Motor Cortex. *Journal of Neurophysiology*, *97*(4), 3109–3117.

Nitsche, M. A., Grundey, J., Liebetanz, D., Lang, N., Tergau, F., & Paulus, W. (2004a). Catecholaminergic consolidation of motor cortical neuroplasticity in humans. *Cerebral cortex (New York, N.Y. : 1991)*, *14*(11), 1240–1245.

Nitsche, M. A., Jaussi, W., Liebetanz, D., Lang, N., Tergau, F., & Paulus, W. (2004b). Consolidation of human motor cortical neuroplasticity by D-cycloserine. *Neuropsychopharmacology : official publication of the American College of Neuropsychopharmacology*, *29*(8), 1573–1578.

Nitsche, M. A., Kuo, M.-F., Karrasch, R., Wächter, B., Liebetanz, D., & Paulus, W. (2009). Serotonin affects transcranial direct current-induced neuroplasticity in humans. *Biological Psychiatry*, *66*(5), 503–508.

Nitsche, M. A., Lampe, C., Antal, A., Liebetanz, D., Lang, N., Tergau, F., & Paulus, W. (2006). Dopaminergic modulation of long-lasting direct current-induced cortical excitability changes in the human motor cortex. *European Journal of Neuroscience*, *23*(6), 1651–1657.

Nitsche, M. A., Liebetanz, D., Lang, N., Antal, A., Tergau, F., & Paulus, W. (2003a). Safety criteria for transcranial direct current stimulation (tDCS) in humans. *Clinical Neurophysiology*, *114*(11), 2220–2222.

Nitsche, M. A., Liebetanz, D., Schlitterlau, A., Henschke, U., Fricke, K., Frommann, K., Lang, N., Henning, S., et al. (2004c). GABAergic modulation of DC stimulation-induced motor cortex excitability shifts in humans. *European Journal of Neuroscience*, *19*(10), 2720–2726.

Nitsche, M. A., Niehaus, L., Hoffmann, K. T., Hengst, S., Liebetanz, D., Paulus, W., & Meyer, B.-U. (2004d). MRI study of human brain exposed to weak direct current stimulation of the frontal cortex. *Clinical neurophysiology : official journal of the International Federation of Clinical Neurophysiology*, *115*(10), 2419–2423. doi:10.1016/j.clinph.2004.05.001

Nitsche, M. A., Schauenburg, A., Lang, N., Liebetanz, D., Exner, C., Paulus, W., & Tergau, F. (2003b). Facilitation of implicit motor learning by weak transcranial direct current stimulation of the primary motor cortex in the human. *Journal of cognitive neuroscience*, *15*(4), 619–626.

Nitsche, M. A., Seeber, A., Frommann, K., Klein, C. C., Rochford, C., Nitsche, M. S., Fricke, K., et al. (2005). Modulating parameters of excitability during and after transcranial direct current stimulation of the human motor cortex. *The Journal of Physiology*, *568*(Pt 1), 291–303.

Palm, U., Keeser, D., Schiller, C., Fintescu, Z., Nitsche, M., Reisinger, E., & Padberg, F. (2008). Skin lesions after treatment with transcranial direct current stimulation (tDCS). *Brain Stimulation*, *1*(4), 386–387.

Palm, U., Schiller, C., Fintescu, Z., Obermeier, M., Keeser, D., Reisinger, E., Pogarell, O., et al. (2011). Transcranial direct current stimulation in treatment resistant depression: a randomized double-blind, placebo-controlled study. *Brain Stimulation*.

Parent, A. (2004). *Giovanni Aldini: from animal electricity to human brain stimulation. The Canadian journal of neurological sciences. Le journal canadien des sciences neurologiques* (Vol. 31, pp. 576–584).

Poreisz, C., Boros, K., Antal, A., & Paulus, W. (2007). Safety aspects of transcranial direct current stimulation concerning healthy subjects and patients. *Brain research bulletin*, *72*(4-6), 208–214.

Priori, A. (2003). Brain polarization in humans: a reappraisal of an old tool for prolonged non-invasive modulation of brain excitability. *Clinical Neurophysiology*, *114*(4), 589–595.

Priori, A., Berardelli, A., Rona, S., Accornero, N., & Manfredi, M. (1998). Polarization of the human motor cortex through the scalp. *Neuroreport*, *9*(10), 2257–2260.

Priori, A., Mameli, F., Cogiamanian, F., Marceglia, S., Tiriticco, M., Mrakic-Sposta, S., Ferrucci, R., et al. (2008). Lie-specific involvement of dorsolateral prefrontal

cortex in deception. *Cerebral cortex (New York, N.Y. : 1991)*, *18*(2), 451–455.

Purpura, D. P., & McMurty, J. G. (1965). Intracellular Activities and Evoked Potential Changes During Polarization of Motor Cortex. *Journal of Neurophysiology*, *28*, 166–185.

Reis, J., Schambra, H. M., Cohen, L. G., Buch, E. R., Fritsch, B., Zarahn, E., Celnik, P. A., et al. (2009). Noninvasive cortical stimulation enhances motor skill acquisition over multiple days through an effect on consolidation. *Proceedings of the National Academy of Sciences of the United States of America*, *106*(5), 1590–1595.

Reis, J., Swayne, O. B., Vandermeeren, Y., Camus, M., Dimyan, M. A., Harris-Love, M., Perez, M. A., et al. (2008). Contribution of transcranial magnetic stimulation to the understanding of cortical mechanisms involved in motor control. *The Journal of Physiology*, *586*(2), 325–351.

Rossi, S., Hallett, M., Rossini, P. M., Pascual-Leone, A., Safety of TMS Consensus Group. (2009). Safety, ethical considerations, and application guidelines for the use of transcranial magnetic stimulation in clinical practice and research. In *Clinical neurophysiology : official journal of the International Federation of Clinical Neurophysiology* (Vol. 120, pp. 2008–2039).

Rossini, P. M., & Rossi, S. (1998). Clinical applications of motor evoked potentials. *Electroencephalography and clinical neurophysiology*, *106*(3), 180–194.

Rossini, P. M., & Rossi, S. (2007). Transcranial magnetic stimulation: Diagnostic, therapeutic, and research potential. *Neurology*, *68*(7), 484–488.

Rush, S., & Driscoll, D. A. (1968). Current distribution in the brain from surface electrodes. *Anesthesia and analgesia*, *47*(6), 717–723.

Sadleir, R. J., Vannorsdall, T. D., Schretlen, D. J., & Gordon, B. (2010). Transcranial direct current stimulation (tDCS) in a realistic head model. *NeuroImage*, *51*(4), 1310–1318.

Schrader, L. M., Stern, J. M., Koski, L., Nuwer, M. R., & Engel, J. (2004). Seizure incidence during single- and paired-pulse transcranial magnetic stimulation (TMS) in individuals with epilepsy. *Clinical neurophysiology : official journal of the International Federation of Clinical Neurophysiology*, *115*(12), 2728–2737.

Stagg, C. J., & Nitsche, M. A. (2011). Physiological Basis of Transcranial Direct Current Stimulation. *The Neuroscientist*, *17*(1), 37–53.

Stagg, C. J., Bestmann, S., Constantinescu, A. O., Moreno Moreno, L., Allman, C., Mekle,

R., Woolrich, M., Near, J., et al. (2011a). Relationship between physiological measures of excitability and levels of glutamate and GABA in the human motor cortex. *The Journal of Physiology*, *589*(Pt 23), 5845–5855.

Stagg, C. J., Jayaram, G., Pastor, D., Kincses, Z. T., Matthews, P. M., & Johansen-Berg, H. (2011b). Polarity and timing-dependent effects of transcranial direct current stimulation in explicit motor learning. *Neuropsychologia*, *49*(5), 800–804. Elsevier Ltd.

Suh, H. S., Kim, S. H., Lee, W. H., & Kim, T.-S. (2009). Realistic simulation of transcranial direct current stimulation via 3-d high-resolution finite element analysis: Effect of tissue anisotropy. *Conference proceedings : ... Annual International Conference of the IEEE Engineering in Medicine and Biology Society. IEEE Engineering in Medicine and Biology Society. Conference*, *2009*, 638–641.

Terao, Y., & Ugawa, Y. (2002). Basic mechanisms of TMS. *Journal of clinical neurophysiology : official publication of the American Electroencephalographic Society*, *19*(4), 322–343.

Thom Oostendorp, Y. H. C. W. J. S. G. V. E. D. S. (2008). Modeling Transcranial DC Stimulation, 1–4.

Utz, K. S., Dimova, V., Oppenländer, K., & Kerkhoff, G. (2010). Electrified minds: Transcranial direct current stimulation (tDCS) and Galvanic Vestibular Stimulation (GVS) as methods of non-invasive brain stimulation in neuropsychologyâ€"A review of current data and future implications. *Neuropsychologia*, *48*(10), 2789–2810. Elsevier Ltd.

Valle, A., Roizenblatt, S., Botte, S., Zaghi, S., Riberto, M., Tufik, S., Boggio, P. S., et al. (2009). Efficacy of anodal transcranial direct current stimulation (tDCS) for the treatment of fibromyalgia: results of a randomized, sham-controlled longitudinal clinical trial. *Journal of pain management*, *2*(3), 353–361.

Wagner, T., Fregni, F., Fecteau, S., Grodzinsky, A., Zahn, M., & Pascual-Leone, A. (2007). Transcranial direct current stimulation: a computer-based human model study. *NeuroImage*, *35*(3), 1113–1124.

Yousry, T. A., Schmid, U. D., Alkadhi, H., Schmidt, D., Peraud, A., Buettner, A., & Winkler, P. (1997). Localization of the motor hand area to a knob on the precentral gyrus. A new landmark. *Brain*, *120 (Pt 1)*, 141–157.

Yuen, T. G., Agnew, W. F., Bullara, L. A., Jacques, S., & McCreery, D. B. (1981).

Histological evaluation of neural damage from electrical stimulation: considerations for the selection of parameters for clinical application. *Neurosurgery*, *9*(3), 292–299.

Zangen, A., Roth, Y., Voller, B., & Hallett, M. (2005). Transcranial magnetic stimulation of deep brain regions: evidence for efficacy of the H-coil. *Clinical neurophysiology : official journal of the International Federation of Clinical Neurophysiology*, *116*(4), 775–779.

Chapter 3: Methods for Imaging the Motor System

Neuroimaging techniques allow for detailed investigation into the organization of the human brain. Chapters 4, 6, and 7 employ magnetic resonance imaging (MRI) to track a variety of neuroplastic changes induced by motor learning and stimulation. Functional MRI is used to assess patterns of activation during task performance and at rest; structural MRI quantifies alterations in cortical and subcortical gray matter; diffusion MRI measures the integrity of the fiber pathways connecting these regions. This chapter explains the basic principles of MRI, then focuses on each modality in turn. Finally, it presents particular considerations that arise in this thesis.

3.1 Overview of Magnetic Resonance Imaging

The origins of imaging can be traced back to the late 1800s and the fortuitous discovery of X-rays and radioactivity. Medical imaging of the type known today, however, began with the invention of Computed Tomography (CT), for which Hounsfield and Cormack won the Nobel Prize for Medicine and Physiology in 1979. Additional imaging techniques such as Single Photon Emission Computed Tomography (SPECT), Positron Emission Tomography (PET), and Magnetic Resonance Imaging (MRI) have gained use as diagnostic and research tools. MR imaging is widely used by clinicians and researchers alike, both for its high degree of sensitivity and relative safety.

3.1.1 PHYSICAL PRINCIPLES

3.1.1.1 The Hydrogen Atom

The hydrogen atom (^{1}H) is the most abundant atom in the human body, and is a primary component of both water and fat molecules. Its nucleus consists of a single proton spinning about its own axis, which gives the hydrogen atom a magnetic moment. The magnetic moment can be visualized as a bar magnet with a north and south pole, and an induced magnetic field. Other atoms such as phosphorus (^{31}P) and carbon (^{13}C) also have magnetic moments. However, because hydrogen's nucleus contains no neutrons, it has a exceptionally large magnetic moment. This, combined with its prevalence in the human body—particularly in the brain, makes the hydrogen nuclei the preferred candidate on which to base MR imaging.

3.1.1.2 Alignment in B_0

In an environment at rest, the magnetic moments of the hydrogen nuclei will be randomly oriented, with their north and south poles facing varying directions (Figure 3.1A). When an external magnetic field (B_0) is applied, the magnetic moments of the nuclei align themselves with B_0. Most magnetic moments will align parallel to B_0, while a smaller portion will align anti-parallel to the field (Figure 3.1B). This difference arises because more energy is required to oppose the magnetic field: moments aligned anti-parallel to B_0 are said to be high energy, while those aligned parallel to it are low energy. The net magnetization vector (NMV) reflects the balance between the parallel and anti-parallel nuclei. At higher magnetic fields, fewer nuclei have the energy required to align anti-parallel to B_0, resulting in a larger NMV.

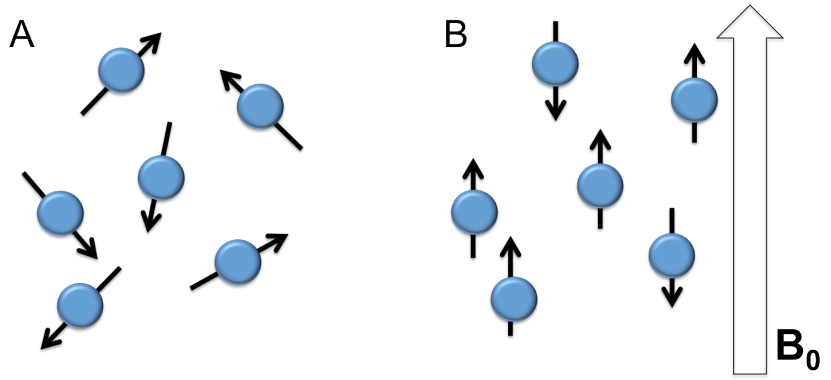

Figure 3.1: Alignment in B_0. (A) The magnetic moments of hydrogen nuclei at rest are randomly oriented. (B) In the presence of an external magnetic field, they align parallel or anti-parallel to B_0.

3.1.1.3 Precession

In addition to orienting the nuclear magnetic moments of the hydrogen atoms, B_0 also causes the magnetic moments to rotate in a circular path around B_0. The frequency with which the nuclei complete this path is termed the precessional frequency (ω_0). This frequency is a property of the atom and B_0, and can be determined using the Larmor equation:

$$\omega_0 = \lambda \times B_0$$

where λ is the gyromagnetic ratio of the nucleus. Critically, the gyromagnetic ratio is a constant particular to each type of atom, and is the same for all nuclei of that atom. That is, all hydrogen nuclei possess the same gyromagnetic ratio of 42.57 MHz/Tesla, which differs from that of carbon nuclei, for example. The precessional (Larmor) frequency is directly proportional to B_0; as one increases, so does the other.

3.1.1.4 Resonance

The Larmor frequency of the hydrogen nuclei is within the radio frequency (RF) band of the electromagnetic spectrum. If an RF pulse of energy is applied at

this Larmor frequency, the hydrogen nucleus gains the energy of the pulse, in a process termed resonance. As a result of this excitation, some low energy nuclei will convert to high energy nuclei and flip orientations to align anti-parallel to B_0. This modification in the balance between high and low energy nuclei moves the NMV out of alignment with B_0. The NMV is now no longer parallel to B_0 and the longitudinal plane, but at an angle to it in the transverse plane. Most RF pulses flip the NMV 90° to B_0. Additionally, the RF pulse causes the hydrogen nuclei to come into phase with each other; that is, the hydrogen nuclei will be at the same position on their precessional paths.

3.1.1.5 The MR Signal

Faraday's laws of induction state that if a conductive coil is placed in a moving magnetic field, a voltage is produced in that coil. Accordingly, when the precession of hydrogen nuclei move across the scanner's coil in the transverse plane, the MR signal is produced. When the RF pulse is turned off, the NMV seeks to realign with B_0. During this processes, termed relaxation, a portion of hydrogen nuclei lose the energy given to them by the prior RF pulse. As relaxation occurs, the amount of magnetization in the longitudinal plane gradually increases (recovery), while the magnetization in the transverse plane decreases (decay). As magnetization in the transverse plane decreases, so too does the MR signal, in a process called the free induction decay (FID).

3.1.2 IMAGE ACQUISITION

3.1.2.1 Overview

The MR signal can be manipulated to create images of different contrasts, allowing for tissue discrimination. A tissue has high signal (and thus appears bright) if there is a large component of coherent transverse magnetization. Parameters of the pulse sequence are used to modify the amount of transverse magnetization in each tissue type at the time the signal is read. This takes advantage of the fact that the rate at which transverse magnetization decays—and longitudinal magnetization recovers, varies between tissue. Particularly important tissue types to consider when imaging the brain are fat and water, two large components of white matter and CSF, respectively.

3.1.2.2 Pulse Timing Parameters

Pulse sequences are a combination of RF pulses, periods of recovery that generate the MR image, and signal readout (Figure 3.2). Two main components are the repetition time (TR) and echo time (TE). TR is the time in milliseconds from one RF pulse application to the next for each brain slice. TE is the time in milliseconds from the application of the RF pulse to the moment of peak signal induction in the coil.

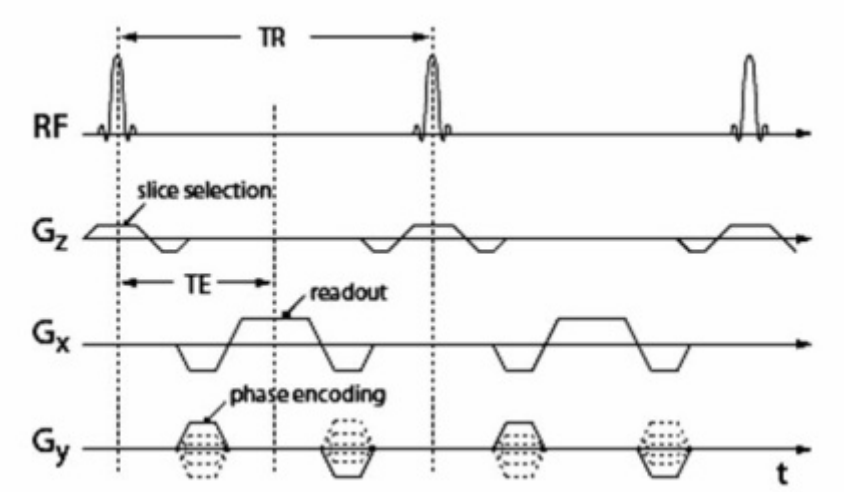

Figure 3.2: Pulse sequence diagram. Figure adapted from http://ipg.epfl.ch/

3.1.2.3 Weighting and Contrast

T1 IMAGES. T1 recovery refers to the restoration of longitudinal magnetization following the end of an RF pulse. It is the result of the hydrogen nuclei releasing their energy into the surrounding environment. T1 relaxation time is the time it takes for 63% of the longitudinal magnetization to be recovered. This varies from tissue to tissue: in fat, it is a relatively rapid process, leading to a short T1. Recovery is slower in water, resulting in a longer T1. For a particular pulse sequence, TR determines the amount of T1 recovery that has occurred when the signal is read. Thus, to maximize the contrast between fat and water, T1-weighted images use a short TR, so that neither tissue has had time to fully recover (Figure 3.3A). After being refocused by the next excitation pulse, fat will appear bright on a T1-weighted image due to its high signal, whereas water will appear dark due to a lower signal.

T2 IMAGES. T2 decay is the loss of transverse magnetization following the end of the RF pulse. It is caused by the hydrogen nuclei exchanging energy with each other due to neighbouring interactions. The T2 relaxation time of a tissue is the time it takes for 63% of the transverse magnetization to be lost. Loss of transverse

magnetization in fat occurs quickly, leading to a short T2, while the T2 of water is long. The amount of T2 decay that has occurred at signal readout is determined by the length of the TE. When generating a T2-weighted image, the TE is be relatively long, to allow both water and fat sufficient time to decay (Figure 3.3B). Because water has a long T2, comparatively less decay of its transverse magnetization will have occurred, and thus it appears bright on a T2-weighted image. Fat, however, with its short T2, has experienced more decay, has less signal, and appears dark. A long TR can be used as well to minimize T1 contrast.

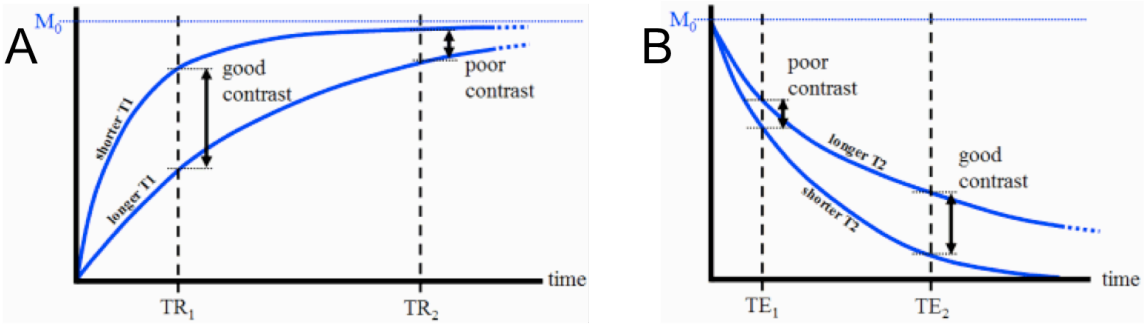

Figure 3.3: Image weighting. (A) T1-weighted images depend primarily on TR, and recovery of longitudinal magnetization. (B) T2-weighted images depend primarily on TE and the amount of decay in the transverse plane. Figures from revisemri.com

T2* IMAGES. T2* decay is the decay of the FID following the RF pulse. It occurs faster than T2 decay, due to the additional dephasing resulting from field inhomogeneities.

3.1.2.4 *Spatial Localization*

The spatial location from which each signal originates must be determined, in 3 dimensions. This is done by first selecting a 2-dimensional slice, and then locating the signal's point of origin along each of the two remaining axes, a process called encoding. Both slice selection and spatial encoding utilise gradients: a

gradient is applied in the x, y, and z directions, causing the magnetic field to vary in a linear fashion emanating from the field's isocentre. Thus, each location within the magnet has nuclei precessing at slightly different rates, allowing the signal to be accurately positioned according to its precessional frequency. This information about the location of each individual signal is then transformed into an image using complex Fourier transforms. Figure 3.4 shows structural images of varying contrasts.

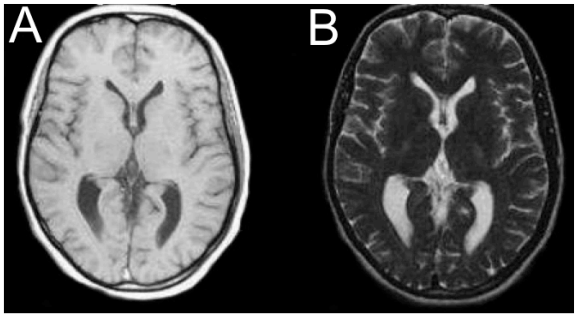

Figure 3.4: Axial structural MRI slices. (A) T1-weighted image. (B) T2-weighted image. Figure adapted from revisemri.com

3.1.3 SAFETY

3.1.3.1 Magnetic Fields

Although MRI does not involve the use of ionizing radiation as some other imaging techniques do, MR imaging does present its own set of safety issues. These primarily arise from the powerful magnetic fields. In particular, the static field (B_0), the time-varying magnetic fields generated by gradients, and the RF pulses can all cause potentially hazardous biological effects. Studies have found no significant adverse affects caused by short-term exposure to the static magnetic field (Shellock & Crues, 2004), though at very high fields, long-term, prolonged exposure could theoretically lead to negative pathological changes (Schenck, 2000). The static field

may also cause mild sensory effects, such as vertigo and nausea (McRobbie, Moore, Graves, & Prince, 2007).

The main concern surrounding gradient fields is the possibility of inducing undesirable peripheral stimulation, especially during EPI sequences (see Section 3.3.2). Experienced as tingling or tapping, this phenomenon is bothersome, but generally not harmful (McRobbie et al., 2007): the threshold for inducing enough stimulation so as to effect cardiac tissue far exceeds the strengths used for clinical and research purposes (Shellock & Crues, 2004). An additional concern is the acoustic noise generated when current is passed through the gradient coil. The sound of the coils moving against their mountings can be in excess of 100 dB on some models (McRobbie et al., 2007). To counteract this, hearing protection is suggested, such as ear plugs or more advanced noise-cancelling headphones (Westbrook, Roth, & Talbot, 2005). The development of 'quiet' gradient systems is an active area of ongoing research.

The primary safety issue arising from RF coils is the heating of tissues. The RF waves are from the nonionizing radiofrequency portion of the electromagnetic spectrum, and therefore lack the energy required to ionise the atoms of the body and cause cellular damage. Thus, while ionizing radiation has the potential to induce irreversible damage on the molecular level, the greatest concern with nonionizing radiation like that delivered by RF pulses is direct heating of the body (Formica & Silvestri, 2004). This is because the majority of the RF power is transformed into heat within the subject's body. The risk is increased when wires or cables, such as those used to connect to stimulation devices, are placed in the scanner with the patient, as it is possible to inadvertently couple the RF energy into the wires. To

combat this, care should be taken that the wires contain no loops, and are not in contact with the participant's body (McRobbie et al., 2007).

3.1.3.2 Ferromagnetic Attraction

In practice, the most common hazard associated with MR imaging is ferromagnetic attraction: when metals such as iron or steel come in close proximity to the scanner's magnet, they experience a force that can turn them into airborne projectiles (McRobbie et al., 2007). It should be noted that the magnetic field extends beyond the confines of the scanner field, creating a perimeter in which a fringe field exists. Thus, all items used in and around the scanner must be MR compatible, including assistive walking apparatus and devices for task performance. The ferromagnetic force can also act on metallic objects implanted within the body, such as aneurysm clips, and can alter the functioning of medical devices like pacemakers and cochlear implants. Because of this, it is important that thorough safety checks are performed before allowing anyone—researcher or participant-into the MRI room.

3.1.3.3 Safety Guidelines

In order to ensure the safety of those administering and undergoing scans, extensive safety guidelines have been established. Particular vigilance should be taken when screening subjects with implanted devices, or occupations that may have caused accidental internal lodging of ferromagnetic materials, such as metal-working. Although many implanted devices today are MR safe (Westbrook et al., 2005), it should not be assumed that all modern medical implants will be non-ferromagnetic. Due to heating concerns, care should be taken with subjects that

have tattoos or permanent makeup. Although no adverse effects on embryos and foetuses have been documented, the scanning of pregnant women is generally advised against, particularly during the first trimester (Westbrook et al., 2005). Due to the small size of the bore hole, some may experience bouts of claustrophobia during scanning. Enquiries should be made prior to scanning about the possibility of this occurring. To promote the safety and comfort of the participant, continual verbal and visual monitoring should occur during the scan.

3.2 STRUCTURAL MRI

3.2.1 OVERVIEW

Structural scans can be used for precise visualization of neuroanatomy and to identify structural abnormalities, such as lesions due to stroke. T1-weighted images are also integral to the registration process that aligns multiple images to each other (discussed further in Section 3.3.3). In addition to these ancillary roles, structural scans can themselves be used to investigate the brain's plasticity. It is known that the structure of the brain changes naturally with age (Good et al., 2001), but recent evidence shows that external influences such as learning or chronic disease can also induce structural changes on a much shortened timescale (Driemeyer, Boyke, Gaser, Büchel, & May, 2008; May et al., 2007). Cross-sectional and longitudinal analyses can be performed on structural images to probe these modifications. Here, we focus on one particular technique, voxel-based morphometry (VBM), which is used to compare local gray matter concentrations between groups. VBM has been applied to study structural changes induced by a variety of influences, such as learning, epilepsy, autism, dementia, back pain, and stroke (Bandettini, 2009).

3.2.2 METHODS

VBM was first introduced in 1995, when Wright and colleagues pioneered the technique in a study of schizophrenia (Wright et al., 1995). In 2000, Ashburner and Friston published a clear set of methods for performing VBM analysis (Ashburner & Friston, 2000), which further increased its popularity and the ease with which the technique could be implemented. Good and colleagues then optimised this process in 2001 (Good et al., 2001). In brief, T1-weighted MR images are spatially normalized and registered into the same stereotactic space using a high resolution standardized image. This alignment is performed, not to precisely match every cortical feature between the brains, but to correct for global differences in brain shape and volume. The images are then segmented into gray matter, white matter, and non-brain tissue (i.e., CSF and skull). The gray matter images are then smoothed with an isotropic Gaussian kernel, which produces voxels whose intensities are the average of their original value along with those of surrounding voxels. To adjust for changes in volume due to registration, these values are then modulated by the Jacobian warpfield. Statistical analysis is then run using a general linear model (GLM, see Section 3.3.4). Finally, voxel-wise parametric statistics are performed to compare the gray matter concentration between groups.

Because minor modifications in the variables used during each of these steps could possibly have a dramatic effect on the final results, care should be taken to specifically report the parameters chosen (Ridgway et al., 2008).

3.2.3 LIMITATIONS

While VBM is a robust technique with a diverse range of applications, there are limitations that arise, both in the analysis and interpretation of results. Currently, how differences in MRI signal intensity affect VBM-derived measures of gray matter concentration has not been fully elucidated (Bandettini, 2009). Moreover, if any of the processing steps (e.g., registration, segmentation) have yielded inaccurate outputs, it is possible that the documented changes will not only reflect differences in gray matter, but of white matter and CSF as well (Bookstein, 2001). Another potential confound is that variations in gyrification patterns may be confused with true differences in gray matter concentration, thus distorting the VBM results. This problem can be partially mitigated by using cortical thickness measurements in tandem (Hutton, Draganski, Ashburner, & Weiskopf, 2009). Additionally, it is difficult to discern the actual mechanisms underlying any structural changes one might find, though it has been posited that such plastic changes may reflect dendritic spine growth and axonal remodelling (Draganski & May, 2008; Johansen-Berg, 2007). This is not a limitation of VBM in particular, but of neuroimaging results in general.

3.3 FUNCTIONAL MRI

Functional MRI (fMRI) is used to acquire images of the brain while at rest and during periods of activity. It depends on T2* contrast, an effect that is enhanced by the Blood Oxygen Level Dependent (BOLD) signal.

3.3.1 THE BOLD SIGNAL

Haemoglobin is an iron containing molecule that transports oxygen through the blood. The presence of iron within haemoglobin gives the molecule magnetic properties. However, when oxygen is bound to haemoglobin (oxyhaemoglobin), the magnetic properties are suppressed. When oxygen is not bound (deoxyhaemoglobin), the iron creates a magnetic field around haemoglobin, which increases T2* decay in the surrounding tissue, resulting in diminished signal from these areas. The BOLD signal is based on the difference in oxygen consumption between brain areas that are active and those that are at rest.

The brain utilizes oxygen to meet its energy demands and perform its activities of normal daily functioning. During periods of activity, metabolic demands are heightened, and thus the need for oxygen rises. To accommodate this increased demand, a surplus of blood is sent to the active cortex, leading to a relative decrease in deoxyhaemoglobin, although total oxygen consumption has increased. The decrease in the deoxyhaemoglobin:oxyhaemoglobin ratio lessens the magnetic properties from the blood, causing decreased T2* decay and increased signal. Figure 3.5 illustrates the timecourse of the BOLD response. Note the several second delay between the increased neuronal activity and the resulting increased BOLD signal.

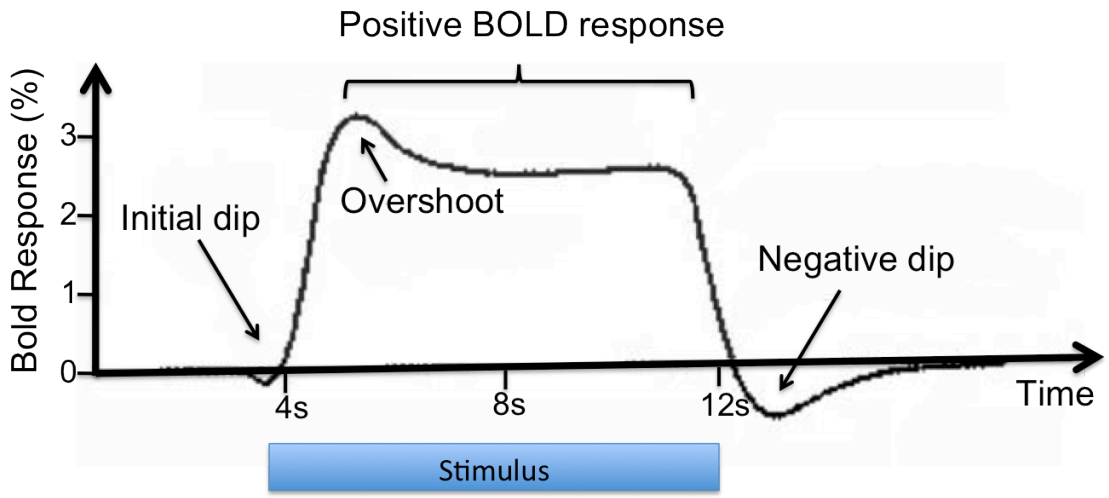

Figure 3.5: BOLD Response. A stable, positive BOLD signal is achieved 4-6 seconds after initiation of neuronal activity. Figure adapted from digitalmediatree.com

3.3.2 Echo Planar Imaging

Because the BOLD signal is fairly transient—on the order of seconds, rapid sequences are needed to capture the effect. One such acquisition technique is Echo Planar Imaging (EPI). EPI sequences are able to image the whole brain within seconds, allowing for meaningful comparisons between brain regions during periods of activity and rest. To exploit T2* effects, EPI sequences tend to use a long TE and a short TR of 2-3 seconds. As a consequence of this rapid acquisition, EPI suffers from a variety of imaging artefacts, such as ghosting and signal dropout. EPI also requires a relatively large voxel size: typically 2-5mm compared to the 1mm of structural scans. These and other limitations of EPI contribute to the overall limitations of fMRI, discussed further in Section 3.3.4

3.3.3 Image Analysis

Because of the artefacts inherent in MR imaging, and the additional artefacts introduced by EPI sequences, fMRI data must be processed prior to analysis. This section provides a brief overview of the preprocessing steps performed on fMRI

images, and outlines the subsequent statistical pipeline used to determine significant voxels. Though multiple image analysis software tools exist, this and all following sections focus on the tools contained within the FMRIB Software Library (FSL), the package of programs used to analyze the imaging data in this thesis (www.fmrib.ox.ac.uk/fsl).

3.3.3.1 Preprocessing

The reconstructed 4-D fMRI data sets (where the dimensions are x,y,z and time) are preprocessed within the FMRI Expert Analysis Tool (FEAT). Motion correction is performed using MCFLIRT (Jenkinson, Bannister, Brady, & Smith, 2002). This uses FMRIB's Linear Registration Tool (FLIRT) to align all of the volumes in the timeseries to the first image, compensating for motion caused by physiological factors (e.g., breathing) as well as mild head movements. B_0 unwarping, performed by FUGUE, uses fieldmaps to rectify the distortions caused by magnetic field inhomogeneities. Slice timing correction adjusts the timeseries for the individual slices within each brain volume, yielding the appearance of an instantaneous acquisition. A brain extraction tool (BET) is used to separate the brain from the skull and other non-brain tissue, so that analyses are performed only on the brain. Spatial smoothing of the data uses a Gaussian kernel to average out the noise within a signal, increasing the SNR. This step also ensures that the signal has a Gaussian spatial distribution, crucial to the statistical analysis performed later (Section 3.3.3.3). In addition to spatial smoothing, temporal smoothing is also performed. High pass temporal filtering removes low frequency artefact, such as that due to slow drift caused by temperature changes in the scanner.

Following these preprocessing steps, the fMRI data is analysed for each individual (first level) and for the group as a whole (higher level). First level analysis is performed using FMRIB's Improved Linear Model (FILM), and higher level statistics performed using FMRIB's Local Analysis of Mixed Effects (FLAME).

3.3.3.2 The General Linear Model (GLM)

The task-based activation paradigms used in Chapters 6 and 7 were based on a blocked ("box car") design, consisting of alternating 30 second rest conditions and 30 second active conditions. This basic design is then convolved with a haemodynamic response function (HRF) to allow for the temporal lag between neuronal activity and the ensuing vascular response. FILM follows a univariate approach to determine the extent to which the BOLD signal from each individual voxel resembles the task design. This is done following the approach of the general linear model (GLM):

$$y = \beta x + e$$

where y is the timecourse from the voxel, x represents the model (i.e., the explanatory variable—EV), β is the parameter estimate (the height of the signal from that voxel, which reflects how well the data is explained by the EV), and e is the remaining error. To determine how activation differs between two conditions (EV1 and EV2, e.g., active and rest), the parameter estimate of EV2 is subtracted from the parameter estimate of EV1, and the result is divided by the standard error of this new estimate. Such values are referred to as contrasts of parameter estimates (COPEs).

3.3.3.3 Single-Subject Statistics

Once the parameter estimates for each voxel have been calculated, it is then necessary to determine which of these voxels represent significant activation. This can be accomplished by thresholding the image at a probabilistic level. As a result of the GLM, each voxel has a probability associated with it (a p-value) that can be used for thresholding purposes. However, thresholding at a standard level of significance, e.g., $p<0.05$, would be inadequate due to the large number of voxels in the brain which necessitates multiple comparisons correction. Conventional methods, such as the Bonferroni correction in which the p-value threshold is divided by the number of tests (i.e., voxels in the brain), would be too stringent, as the voxels in the brain are not independent of each other (due to natural physiological factors as well as external factors such as spatial smoothing).

Statistical thresholding can also be performed by using Gaussian random field theory. In Gaussian random field theory, the smoothness of the image is estimated from the data, and this information is used to calculate the number of *independent* resolution elements, or 'resels'. The number or resels will always be smaller than the number of voxels. This smaller number is then used to correct for multiple comparisons. An additional thresholding method employing Gaussian random field theory, and the approach used in this thesis, is to detect statistically significant groups of activated voxels ("clusters"), rather than individual voxels. This cluster-based approach may better reflect the physiological response, as activated regions can typically be expected to span more than a single voxel. To perform cluster-based thresholding, the statistical map is thresholded at a manually specified value (typically around Z=2.3). The surviving clusters of voxels are then assigned a p-value according to the size of the cluster and the initial threshold.

3.3.3.4 Multi-Subject Statistics

Following first-level statistics, and before any multi-subject or multi-session analyses can be performed, individual data sets must be aligned to a standard template (in this thesis, the Montreal Neurological Institute (MNI) 152 brain). In Chapter 4, this is performed using a combination of FMRIB's Linear Image Registration Tool (FLIRT) and FMRIB's Nonlinear Image Registration Tool (FNIRT). Chapters 6 and 7 also use boundary based registration (BBR), (Greve & Fischl, 2009), a process which utilises image contrast across tissue boundaries. Registering each EPI dataset to standard space is performed in three general steps. First, the EPI images are registered to subject's T1-weighted structural image. The T1-weighted structural image is then registered to the standard image, also T1-weighted. Finally, these two transformations are combined and used to register the EPI image to the standard image. This final step also transforms the statistical maps generated in the first level analysis into standard space, to be used in later higher level analysis.

Higher level modelling uses variance estimation to assess group activation, and can be performed with either fixed effects (FE) or mixed effects (ME). FE modelling ignores between-subject and between-session variance, and thus inferences drawn from the results are applicable only to the sample studied. ME modelling does include between-subject and between-session variance, allowing for inferences about the wider population. This thesis employed ME modelling using FLAME. ME variance is the sum of FE variance (single subject, single session variance calculated at the first level) and random effects (RE) variance (cross-sectional variance). By combining measures of intra-subject variance with measures of between-subject variance, FLAME estimates the higher level parameter estimates

(essentially group mean activations) and the mixed effects variance separately for each group. Finally, statistical thresholding similar to that described in Section 3.3.3.3 is performed.

3.3.4 LIMITATIONS

As mentioned earlier, EPI sequencing is accompanied by various limitations, including signal dropout and larger voxel size (see Section 3.3.2). In addition to a diminished spatial resolution, the temporal resolution of fMRI is also limited. This is partially due to the temporal delay in the haemodynamic response. As the HRF is normally convolved with the model, the temporal lag itself is not a problem. The issue occurs due to the variability in the lag between individuals (Aguirre, Zarahn, & D'esposito, 1998) and in disease states, including stroke (Pineiro, Pendlebury, Johansen-Berg, & Matthews, 2002). The HRF models the behaviour of blood flow in response to neuronal activity, but it is worth noting that the degree to which increased blood flow as a result of heightened metabolic demand accurately reflects neuronal activity is still debated (Logothetis, 2002).

In addition to limitations stemming from the physical basis of fMRI, difficulties may arise from the analysis methods as well. In particular, fMRI is highly sensitive to head motion, particularly that which is correlated with the model (e.g., movement at the beginning of a task block). This is a particular concern when imaging stroke patients who may lack fine, independent motor control. Both gross movements and smaller head movements may be removed using independent component analysis (ICA), discussed further in Section 3.3.5.3. In performing higher level modelling, group analysis relies strongly on the integrity of the registration process. In particular, for activation to be significant, it must be spatially co-

localized across subjects, both anatomically and when the statistical maps are transformed into standard space.

3.3.5 MODEL-FREE ANALYSIS

In addition to using a model to compare activity changes between two or more conditions, fMRI data can also be used to investigate BOLD activity in a model-free manner. This is generally performed on data acquired from the resting brain, that is, when the scan was administered in the absence of a task. First established by Biswal and colleagues in 1995, resting state imaging examines low frequency fluctuations (generally <0.1 Hz) of the BOLD signal (Biswal, Yetkin, Haughton, & Hyde, 1995). Temporally correlated fluctuations between regions are thought to reflect underlying functional connectivity. A variety of methods have been employed to gain meaningful insights into resting state activity, including region of interest approaches, seed-based correlations, whole-brain analysis, and more recently, graph theory (see (Margulies et al., 2010) for a review). This thesis uses Independent Component Analysis (ICA) to probe resting state activity, a technique whose methods and applications are discussed further in the following sections.

3.3.5.1 Independent Component Analysis (ICA)

The ICA process does not require *a priori* definition of spatial or temporal inputs, and thus is a model-free method. ICA parcellates patterns of activation across the brain, producing as its output independent spatial component maps and their timeseries (Beckmann, DeLuca, Devlin, & Smith, 2005). In this thesis, ICA has been used in two separate ways: to generate resting state networks, and to remove artefacts from task fMRI data.

3.3.5.2 Resting fMRI

To generate resting state networks (RSN) via ICA, the Multivariate Exploratory Linear Optimized Decomposition into Independent Components (Melodic) tool was used (Beckmann & Smith, 2004). Following preprocessing and registration as detailed in sections 3.3.3.1 and 3.3.3.4, the fMRI datasets are analysed using a multi-session temporal concatenation approach. The images from all subjects are combined into a single 2D time x space data matrix, in which the subjects' data sets are "stacked" on top of one another (Figure 3.6). Melodic then decomposes this matrix into its component spatial maps and their corresponding timecourses. The number of components can be automatically estimated by Melodic, or constrained by user-defined input.

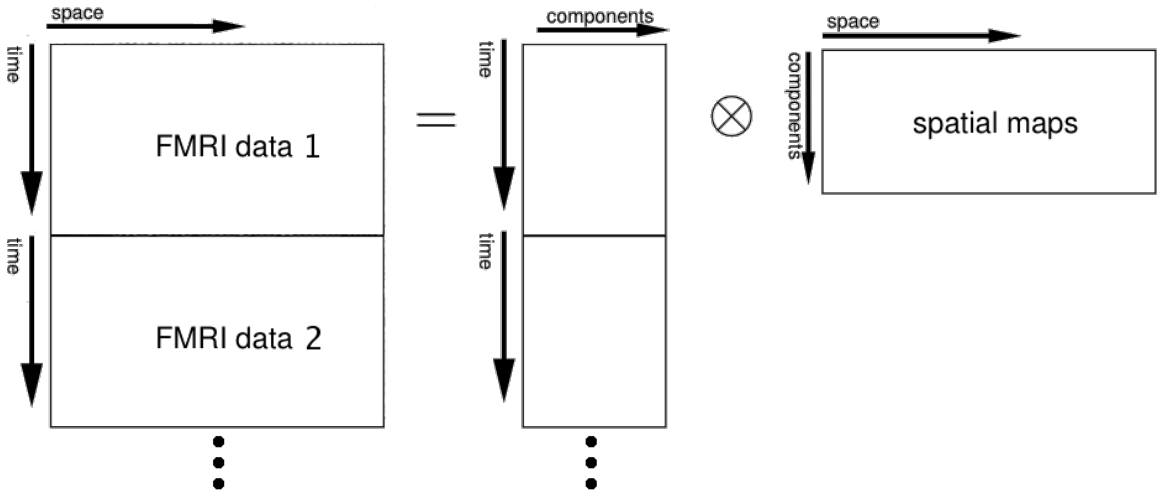

Figure 3.6: Schematic illustrating the pipeline for multi-session temporal concatenation analysis within Melodic. Figure from www.fmrib.ox.ac.uk/fsl

After the components are created from the group data, the components need to be identified from each individual's dataset. To accomplish this, a dual regression can be performed (Filippini et al., 2009). For each subject, the group-ICA spatial

maps are used as a spatial regressor in separate GLM analyses to extract a timeseries of the BOLD signal from the EPI data. This timeseries is then used as a temporal regressor in a second GLM to create the subject-specific spatial maps for each component. The resulting spatial maps for each component are then merged into a single 4D file containing all subjects, which can then be used to perform group statistics as described above.

Some of the components identified by the group-ICA will be those caused by artefacts (e.g., head motion), while others may represent resting state networks (RSN). Resting state networks are patterns of functional connectivity that have been found to correspond to various cognitive and sensory domains (Beckmann et al., 2005). Figure 3.7 shows eight of the most widely reported RSNs.

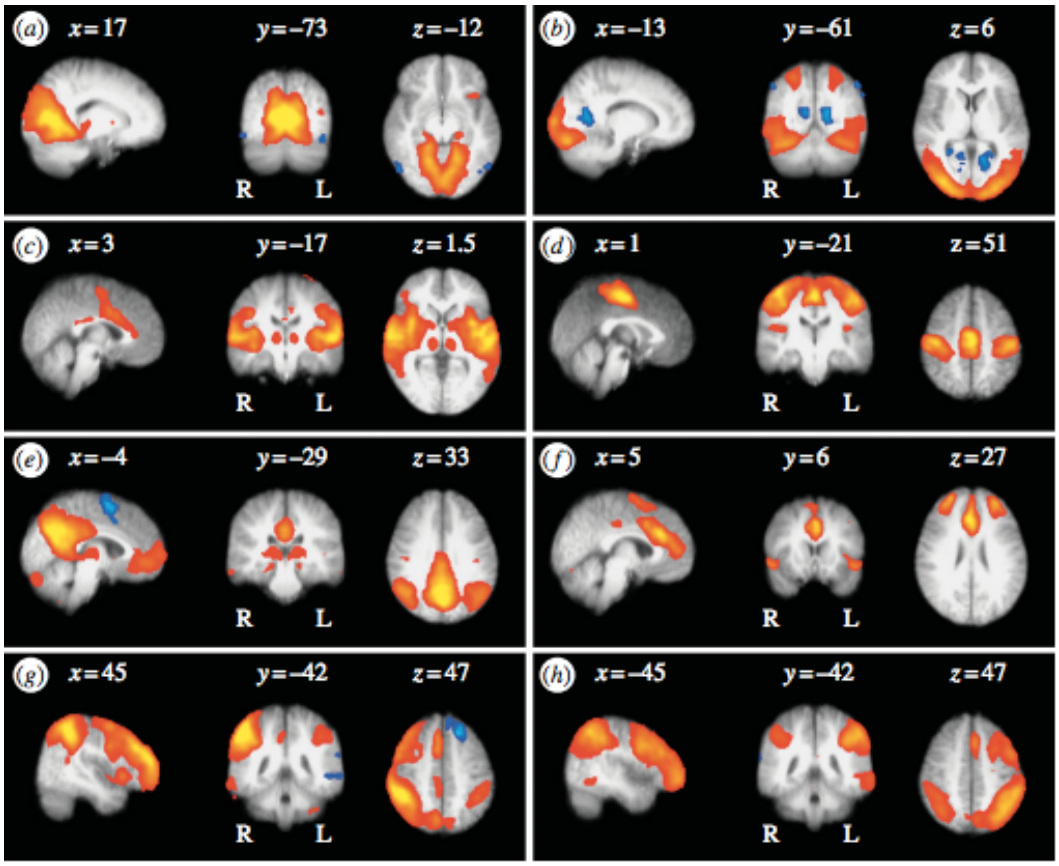

Figure 3.7: Image of the eight established resting state networks. (a) medial visual (b) lateral visual (c) auditory (d) motor (e) default mode (f) executive control (g) right dorsal visual stream (h) left dorsal visual stream. Figure from Beckmann et al., 2005.

RSNs have been identified as robust across individuals and imaging modalities (De Luca, Beckmann, De Stefano, Matthews, & Smith, 2006), and both behaviourally and clinically relevant (Rosazza & Minati, 2011). An important, and as yet unresolved, question is what the low-frequency fluctuations that support these networks actually represent. One current hypothesis is that they are a combination of conscious activity and prior memory traces that support subsequent behaviour (Buckner, 2010).

3.3.5.3 Task fMRI

While much of the interest in ICA has focused on resting state imaging, ICA can also be useful in task fMRI analysis to identify both task-related activity and artefactual structured noise. In this thesis ICA has been used with task fMRI data purely to denoise the data prior to model-based analysis of task-related signals. For ICA-based denoising, rather than performing a multi-session ICA as described above, a single-session ICA is run on each individual 4-D dataset. Visual inspection of the ICA output can then identify components that are primarily artefactual (Figure 3.8). Such components can be identified based on their spatial distribution (e.g., ringing around the brain, activation of an entire brain slice, streaking), timeseries (e.g., sudden, transient activation indicative of rapid head movement), or power spectrum (e.g., frequencies lying outside the range of biologically plausible BOLD fluctuations). These components can then be removed from the image prior to performing any statistical analysis, resulting in a cleaner dataset. Such "denoising" is of particular use in Chapters 6 and 7, when imaging the stroke population. However, overzealous denoising runs the risk of eliminating true activation, so the removal of components should be kept to a minimum as much as possible.

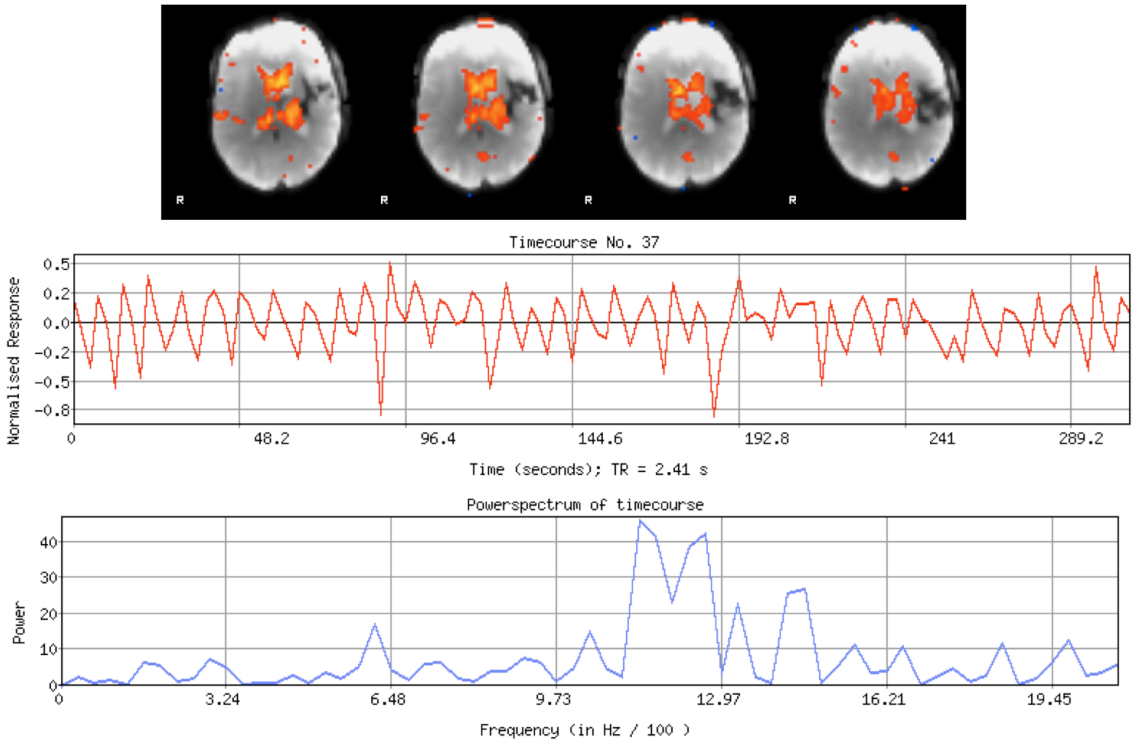

Figure 3.8: Example of artefactual activation identified by Melodic. Here, activation is primarily confined to the ventricles (note that the dark area on the left is the stroke infarct). Both the timeseries and powerspectrum are biologically implausible: the timeseries is too rapid; the powerpectrum is too high.

3.4 Diffusion MRI

Diffusion MRI is an imaging technique used in conjunction with our stroke patients in Chapter 7 of this thesis. It is used to measure global diffusion values across the whole brain, as well as to probe the structural integrity of specific white matter pathways.

3.4.1 Overview

Diffusion-weighted MRI is based on the movement of water molecules within the brain, which can either be freely moving or restricted. Freely moving water molecules are equally likely to move in any direction, called isotropic movement. This is the primary type of movement present in cerebrospinal fluid, and also predominates in gray matter (at conventional imaging resolution). Isotropic

movement contrasts with anisotropic movement in which molecular motion is restricted in one direction. This occurs when normal random motion is constrained by physical barriers, such as cell walls. Movement within healthy axons is primarily anisotropic, with movement progressing parallel to the axon and perpendicular movement being restricted.

3.4.2 DIFFUSION-WEIGHTING

The apparent diffusion coefficient (ADC) models the net displacement of molecules due to their diffusion. On an ADC map, areas of free diffusion appear bright, while areas of restricted diffusion are dark. Diffusion-weighted MR sequences are designed to capture differences in ADC by applying strong gradients on either side of the 180° RF pulse. These gradients are introduced along the axis in which the ADC is being measured. In this thesis, 60 different directions are used to allow for probabilistic modelling of diffusion properties (see Section 3.4.4). The phase of molecules with stationary spins (i.e., a low ADC) will be unaffected by the gradients yielding a high signal, whereas moving spins (i.e., a high ADC) will acquire a phase change that results in a low signal.

As explained in Section 3.1.2.3, extrinsic factors ultimately control the weighting of an image. The strength of the gradients determines the signal intensity of the diffusion-weighted image, the amplitude of which is modulated by the b-value. A sequence with a long TR and TE, and a b-value of 0 will produce a T2-weighted image. However, if the b-value is increased to between 500 and 1000 s/mm^2, the resulting image will be diffusion-weighted. Areas with a low ADC will have a high signal. That is, tissue in which movement is restricted and thus anisotropic will appear bright on a raw diffusion-weighted image, and vice-versa.

3.4.3 DIFFUSION TENSOR IMAGING

Following reconstruction of the raw diffusion-weighted data from the scanner, images are analysed using programs from FMRIB's Diffusion Toolbox (FDT). Preprocessing is performed to correct for subject motion and distortions caused by eddy currents. DTIfit is then run on these images to fit a diffusion tensor model to each voxel, which gives at its output multiple variables describing molecular movement at the voxel level. Fractional anisotropy (FA) measures the degree to which molecular diffusion is anisotropic, and assumes values from 0 (freely diffusing) to 1 (diffusion along one direction only). Intermediate values reflect more moderate degrees of directional preference.

In addition to producing values reflecting anisotropy, FDT also calculates the preferred diffusion direction in each voxel, using as its template the 3 axes of an ellipsoid. The long axis of the ellipsoid is the principal diffusion direction; the remaining 2 shorter axes describe its width and depth. These three axes can be modelled mathematically as eigenvectors (V), with their associated eigenvalues (λ) representing the strength of diffusion along that direction. The principal diffusion direction (V1) is the direction of the longest eigenvector. In addition to the principal diffusion direction, FDT also generates maps showing the secondary (V2) and tertiary (V3) diffusion directions. The mean diffusivity (MD) within a voxel is calculated by averaging the voxel's 3 eigenvalues (λ1, λ2, λ3). Statistical processing and analysis of FA, eigenvalues, and MD can then performed using Tract-Based Spatial Statistics (TBSS) (Smith et al., 2006).

3.4.4 PROBABILISTIC TRACTOGRAPHY

FDT can also be used to fit a probabilistic model of diffusion at each voxel and this can then be used to estimate white matter connectivity within the brain. Voxel-wise probabilistic modelling of diffusion properties is done with Bayesian Estimation of Diffusion Parameters Obtained using Sampling Techniques (bedpostx) and probabilistic tractography is then performed on the resulting outputs using probtrackx (Behrens, Johansen-Berg, Jbabdi, Rushworth, & Woolrich, 2007). Bedpostx models the local diffusion within each voxel, including those which contain multiple fibre orientations. It produces as its output estimates of the diffusion directions present, along with probability distributions on those estimates. As used in this thesis, probtrackx delineates the pathways originating in one user-specified seed region and terminating in a user-specified target region. Each voxel within the seed mask is used as a starting point for a probabilistic streamline, which proceeds to the target by sampling from the distribution of directions in each voxel that it encounters. Initiating multiple streamlines from each seed voxels produces a connectivity distribution for each voxel within the seed. The distributions from all seed voxels are summed to produce the a global connectivity distribution representing the connectivity from seed to target.

3.5 SPECIAL CONSIDERATIONS

3.5.1 PATIENT POPULATIONS

The MRI study contained in Chapters 6 and 7 was performed on patients with cortical and subcortical lesions due to stroke. Imaging this population presents unique challenges, both during the scanning session and when analysing the data. Patients with diminished motor control may move more during image acquisition,

resulting in increased artefacts that must be corrected or accounted for during initial data processing. All patients in our study exhibited motor deficits, although the degree of this impairment varied widely across subjects. As our experiment was primarily concerned with changes in motor performance, it was important to consider this diverse range of movement abilities when planning the task fMRI paradigm. Thus, rather than using patient-initiated, voluntary movements as the task, the affected limb was moved by the researcher. While this compromise allowed for the inclusion of patients with more severe levels of impairment, the conclusions drawn on externally versus internally mediated movements are not identical.

Moreover, the presence of stroke-induced lesions presents an additional challenge, as lesion location varied across participants. One method to compensate for these spatially-varying lesions is to mask out the lesion of each individual, performing statistics only on intact tissue within each patient. Lesions which impinge on white matter tracts increase the difficulty of interpreting DTI analyses, particularly when performing tractography.

3.5.2 LONGITUDINAL DESIGNS

The stroke study employed a longitudinal experimental design in which patients were scanned at multiple timepoints before and after the intervention. Compared to cross-sectional designs, longitudinal designs tend to have increased power. This is because longitudinal studies collect multiple within-subject datapoints, the variability of which is likely much smaller than the between-subject variability (Skup, 2010). However, longitudinal designs also carry the potential of additional confounds. As patients are seen over a period of several months, external

factors can change over the course of the study, influencing the experimental results. These may be variables related to the scanner itself, such as drift or hardware malfunctions, or variables related to the patients. In particular, it is important to ensure that patients do not begin any new therapies within the experimental timeframe that may affect both imaging and behavioural outcomes (e.g., additional physiotherapy, Botox injections). However, the randomised controlled design of the study presented here should mitigate the possibility of such confounds producing spurious results. An additional concern with longitudinal imaging of patients is the spontaneous resolution or worsening of pathology. Because we are imaging stroke patients who are well into the chronic recovery phase of their impairment, we would not expect any significant spontaneous changes to occur over the course of the study.

REFERENCES

Aguirre, G. K., Zarahn, E., & D'esposito, M. (1998). The variability of human, BOLD hemodynamic responses. *NeuroImage*, *8*(4), 360–369.

Ashburner, J., & Friston, K. J. (2000). Voxel-based morphometry--the methods. *NeuroImage*, *11*(6 Pt 1), 805–821.

Bandettini, P. A. (2009). What's new in neuroimaging methods? *Annals of the New York Academy of Sciences*, *1156*, 260–293.

Beckmann, C. F., & Smith, S. M. (2004). Probabilistic independent component analysis for functional magnetic resonance imaging. *IEEE transactions on medical imaging*, *23*(2), 137–152.

Beckmann, C. F., DeLuca, M., Devlin, J. T., & Smith, S. M. (2005). Investigations into resting-state connectivity using independent component analysis. *Philosophical transactions of the Royal Society of London. Series B, Biological sciences*, *360*(1457), 1001–1013.

Behrens, T. E. J., Berg, H. J., Jbabdi, S., Rushworth, M. F. S., & Woolrich, M. W. (2007). Probabilistic diffusion tractography with multiple fibre orientations: What can we gain? *NeuroImage*, *34*(1), 144–155.

Biswal, B., Yetkin, F. Z., Haughton, V. M., & Hyde, J. S. (1995). Functional connectivity in the motor cortex of resting human brain using echo-planar MRI. *Magnetic resonance in medicine : official journal of the Society of Magnetic Resonance in Medicine / Society of Magnetic Resonance in Medicine*, *34*(4), 537–541.

Bookstein, F. L. (2001). "Voxel-based morphometry" should not be used with imperfectly registered images. *NeuroImage*, *14*(6), 1454–1462.

Buckner, R. L. (2010). Human functional connectivity: new tools, unresolved questions. *Proceedings of the National Academy of Sciences of the United States of America*, *107*(24), 10769–10770.

De Luca, M., Beckmann, C. F., De Stefano, N., Matthews, P. M., & Smith, S. M. (2006). fMRI resting state networks define distinct modes of long-distance interactions in the human brain. *NeuroImage*, *29*(4), 1359–1367.

Draganski, B., & May, A. (2008). Training-induced structural changes in the adult human brain. *Behavioural brain research*, *192*(1), 137–142.

Driemeyer, J., Boyke, J., Gaser, C., Büchel, C., & May, A. (2008). Changes in gray

matter induced by learning--revisited. *PloS one*, *3*(7), e2669.

Filippini, N., MacIntosh, B. J., Hough, M. G., Goodwin, G. M., Frisoni, G. B., Smith, S. M., Matthews, P. M., et al. (2009). Distinct patterns of brain activity in young carriers of the APOE-epsilon4 allele. *Proceedings of the National Academy of Sciences of the United States of America*, *106*(17), 7209–7214.

Formica, D., & Silvestri, S. (2004). Biological effects of exposure to magnetic resonance imaging: an overview. *Biomedical engineering online*, *3*, 11.

Good, C. D., Johnsrude, I. S., Ashburner, J., Henson, R. N., Friston, K. J., & Frackowiak, R. S. (2001). A voxel-based morphometric study of ageing in 465 normal adult human brains. *NeuroImage*, *14*(1 Pt 1), 21–36.

Greve, D. N., & Fischl, B. (2009). Accurate and robust brain image alignment using boundary-based registration. *NeuroImage*, *48*(1), 63–72.

Hutton, C., Draganski, B., Ashburner, J., & Weiskopf, N. (2009). A comparison between voxel-based cortical thickness and voxel-based morphometry in normal aging. *NeuroImage*, *48*(2), 371–380.

Jenkinson, M., Bannister, P., Brady, M., & Smith, S. (2002). Improved optimization for the robust and accurate linear registration and motion correction of brain images. *NeuroImage*, *17*(2), 825–841.

Johansen-Berg, H. (2007). Structural plasticity: rewiring the brain. *Current Biology*, *17*(4), R141–4.

Logothetis, N. K. (2002). The neural basis of the blood-oxygen-level-dependent functional magnetic resonance imaging signal. *Philosophical transactions of the Royal Society of London. Series B, Biological sciences*, *357*(1424), 1003–1037.

Margulies, D. S., Böttger, J., Long, X., Lv, Y., Kelly, C., Schäfer, A., Goldhahn, D., et al. (2010). Resting developments: a review of fMRI post-processing methodologies for spontaneous brain activity. *Magma (New York, N.Y.)*, *23*(5-6), 289–307.

May, A., Hajak, G., Gänssbauer, S., Steffens, T., Langguth, B., Kleinjung, T., & Eichhammer, P. (2007). Structural brain alterations following 5 days of intervention: dynamic aspects of neuroplasticity. *Cerebral cortex (New York, N.Y. : 1991)*, *17*(1), 205–210.

McRobbie, D. W., Moore, E. A., Graves, M. J., & Prince, M. R. (2007). *MRI from Picture to Proton* (2nd ed. p. 406). Cambridge University Press.

Pineiro, R., Pendlebury, S., Johansen-Berg, H., & Matthews, P. M. (2002). Altered

hemodynamic responses in patients after subcortical stroke measured by functional MRI. *Stroke*, *33*(1), 103–109.

Ridgway, G. R., Henley, S. M. D., Rohrer, J. D., Scahill, R. I., Warren, J. D., & Fox, N. C. (2008). Ten simple rules for reporting voxel-based morphometry studies. *NeuroImage*, *40*(4), 1429–1435.

Rosazza, C., & Minati, L. (2011). Resting-state brain networks: literature review and clinical applications. *Neurological sciences : official journal of the Italian Neurological Society and of the Italian Society of Clinical Neurophysiology*, *32*(5), 773–785.

Schenck, J. F. (2000). Safety of strong, static magnetic fields. *Journal of magnetic resonance imaging : JMRI*, *12*(1), 2–19.

Shellock, F. G., & Crues, J. V. (2004). MR procedures: biologic effects, safety, and patient care. *Radiology*, *232*(3), 635–652.

Skup, M. (2010). Longitudinal fMRI analysis: A review of methods. *Statistics and its interface*, *3*(2), 232–252.

Smith, S. M., Jenkinson, M., Johansen-Berg, H., Rueckert, D., Nichols, T. E., Mackay, C. E., Watkins, K. E., et al. (2006). Tract-based spatial statistics: voxelwise analysis of multi-subject diffusion data. *NeuroImage*, *31*(4), 1487–1505.

Westbrook, C., Roth, C. K., & Talbot, J. (2005). *MRI in Practice (3rd Edition)* (3rd ed. p. 424). Wiley-Blackwell.

Wright, I. C., McGuire, P. K., Poline, J. B., Travere, J. M., Murray, R. M., Frith, C. D., Frackowiak, R. S., et al. (1995). A voxel-based method for the statistical analysis of gray and white matter density applied to schizophrenia. *NeuroImage*, *2*(4), 244–252.

Chapter 4: The Effect of tDCS to Primary Motor Cortex on Resting State Activity

The overarching aim of this thesis is to investigate how tDCS alters the underlying substrates engaged in performance of motor behavior and learning. The imaging correlates of tDCS-induced modifications in brain activity are fairly well documented during task performance, but have only recently been studied in the resting brain. Examining resting activity affords the opportunity to understand how tDCS modifies intrinsic connectivity within the brain, which may in turn influence the processing of motor tasks. This first experiment explores how tDCS affects resting state activity on a global, yet network-specific, level.

4.1 INTRODUCTION

Transcranial direct current stimulation has found therapeutic use in the treatment of a variety of motor disorders (Fregni & Pascual-Leone, 2007), yet our understanding of how tDCS affects basic brain function is still incomplete. In the resting brain, it has been shown that tDCS applied to M1 affects the subsequent physiology (Nitsche & Paulus, 2000) and neurotransmitter profile (Stagg et al., 2009a) of M1. However, the ability of tDCS to modify large scale networks beyond M1 is yet to be firmly established in the resting brain. Task fMRI has revealed that tDCS alters *task-based* activity across the sensorimotor network (Stagg, 2009b), but it is difficult to disentangle the effects of tDCS from the effects of task performance itself. That is, because anodal tDCS generally improves behaviour, and cathodal tDCS often worsens behaviour (Nitsche et al., 2003; Stagg et al., 2011), it is unclear whether the modifications in activation patterns are caused purely by tDCS application, or by the differing levels of motor performance.

One way to examine the effects of tDCS on functional networks without the potentially confounding effects of the task is to employ resting state imaging. Resting fMRI has yielded behaviourally and clinically relevant insights into functional brain networks (Rosazza & Minati, 2011). A variety of imaging methods and modalities can be used to investigate changes in the functional connectivity and organization of the resting brain (Margulies et al., 2010), such as those that occur in response to tDCS. For example, region-of-interest approaches have revealed changes that occur within predefined, specific brain areas following tDCS to M1, including reorganization within M1 (Polanía et al., 2012), secondary motor areas (Antal et al., 2011), and subcortical structures (Polanía et al., 2011a). Similar seed-based studies use a predefined model—such as changes in activity found within M1, to identify additional regions that exhibit an analogous pattern of change (Alon et al., 2011). Whole brain analyses have been employed to extract global changes in resting state activity, via fluctuations in regional cerebral blood flow (Lang et al., 2005), or changes in nodal connectivity as elucidated by graph theory (Polanía et al., 2011b).

The present experiment builds upon these results by examining resting state activity using both ROI-based correlation approaches to assess interhemispheric interactions within the motor system, and Independent Component Analysis (ICA) (Beckmann et al., 2005) to explore functional connectivity changes across the whole brain. ICA is a model-free method that parcellates patterns of activation across the brain, producing as its output networks representing various cognitive and sensory domains. Thus, it capitalizes on the advantages of both ROI and whole brain analyses, while eliminating some of their shortcomings. Like ROI-based analysis, the identified resting state networks (RSN) are functionally distinct; unlike ROI or seed-

based analyses, the ICA method does not require *a priori* definition of spatial or temporal components. ICA is a whole-brain analysis technique, but one that affords the opportunity to draw conclusions on intrinsic brain networks—such as motor, executive control, or the default mode, rather than distinct areas of the brain that may not be functionally connected (van den Heuvel & Hulshoff Pol, 2010).

Previously, ICA has been used to examine how tDCS to the DLPFC affects resting state fMRI networks (Keeser et al., 2011; Peña-Gómez et al., 2011). However, to date, there have been no studies using ICA to examine the effects of tDCS to M1 on such networks. An MEG study by Venkatakrishnan and colleagues used ICA to investigate the effects of tDCS to M1 on resting state MEG activity, but did not look within any of the 'canonical' networks, and found no difference between anodal and cathodal stimulation (Venkatakrishnan et al., 2011). This difference in approach may partially be explained by the fact that resting state networks are more thoroughly characterized for BOLD fMRI, and have only recently been correlated to networks found with MEG (Brookes et al., 2011).

The present study assessed how anodal and cathodal tDCS to M1 modify resting state functional connectivity between motor areas and across the whole brain. Given the interconnected nature of motor cortical regions, and the ability of anodal and cathodal tDCS to increase and decrease neuronal excitability, respectively, we hypothesized that anodal tDCS to M1 would result in concomitant increases of activity across the motor network, while cathodal tDCS would have the opposite effect, decreasing motor network strength.

4.2 METHODS

4.2.1 OVERVIEW

Data was collected by other members of the research group in 2009. During each of the three sessions, participants received either anodal, cathodal, or sham tDCS in the scanner. Prior to and following tDCS, ten minutes of resting state fMRI data was acquired, during which time subjects were instructed to relax and keep their eyes closed. During the sham tDCS session, subjects also performed a motor task following the final resting state scan. The order of the sessions was randomly determined for each subject, and counterbalanced across the group. Experimental sessions were separated by at least 48 hours and real tDCS sessions by at least 1 week. Subjects were blind to the type of stimulation they received in any session.

4.2.2 SUBJECTS

Eleven healthy, right-handed subjects (age 21-24, mean age 22.9, 7 female) participated in this study, in accordance with local ethics committee approval. Due to personal reasons, one subject completed the cathodal and sham, but not anodal, sessions.

4.2.3 TDCS ADMINISTRATION

Prior to entering the scanner, tDCS electrodes were fitted to the participant's scalp. The stimulating electrode was centred over the dominant (left) motor cortex, as measured to be 5 cm lateral and 2 cm anterior to Cz. The reference electrode was placed over the right supraorbital ridge. Both electrodes were affixed to the scalp using high chloride EEG paste as a conducting medium (Eldith, Germany). The

electrodes were secured to the head using rubber straps. To ensure that the electrodes did not move while subjects lay in the scanner, a snugly fitting swimming cap was worn. The subjects were then positioned in the scanner, ensuring that the electrode wires contained no loops and ran parallel to the body without touching it. To administer anodal and cathodal tDCS, a DC stimulator (Magstim Eldith, Germany) gradually generated a 1 mA current over 10 seconds. This current was administered for 10 minutes, after which time it was slowly ramped down over 10 seconds. During the sham condition, after the initial 10 second ramp up period, the DC stimulator was turned off.

4.2.4 Behavioral Task

Upon conclusion of the sham stimulation session, subjects performed a sequence learning task while EPI data were acquired. This served as a localizer for motor activation, which was ultimately used to define functional ROIs of motor areas (see below). Subjects held a button-box in their right hand, and Presentation (Neurobehavioral Systems) was used to display four horizontal bars, each of which corresponded to a button on the button-box. The subjects were told that when a bar changed into an asterisk, they were to press the corresponding button as quickly as possible. They were also informed that these button presses would form a sequence that was 10 cues long, and that they should try to learn the sequence.

4.2.5 Image Acquisition

All scans were acquired on a 3T Varian Scanner. In brief, two resting state scans and a field map were acquired for each session. One T1-weighted scan was also acquired for registration purposes. T1-weighted axial anatomical images were

acquired for each subject using a 3D Turbo Flash sequence (TR=13ms, TE=4.9ms, flip angle=8, FOV=256x256). Axial echo-planar volumes were acquired during the resting state scans using a 4 channel head coil (TR=3000ms, TE=28ms, FOV=192x192). During the sham session, an additional axial echo-planar scan was acquired while the subject performed the behavioural task described above, using the same sequence parameters.

4.2.6 IMAGE ANALYSIS

PREPROCESSING. All image analysis steps were performed using tools from the FMRIB Software Library (FSL, www.fmrib.ox.ac.uk/fsl). Prior to beginning statistical analysis on the resting state scans, the following preprocessing steps were taken: Motion correction using MCFLIRT (Jenkinson et al., 2002); B0 unwarping with fieldmaps using FUGUE; spatial smoothing with a Gaussian kernel of 5mm; and highpass temporal filtering at 150 seconds to remove low frequency artefacts. Registration to individual T1-weighted structural images and standard MNI space was performed using FLIRT and FNIRT.

ROI-BASED ANALYSIS First, anatomical ROIs were defined on a standard-space brain as previously for the primary motor cortex (M1), hand area of the M1, PMC and SMA as follows:

-*Primary motor cortex (M1):* Lateral and medial half of the anterior bank of the central sulcus, extending from the dorsal surface of the lateral ventricles to the top of the brain.

-*Hand area of M1:* The knob of the precentral gyrus, posterior to the junction of the superior frontal sulcus with the precentral sulcus.

-*Premotor cortex (PMC):* Precentral gyrus and precentral sulcus, extending from the dorsal surface of the lateral ventricles to the top of the brain.

-*Supplementary motor area (SMA):* The medial surface of the brain above the cingulate sulcus posterior to the vertical plane above the anterior commissure (VCA line) and anterior to the vertical plane above the posterior commissure (VCP line).

Then, functionally defined motor regions of interest were created from the EPI images acquired during performance of the behavioural task following the sham stimulation session. The task EPI data was preprocessed as outlined above. Statistical analysis was carried out using FILM with local autocorrelation correction (Woolrich et al., 2001). FEAT was used to create activation maps for each individual (Beckmann et al., 2003), and the resulting Z statistic images were thresholded at $Z>2.0$ with a corrected cluster extent threshold of $p<0.01$. For each pre-defined anatomical region, functional ROI masks were created for each subject by dilating the maximally active voxel within each anatomical ROI to produce a spherical ROI within a fixed volume of 8x8x8 mm centred on the peak voxel. As the task-induced activation was primarily left lateralized, functional ROI masks were created for the left hemispheric ROIs, then flipped about the y-axis to create right hemispheric ROIs.

Using as masks the functionally defined ROIs for M1, the hand area, PMC, and SMA, the timecourse of the resting BOLD signal was extracted from each subject's images for each stimulation condition (i.e., anodal, cathodal and sham) and timepoint (i.e., pre and post stimulation). The resulting timecourses were then correlated between hemispheres for each ROI (e.g., left-M1 with right-M1), to give a

measure of inter-hemispheric functional connectivity. Statistical analysis of all extracted values were carried out in SPSS (IBM, version 19.0.0).

INDEPENDENT COMPONENT ANALYSIS. Preprocessed resting state scans were then analysed using independent component analysis (ICA), implemented by MELODIC (Beckmann & Smith, 2004). Initially, all scans from all sessions were combined and run in a group ICA using the temporal concatenation method within MELODIC, constrained to identify 25 components. Individual components were visually inspected to determine which resting state networks they resembled, with reference to previous descriptions of typical resting networks (Beckmann et al., 2005). The identified networks were confirmed using an automated approach by calculating the spatial correlation with standard masks of those networks, as described previously (Beckmann et al., 2005). A dual-regression approach (Filippini et al., 2009) was then taken as follows: Group-defined RSNs were used as a regressor in separate GLM analyses to extract a timeseries of the BOLD signal from the EPI data from each subject and each session independently. Each individual timeseries was then used in a second GLM to extract the spatial maps that corresponded to each RSN timecourse for each subject and session separately.

Permutation-based statistics were run on these individually defined resting networks, using "randomise" as implemented within FSL to create within and between condition activation maps for each network. The resulting t-statistic images were thresholded at $t>2.0$, and significant clusters defined at a corrected cluster extent threshold of $p<0.05$.

Additionally, the mean resting BOLD signal was extracted from each of the binarized MELODIC-defined resting networks to determine their overall strength.

4.3 RESULTS

ROI analysis: Cathodal tDCS Increases the Correlation of Motor Activity Between Hemispheres

We investigated whether M1 tDCS caused changes in the correlation of resting BOLD signal between motor cortical areas. We specifically investigated M1, the hand area of M1, SMA, and PMC of the left and right hemispheres.

Correlations in the timeseries of resting activity between the left and right M1, hand area, SMA, and PMC were determined for each subject, before and after each type of stimulation. For statistical analysis, to ensure normality of the data the resulting r-values were transformed into Z scores using the Fisher r-to-Z transformation (Figure 4.1). These Z scores were entered into a RM-ANOVA with one factor of ROI (the hand area, PMC, SMA), one factor of Stim (anodal, cathodal and sham) and one factor of time (pre and post). There was a significant ROI x Stim x Time interaction ($F(4, 36)= 3.319$, $p= 0.021$). To determine what stimulation condition was driving this three-way interaction, separate RM-ANOVAs were performed for anodal or cathodal stimulation versus sham (ROI x Stim x Time). When comparing anodal to sham stimulation, there were no significant interactions. When comparing cathodal to sham, there was a significant ROI x Stim x Time interaction $F(2, 20)= 4.001$, $p= 0.035$. To determine in which ROIs these effects were occurring, RM-ANOVA were then performed for each ROI separately (Stim x Time). There was a significant Stim x Time interaction for the hand area of M1 and SMA (hand: $F(1, 10)= 9.874$, $p= 0.010$; SMA: $F(1, 10)= 9.041$, $p= 0.013$). t-tests between the left and right hand area, and left and right SMA before and after cathodal stimulation showed a significant increase in interhemispheric connectivity

in both regions (hand: t(10)= 4.591, p= 0.001; SMA: t(10)= 2.874, p=0.017). In addition, a strong trend toward an increase in interhemispheric connectivity was found for the PMC (t(10)= 2.123, p= 0.060; Figure 4.1).

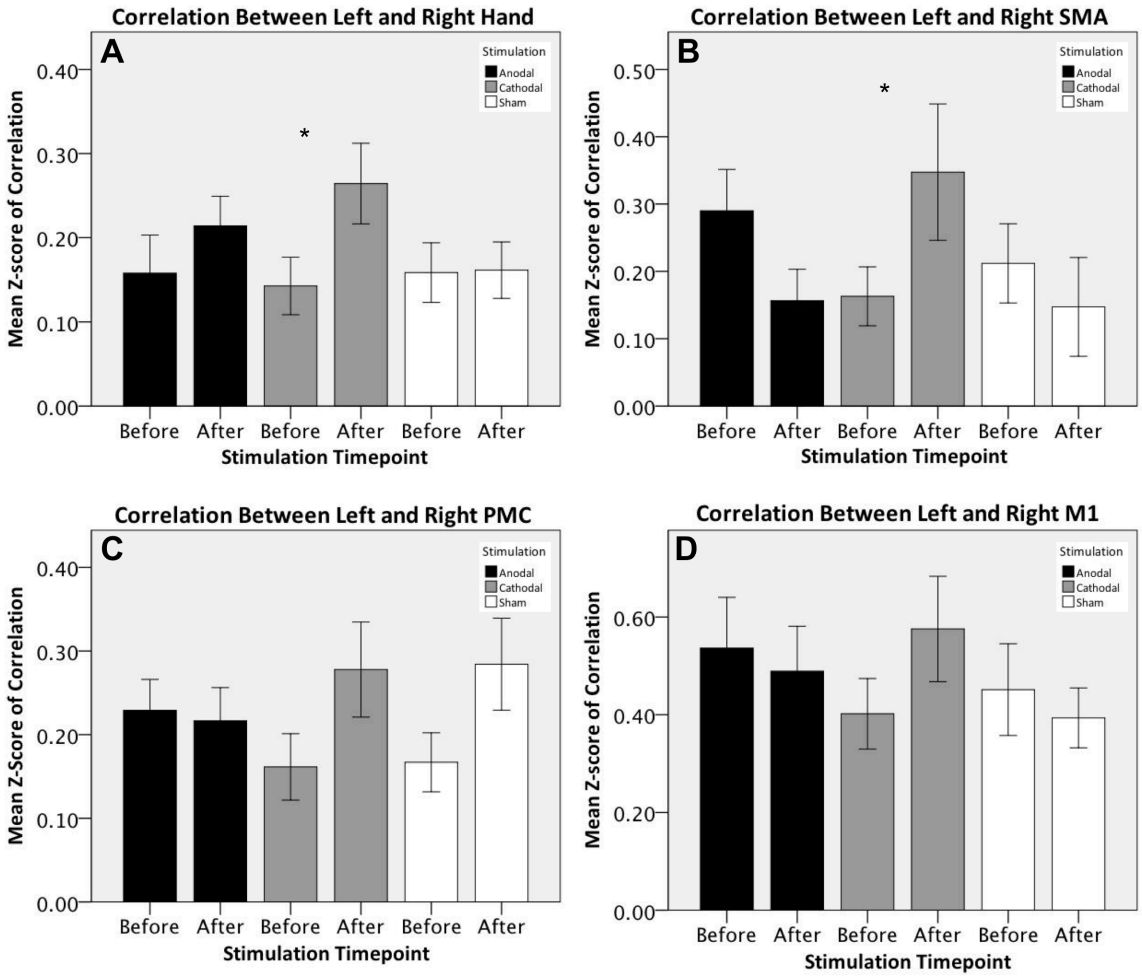

Figure 4.1: Cathodal stimulation significantly increases the correlations between left and right hand area of M1 and the left and right SMA. Increases were also observed in other regions; these showed a trend for PMC and were nonsignificant for M1. Black bars, anodal; gray bars, cathodal; white bars, sham. Error bars ±1 SEM.

ICA generation of resting state networks

From the MELODIC output, eight components were identified that corresponded to the motor, default mode, medial visual, lateral visual, executive control, auditory, right dorsal visual stream, and left dorsal visual stream resting state networks as previously described (Figure 4.2).

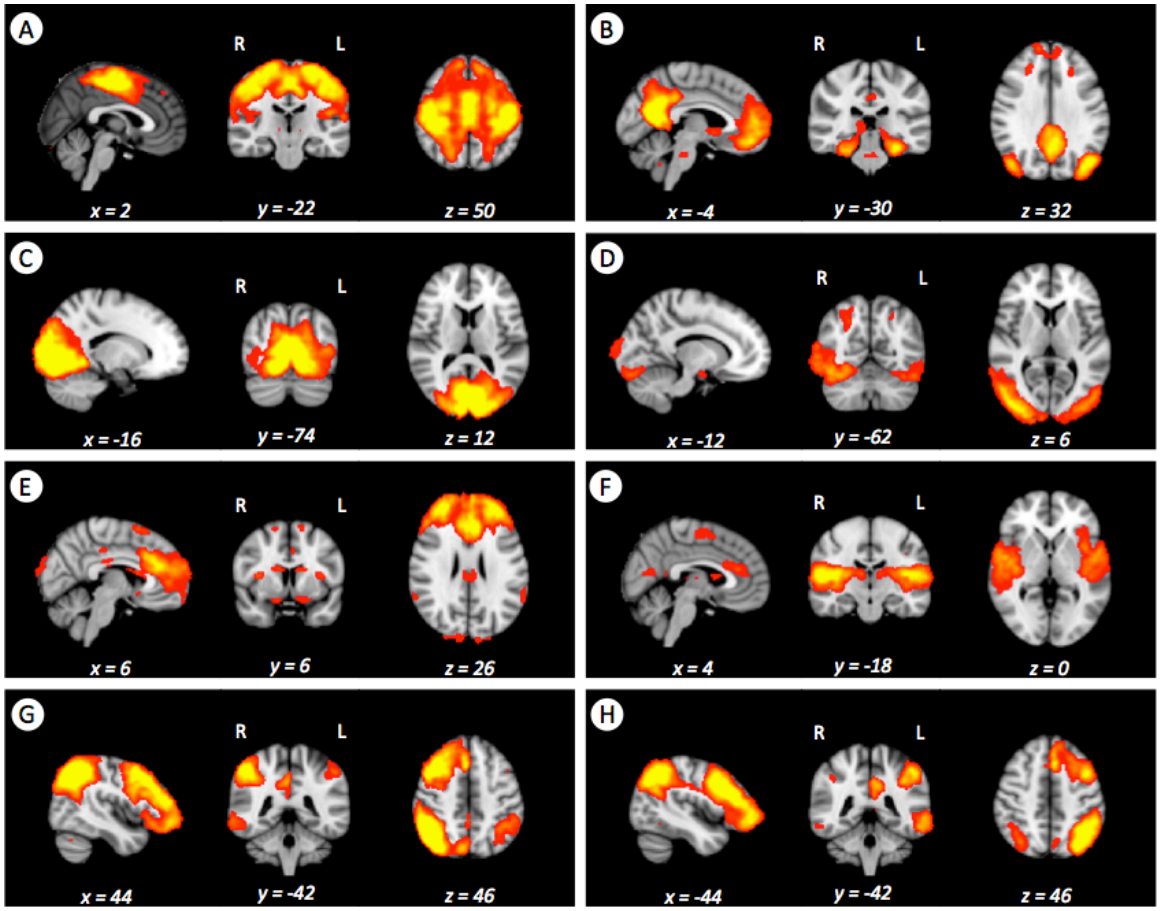

Figure 4.2: Melodic ICA generated resting networks. Sagittal, coronal, and axial views of different spatial maps corresponding to the eight established resting state networks. A) motor (0.69), B) default mode (0.42), C) medial visual (0.70), D) lateral visual (0.56), E) executive control (0.49), F) auditory (0.47), G) right dorsal visual stream (0.44), H) left dorsal visual stream (0.60). Correlation values of each RSN with its canonical RSN are listed in parentheses. Images are presented in MNI space; coordinates are mm from the anterior commissure.

Cathodal tDCS Increases the Overall Strength of the Default Mode Network

We then tested whether tDCS could modify the overall strength of resting state networks. The mean resting activity in each of the 8 identified networks (Figure 4.2), before and after each period of stimulation (anodal, cathodal, sham), was compared. A RM-ANOVA (RSN x Stim x Time) found an RSN x Stim interaction ($F(14,126)= 1.860$, $p= 0.037$) suggesting that the effects of stimulation varied between RSNs. Subsequent RM-ANOVAs comparing anodal to sham, and cathodal to sham were run for each RSN. There was no significant effect of tDCS on any network

when comparing anodal to sham. When comparing cathodal to sham, the only RSN where there was a significant effect of tDCS was the default mode network (DMN), which showed a Stim x Time interaction ($F(1,10)= 5.977$, $p= 0.035$) (Figure 4.3A). Paired t-tests on the mean DMN strength before and after stimulation found a significant increase in resting activity following cathodal tDCS ($t(9)= 3.046$, $p= 0.012$), but not following anodal or sham tDCS (anodal: $t(9)= 1.543$, $p= 0.157$; sham: $t(10)= 0.725$, $p= 0.485$). As we had an *a priori* hypothesis for the effects of tDCS on the motor network, although no significant effects of tDCS were identified on resting activity changes within the motor network, we investigated polarity-specific effects within this network. This analysis revealed a trend toward increased resting activity following anodal stimulation (anodal: $t(9)= 1.993$, $p= 0.077$; cathodal: $t(10)= 1.401$, $p=0.191$; sham: $t(10)= 0.221$, $p=0.830$). The results of this exploratory analysis are shown in Figure 4.3B.

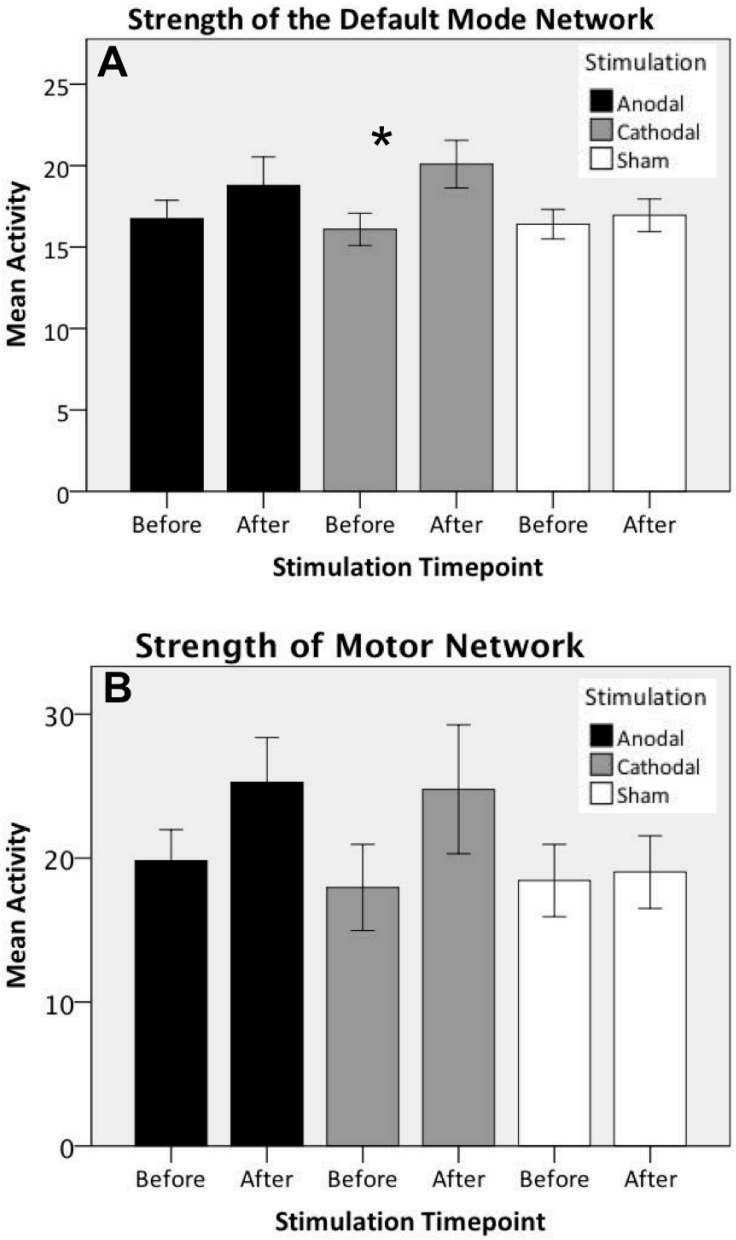

Figure 4.3: Cathodal tDCS increases the strength of the default mode network. A) Default mode network. A significant ($p < 0.05$) increase in activity in the DMN can be seen following cathodal, but not anodal or sham, tDCS. B) Motor network. The strength of the motor network is not significantly changed over time by tDCS, although a trend towards an increase was demonstrated with anodal tDCS. Error bars: ±1 SEM.

Cathodal tDCS Increases Connectivity within the Motor and Default Mode Networks

Positing that stimulation may increase connectivity between specific areas of the resting state networks in addition to (or independent of) affecting the overall strength of the network, we ran an exploratory voxel-wise whole brain analysis

comparing pre and post stimulation resting activity in the motor and default mode networks for each stimulation type. Cathodal stimulation led to significant increases in connectivity for specific clusters within both the motor and default mode networks (Figure 4.4). No significant changes were found for equivalent whole brain analysis of anodal or sham stimulation. For exploratory purposes, we plotted the extracted parameter estimates before and after each stimulation type from voxels within the clusters that showed significant changes due to cathodal stimulation (Figure 4.5). There was no evidence for change in these clusters following anodal or sham stimulation.

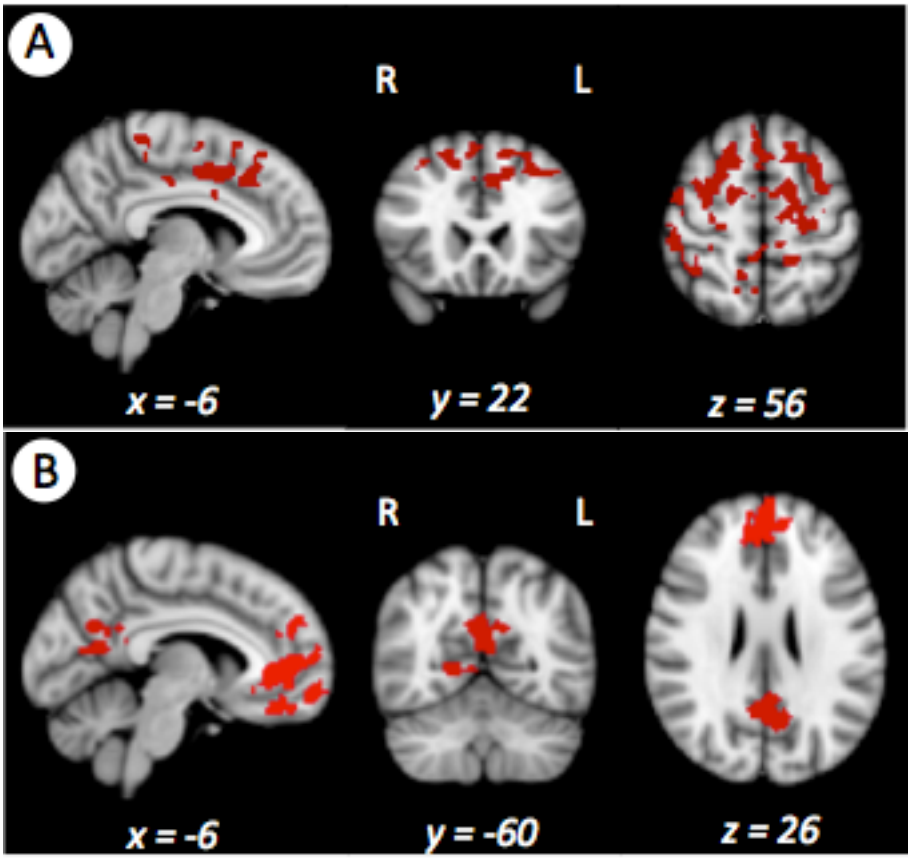

Figure 4.4: Cathodal stimulation modifies connectivity between specific areas of the motor and default mode networks. A) Motor network, B) Default mode network. T-statistic images of increases due to cathodal stimulation in the RSN. Images are in MNI space; coordinates are mm from the anterior commissure.

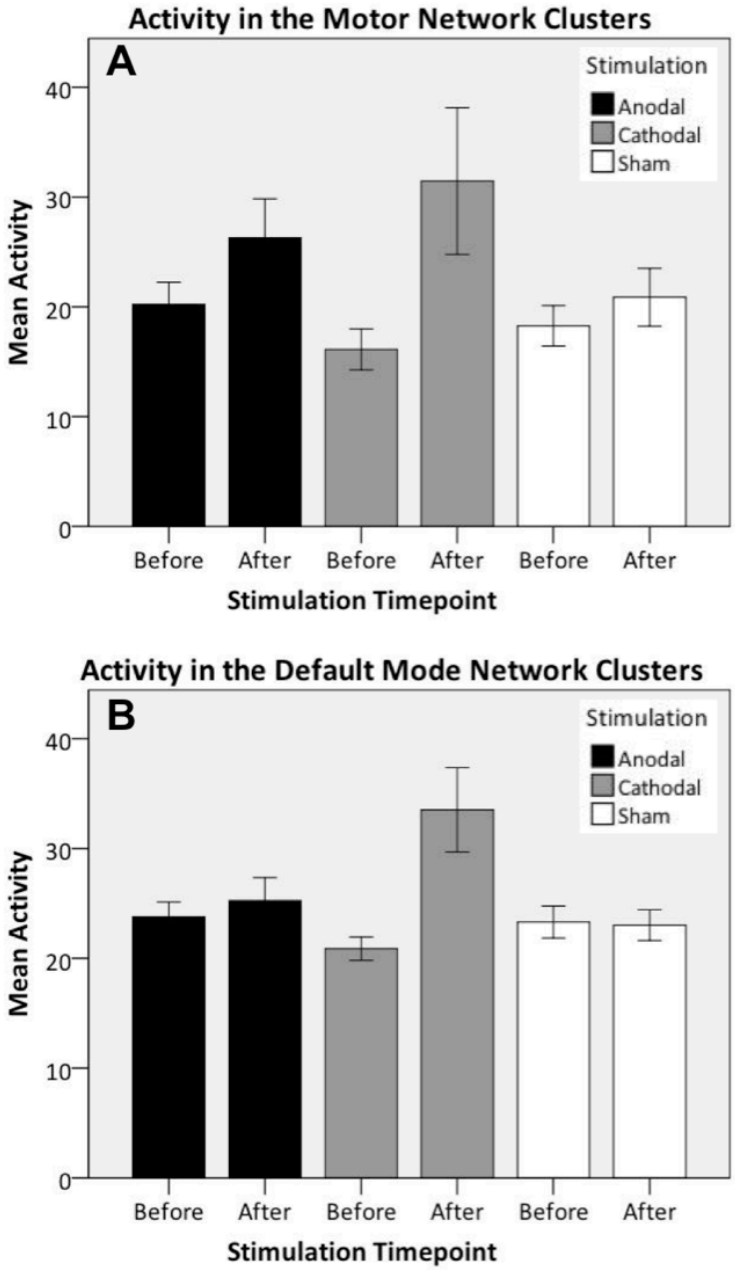

Figure 4.5: Clusters which showed increased connectivity after cathodal stimulation did not show any evidence for significant change after anodal or sham stimulation. A) Motor network, B) Default mode network. Bar graphs represent the amount of activity in the clusters shown in Figure 4.4 before and after anodal, cathodal, and sham stimulation. Error bars ±1 SEM.

4.4 DISCUSSION

This study demonstrated that tDCS to the motor cortex modulates resting state activity in a polarity and network-specific manner. These effects were primarily found when cathodal tDCS was applied to M1. A region of interest analysis probing the coherence of activity between major nodes within the motor network (M1, the hand area, SMA, and PMC) between hemispheres found increased interhemispheric connectivity between the hand areas and SMAs following cathodal tDCS. An ICA analysis identified the major resting state networks and found that cathodal tDCS increased the overall strength of the default mode network (DMN), and increased functional connectivity for specific regions within both the DMN and the motor network. No significant results were found in any of these analyses when probing the effects of anodal tDCS.

Though the overall strength of the motor network was not significantly modulated by tDCS, the ROI analysis revealed increased interhemispheric functional connectivity within the network following cathodal stimulation. Specifically, we found an increase in correlations between the left and right hand area of M1, and left and right SMA following cathodal tDCS. We did not, however, find evidence for changes in interhemispheric functional connectivity following anodal tDCS for any ROI. These results contrast with previous findings concerning changes in resting motor activity following anodal tDCS. Alon and colleagues reported a decrease in interhemispheric interactions between the left and right M1 after anodal tDCS, though they did not test cathodal stimulation (Alon et al., 2011).

The discrepancy between the anodal tDCS results from Alon's study and ours may be due to a variety of factors. First, Alon found significant effects when using transcranial pulsed current stimulation (tPCS), noting only a trend when tDCS, the

stimulation method we employed, was applied. Additionally, the present study compares resting activity before and after stimulation, while the Alon study compares resting activity before stimulation to resting activity *during* stimulation. As the neurophysiological basis of the effects of tDCS during and after stimulation differ (Stagg & Nitsche, 2011), our two studies may be investigating essentially different mechanisms. Moreover, the experimental setups of the two studies varied widely. We followed a "Rest – Stimulation – Rest" design, while the Alon study used a "Rest 1 – Task – Stimulation 1 – Rest 2 – Stimulation 2" design. They found significant effects when comparing Stimulation 2 to Rest 1. If the stimulation block is compared to the rest block immediately preceding it (i.e., Stimulation 2 to Rest 2), there is no effect. In the intervening 20 minutes between the end of Rest 1 and the beginning of Stimulation 2, the subjects performed a finger-thumb opposition task. It is possible that the performance of the motor task may have metaplastically raised the threshold for LTP induction, favouring the induction of LTD, and thus modifying the subsequent effect of stimulation (Iezzi et al., 2008). Indeed, the largest sequential change in resting activity correlation is seen between Rest 1 and Stimulation 1 (between which the task was performed, with no imaging acquired). This raises the possibility that it may have been performance of the task, rather than stimulation, that lead to the reported decrease in coherent activity between left and right M1.

The incongruence between the scale of action of anodal and cathodal tDCS in the current study may partially be due to the functional architecture of M1. A study investigating stimulation-mediated reorganization within M1 found that cathodal tDCS increased local connectedness in the hand area, but not globally across M1; anodal tDCS had the opposite effect, increasing long distance connections across M1

but not local connectedness (Polanía et al., 2012). Our result of increased interhemispheric synchronization between the hand areas, but not M1 as a whole, following cathodal tDCS is in accord with this finding. It has been proposed that such modifications in connectivity and synchronization are the result of changes in the signal to noise ratio (SNR) (Polanía et al., 2012). Cathodal tDCS causes neuronal hyperpolarization and decreased spontaneous firing (Bindman et al., 1964), effectively decreasing neuronal noise (Antal et al., 2004). This may result in increased SNR from the stimulated area, promoting better communication with other regions and increasing synchronization (Polanía et al., 2011b).

How might the increased synchronicity between hemispheres documented in this study translate to the detrimental behavioural effects seen on unimanual motor learning tasks following cathodal tDCS? Such unimanual movements recruit contralateral motor areas, with ipsilateral signals effectively treated as noise (Cincotta & Ziemann, 2008). During unimanual task performance, contralateral motor regions are positively modulated, while ipsilateral areas are inhibited (Grefkes et al., 2008). The increased signal from contralateral areas, combined with decreased noise from ipsilateral areas, results in improved efferent SNR from the contralateral motor area. This may lead to more efficient synaptic transmission and, ultimately, faster motor execution (Grefkes et al., 2008). Cathodal tDCS, by synchronizing activity between the hand areas of the two hemispheres, may interfere with the ability of intrinsic mechanisms to perform this decoupling, resulting in impaired motor performance. Such work also suggests that the SMAs, and to a lesser extent the PMCs, mediate these interhemispheric interactions, modulating M1 activity in favour of the hemisphere responsible for the unimanual movement (Grefkes et al., 2008). Our study documented increased correlations

between activity in the SMAs following cathodal tDCS, and a similar trend in the PMCs. This may reflect the SMA of both hemispheres working in concert to promote activity within both motor cortices, rather than the contralateral cortex exclusively.

Our findings also report an unexpected increase in strength of the DMN following cathodal tDCS. The DMN is thought to underlie processes necessary for passive cognitive states, such as introspection and "mind wandering" (Broyd et al., 2009; Rosazza & Minati, 2011). In line with this, and in contrast with other RSNs, the DMN exhibits increased activity during rest and decreased activity during task performance (Raichle et al., 2001). As such, it has been labelled as a task-negative network, the deactivation of which allows task-positive networks to more effectively facilitate task performance (Peña-Gómez et al., 2011). Indeed, increases in DMN activity have been shown to precede and predict worsened performance on behavioural tasks (Eichele et al., 2008; Li et al., 2007; Weissman et al., 2006). The default mode interference hypothesis proposes that overactivity of the task-negative component of the DMN results in attentional lapses during goal-directed actions, increasing error rates (Mason et al., 2007; Sonuga-Barke & Castellanos, 2007). Studies investigating the effects of tDCS on motor performance often find that cathodal tDCS impairs motor learning and behaviour (Stagg et al., 2011). Taken together, these results suggest that cathodal tDCS may worsen motor performance via the DMN in two complementary ways. First, increased task-negative activity might interfere with the ability of task-positive networks (e.g., the motor network) to execute the behavioural task. Secondly, impaired top-down control caused by increased DMN strength may result in more attentional lapses, contributing to the reduction in motor learning apparent during cathodal stimulation.

While this experiment expands upon those that preceded it, namely by the inclusion of both anodal and cathodal tDCS, and the use of ICA to define resting state networks, room remains for future development. One confound of this study originates from the electrode configuration itself: anodal tDCS to M1 simultaneously delivers cathodal stimulation to the prefrontal cortex, and vice versa for cathodal tDCS. This is not a critique of the present experiment exclusively, as any study using a similar electrode montage must contend with the same duality. However, it is particularly pertinent in the interpretation of results from this study, as many findings concern the default mode network. Because the DMN partially encompasses the PFC, it is difficult to discern whether the increased strength of the DMN is a result of cathodal stimulation to M1 specifically, or if it was driven by anodal stimulation of the PFC. While an interesting question, it lies beyond the scope of this experiment. Studies wishing to address this concern may consider increasing the size of the reference electrode, or delivering bipolar tDCS to both motor cortices. Though both options diminish or eliminate stimulation to the PFC, they would also render comparisons with prior and future studies more difficult, as such configurations are not as commonly used in practice.

A second, and perhaps more salient, limitation of this study is that the behavioural task was only performed on the sham tDCS day, to provide a localizer of motor activation. This did not provide the opportunity to investigate how tDCS-induced changes in RSN activity predict or modify motor performance. To properly form such conclusions, the motor learning task should also be performed on the anodal and cathodal tDCS days. A single session of the task following the second resting state scan would allow for inferences regarding how changes in resting state activity predict motor performance. In order to understand how such changes not

just predict, but modify learning, the task would need to be performed after both resting state scans. This design may introduce other complications, as motor learning itself modifies resting state activity (Albert et al., 2009).

4.5 CONCLUSION

The results of this experiment provide new evidence on the ways in which cathodal tDCS modifies resting functional activity in the human brain. Cathodal tDCS was shown to significantly increase interhemispheric functional coupling between motor regions at rest and to increase the strength of the default mode network. Though trends regarding change due to anodal tDCS were noted, none reached significance. The absence of clear alterations in resting state activity following anodal tDCS suggests that the effects of anodal tDCS may be more reliant on task performance. Therefore, rather than continuing to explore the interaction between tDCS and resting state activity, Chapter 5 focuses on the interaction between tDCS and task performance. The beneficial effects of tDCS as related to motor behaviour are more frequently documented for anodal than cathodal tDCS. Pursuing anodal tDCS in the remaining experiments allows for a more thorough investigation into the means by which tDCS promotes improvements in motor learning.

REFERENCES

Albert, N. B., Robertson, E. M., & Miall, R. C. (2009). The resting human brain and motor learning. *Current biology : CB*, *19*(12), 1023–1027.

Alon, G., Roys, S. R., Gullapalli, R. P., & Greenspan, J. D. (2011). Non-invasive electrical stimulation of the brain (ESB) modifies the resting-state network connectivity of the primary motor cortex: a proof of concept fMRI study. *Brain research*, *1403*, 37–44.

Antal, A., Nitsche, M. A., Kruse, W., Kincses, T. Z., Hoffmann, K.-P., & Paulus, W. (2004). Direct current stimulation over V5 enhances visuomotor coordination by improving motion perception in humans. *Journal of cognitive neuroscience*, *16*(4), 521–527.

Antal, A., Polanía, R., Schmidt-Samoa, C., Dechent, P., & Paulus, W. (2011). Transcranial direct current stimulation over the primary motor cortex during fMRI. *NeuroImage*, *55*(2), 590–596.

Beckmann, C. F., & Smith, S. M. (2004). Probabilistic independent component analysis for functional magnetic resonance imaging. *IEEE transactions on medical imaging*, *23*(2), 137–152.

Beckmann, C. F., DeLuca, M., Devlin, J. T., & Smith, S. M. (2005). Investigations into resting-state connectivity using independent component analysis. *Philosophical transactions of the Royal Society of London. Series B, Biological sciences*, *360*(1457), 1001–1013.

Beckmann, C. F., Jenkinson, M., & Smith, S. M. (2003). General multilevel linear modeling for group analysis in FMRI. *NeuroImage*, *20*(2), 1052–1063.

Bindman,L. J., Lippold, O. C., & Redfearn, J. W. (1964). The action of brief polarizing currents on the cerebral cortex of the rat (1) during current flow and (2) in the production of long-lasting after-effects. *The Journal of Physiology*, *172*, 369–382.

Brookes, M. J., Woolrich, M., Luckhoo, H., Price, D., Hale, J. R., Stephenson, M. C., Barnes, G. R., et al. (2011). Investigating the electrophysiological basis of resting state networks using magnetoencephalography. *Proceedings of the National Academy of Sciences of the United States of America*, *108*(40), 16783–16788.

Broyd, S. J., Demanuele, C., Debener, S., Helps, S. K., James, C. J., & Sonuga-Barke, E. J. S. (2009). Default-mode brain dysfunction in mental disorders: a systematic

review. *Neuroscience and biobehavioral reviews*, *33*(3), 279–296.

Cincotta, M., & Ziemann, U. (2008). Neurophysiology of unimanual motor control and mirror movements. *Clinical neurophysiology : official journal of the International Federation of Clinical Neurophysiology*, *119*(4), 744–762.

Eichele, T., Debener, S., Calhoun, V. D., Specht, K., Engel, A. K., Hugdahl, K., Cramon, von, D. Y., et al. (2008). Prediction of human errors by maladaptive changes in event-related brain networks. *Proceedings of the National Academy of Sciences of the United States of America*, *105*(16), 6173–6178.

Filippini, N., MacIntosh, B. J., Hough, M. G., Goodwin, G. M., Frisoni, G. B., Smith, S. M., Matthews, P. M., et al. (2009). Distinct patterns of brain activity in young carriers of the APOE-epsilon4 allele. *Proceedings of the National Academy of Sciences of the United States of America*, *106*(17), 7209–7214.

Fregni, F., & Pascual-Leone, A. (2007). Technology Insight: noninvasive brain stimulation in neurology—perspectives on the therapeutic potential of rTMS and tDCS. *Nature Clinical Practice Neurology*, *3*(7), 383–393.

Grefkes, C., Eickhoff, S. B., Nowak, D. A., Dafotakis, M., & Fink, G. R. (2008). Dynamic intra- and interhemispheric interactions during unilateral and bilateral hand movements assessed with fMRI and DCM. *NeuroImage*, *41*(4), 1382–1394.

Iezzi, E., Conte, A., Suppa, A., Agostino, R., Dinapoli, L., Scontrini, A., Berardelli, A. (2008). Phasic voluntary movements reverse the aftereffects of subsequent theta-burst stimulation in humans. *Journal of Neurophysiology, 100(4),* 2070-2076.

Jenkinson, M., Bannister, P., Brady, M., & Smith, S. (2002). Improved optimization for the robust and accurate linear registration and motion correction of brain images. *NeuroImage*, *17*(2), 825–841.

Keeser, D., Meindl, T., Bor, J., Palm, U., Pogarell, O., Mulert, C., Brunelin, J., et al. (2011). Prefrontal Transcranial Direct Current Stimulation Changes Connectivity of Resting-State Networks during fMRI. *Journal of Neuroscience*, *31*(43), 15284–15293.

Lang, N., Siebner, H. R., Ward, N. S., Lee, L., Nitsche, M. A., Paulus, W., Rothwell, J. C., et al. (2005). How does transcranial DC stimulation of the primary motor cortex alter regional neuronal activity in the human brain? *European Journal of Neuroscience*, *22*(2), 495–504.

Li, C.-S. R., Yan, P., Bergquist, K. L., & Sinha, R. (2007). Greater activation of the "default" brain regions predicts stop signal errors. *NeuroImage*, *38*(3), 640–648.

Margulies, D. S., Böttger, J., Long, X., Lv, Y., Kelly, C., Schäfer, A., Goldhahn, D., et al. (2010). Resting developments: a review of fMRI post-processing methodologies for spontaneous brain activity. *Magma (New York, N.Y.)*, *23*(5-6), 289–307.

Mason, M. F., Norton, M. I., Van Horn, J. D., Wegner, D. M., Grafton, S. T., & Macrae, C. N. (2007). Wandering minds: the default network and stimulus-independent thought. *Science (New York, N.Y.)*, *315*(5810), 393–395.

Nitsche, M. A., & Paulus, W. (2000). Excitability changes induced in the human motor cortex by weak transcranial direct current stimulation. *The Journal of Physiology*, *527 Pt 3*, 633–639.

Nitsche, M. A., Schauenburg, A., Lang, N., Liebetanz, D., Exner, C., Paulus, W., & Tergau, F. (2003). Facilitation of implicit motor learning by weak transcranial direct current stimulation of the primary motor cortex in the human. *Journal of cognitive neuroscience*, *15*(4), 619–626.

Peña-Gómez, C., Sala-Lonch, R., Junqué, C., Clemente, I. C., Vidal, D., Bargalló, N., Falcón, C., et al. (2011). Modulation of large-scale brain networks by transcranial direct current stimulation evidenced by resting-state functional MRI. *Brain Stimulation*.

Polanía, R., Paulus, W., & Nitsche, M. A. (2011a). Modulating cortico-striatal and thalamo-cortical functional connectivity with transcranial direct current stimulation. *Human brain mapping*.

Polanía, R., Paulus, W., & Nitsche, M. A. (2012). Reorganizing the intrinsic functional architecture of the human primary motor cortex during rest with non-invasive cortical stimulation. *PloS one*, *7*(1), e30971. doi:10.1371/journal.pone.0030971

Polanía, R., Paulus, W., Antal, A., & Nitsche, M. A. (2011b). Introducing graph theory to track for neuroplastic alterations in the resting human brain: A transcranial direct current stimulation study. *NeuroImage*, *54*(3), 2287–2296.

Raichle, M. E., MacLeod, A. M., Snyder, A. Z., Powers, W. J., Gusnard, D. A., & Shulman, G. L. (2001). A default mode of brain function. *Proceedings of the National Academy of Sciences of the United States of America*, *98*(2), 676–682.

Rosazza, C., & Minati, L. (2011). Resting-state brain networks: literature review and clinical applications. *Neurological sciences : official journal of the Italian*

Neurological Society and of the Italian Society of Clinical Neurophysiology, *32*(5), 773–785.

Sonuga-Barke, E. J. S., & Castellanos, F. X. (2007). Spontaneous attentional fluctuations in impaired states and pathological conditions: a neurobiological hypothesis. *Neuroscience and biobehavioral reviews*, *31*(7), 977–986.

Stagg, C. J., Best, J. G., Stephenson, M. C., O'Shea, J., Wylezinska, M., Kincses, Z. T., Morris, P. G., Matthews, P. M., et al. (2009a). Polarity-sensitive modulation of cortical neurotransmitters by transcranial stimulation. *Journal of Neuroscience*, *29*(16), 5202–5206.

Stagg, C. J., Jayaram, G., Pastor, D., Kincses, Z. T., Matthews, P. M., & Johansen-Berg, H. (2011). Polarity and timing-dependent effects of transcranial direct current stimulation in explicit motor learning. *Neuropsychologia*, *49*(5), 800–804.

Stagg, C. J., & Nitsche, M. A. (2011). Physiological Basis of Transcranial Direct Current Stimulation. *The Neuroscientist*, *17*(1), 37–53.

Stagg, C. J., O'Shea, J., Kincses, Z. T., Woolrich, M., Matthews, P. M., & Johansen-Berg, H. (2009b). Modulation of movement-associated cortical activation by transcranial direct current stimulation. *European Journal of Neuroscience*, *30*(7), 1412–1423.

van den Heuvel, M. P., & Hulshoff Pol, H. E. (2010). Exploring the brain network: a review on resting-state fMRI functional connectivity. *European neuropsychopharmacology : the journal of the European College of Neuropsychopharmacology*, *20*(8), 519–534.

Venkatakrishnan, A., Contreras-Vidal, J. L., Sandrini, M., & Cohen, L. G. (2011). Independent component analysis of resting brain activity reveals transient modulation of local cortical processing by transcranial direct current stimulation. *Conference proceedings : ... Annual International Conference of the IEEE Engineering in Medicine and Biology Society. IEEE Engineering in Medicine and Biology Society. Conference*, *2011*, 8102–8105.

Weissman, D. H., Roberts, K. C., Visscher, K. M., & Woldorff, M. G. (2006). The neural bases of momentary lapses in attention. *Nature neuroscience*, *9*(7), 971–978.

Woolrich, M. W., Ripley, B. D., Brady, M., & Smith, S. M. (2001). Temporal autocorrelation in univariate linear modeling of FMRI data. *NeuroImage*, *14*(6), 1370–1386.

Zheng, X., Alsop, D. C., & Schlaug, G. (2011). Effects of transcranial direct current stimulation (tDCS) on human regional cerebral blood flow. *NeuroImage*, *58*(1), 26–33.

Chapter 5: Online and Offline tDCS Differentially Modulate Motor Learning and Excitability

The previous chapter demonstrated that tDCS to M1 modulates subsequent connectivity across the motor network in the resting brain. However, the behavioural effects of tDCS are variable: administering anodal tDCS prior to task performance has been shown to worsen learning, whereas the same stimulation applied concurrently with task performance generally enhances motor learning. Here, we investigate how the relative timing of anodal tDCS application and task performance modulates learning on an explicit motor learning task. In particular, we ask what neurophysiological correlates may form the basis of these behavioural responses.

5.1 INTRODUCTION

Anodal tDCS to the motor cortex has been shown to increase excitability, as measured by larger motor evoked potentials (MEPs) elicited by TMS (Nitsche & Paulus, 2000). The effect of this excitability change on motor learning can be probed using a sequence learning task. When anodal tDCS is applied during such a task, levels of learning increase on both explicit (Stagg et al., 2011b) and implicit variants (Nitsche et al., 2003). Though tDCS-induced increases in excitability can outlast stimulation termination by up to ninety minutes (Nitsche & Paulus, 2001), augmented motor learning is only reliably documented if stimulation is concurrent with performance of the task (Stagg et al., 2011b). Applying stimulation prior to sequence learning tasks has been shown to have no effect at all (Kuo et al., 2008) or to even worsen performance (Stagg et al., 2011b).

A growing body of work proposes that the mechanisms of homeostatic plasticity may be helpful in understanding the differing effects of performing a task after tDCS (offline) and performing the same task concurrently (online) with tDCS application (Ziemann & Siebner, 2008). The principle of homeostatic plasticity proposes that the brain's capacity for plasticity (and as a result, learning) at any point in time depends on its background activity (see Chapter 1.2.2.4). Homeostatic plasticity has been modelled using the Bienenstock-Cooper-Munro (BCM) rule (Bienenstock et al., 1982). In this model, a decrease in background activity prior to an intervention leads to an increase in facilitatory plasticity induced during that intervention (or a decrease in inhibitory plasticity). Likewise, an increase in prior background activity decreases the brain's ability for subsequent facilitatory plasticity induction (and increases its ability for inhibitory plasticity). The first experiment to demonstrate such homeostatic properties in humans was performed by Iyer and colleagues in 2003. They found that increasing cortical excitability using 6 Hz rTMS enhanced the inhibitory effect of subsequent 1 Hz rTMS application (Iyer, Schleper, & Wassermann, 2003).

The homeostatic model is itself dependent on the relative timing of any change in background activity and learning or plasticity. This is often demonstrated by experiments that have modified background activity using tDCS and induced plasticity using TMS: If anodal tDCS (which increases background activity) is applied concurrently with a plasticity-inducing TMS protocol, the resultant effects can be explained homeostatically (Nitsche et al., 2007). However, if tDCS is applied prior to the plasticity-inducing protocol, the effects have been shown to be variously nonhomeostatic (Nitsche et al., 2007), homeostatic (Fricke et al., 2011), or non-

existent (Fricke et al., 2011), depending on the interval between the two interventions and the nature of those interventions.

The results of such tDCS-TMS studies suggest that the relative timing of tDCS and a plasticity-inducing protocol has a strong impact on plasticity and, by inference, on learning. The effect of timing on the applicability of the homeostatic model has also been demonstrated behaviourally. Jung and Ziemann showed that LTP-like increases in motor cortical excitability induced by paired associative stimulation (PAS) facilitated subsequent learning of a thumb flexion movement if there was a 0 minute delay between protocols (nonhomeostatic interaction). However, if there was a delay of 90 minutes between the two protocols, subsequent learning was *decreased* (homeostatic interaction) (Jung & Ziemann, 2009). That results concerning the relevance of homoeostatic mechanisms to plasticity and learning are conflicting behoves further investigation into the matter.

Evidence from animal studies suggests that homeostatic plasticity is synapse-specific (Huang et al., 1992), and therefore seen most clearly when both stimuli directly modulate activity across the same synaptic circuits. Separate experiments have previously reported a decrease in cortical GABA following both anodal tDCS (Stagg et al., 2009) and motor learning (Floyer-Lea et al., 2006), leading to the tentative hypothesis that GABAergic synapses may act as the site of homeostatic interactions between these two interventions. Moreover, using TMS, both anodal tDCS and motor learning have been demonstrated to increase MEP amplitude and decrease inhibition, when performed independently of each other (Nitsche & Paulus, 2000; Rosenkranz & Rothwell, 2006). However, no study to date has used such TMS protocols to examine the homeostatic interactions between tDCS and motor learning.

To address the inconsistent results regarding the applicability of the homeostatic model to plasticity-inducing protocols, and following the behavioural results previously reported by our lab in (Stagg et al., 2011b), Experiment 1 sought to understand the interaction between tDCS application and motor learning by asking the following four questions:

1. What effect does receiving online or offline anodal tDCS have on rates and levels of learning?

2. Can the differential effects of online and offline anodal tDCS on behaviour be explained by changes in motor cortical excitability?

3. Can the differential effects of online and offline anodal tDCS on behaviour be explained by changes in motor cortical inhibition?

4. Are GABAergic homeostatic processes limited to synaptic $GABA_A$ activity, or are other GABAergic pools, such as extrasynaptic $GABA_A$ activity, involved in the creation of these effects?

Experiment 2 then examined whether changes in these measures were modulated by the level of task-involvement of the recorded muscle.

Motor evoked potentials (MEPs) were used to measure motor cortical excitability. Specifically, as discussed in detail in Chapter 2.1, we used single-pulse TMS to give a measure of cortical excitability and paired-pulse TMS to give measures of short-interval intracortical inhibition (SICI). By performing SICI measurements with both an interstimulus interval of 1 ms and 2.5 ms we aimed to differentiate between inhibitory effects due to extrasynaptic $GABA_A$ tone, as indicated by changes in 1 ms paired-pulse TMS, or modifications in synaptic $GABA_A$ activity, as indicated by changes in 2.5 ms paired-pulse TMS (Stagg et al., 2011a).

Additionally, in Experiment 2, simultaneous recordings from three muscles during task performance were used to establish each muscle's level of involvement in execution of the motor task.

We predicted that online anodal tDCS would enhance learning, while offline anodal tDCS would decrease learning. As results from MRS studies suggest that the excitability changes induced by anodal tDCS and by motor learning may be due to a decrease in GABA (Floyer-Lea, 2006; Stagg et al., 2009), we expected to find decreased inhibition (as measured by SICI) both following tDCS and following learning task performance. Task performance in the absence of stimulation was anticipated to result in increased excitability as measured by MEP amplitude, as reported previously (Rosenkranz & Rothwell, 2006).

5.2 METHODS

Study Design

Thirteen healthy, right-handed volunteers participated in each of the five sessions of this study (Figure 5.1). Experiment 1 consisted of one session each of paradigms A through D; the order of sessions was counterbalanced across subjects and each session was separated by at least one week. Experiment 2 consisted of a single session of paradigm D.

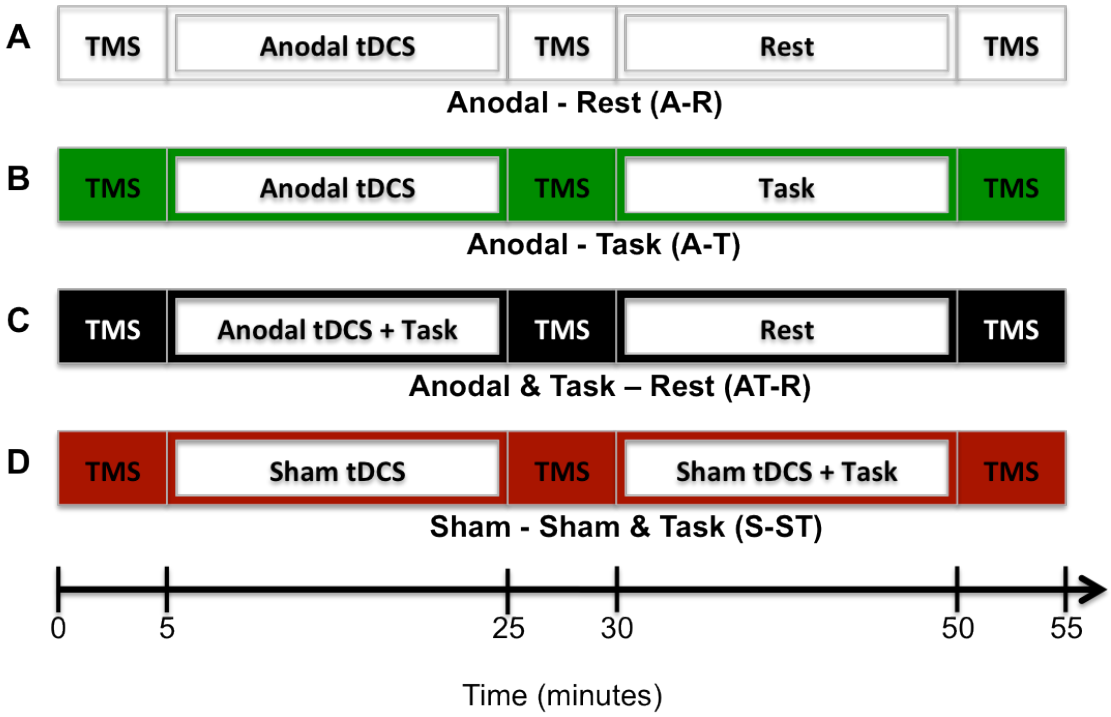

Figure 5.1: The four paradigms used in this study. For all paradigms, TMS was used at three timepoints to assess motor cortical excitability and inhibition. Between these TMS assessments, two 20 minute intervention epochs were included, the content of which varied across paradigms as follows: A) Stimulation alone, followed by rest (A-R). B) Stimulation alone, followed by task (A-T). C) Concurrent stimulation and task, followed by rest (AT-R). D) Sham tDCS, followed by concurrent sham tDCS and task (S-ST). Experiment 1 used all 4 paradigms; experiment 2 used paradigm D, S-ST, only.

5.2.1 Experiment 1

Overview

Neonatal ECG electrodes (Tyco Healthcare, Germany) were used to measure EMG responses and were attached to the participant's right hand on the first dorsal interosseous muscle (FDI) in a belly-tendon montage. The motor hotspot for the FDI was then identified (defined as the scalp location that consistently elicited maximum MEPs at 120% of resting threshold) and was marked on the scalp. TMS was applied over the demarcated hand area using a 70cm figure-of-eight coil attached to a BiStim module connecting two monophasic Magstim200 systems. The coil was held tangentially to the scalp and rotated 45° away from the midline to

ensure optimal neuronal recruitment. To determine the participant's resting motor threshold (RMT), single pulses of TMS were given at varying intensities while the subject was at rest. The RMT_{1mV} was defined as the lowest intensity that elicited peak-to-peak MEP amplitudes of 1 mV on EMG and observable twitches in the hand. The active motor threshold (AMT) was determined during an isometric contraction of approximately 20% of the maximum contraction, and was defined as the lowest intensity that produced observable MEPs on five out of ten trials. Signal for Windows (Cambridge Electronic Design, version 3.07) was used to record the elicited MEPs, which were sampled at 5 kHz, amplified, and filtered (10 Hz to 1 kHz) using a CED 1902 amplifier and 1401 analog to digital converter.

TMS

TMS measures were recorded three times in each experimental session, with the hand at rest. In each TMS block, single pulses of TMS were used to provide simple measures of cortical excitability and were given at an intensity equal to RMT_{1mV}. Paired-pulse TMS paradigms were used to elicit short-interval intracortical inhibition (SICI) using interstimulus intervals (ISI) of 1 ms or 2.5 ms. For paired pulses, the conditioning pulse was set to 70% of each subject's AMT, and the test pulse was given at their RMT_{1mV}. During each TMS administration a total of 60 TMS pulses were delivered: 30 single pulses, 15 paired pulses with a 1 ms ISI and 15 paired pulses with a 2.5 ms ISI. Pulses were administered in a pseudo-random order as generated within the Signal software. In the event that the participant's RMT_{1mV} changed within a session, as evidenced by MEPs substantially larger or smaller than 1 mV, ten single pulses were acquired at the initial RMT_{1mV} and the intensity was

then decreased until the elicited MEPs were again at 1 mV. This new RMT_{1mV} was used for the remainder of the TMS component.

MEP analysis was conducted on each block separately. EMG activity in the 50ms period prior to the first TMS pulse was analysed, and any trace with visible pre-contraction of the FDI was excluded. Peak-to-peak amplitudes of each MEP for all three pulse types were then calculated separately within Signal. For each block of TMS and each pulse type separately, a single iteration of Grubbs' test with a significance level of 0.05 was performed. Outliers were identified and subsequently discarded. Any remaining MEPs that fell outside of 2 standard deviations from the mean were also excluded from the analysis. The mean MEP amplitude was then computed for the single pulse condition. For each paired pulse administration, inhibition was calculated as the conditioned MEP amplitude divided by the mean MEP amplitude from the single (unconditioned) pulses. These values were then used to determine the mean inhibition for each paired pulse condition. All statistics were performed in SPSS (IBM, version 19.0.0). Repeated measures ANOVAs were run, followed by t-tests for specific comparisons.

tDCS

Two electrodes measuring 5x7 cm were inserted in saline-soaked sheaths and placed on the scalp. The stimulating electrode was centred over the hand area measured as 5cm lateral to Cz, as described previously, and the reference electrode was positioned over the contralateral supraorbital ridge. During real stimulation, 1mA anodal tDCS was applied for 20 minutes via a DC-stimulator (Magstim eldith). The current was increased at the beginning of stimulation over 10 seconds and diminished over 10 seconds at the end of the stimulation period. For the sham

condition, the current was ramped up for 10 seconds and then turned off. For sessions during which tDCS was applied concurrently with the learning task, the electrodes were attached first, and the current was allowed to ramp up fully prior to the participant starting the learning task. The current ran for the duration of the task and was allowed to run and ramp down after the task had ceased.

Motor Task

Participants performed a visually-cued explicit sequence learning task lasting approximately 20 minutes. Participants held a button-box in their right hand, and Presentation (Neurobehavioral Systems, Version 14.9) was used to display four horizontal bars, each of which corresponded to a button on the button-box. The participants were told that when a bar changed into an asterisk, they were to press the corresponding button as quickly and accurately as possible. They were also informed that these button presses would form a sequence that was 10 cues long, and that they should try to learn the sequence of these button presses. There were 15 sequence blocks. During each block, the sequence repeated three times, giving a total of 30 button presses per block. There were two blocks (1st and 15th blocks) that consisted of 30 visual cues appearing in a pseudo-random order. Participants were alerted, via the words "Sequence" or "Random" appearing on the screen, as to which type of block was to follow. Four sequences of equal difficulty were used in an order counter-balanced across the group; each sequence was constrained to the same ratio of button presses (3:3:2:2), to control for reaction time differences between fingers.

Offline, the number of correct button presses was tallied for each block. Anticipatory responses, i.e. those that occurred prior to the cue, were discarded.

Reaction time was calculated as the time from cue onset to button press. Reaction times falling out of ±2 standard deviations from the mean were also excluded. Change in reaction times (ΔRT) was defined as the ratio of the mean reaction time for that block to the mean reaction time for the first learning block (block 2). The ΔRT for all of the sequence blocks were then fed into a 3 by 15 repeated measures ANOVA including factors of stimulation type (A-T, AT-R, and S-ST) and time.

5.2.2 EXPERIMENT 2

Overview

Experiment 2 consisted of a single session of paradigm D, the sham stimulation, control condition (see Figure 5.1). Neonatal ECG electrodes were attached to three muscles of the participant's right hand to measure EMG responses: the FDI as above, the abductor pollicis brevis (APB), and the abductor digiti minimi (ADM). Localization of the hand area, establishment of motor thresholds, TMS application, and performance of the motor task proceeded as in Experiment 1. Data from three participants were excluded, as simultaneous recordings from all three muscles could not be reliably achieved.

Motor Activity Recording

Activity was recorded from each of the three muscles (FDI, APB, ADM) for the duration of performance of the motor sequence learning task. Spike2 for Windows (Cambridge Electronic Design, version 6.00) was used to analyse this activity, which was sampled at 3.33 kHz, amplified, and filtered (10 Hz to 1 kHz) using a CED 1902 amplifier and 1401 analog to digital converter. Each muscle's

waveform was separated into blocks during which the sequence was being performed ("active"), and rest blocks in which the hand was held still ("rest"). A partial waveform, illustrating both active and rest blocks, is shown in Figure 5.2. Mean activity during each block was extracted from Spike2, and statistics performed in SPSS.

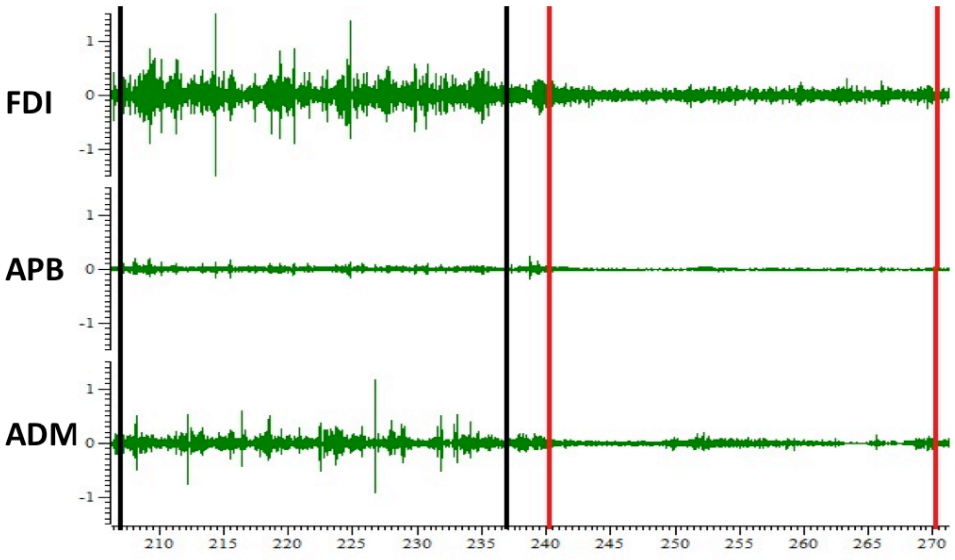

Figure 5.2: Partial waveform from one participant. The three channels, recording from the FDI, APB, and ADM are illustrated. Between the vertical black bars is an active block of sequence tapping; between red bars is a rest block. The x-axis shows time (in seconds); the y-axis gives the amplitude of the EMG response (in mV).

5.3 RESULTS

5.3.1 EXPERIMENT 1

Differential effects of online and offline tDCS on motor learning

Reaction times for performance of the task decreased over time in all sessions, indicating that the paradigms resulted in learning of the task (RM-ANOVA; main effect of time: $F(14,168)=14.516$, $p<0.001$) (Figure 5.3). However, the degree of learning was not equivalent for the three paradigms (RM-ANOVA, main effect of paradigm: $F(2,24)=4.383$, $p=0.024$). Offline stimulation (A-T) led to decreased learning when compared to control (S-ST) (RM-ANOVA, main effect of paradigm:

F(1,12)=4.900, p=0.047) and to online stimulation (AT-R) (RM-ANOVA, main effect of paradigm: F(1,12)=4.877, p=0.047). Learning did not differ between online stimulation (AT-R) and control (S-ST) (RM-ANOVA, main effect of paradigm: F(1,12)=.004, p=0.949).

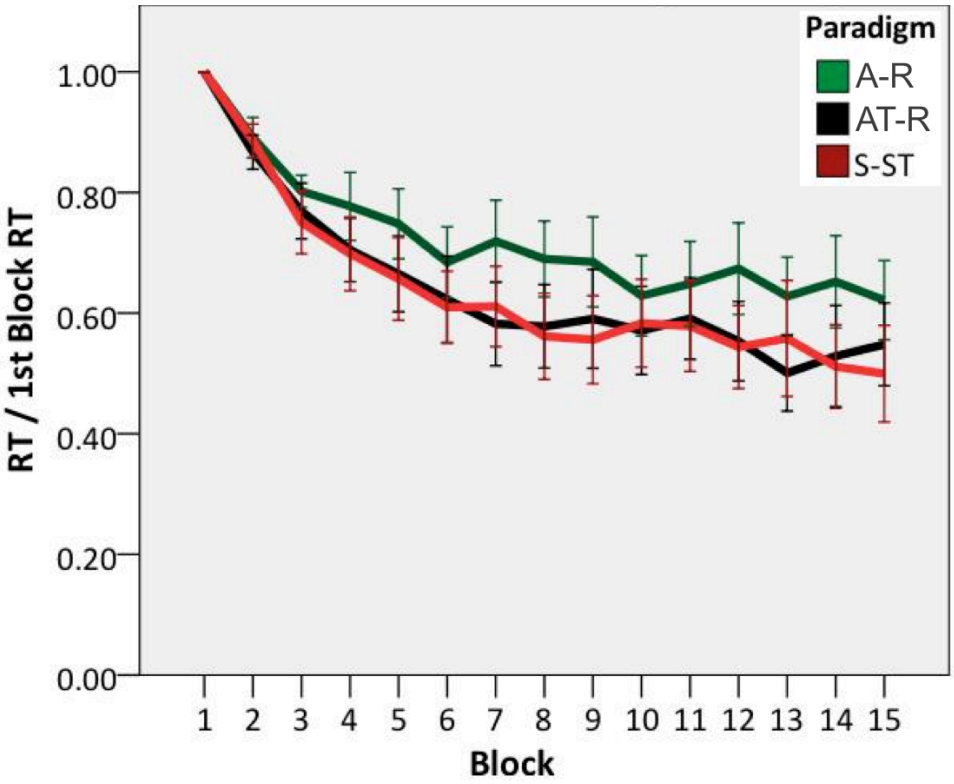

Figure 5.3: Reaction times during the learning blocks of the motor task. Offline tDCS (A-T) led to decreased learning compared to online tDCS (AT-R) and control (S-ST). The two blocks containing random sequences (before Block 1 and after Block 13) have been excluded. Error bars ±1 SEM.

Cortical excitation is modulated by tDCS and by task performance

As expected, twenty minutes of anodal tDCS alone (i.e., as delivered during the first phase of the A-R condition, see Figure 5.1) increased cortical excitability, as measured by increased MEP size (t(12)=2.880, p=0.014). However, this excitability increase was not seen when anodal tDCS was delivered concurrently with task performance (AT-R) (t(12)=0.077, p=0.940), and there was a significant difference in the change in MEP size between the two paradigms (RM-ANOVA, paradigm*time:

F(1,12)=5.307, p=0.040) (Figure 5.4A). In order to more easily visualise the excitability changes induced by tDCS, the ratio of MEP size after stimulation to that prior to stimulation was also calculated (Figure 5.4B). A significant difference between the two paradigms was found (t(12)=2.319, p=0.039). For anodal tDCS alone, increased excitability following anodal tDCS was demonstrated, as indicated by an MEP ratio significantly greater than 1. This was not the case when anodal tDCS was given concurrently with the motor task (A-R: t(12)=2.561, p=0.025; AT-R: t(12)=0.064, p=0.950) (Figure 5.4B).

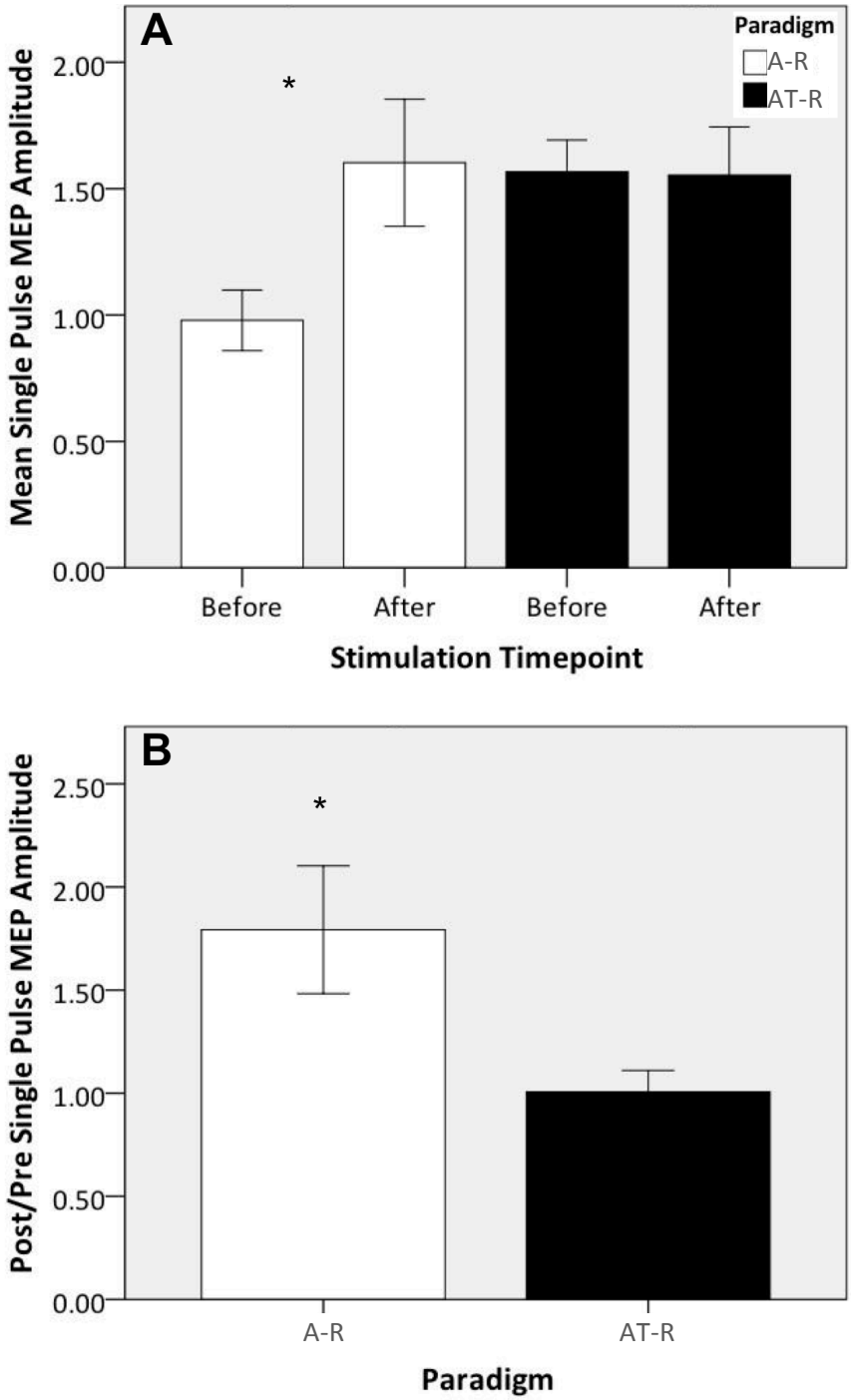

Figure 5.4: Anodal tDCS increases cortical excitability. A) Anodal tDCS increases MEP size, an effect that is not seen if stimulation is applied concurrently with task performance (online tDCS, AT-R. B) Increase in excitation expressed as a ratio of post-stimulation to pre-stimulation MEP size. Error bars ±1 SEM.

Next, we asked what effect task performance had on cortical excitability (Figure 5.5). A RM-ANOVA comparing MEP size before and after task performance showed no significant difference between paradigms (RM-ANOVA, main effect of paradigm: $F(2,24)= 1.615$, $p=0.220$), though a trend toward an effect of time was noted (RM-ANOVA, main effect of time: $F(1,12)= 4.124$, $p=0.065$). However, as we had a strong *a priori* hypothesis that task performance would modulate cortical excitability, we proceeded to perform t-tests within each paradigm. Contrary to the previously reported increase in MEP size following motor learning (Rosenkranz & Rothwell, 2006), performance of the task in the absence of stimulation (i.e., S-ST) led to a significant decrease in MEP size ($t(12)=2.800$, $p=0.016$) (Figure 5.5A). This effect was not present when the task was performed either during anodal stimulation (AT-R: $t(12)=0.077$, $p=0.940$) or after stimulation (A-T: $t(12)=0.772$, $p=0.297$).

To better visualize the changes in cortical excitability induced by task performance, the ratio of the MEP size after task performance to before task performance was analysed. This approach showed a strong trend toward motor learning leading to a decrease in excitability for task performance in the absence of stimulation (S-ST: $t(12)=2.084$, $p=0.059$) (Figure 5.5B). As previously, no such effect was found for MEP amplitude when task performance followed stimulation (A-T) or was concurrent with stimulation (AT-R) (A-T: $t(12)=0.297$, $p=0.771$; AT-R: $t(12)=0.064$, $p=0.950$) (Figure 5.5B).

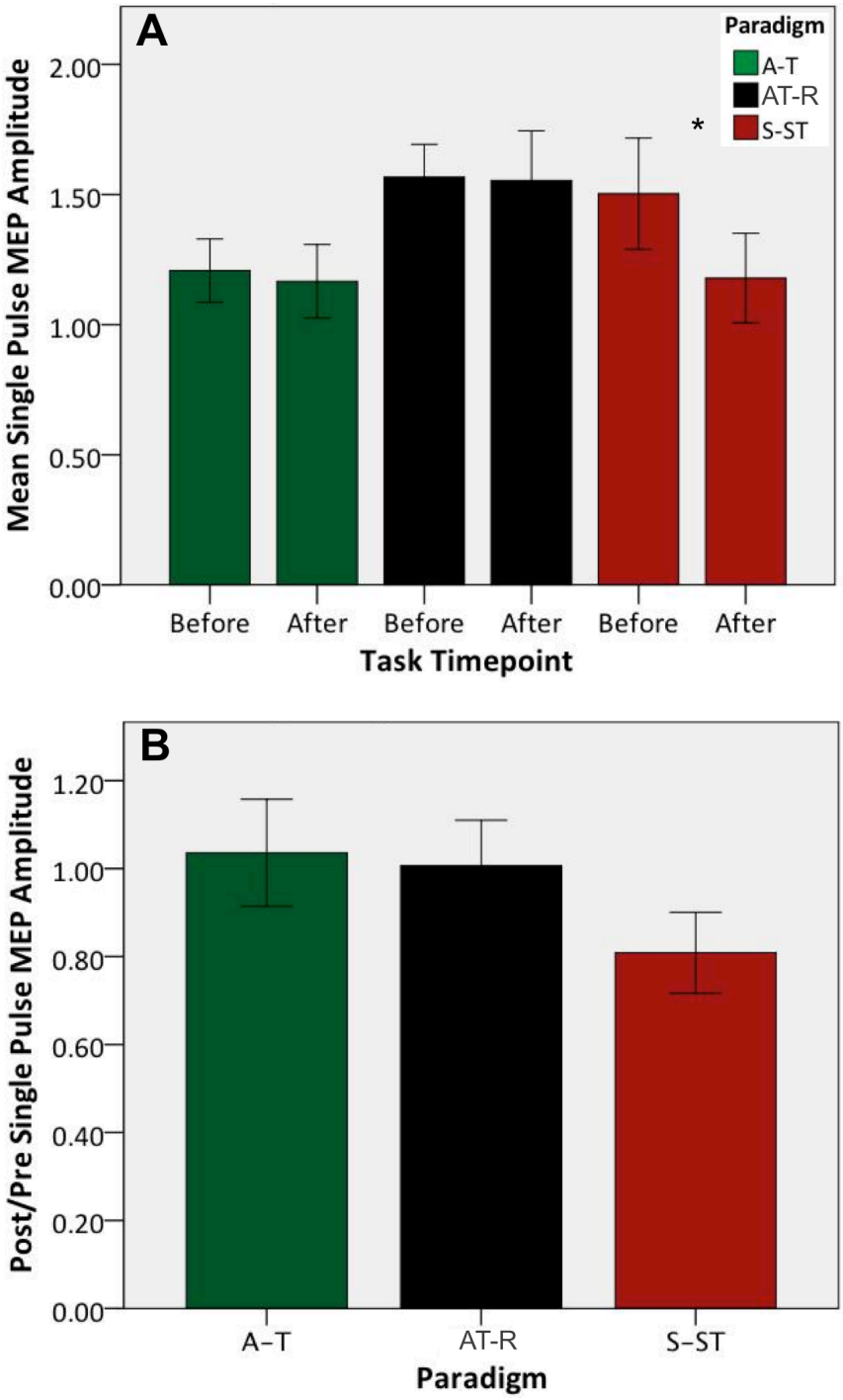

Figure 5.5: Task performance decreases cortical excitability. A) Performance of the task alone (S-ST) decreases MEP size, an effect that is not present if anodal tDCS is applied prior to (A-T) or concurrent with (AT-R) task performance. B) Changes in excitation expressed as a ratio of post- to pre- task performance MEP size. Error bars ±1 SEM.

Cortical Inhibition: 1 and 2.5 ms SICI

We then went on to look at the effects of stimulation and task performance on measures of inhibition. A RM-ANOVA comparing SICI before and after the two stimulation conditions (as administered during the first portions of the A-R and AT-R paradigms) showed a main effect of SICI Type ($F(1,12)=16.961$, $p=0.001$). A similar RM-ANOVA investigating the effects of task performance on SICI also showed a main effect of SICI type ($F(1,12)=9.961$, $p=0.008$). Because of these results, and the mechanistic independence of 1 and 2.5 ms SICI, the effects of stimulation and task performance were analysed for each SICI type separately.

Cortical inhibition: 1 ms SICI

We first investigated the effects of stimulation on 1 ms SICI. Neither anodal tDCS alone nor anodal tDCS delivered concurrently with task performance affected levels of 1 ms SICI (RM-ANOVA, main effect of paradigm: $F(1,12)=0.487$, $p=0.499$). A comparison of 1 ms SICI levels before and after task performance showed a significant effect of time across the three task conditions (RM-ANOVA, main effect of time: $F(1,12)=6.073$, $p=0.030$). Given the apparent lack of specificity of this effect, we then inquired whether it could be due to the passage of time, independent of task performance. We analysed the sham only condition (i.e., the first portion of the S-ST paradigm), and found no change over time in 1 ms SICI ($t(12)=0.299$, $p=0.770$). Subsequent t-tests to determine the relative strengths of this effect in the three task conditions did not identify any significant differences between pre- and post-task levels of 1 ms SICI (S-ST: $t(12)=0.314$, $p=0.759$; AT-R: $t(12)=0.670$, $p=0.516$; A-T: $t(12)=1.728$, $p=0.110$).

Task performance affects cortical inhibition: 2.5 ms SICI

An identical series of analysis to above was then performed for 2.5 ms SICI. Stimulation did not significantly modulate 2.5 ms SICI, although a trend toward a differential effect of paradigms was noted (RM-ANOVA, main effect of paradigm: $F(1,12)=2.737$, $p=0.124$). Task performance did modulate inhibition levels (RM-ANOVA, main effect of time: $F(1,12)=8.132$, $p=0.015$). Although no interactions were found, exploratory t-tests were performed to determine which paradigm, if any, was driving this effect. No significant effect of task performance on 2.5ms SICI was found in the absence of stimulation (S-ST: $t(12)=0.502$, $p=0.625$), nor when the task was performed during stimulation (AT-R: $t(12)=0.785$, $p=0.448$). However, performance of the task after stimulation showed a significant increase in 2.5ms SICI (A-T: $t(12)=2.983$, $p=0.011$). (Figure 5.6, note that smaller values reflect greater inhibition.) For this paradigm (A-T), a trend toward post-task inhibition being greater than baseline inhibition (i.e., at the beginning of the session, before tDCS application) was noted ($t(12)=1.850$, $p=0.089$), suggesting that this increase in inhibition was not simply a natural return to baseline.

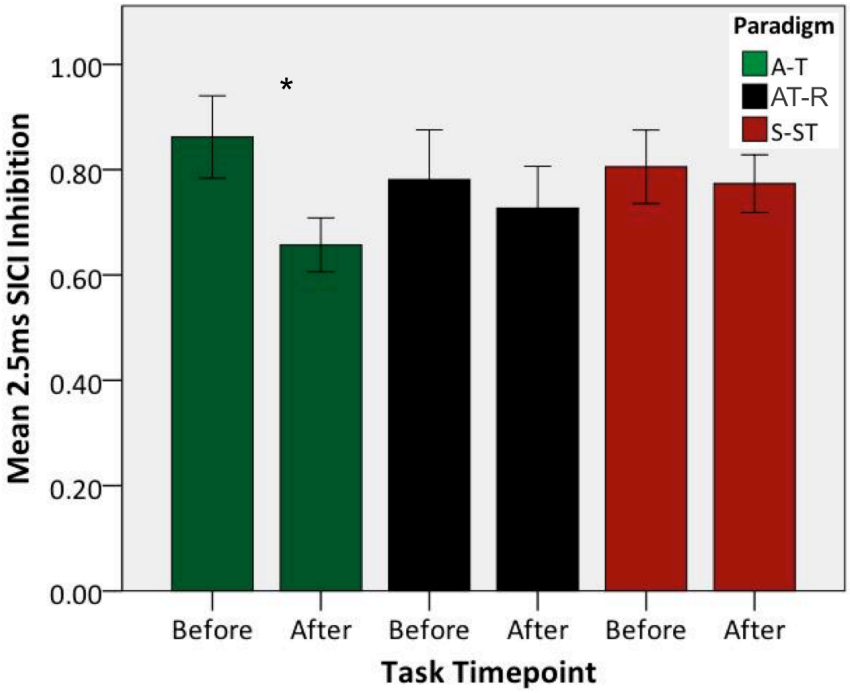

Figure 5.6: Task performance increases cortical inhibition. Anodal tDCS applied prior to task performance (A-T), increases inhibition as measured by 2.5 ms SICI following the task. Error bars ±1 SEM.

5.3.2 EXPERIMENT 2

Muscle activity during task performance

Given the unexpected finding of decreased MEP size following task performance (Figure 5.5), we examined whether the effect could be attributed to the level of FDI involvement in performance of the motor task. Recordings from the FDI, APB (a muscle not involved in tapping the sequence), and ADM (a muscle more directly involved in tapping the sequence) were analysed. It was noted that, even during the rest blocks, there was activity within all muscles, potentially reflective of the grip force required to hold the button box in hand. This was not the case when MEPs were recorded in the intervals surrounding task performance (as reported in the previous and following sections): during these periods, subjects were not required to hold the button box and background muscle activity was near zero—

any traces in which muscle activity was observed on the EMG prior to the TMS pulse were excluded.

A RM-ANOVA demonstrated that the overall levels of activity differed between muscles (main effect of muscle: $F(2,18)=15.596$, $p<0.001$, Figure 5.7A). Moreover, a main effect of task was also found ($F(1,9)=27,998$, $p<0.001$), suggesting different amounts of activity during the active and rest blocks (Figure 5.7A). Subsequent t-tests showed that all muscles increased their activity during the active blocks compared to rest blocks (FDI: $t(9)=2.894$, $p=0.018$; APB: $t(9)=5.955$, $p<0.001$; ADM: $t(9)=6.674$, $p<0.001$). When comparing activity in each of the three muscles, a strong trend toward differential effects of task performance was found (RM-ANOVA, muscle by task interaction: $F(2,18)=3.373$, $p=0.057$). We then compared the percent increase in activity from rest to active in each pair of muscles (Figure 5.7B). The ADM showed a significantly larger increase in activity from rest to active blocks when compared to both the FDI and APB (FDI: $t(9)=5.457$, $p<0.001$; APB $t(9)=2.717$, $p=0.024$). There was no difference between the activity increase in the FDI and APB ($t(9)=1.020$, $p=0.334$), suggesting that activity in the FDI more closely resembles that of an uninvolved muscle, the APB, than in a muscle directly involved in learning the task, the ADM.

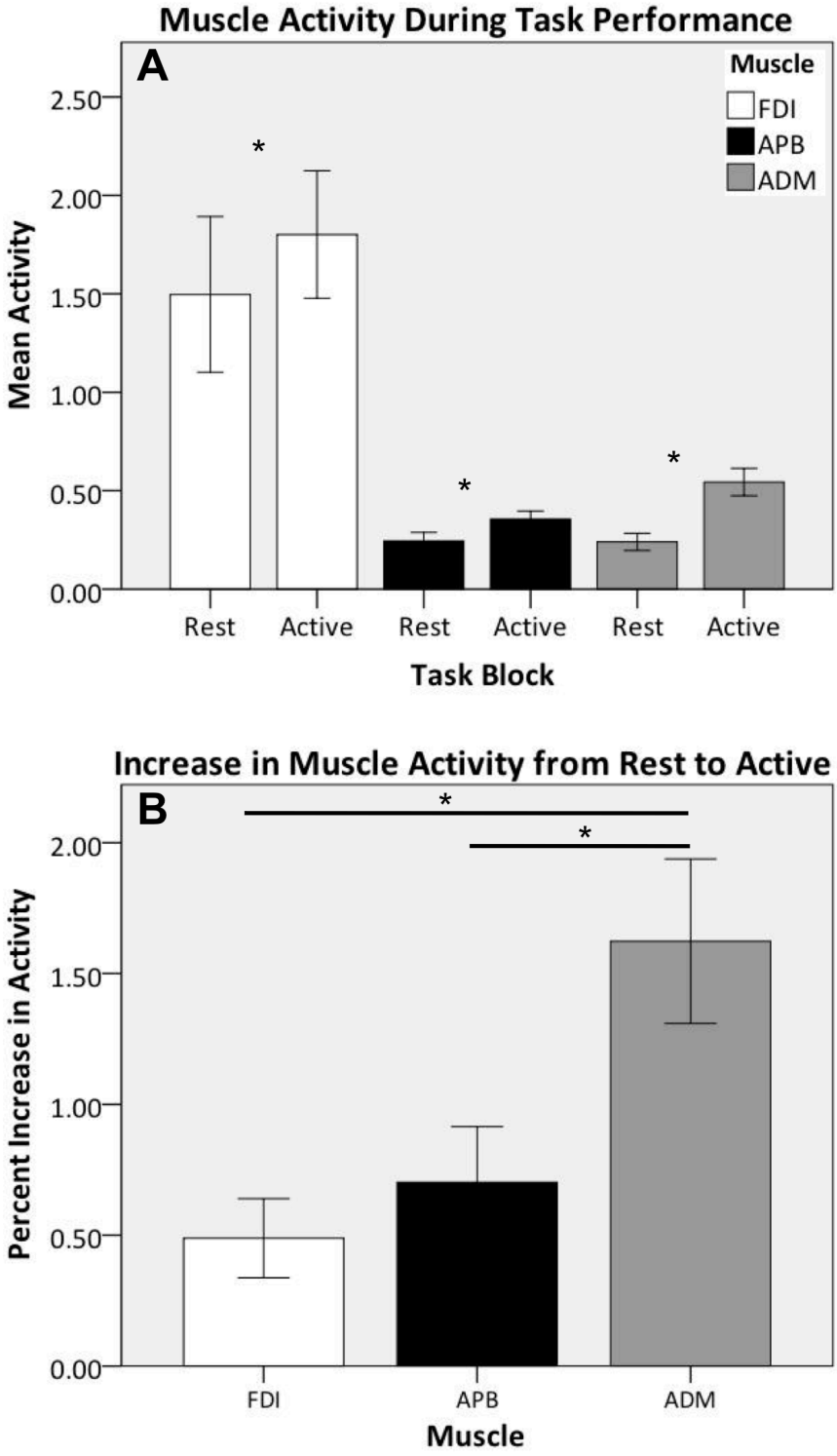

Figure 5.7: The FDI, APB, and ADM are differentially active during task performance. A) All three muscles increase their activity during active blocks of the task compared to rest. B) The ADM shows a significantly larger increase in activity from rest to active blocks than the FDI or APB. Error bars ±1 SEM. Mean activity is given in mV.

Level of muscle involvement affects task-induced excitation changes

In Experiment 1, we observed a decrease in cortical excitability within the FDI during task performance in the absence of stimulation. We wished to investigate whether this decrease was specific to the FDI, or whether similar decreases in cortical excitability within other muscle representations could be demonstrated. When comparing measures of cortical excitability before versus after the task for each muscle separately, we did not find a main effect of muscle or of time, but we noted a significant differential effect of task-induced excitability changes between muscles (RM-ANOVA, muscle*time: $F(2,18)=4.865$, $p=0.020$). To determine which muscles were driving this interaction, RM-ANOVAs between muscle pairs were performed. A strong trend toward a difference between the FDI and ADM was found (muscle*time: $F(1,9)=4.905$, $p=0.054$), suggesting that excitability in the FDI was affected differently than in a muscle directly involved in task performance (the ADM). Moreover, a significant difference between the FDI and APB was also found (muscle*time: $F(1,9)=9.419$, $p=0.013$), implying that the FDI was affected differently than a primarily uninvolved muscle (APB). There was no difference between the APB and ADM (muscle*time: $F(1,9)=0.058$, $p=0.598$). Although the ANOVA's suggest that the effects of task on excitability vary between muscles, subsequent t-tests revealed no significant differences in excitation before and after task performance for any muscle (FDI: $t(9)= 1.364$, $p=0.206$; APB: $t(9)=-0.571$, $p=0.582$; ADM: $t(9)=0.624$, $p=0.548$) (Figure 5.8).

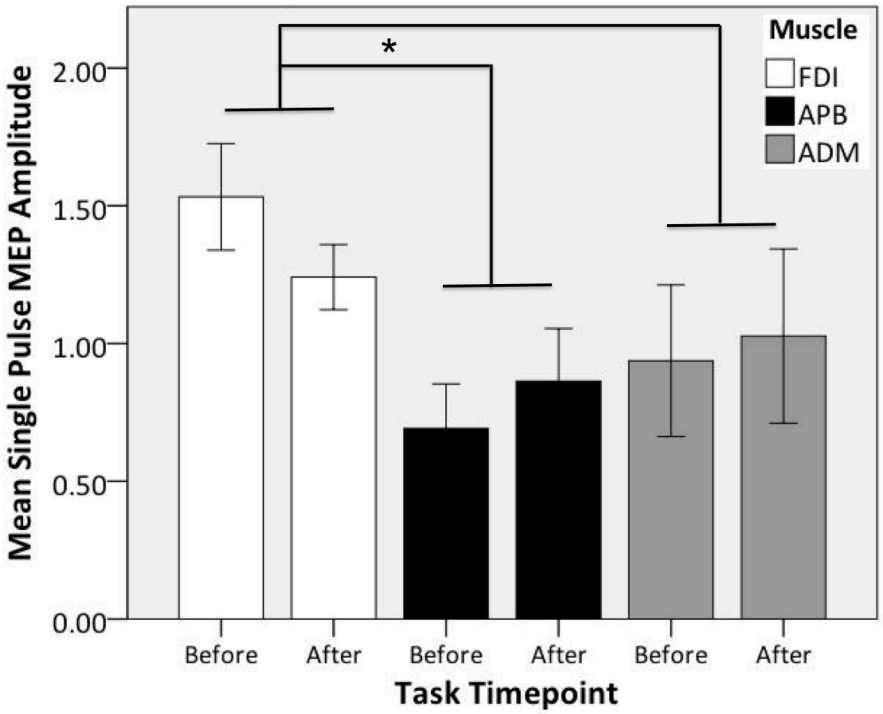

Figure 5.8: Excitability changes following task performance. Excitation of the FDI was differentially changed by task performance when compared to the APB and ADM. There was a significant difference between the FDI and APB, and a strong trend between the FDI and ADM. There was no difference between the APB and ADM. The FDI showed a decrease in excitability, as in Experiment 1, but this change was not statistically significant here. Error bars ±1 SEM.

5.4 DISCUSSION

This study investigated the interaction between the timing of tDCS application and motor learning, and the corresponding effect on cortical neurophysiology. In line with the theory of homeostatic plasticity, the effects of tDCS on motor learning were dependent on the relative timing of the two interventions. Applying excitatory anodal tDCS prior to task performance resulted in decreased learning, whereas applying anodal tDCS during task performance led to no change in behaviour. These timing-dependent behavioural effects were also seen in neurophysiological measures: applying anodal tDCS alone led to a significant increase in cortical excitability, as previously reported, but when delivered conccurently with motor learning, no significant effects were seen. Finally, cortical

inhibition was not changed by application of anodal tDCS alone, by task performance alone, or by concurrent anodal tDCS and task. However, when anodal tDCS preceded task performance, then task performance resulted in an increase in cortical inhibition. That is, inhibition assessed by SICI was greater after task performance compared to before task performance.

Homeostatic Plasticity

Applying anodal tDCS prior to task performance resulted in decreased learning compared to the control condition, consistent with homeostatic mechanisms. Homeostatic rules state that increased background activity prevents further facilitation by subsequent excitatory stimuli. Anodal tDCS increases background activity by increasing neuronal firing rates (Bindman, 1964), an effect demonstrated by TMS measures as an increase in MEP size, usually said to reflect cortical excitability (Nitsche & Paulus, 2000). In this heightened state, then, processes relying on further excitation should be blocked, and with it, their behavioural correlates. Accordingly, as motor learning is associated with facilitory LTP-like processes (Ziemann et al., 2004), post-tDCS learning levels are decreased. The results of our study are in agreement with this homeostatic model.

However, previous studies employing anodal tDCS to explore homeostatic mechanisms have had varying results. This may be in some part due to a time-dependence of homeostatic applicability (Jung & Ziemann, 2009). A study by Fricke in 2011 demonstrated that homeostatic rules govern the interaction of two sequentially administered sessions of anodal tDCS if the temporal gap between the two administrations is between 3 and 10 minutes for 5 minutes of stimulation (Fricke et al., 2011). In our paradigm, the motor learning task began approximately

5 minutes after stimulation termination, well within the window during which one might expect homeostatic rules to apply.

Moreover, the decreased learning documented in the offline condition (A-T) is associated with increased cortical inhibition. There was a strong trend toward this level of post-task inhibition being more than that seen at baseline, suggesting that the inhibition increase is associated with the task in particular, and is not a natural return to baseline levels present before the application of tDCS. That more inhibition is associated with decreased learning conforms to the theory of metaplasticity. Referring to the "plasticity of synaptic plasticity" (Abraham & Bear, 1996), metaplasticity describes synaptic changes that regulate the ability for LTD or LTP to be induced over time.

One particularly influential model of metaplasticity is the Bienenstock-Cooper-Munro (BCM) theory first introduced in 1982. The BCM model proposes that there is a level of post-synaptic activity, termed the modification threshold (θ_m), above which gives LTP and below which results in LTD (Bienenstock, Cooper, & Munro, 1982). The modification threshold is a dynamic entity, and can be raised or lowered based on the previous time-averaged level of postsynaptic cell firing. Accordingly, anodal tDCS, which increases post-synaptic activity, would raise the θ_m, decreasing the likelihood of LTP formation and increasing the likelihood of LTD. Thus, the level of task-induced post-synaptic activity that would normally result in LTP, may now induce in LTD, inhibition, and as a result, decreased learning and greater cortical inhibition.

Metaplasticity according to the BCM model is thought to occur via modifications in synaptic mechanisms, and is well characterized for glutamatergic changes (Lee, Yasuda, & Ehlers, 2010). The contribution of GABA to such

metaplastic processes has primarily focused on its ability to indirectly shift θ_m via increasing the NMDA response and intracellular Ca^{2+} concentration (Abraham & Tate, 1997), or by autoregulatory inhibition of GABA release as a result of postsynaptic excitation of neighbouring terminals (Chevaleyre & Castillo, 2004). However, whether plasticity of GABAergic signalling is in itself a type of metaplasticity is still unclear (Abraham, 2008), although rodent work was shown it to be involved in metaplasticity in the spinal dorsal horn (G. Miletic & Miletic, 2001) and hippocampus (Bukalo, Schachner, & Dityatev, 2007). Here, we report changes in 2.5 ms, but not 1 ms, SICI associated with learning after anodal tDCS, supporting the view that metaplasticity is a primarily synaptic mechanism. Moreover, this result suggests a direct role for $GABA_A$ in the mediation of metaplasticity as evoked by our paradigm.

Surround Inhibition

In the control condition, in which the motor task was performed in the absence of tDCS, we demonstrated that motor learning led to decreased cortical excitation in the FDI. This result contrasts with the findings previously reported by Rosenkranz and Rothwell (Rosenkranz & Rothwell, 2006). In their study, MEP size increased following motor learning. A potential reason for this disparity lies in the specifics of the task employed by our studies. Rosenkranz's study used self-paced thumb abduction, which is highly dependent on the muscle from which they recorded, the APB. In Experiment 1, we recorded from the FDI, a muscle that is not directly involved in learning our sequence task, as evidenced by the results from Experiment 2. These findings suggest that task-induced decreases in cortical excitability may be specific to muscles peripherally involved in learning the task,

like the FDI in our study, and not to muscles that are critically involved, like the APB in the Rosenkranz study.

Indeed, decreased excitation of the nearby muscle may be a cooperative mechanism that paves the way for increased excitation of the target muscle, exploiting center-surround organization. In this model, surround inhibition works to focus neuronal activity on the processes that are actively required for task performance, by filtering out extraneous inputs (Beck & Hallett, 2011). Though most thoroughly characterized in the visual system, surround inhibition has been reported in the sensorimotor system as well, particularly in fine finger movements (Beck et al., 2005), and for the initiation of voluntary movements (Sohn & Hallett, 2004). Beck and colleagues demonstrated facilitation of MEPs recorded from the FDI, a synergistic muscle in their task, while those of the APB, an adjacent muscle, were decreased (Beck et al., 2008). Likewise, in our study, we found decreased MEPs in the adjacent muscle of our task, the FDI. As expected, no changes were found in the APB, a muscle that was neither adjacent nor synergistic in our task. We did not, however, find significantly increased excitation of a synergistic muscle (i.e., the ADM). This may be because the ADM is used slightly less in our task, as the ratio of button presses among fingers is 3-3-2-2. As a result of the cumulative effect of this difference, any increase in excitation may still lie below a statistical threshold.

The finding of decreased excitation following task performance helps explain the behavioural results for the motor learning task, illustrated in Figure 5.3, in which offline anodal tDCS decreases learning compared to control. When applied alone, anodal tDCS increases MEP size; when applied during task performance, it does not. This may reflect the two processes effectively negating each other: anodal tDCS tends to increase excitation, while task performance tends to decrease

excitation, leading to a zero-sum effect. That these neurophysiological results interact with each other suggests motor learning and tDCS rely on similar or cooperative neurochemical mechanisms. One such possibility is through specific synaptic changes, either in GABAergic or glutamatergic synapses. Inhibitory plasticity has been documented at GABAergic synapses previously (Maffei, 2011), and both anodal tDCS and motor learning have been shown to increase levels of cortical GABA (Floyer-Lea et al., 2006; Stagg et al., 2009). This, combined with our finding of increased 2.5 ms SICI following motor learning, raises the possibility that GABAergic synapses may be a substrate for the interaction between tDCS and motor learning. An alternative putative site for these modulations to occur are the glutamatergic synapses. Motor learning occurs via LTP-like processes that increase synaptic Ca^{2+} concentration (Ziemann et al., 2004). Via surround inhibition, this targeted LTP-like increase in synergistic muscles may lead to corresponding decreases in the FDI, thereby eliminating the prospective increase in MEP size. During the intrastimulation period, anodal tDCS is thought to exert its effects primarily through a widespread decrease in resting membrane potential (Stagg & Nitsche, 2011). Indeed, pharmacological studies have shown that blockading Ca^{2+} and Na^{+} channels abolishes or greatly reduces the excitability enhancement normally elicited by anodal tDCS (Nitsche, 2003). Thus, an additional avenue through which motor learning may have suppressed increases in MEP size in the FDI is via modulation of resting membrane potentials.

Future Directions

Previous studies have reported enhanced motor leaning with online anodal tDCS (Nitsche, 2003; Stagg et al., 2011b). Our study did not replicate this finding in

the AT-R condition, although studies employing very similar paradigms have done so (Stagg et al., 2011b). This may partially be due to the length of the inactive "rest" blocks in comparison to our active "sequence" blocks. In the previous study from our lab utilising a similar motor sequence learning task, the rest blocks lasted for 12 seconds, while they lasted for 30 seconds in the present study. It is conceivable that the longer rest periods resulted in an attenuation of the behavioural affects of anodal tDCS, as approximately half of the stimulation period was administered while no actual learning was occurring. To address this issue, future studies using a sequence task would employ one identical to that in the previous study. Moreover, one might repeat this experiment using a different motor task altogether, such as thumb abduction, to directly test the surround inhibition hypothesis put forward here. Independent of the motor task used, subsequent studies should consider recording from multiple muscles during each of the stimulation paradigms, and not just the control condition. Doing so would allow for more concrete conclusions on how tDCS might affect surround inhibition to affect behaviour.

5.5 CONCLUSIONS

Taken together, these two experiments help elucidate the mechanisms responsible for behavioural modifications caused by anodal tDCS. In particular, the results suggest that surround inhibition focuses activity on muscles critically involved in task performance. This activity is then transformed into augmented or decreased learning in accordance with a sliding threshold of LTP/LTD induction, initiated by tDCS application. Our neurophysiological recordings provide evidence that these metaplastic mechanisms occur synaptically, particularly with regard to $GABA_A$ activity. Behaviourally, these alterations manifest themselves as changes in

motor learning in our healthy volunteers. The remaining two chapters of this thesis investigate whether similar changes in motor performance and cortical properties can be elicited in chronic stroke patients. By doing this, we aim to investigate the clinical relevance of anodal tDCS in the motor domain.

REFERENCES

Abraham, W. C. (2008). Metaplasticity: tuning synapses and networks for plasticity. *Nature Reviews Neuroscience*, *9*(5), 387–387.

Abraham, W. C., & Bear, M. F. (1996). Metaplasticity: the plasticity of synaptic plasticity. *Trends in neurosciences*, *19*(4), 126–130.

Abraham, W. C., & Tate, W. P. (1997). Metaplasticity: a new vista across the field of synaptic plasticity. *Progress in neurobiology*, *52*(4), 303–323.

Beck, S., & Hallett, M. (2011). Surround inhibition in the motor system. *Experimental Brain Research*, *210*(2), 165–172.

Beck, S., Richardson, S. P., Shamim, E. A., Dang, N., Schubert, M., & Hallett, M. (2008). Short intracortical and surround inhibition are selectively reduced during movement initiation in focal hand dystonia. *Journal of Neuroscience*, *28*(41), 10363–10369.

Beck, S., Schubert, M., Richardson, S. P., & Hallett, M. (2009). Surround inhibition depends on the force exerted and is abnormal in focal hand dystonia. *Journal of applied physiology (Bethesda, Md. : 1985)*, *107*(5), 1513–1518.

Bienenstock, E. L., Cooper, L. N., & Munro, P. W. (1982). Theory for the development of neuron selectivity: orientation specificity and binocular interaction in visual cortex. *The Journal of neuroscience : the official journal of the Society for Neuroscience*, *2*(1), 32–48.

Bukalo, O., Schachner, M., & Dityatev, A. (2007). Hippocampal metaplasticity induced by deficiency in the extracellular matrix glycoprotein tenascin-R. *Journal of Neuroscience*, *27*(22), 6019–6028.

Chevaleyre, V., & Castillo, P. E. (2004). Endocannabinoid-mediated metaplasticity in the hippocampus. *Neuron*, *43*(6), 871–881. doi:10.1016/j.neuron.2004.08.036

Floyer-Lea, A., Wylezinska, M., Kincses, T., & Matthews, P. M. (2006). Rapid modulation of GABA concentration in human sensorimotor cortex during motor learning. *Journal of Neurophysiology*, *95*(3), 1639–1644.

Fricke, K., Seeber, A. A., Thirugnanasambandam, N., Paulus, W., Nitsche, M. A., & Rothwell, J. C. (2011). Time course of the induction of homeostatic plasticity generated by repeated transcranial direct current stimulation of the human motor cortex. *Journal of Neurophysiology*, *105*(3), 1141–1149.

Huang, Y. Y., Colino A., Selig D. K., & Malenka R. C. (1992). The influence of prior synaptic activity on the induction of long-term potentiation. *Science, 255*(504), 730-733.

Iyer, M. B., Schleper, N., & Wassermann, E. M. (2003). Priming stimulation enhances the depressant effect of low-frequency repetitive transcranial magnetic stimulation. *Journal of Neuroscience*, *23*(34), 10867–10872.

Jung, P., & Ziemann, U. (2009). Homeostatic and nonhomeostatic modulation of learning in human motor cortex. *Journal of Neuroscience*, *29*(17), 5597–5604.

Kuo, M.-F., Unger, M., Liebetanz, D., Lang, N., Tergau, F., Paulus, W., & Nitsche, M. A. (2008). Limited impact of homeostatic plasticity on motor learning in humans. *Neuropsychologia*, *46*(8), 2122–2128.

Lee, M.-C., Yasuda, R., & Ehlers, M. D. (2010). Metaplasticity at single glutamatergic synapses. *Neuron*, *66*(6), 859–870. doi:10.1016/j.neuron.2010.05.015

Maffei, A. (2011). The many forms and functions of long term plasticity at GABAergic synapses. *Neural Plasticity, 2011*(254724).

Miletic, G., & Miletic, V. (2001). Contribution of GABA-A receptors to metaplasticity in the spinal dorsal horn. *Pain*, *90*(1-2), 157–162.

Nitsche, M. A. (2003). Pharmacological modulation of cortical excitability shifts induced by transcranial direct current stimulation in humans. *The Journal of Physiology*, *553*(1), 293–301.

Nitsche, M. A., & Paulus, W. (2000). Excitability changes induced in the human motor cortex by weak transcranial direct current stimulation. *The Journal of Physiology*, *527 Pt 3*, 633–639.

Nitsche, M. A., & Paulus, W. (2001). Sustained excitability elevations induced by transcranial DC motor cortex stimulation in humans. *Neurology*, *57*(10), 1899–1901.

Nitsche, M. A., Roth, A., Kuo, M.-F., Fischer, A. K., Liebetanz, D., Lang, N., Tergau, F., et al. (2007). Timing-dependent modulation of associative plasticity by general network excitability in the human motor cortex. *Journal of Neuroscience*, *27*(14), 3807–3812.

Nitsche, M. A., Schauenburg, A., Lang, N., Liebetanz, D., Exner, C., Paulus, W., & Tergau, F. (2003). Facilitation of implicit motor learning by weak transcranial direct current stimulation of the primary motor cortex in the human. *Journal of*

cognitive neuroscience, *15*(4), 619–626.

Rosenkranz, K., & Rothwell, J. C. (2006). Differences between the effects of three plasticity inducing protocols on the organization of the human motor cortex. *European Journal of Neuroscience*, *23*(3), 822–829.

Sohn, Y. H., & Hallett, M. (2004). Surround inhibition in human motor system. *Experimental Brain Research*, *158*(4), 397–404.

Stagg, C. J., & Nitsche, M. A. (2011). Physiological Basis of Transcranial Direct Current Stimulation. *The Neuroscientist*, *17*(1), 37–53.

Stagg, C. J., Best, J. G., Stephenson, M. C., O'Shea, J., Wylezinska, M., Kincses, Z. T., Morris, P. G., et al. (2009). Polarity-sensitive modulation of cortical neurotransmitters by transcranial stimulation. *Journal of Neuroscience*, *29*(16), 5202–5206.

Stagg, C. J., Bestmann, S., Constantinescu, A. O., Moreno Moreno, L., Allman, C., Mekle, R., Woolrich, M., Near, J., et al. (2011a). Relationship between physiological measures of excitability and levels of glutamate and GABA in the human motor cortex. *The Journal of Physiology*, *589*(Pt 23), 5845–5855.

Stagg, C. J., Jayaram, G., Pastor, D., Kincses, Z. T., Matthews, P. M., & Johansen-Berg, H. (2011b). Polarity and timing-dependent effects of transcranial direct current stimulation in explicit motor learning. *Neuropsychologia*, *49*(5), 800–804.

Tamburin, S., Fiaschi, A., Andreoli, A., Marani, S., & Zanette, G. (2005). Sensorimotor integration to cutaneous afferents in humans: the effect of the size of the receptive field. *Experimental Brain Research*, *167*(3), 362–369.

Vines, B. W., Cerruti, C., & Schlaug, G. (2008). Dual-hemisphere tDCS facilitates greater improvements for healthy subjects' non-dominant hand compared to uni-hemisphere stimulation. *BMC neuroscience*, *9*, 103.

Ziemann, U., & Siebner, H. R. (2008). Modifying motor learning through gating and homeostatic metaplasticity. *Brain Stimulation*, *1*(1), 60–66.

Ziemann, U., Ilić, T. V., Iliać, T. V., Pauli, C., Meintzschel, F., & Ruge, D. (2004). Learning modifies subsequent induction of long-term potentiation-like and long-term depression-like plasticity in human motor cortex. *Journal of Neuroscience*, *24*(7), 1666–1672.

Chapter 6: tDCS and Motor Training Induce Functional and Structural Changes in Chronic Stroke Patients

The first two experimental chapters of this thesis focused on elucidating the mechanisms responsible for the effects of tDCS in healthy controls. We demonstrated that behavioural modifications and neuroimaging changes were possible following stimulation. The remainder of this thesis seeks to extend this work to a clinical population: chronic stroke patients. We ask whether the behavioural improvements caused by coupling motor training with tDCS are reflected in brain changes apparent using MR imaging. In particular, we investigate changes in task-induced activation and grey matter. The final chapter then uses these and other baseline neuroimaging measures to predict patients' response to the rehabilitation program.

6.1 INTRODUCTION

Natural recovery of post-stroke motor function plateaus within three to six months of the incident (Halsband & Lange, 2006; Leonard, 1997; Studenski et al., 2001) (For an in depth review of stroke recovery, see section 1.3.3.). Concurrent with a tapering off of behavioural gains, the gradual transition into the chronic phase of stroke recovery is associated with functional and structural brain changes. Knowledge of these potential changes has formed the basis of rehabilitation programs aimed at improving behaviour in chronic stroke patients.

6.1.1 FUNCTIONAL CHANGES

The most striking neurological change that evolves with advancing time post-stroke is most readily apparent during task performance. Longitudinal studies document heightened contralesional activation of motor areas during the acute phase, which slowly decreases as recovery plateaus in the chronic stage (Feydy et al., 2002; Tombari et al., 2004; Ward et al., 2003). Patients in whom this response pattern has normalised to a profile more consistent with that seen in healthy adults (i.e., ipsilesional, contralateral to the moving limb, and primarily unilateral) tend to be better recovered than their counterparts who still exhibit a strongly bilateral activation pattern (Cramer, 2008; Synofzik et al., 2008).

Research regarding the extent to which the imbalance caused by this contralesional activity is associated with worsened motor ability is at times unclear (Feydy et al., 2002; Ward et al., 2003). However, the phenomenon is generally viewed as maladaptive, particularly with respect to altered competitive hemispheric interactions (Duque et al., 2007). This occurs as a result of disturbed processes in both hemispheres (Takeuchi & Izumi, 2012). M1 of the lesioned hemisphere experiences increased inhibition from within its own circuitry (Liepert et al., 2005), which may decrease its ability to naturally downregulate the contralesional hemisphere via inhibitory transcallosal pathways. The contralesional motor cortex becomes hyperexcitable (Ward et al., 2003; 2006), and in turn is able to exert excessive inhibition over the lesioned hemisphere (Hikosaka et al., 2002; Murase et al., 2004; Nachev et al., 2008), further perpetuating the hemispheric imbalance and leading to stunted recovery.

6.1.2 Structural Changes

In addition to performance-based changes, post-stroke recovery of behaviour is also accompanied by modifications in brain structure, often colocalised with the functional changes (Schaechter et al., 2006). Longitudinal studies following stroke patients over the course of several months to a year have documented grey matter decreases in motor areas directly and indirectly connected to the lesion site (Fan et al., 2012; Kraemer et al., 2004). Conversely, non-motor regions such as the hippocampus and precuneus experience increased grey matter density that is correlated with motor ability, suggesting that increased recruitment of regions involved in memory and cognition may help modulate the improved motor performance thought to indicate motor recovery (Fan et al., 2012).

Recent work suggests that this decline in grey matter density within motor regions following a stroke can be partially mitigated by rehabilitation techniques. Gauthier and colleagues demonstrated that ten days of constraint induced movement therapy (CIMT) resulted in diffuse grey matter increases in bilateral sensory and motor regions (Gauthier et al., 2008). These changes were correlated with increased use of the affected limb and behavioural improvements. Similar results have been found in healthy subjects: performance of a sequential pinch force task over five days led to increased grey matter in the contralateral M1, ipsilateral PMv, and DLPFC (Gryga et al., 2012).

6.1.3 Behavioural Modifications

Further to these modifications occurring in the brain, stroke patients also decrease their use of the affected limb, relying more heavily on the unaffected limb in a form of behavioural compensation (Levin et al., 2009). While such

compensatory strategies are initially beneficial in performing activities of daily living, they may be detrimental to long-term recovery. Overuse of the unaffected limb can lead to learned non-use of the affected limb, resulting in loss of what motor function may have been spared by the stroke, further hindering the ability to re-establish appropriate arm function (Levin et al., 2009). Moreover, as evidenced from rodent studies, these changes in motor behaviour may in turn worsen and propagate the maladaptive plasticity discussed above (Allred & Jones, 2008; Allred et al., 2010).

Rehabilitation strategies have endeavoured to promote motor recovery in chronic stroke patients by attempting to normalise both motor behaviour as well as neuronal profiles. Traditional behavioural therapy focuses on task-specific training of the affected limb, with the aim of restoring a portion of its lost motor function (Hubbard et al., 2009). Other rehabilitation techniques, such as constraint-induced movement therapy (CIMT), attempt to overcome learned non-use of the affected limb. CIMT restrains the unaffected limb, substantially hindering its range of movement, thus compelling the patient to use the affected limb. Behavioural improvements following CIMT have been shown to last for up to one year (Wolf et al., 2006).

6.1.4 Brain Stimulation to Augment Physiotherapy

In addition to modifying patient behaviour, therapies can also target the brain structures and processes underlying maladaptive post-stroke plasticity. In particular, interhemispheric imbalance can be attenuated by increasing the function of the ipsilesional motor cortex, decreasing the function of the contralesional motor cortex, or both. In combination with motor training, such interventions are

performed with the brain stimulation techniques of rTMS and tDCS, introduced in Chapter 2 (Nowak at al., 2009). While rTMS has been demonstrated to produce behavioural improvements (Corti et al., 2012; Nowak et al., 2009), we focused on tDCS as it is less obviously intrusive, and has a better placebo condition (Gandiga et al., 2006).

When combined with motor training, a single session of tDCS can improve motor ability of the affected limb. Anodal tDCS to the ipsilesional M1 has been shown to increase performance on clinical and behavioural measures of hand function (Fregni et al., 2005; Hummel & Cohen, 2005; Stagg et al., 2012). This improvement is associated with reduced inhibition in M1 as measured by short intracortical inhibition (SICI) (Hummel, 2005). Cathodal tDCS to the contralesional M1 can produce similar results. Following cathodal stimulation, motor improvements have been documented (Fregni et al., 2005; Zimerman et al., 2012) that correlate with the tDCS-induced decreases in inhibition within the lesioned M1 (Zimerman et al., 2012). Both ipsilesional anodal tDCS and contralesional cathodal tDCS promote increased task-related fMRI activity in motor regions, particularly in the hand area of the ipsilesional M1, suggesting that this region may be the cortical substrate of the reported behavioural improvements (Stagg et al., 2012).

6.1.5 Repeated Sessions of Tdcs and Training

Given the encouraging results produced by a single session of tDCS, Boggio et al. investigated the effects of weekly sessions of tDCS given over one month. Although patients performed better after each individual session, there was no cumulative effect of either anodal or cathodal stimulation (Boggio et al., 2007). However, if five consecutive sessions of cathodal tDCS were given, they reported a

behavioural enhancement that lasted for 2 weeks following intervention (Boggio et al., 2007). Similar results have since been replicated, with the additional finding that immediately following the intervention, improved motor outcome is correlated with decreased contralesional task-related fMRI activity (Nair at al., 2011). The functional potential of bihemispheric tDCS, in which ipsilesional anodal and contralesional cathodal tDCS are delivered simultaneously, has also been explored. Ten days of 1 mA bihemispheric tDCS and occupational therapy resulted in behavioural improvements that persisted for one week following intervention (Lindenberg et al., 2010). For those patients receiving real tDCS, these gains were accompanied by stronger activation in ipsilesional motor regions, a result not seen in the placebo condition. Bolognini and colleagues performed a study in which patients received 40 minutes of 2 mA bihemispheric tDCS while also undergoing two weeks of CIMT. Patients receiving stimulation and CIMT, as well as those in the control condition receiving CIMT alone, showed behavioural improvements and a decrease in TMS measures of excitability in the contralesional hemisphere (Bolognini et al., 2011). Interestingly, only those receiving tDCS showed increased excitability in the lesioned hemisphere, as well as a reduction in transcallosal inhibition from the contra- to ipsi-lesional hemisphere. This suggests that tDCS augments training-induced behavioural gains via multiple neural mechanisms.

The aforementioned repeated-sessions studies all utilised either cathodal or bihemispheric tDCS; none used multiple sessions of daily anodal tDCS in rehabilitation for chronic stroke patients (although a 2011 study by Geroin investigating lower limb function has). Evidence suggests that it is likely that such a protocol would impart significant, sustained behavioural improvements: if repeated

sessions of anodal tDCS are provided to healthy controls, the enhancement of motor ability continues for at least 3 months (Reis et al., 2009). Moreover, work from our lab comparing single sessions of anodal, cathodal, and sham tDCS suggest that anodal tDCS more robustly elicits behavioural gains in stroke patients, particularly within a heterogeneously impaired population (Stagg et al., 2012). The present study intended to fill this gap regarding the effect of repeated sessions of anodal tDCS on motor recovery in chronic stroke patients. We designed a double-blind, randomised-controlled trial in which patients received simultaneous ipsilesional anodal tDCS to M1 and motor training for ten days over a period of two weeks. We included multiple post-intervention followups and neuroimaging modalities to assess the longevity and neural correlates of motor improvements. We predicted that anodal tDCS would result in performance gains on our clinical measures above and beyond that seen with motor training alone, an effect that would outlast the intervention by weeks to months. Moreover, we suspected that these changes would be associated with increased activation of ipsilesional motor areas.

6.2 METHODS

6.2.1 OVERVIEW

This double-blind, randomised-controlled trial investigated the effect of a combined motor training and tDCS program in chronic stroke patients (Figure 6.1).

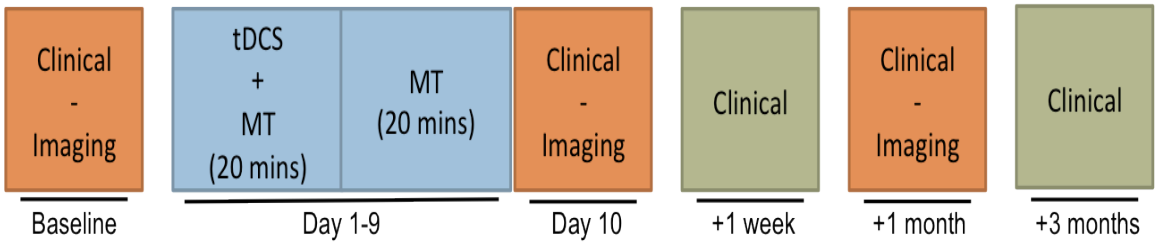

Figure 6.1: Study design. Patients were seen over several months. Clinical: clinical measures (Fugl-Meyer and ARAT); tDCS: anodal or sham tDCS. This and the following chapter are primarily concerned with the sessions which included imaging: baseline, day 10 post-intervention followup, and the one month followup.

Following an initial consultation with a physiotherapist to determine suitability for inclusion in the study, patients were randomly assigned to receive either anodal or sham tDCS. Prior to beginning the intervention, patients each underwent a baseline session of clinical measures and imaging. The intervention period lasted for nine days (Monday through Friday of week one, Monday through Thursday of week 2), and contained daily motor training and tDCS. Post-intervention follow-ups consisting of clinical measures and imaging were administered immediately following the end of the intervention (Day 10), and one month later (Day 39).

6.2.2 SUBJECTS

Twenty-two patients are included in this analysis (11 anodal, 11 sham). At least six months had lapsed since each participant's first and only stroke, and all had lost some motor function of their hand, to varying degrees. Both cortical and subcortical strokes were included; no infarcts impinged on M1. Patients had no other neurological or psychiatric disorders, nor any contraindications for fMRI or tDCS. Prior to inclusion in the study, all patients gave their written informed

consent in accordance with local ethics committee approval. Table 6.1 provides a summary of relevant patient characteristics; Figure 6.2 shows their lesions.

tDCS condition	Subject	Gender	Age at intervention (years)	Time post-stroke (months)	Baseline UE-FM (maximum 66)	Baseline ARAT (maximum 57)	GRASP Level (1/2/3)
Anodal	02	M	74	44	13	0	1
	04	M	58	72	59	30	3
	07	F	45	54	61	43	3
	10	M	65	52	34	31	2
	11	M	71	44	36	19	2
	14	M	72	109	25	3	1
	20	M	58	105	52	43	3
	21	F	52	17	28	9	1
	22	M	70	41	56	37	3
	24	M	53	6	27	3	1
	26	F	37	19	35	3	1
		3F	**59.55**	**51.18**	**38.73**	**20.09**	**5/2/4**
Sham	01	F	76	47	16	4	1
	03	M	67	47	62	55	3
	05	M	56	29	40	35	2
	06	M	55	92	62	48	3
	12	F	79	68	14	3	1
	13	M	72	31	14	0	1
	16	M	78	141	47	23	3
	17	M	68	97	37	40	2
	18	M	64	39	50	49	3
	23	M	69	99	46	27	3
	25	F	44	9	21	3	1
		3F	**66.18**	**63.55**	**37.81**	**26.09**	**4/2/5**
Overall Mean		**6F/16M**	**62.86**	**57.36**	**37.95**	**23.09**	**9/4/9**

Table 6.1: Patient characteristics. UE-FM: Upper extremity Fugl-Meyer. ARAT: Action reaction arm test. GRASP: Graded repetitive arm supplementary program.

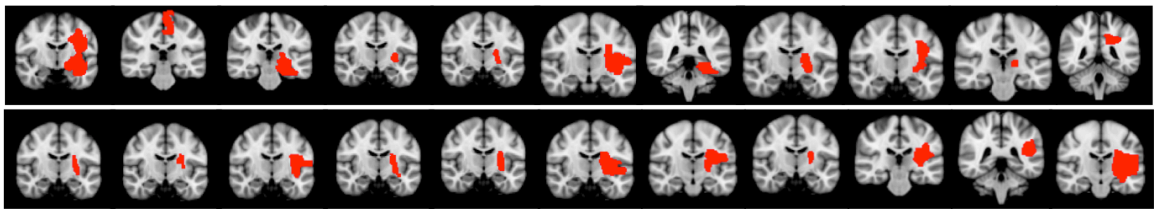

Figure 6.2: Lesion locations of anodal (top row) and sham tDCS (bottom row) groups.

6.2.3 Clinical Measures

Multiple clinical measures were used to assess motor ability. The full range of these clinical outcomes lies outside the scope of this thesis. (They have been collected and analysed in depth by another student in the group). Here, we concentrate on two complementary clinical measures: the Upper Extremity Fugl-Meyer Assessment (UE-FM) and the Action Reaction Arm Test (ARAT). Both measures are sensitive to recovery-related motor changes present in stroke patients. However, they are attuned to different dimensions of the recovery process.

The UE-FM measures motor recovery as indicative of impairment; the ARAT measures functional recovery as indicative of disability level (DeWeerdt, 1985). While related, there is no simple relationship between impairment and disability, as the two are distinct entities (Roth et al., 1998; van der Lee et al., 2001). Impairment has been defined as "any loss or abnormality of psychological, physiological or anatomical structure or function" (World Health Organisation). Disability has been defined as "any restriction or lack (resulting from any impairment) of ability to perform an activity in the manner or within the range considered normal for a human being" (World Health Organisation). Thus, by measuring impairment, the UE-FM is more attuned to anatomical changes within the brain. The ARAT, by measuring disability, more accurately reflects motor performance and the execution of tasks.

6.2.4 MOTOR TRAINING

The Graded Repetitive Arm Supplementary Program (GRASP) formed the basis of our motor training regimen (Halsband & Lange, 2006; Pang et al., 2006). Previous studies have shown that patients who complete the GRASP program experience motor improvements as measured by the UE-FM and other behavioural scales (Halsband & Lange, 2006; Pang et al., 2006). Tasks performed ranged from gross movements (e.g., lifting the affected arm) to exercises requiring finer dexterity and coordination (e.g., buttoning a shirt using the affected hand). Following an initial assessment by a physiotherapist, each patient was stratified into one of three GRASP levels (1: most impaired, through to 3: least impaired), according to their degree of paralysis. For each patient, the tasks administered from within the prescribed GRASP level were tailored to the individual's motor ability.

6.2.5 TDCS ADMINISTRATION

On each day of the intervention, the subjects were fitted with saline soaked tDCS electrodes (5 x 7 cm). The reference cathode was positioned over the contralesional supraorbital ridge, while the stimulating anode was placed over M1 of the lesioned cortex, centered over the hand area as measured to be 5cm lateral to Cz. The current generated by the tDCS machine (Magstim eldith) was steadily increased to 1 mA over 10 seconds and, for the anodal condition, continued for 20 minutes. For those subjects receiving sham stimulation, the current was allowed to reach 1 mA, and then turned off. During this 20 minutes of anodal or sham stimulation, all patients received modified versions of the GRASP. After 20 minutes,

the electrodes were removed. The GRASP program was continued for an additional 20 minutes.

6.2.6 IMAGE ACQUISITION AND ANALYSIS

Three imaging sessions were performed: at baseline, immediately following intervention cessation on Day 10, and Day 30. Each scanning session lasted approximately fifty minutes and was performed on a 3T Verio scanner (Siemens, Erlangen, Germany). T1 and T2 weighted structural scans, task fMRI, resting fMRI and DTI were collected, as detailed below.

6.2.6.1 Task fMRI

ACQUISITION. Axial echo-planar volumes were acquired (TR=2410ms, TE=30ms, flip angle=90°, voxel size=3x3x3mm). During acquisition passive flexion-extension of the stroke affected hand was performed, cued by a 1Hz clicker presented to the experimenter via headphones attached to the scanner. Movements were manually guided by the experimenter, as not all patients retained independent use of their stroke affected hand. Movement and rest blocks alternated in 30 second periods. Using an MPRAGE sequence, T1-weighted structural images were also collected and used in the registration process.

ANALYSIS. For analysis purposes, images from patients with right hemispheric strokes were flipped about the midline after registration to standard space so that all lesions appeared on the left side. All analysis was performed using tools from FSL (www.fmrib.ox.ac.uk/fsl).

The following pre-processing steps were applied: high-pass temporal filtering at 100 seconds; motion correction using MCFLIRT (Jenkinson et al., 2002); removal

of non-brain tissue using BET; spatial smoothing using a Gaussian kernel of 5mm; B_0 unwarping with fieldmaps using FUGUE. To remove artefactual components, the pre-processed EPI data were then denoised using Independent Component Analysis from within MELODIC, as detailed in section 3.3.5.3 (Beckmann & Smith, 2004).

Statistical analyses were performed on this denoised data using FILM with local autocorrelation correction (Woolrich et al., 2001). Registration of each patient's individual EPI and structural images to standard space was performed using FNIRT and Boundary Based Registration (BBR) (Greve & Fischl, 2009). Within FEAT, a boxcar regressor modelling the 30-second task and rest blocks was used to create first-level statistical activation maps for each patient at each timepoint: baseline (base), post-intervention on Day 10 (post), one month follow-up (month).

Higher-level, mixed effects analyses were then run using FLAME. Two analyses were performed. The first compared activations between the three timepoints for all subjects, collapsed across stimulation conditions (all patients: post – base, month – base, month – post), with individual subject regressors. The second analysis compared the three timepoints within stimulation condition (anodal: post – base, month – base, month – post; sham: post – base, month – base, month – post), and between conditions (anodal – sham: post – base, month – base, month – post). For each of these analyses, resulting Z statistic images were thresholded using clusters formed at $Z = 2.0$, $p < 0.01$.

To explore the data, each of the significant clusters determined by the higher-level analyses was binarised and used as a mask to extract the mean contrast of parameter estimate (COPE) from each patient's individual EPI data file. These COPEs were then used to create bar graphs to better visualise the changes occurring within some of these areas.

6.2.6.2 Structural MRI

ACQUISITION. T1-weighted structural images were acquired for all subjects using an MPRAGE sequence (voxel size= 1mm isotropic, TR=2040ms, TE=4.7ms, flip angle=8°). For some subjects, an additional T2-weighted structural image was also acquired (voxel size= 0.6 x 0.5 x 3mm; TR=5220ms; TE=71ms; flip angle=120°).

VBM ANALYSIS. A standard FSL-VBM pipeline was used to analyse longitudinal changes in grey matter (Douaud et al., 2007). For each subject, the following steps were taken: the three T1-weighted structural images (baseline, post-intervention, and one month follow-up) were aligned to one another and a "midpoint space" was created that was equidistant from all three images. The scans were averaged together in this space and the resulting image was then brain-extracted using BET, creating a brain mask. This brain mask was then transformed back to each scan's original space and used to mask each scan equivalently. Each scan was then segmented in its native space using FAST. The grey matter for the three scans for each subject were then transformed to the subject's midpoint space, where they were averaged together. These average grey matter images were then nonlinearly aligned to standard MNI space using FNIRT.

The standard-space aligned, average grey matter images of all the subjects (i.e., one per subject) were then combined to build a study-specific template. The average grey matter images were then re-aligned to this study-specific template. The grey matter for each individual scan (i.e., three scans per subject) was then transformed to standard space using the combination of rigid transformation from native space to midpoint space and the warp from midpoint space to MNI space. The images were then modulated for local expansion and contraction caused by the

non-linear registration and smoothed with a sigma of 4mm. These pre-processed images were then analysed using permutation-based testing, as implemented in Randomise within FSL, to test for statistical differences between timepoints and groups, using the same contrasts as outlined above for the higher-level FEAT analysis. Threshold-free cluster enhancement was used to determine areas of significant differences at a level of $p<0.05$, corrected for family-wise error.

T2 ANALYSIS. The T2-weighted structural images from each subject were brain-extracted using BET, then registered to the subject's corresponding T1-weighted structural images using BBR. The nonlinear warp fields generated by the T1 VBM analysis were then used to register the T2-weighted images to standard space. As these images are T2-weighted, and thus the value of each voxel has no intrinsic meaning, each subject's image was normalised by the median of all values across the brain. These median-normalised T2-weighted images were then analysed using non-parametric statistical methods implemented by Randomise.

6.2.6.3 Diffusion MRI

ACQUISITION. Two sets of diffusion weighted volumes were acquired (voxel size= 2mm isotropic; TR=9600ms; TE= 87ms; 60 directions with a b-value 1000 s/mm^2; and 8 volumes without diffusion weighting, b-value=0 s/mm^2).

MEAN DIFFUSIVITY ANALYSIS. Diffusion data was analysed using FMRIB's Diffusion Toolbox (FDT). Eddy current correction was run to reduce the distortions induced by the gradient coils, and to correct for head motion by affine registering all images acquired for one subject to one another. DTIfit then fit a diffusion tensor at each brain voxel, which was subsequently used to generate voxel-wise estimates of mean diffusivity (MD). The longitudinal voxel-based analysis of the MD images

proceeded as above for the T2-weighted images; as MD is a quantitative value, no normalisation of the data was required prior to analysis.

6.2.6.4 Resting fMRI

ACQUISITION. Axial echo-planar volumes were acquired (TR=2410ms, TE=30ms, flip angle=90°, voxel size=3mm isotropic). During this time, subjects were instructed to relax with their eyes open; no task was performed.

6.3 RESULTS

6.3.1 BEHAVIOURAL IMPROVEMENTS

When considering the full set of patients and follow-up timepoints, a RM-ANOVA found a significant main effect of time on both clinical measures (ARAT: $F(4, 72)= 25.09$, $p<0.001$; UE-FM: $F(4, 72)= 24.07$, $p<0.001$), demonstrating that, overall, patients' behavioural scores improved over time. Moreover, RM-ANOVA on the absolute change in clinical scores for post-tDCS timepoints relative to baseline showed a significant main effect of tDCS on the ARAT ($F(1,18)=4.49$, $p=0.048$), demonstrating that the two interventions (motor training alone, simultaneous motor training and anodal tDCS) have differential effects on behaviour. For the subset of patients and timepoints presented in this chapter (those that contain imaging measures), similar results were found (RM-ANOVA, main effect of time. ARAT: $F(2,40)= 30.345$, $p<0.001$; UE-FM: $F(2,40)=37.312$, $p<0.001$; RM-ANOVA, time by intervention interaction. ARAT: $F(2,40)= 1.519$, $p=0.231$). Figure 6.2 illustrates improvements in motor ability as measured by increased scores on the ARAT (Figure 6.3A) and Fugl-Meyer (6.3B).

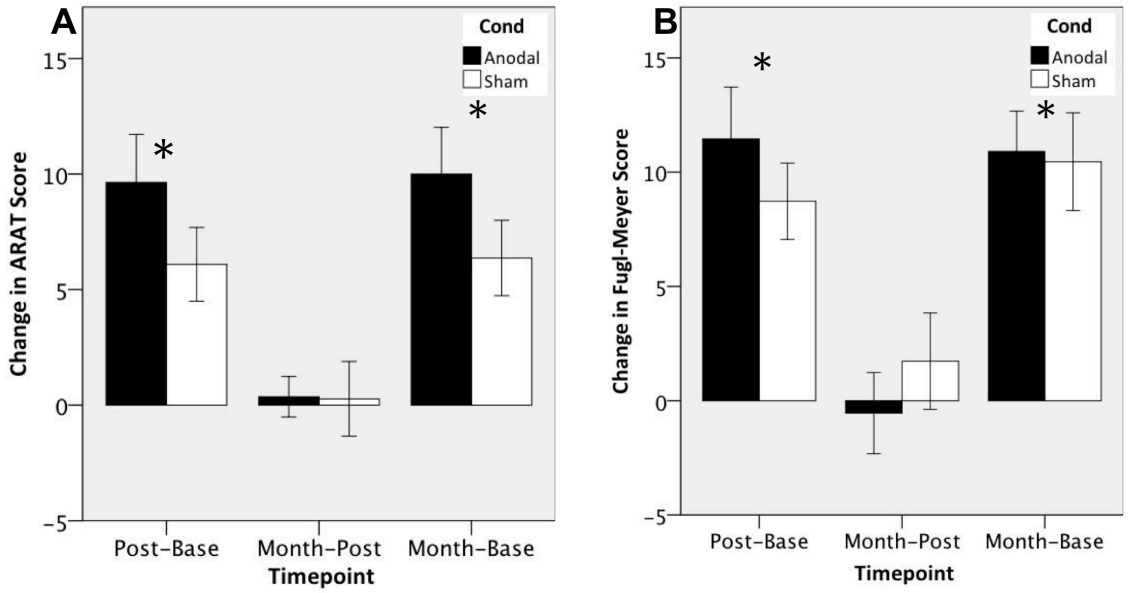

Figure 6.3: Behavioural changes. (A) Increase in ARAT score. (B) Increase in UE-FM score. For both clinical measures, positive numbers reflect greater improvement.

6.3.2 RESTING FMRI AND DTI

No significant longitudinal changes were found within the resting state fMRI data or the DTI data so those modalities are not considered further in this chapter.

6.3.3 TASK FMRI

Rehabilitation causes greater deactivation of medial parietal-occipital areas during task-performance

We first determined whether our rehabilitation program produced functional changes in task-based activation in the stroke patients. A voxel-wise analysis of all patients (in both the anodal and sham groups) comparing activation patterns between the three timepoints found significant differences between baseline and post-intervention (Figure 6.4A). These changes were primarily posterior, including the precuneus and posterior cingulate cortex (Table 6.2). Bar graphs plotting the COPEs extracted from these areas showed that these regions showed deactivation during task performance at all time points, but that this was

greater in magnitude post-intervention (Figure 6.4B). Whole brain analyses of the contrasts between other timepoint pairs (post-intervention and one month follow-up; baseline and one month follow-up) were non-significant.

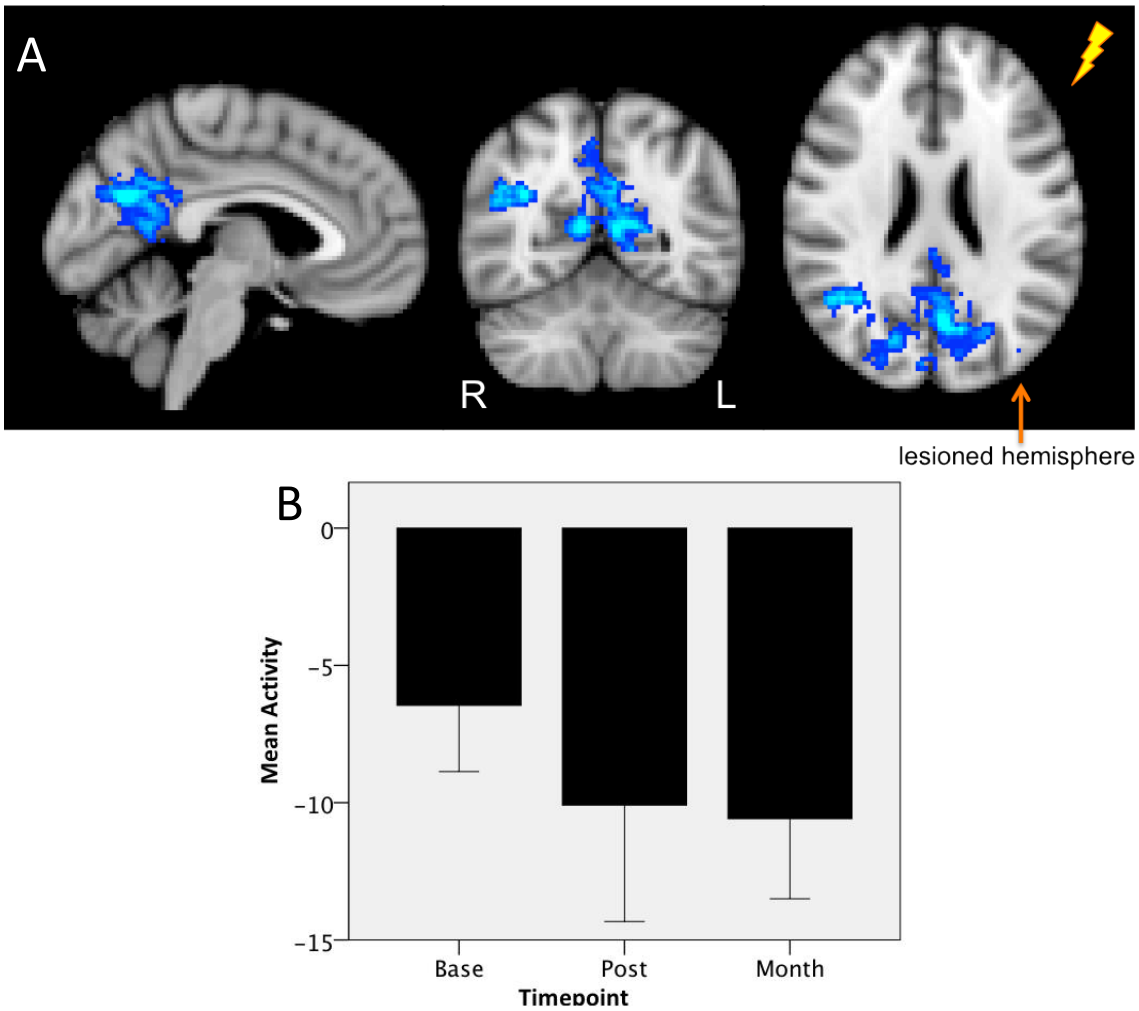

Figure 6.4: Task based changes from baseline to post-intervention. (A) Decreased activation in posterior areas is apparent. Clusters were formed at z=2.0, p<0.01. The resulting image has been thresholded at z=3.5 for display purposes. Coordinates are (-4, -58, 28). (B) Bar graph of extracted copes from the regions illustrated in (A). Left hemisphere is the lesioned hemisphere.

Anatomical Region	Cluster size (voxels)	Maximum Z score	Coordinates of maximum Z statistic		
			x	y	z
Base to Post - Decrease					
Cluster 1	3411				
L Precuneus		4.34	-4	-66	26
L cingulate		4.13	-8	-46	6
R angular gyrus		4.03	34	-56	26
L precuneus		3.95	-12	-70	22
L posterior cingulate gyrus		3.89	-8	-52	16
L intracalcarine cortex		3.86	-10	-62	8

Table 6.2: Location and Z statistic of peak voxels. Regions experiencing altered task-based activation following the rehabilitation program.

Differential activation changes between anodal and sham tDCS groups

We then directly compared longitudinal changes in activation patterns between the anodal and sham tDCS groups. In progressing from baseline to post-intervention, the anodal tDCS group experienced larger increases in activation in primarily ipsilesional motor areas than those in the sham group (Figure 6.5A, B; Table 6.3). A correlation analysis across all patients between the change in activity within these clusters and improvements on the ARAT approached significance ($r=0.418$, $p=0.053$, Figure 6.5C), such that patients showing a greater increase in ipsilesional motor activity had greater improvements in ARAT score. Relative to immediately post-intervention, at the one month follow-up the anodal tDCS group showed greater activation in ipsilesional subcortical areas than did the sham tDCS group (Figure 6.5D, F). Lastly, a comparison of the overall change in task-based activation from baseline to the one month follow-up revealed diffuse ipsilesional increases in primary and secondary motor areas for the anodal tDCS group compared to sham tDCS (Figure 6.5E, G).

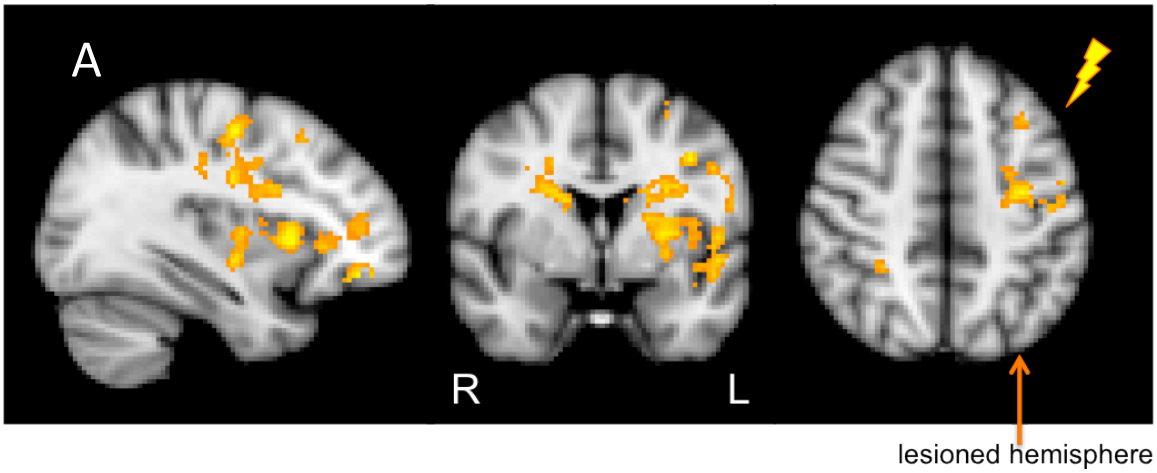

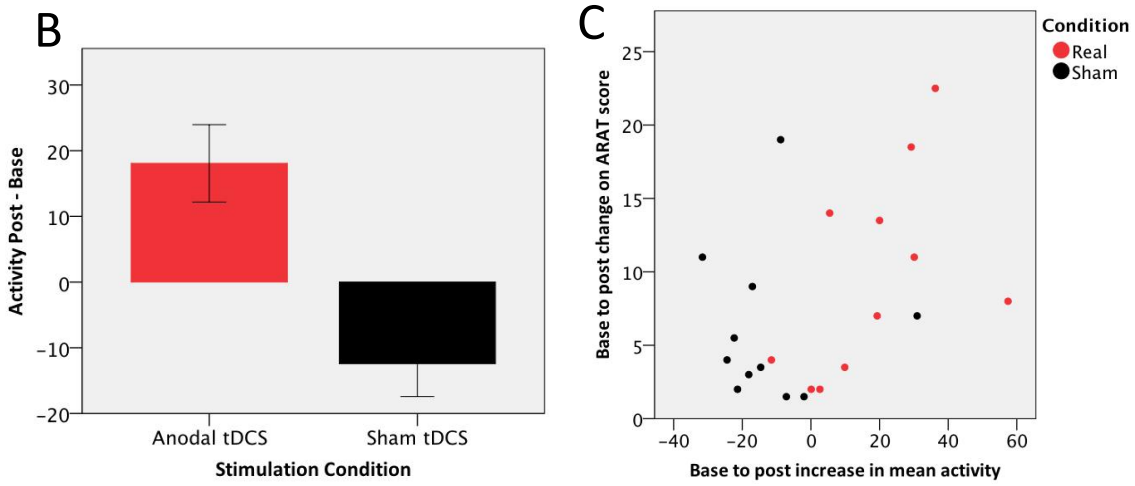

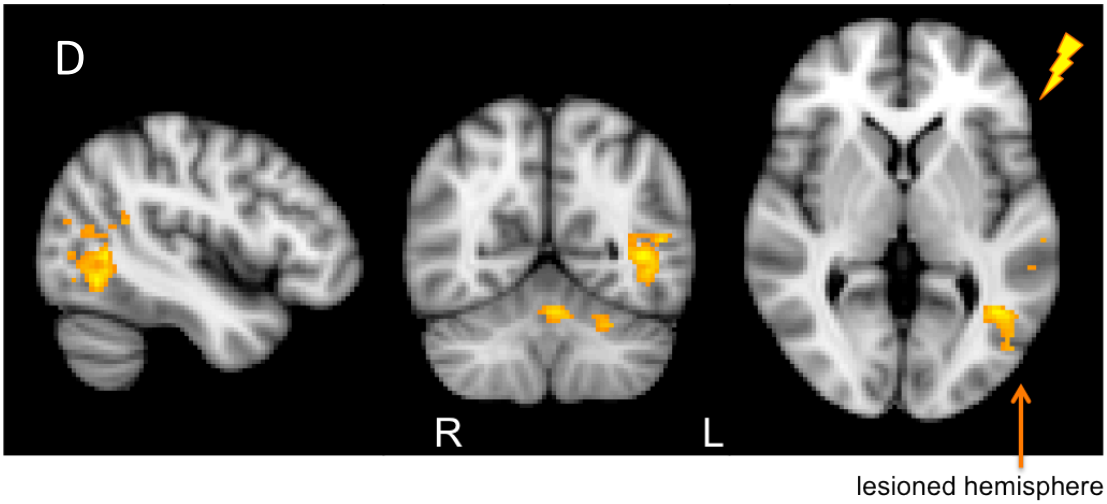

Figure 6.5: Task-based changes when comparing the anodal tDCS and sham tDCS groups. A) Changes from baseline to post-intervention. Coordinates are (-34, 0, 48). B) Bar graph of the changes from regions in (A). C) Change in the regions identified in (A) show a trend toward correlating with improvements on the ARAT. D) Changes from post-intervention to one month follow-up. Coordinates are (-44, -58, 2).

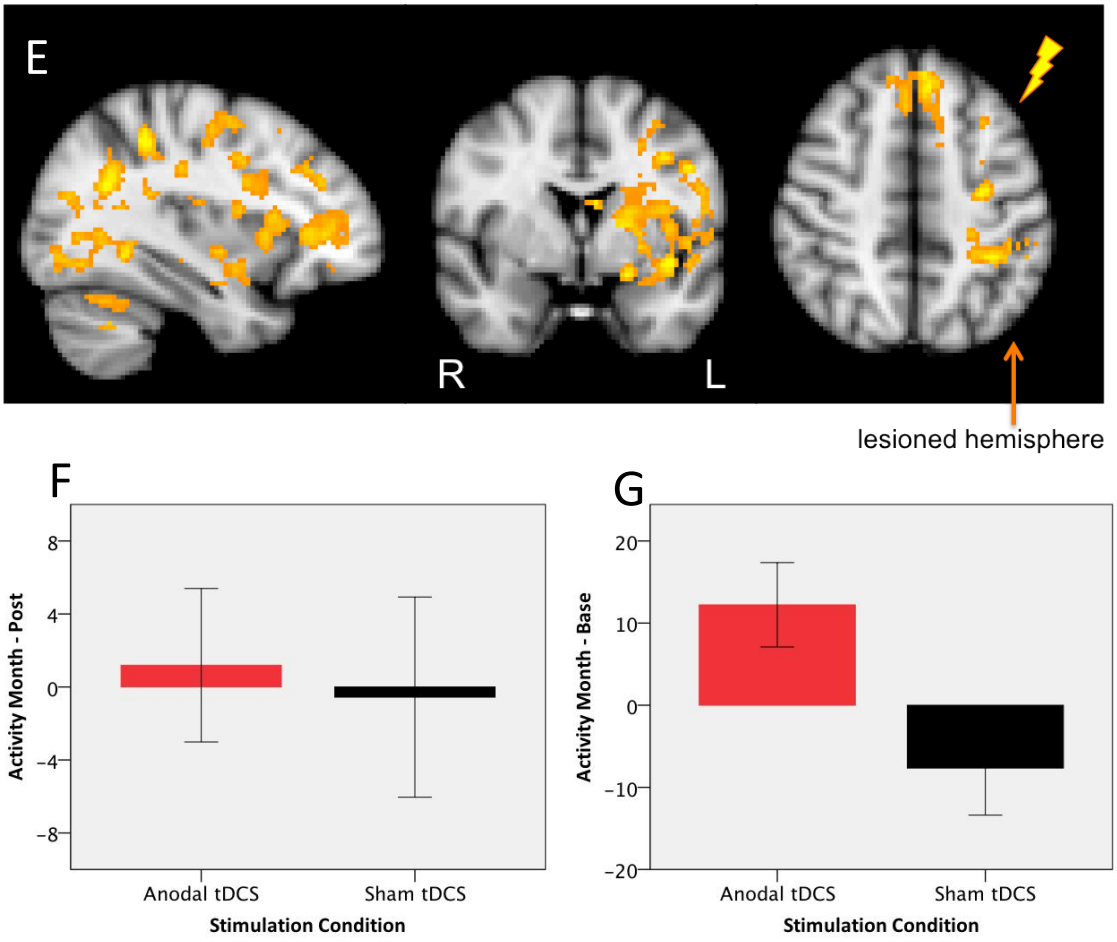

Figure 6.5 (cont.): Task-based changes when comparing the anodal tDCS and sham tDCS groups. E) Changes from baseline to one month follow-up. Coordinates are (-34, 0, 48). F) Bar graph of changes from (D). G) Bar graph from changes in (E). Clusters in (A), (C), and (D) were formed at z=2.0, p<0.01. The resulting images were thresholded at z=3.5 for display purposes. Left hemisphere is lesioned hemisphere.

Anatomical Region	Cluster size (voxels)	Maximum Z score	Coordinates of maximum Z statistic		
			x	y	z
Base to Post - Increase					
Cluster 1	5567				
L insula		4.19	-40	-10	-2
L putamen		4.08	-28	4	4
L ventral premotor cortex		4.06	-40	-4	38
L caudate		3.83	-18	-6	24
L sensory cortex		3.83	-52	-14	44
L frontal pole		3.70	-16	56	-8
Cluster 2	1529				
R putamen		3.83	24	10	8
R cerebral white matter		3.71	36	-32	0
R thalamus		3.49	18	-8	18

R supramarginal gyrus		3.38	50	-38	8
R caudate		3.38	14	16	20
R thalamus		3.37	14	-14	18
Post to Month - Increase					
Cluster 1	857				
L middle temporal gyrus		3.72	-42	-58	2
L inferior temporal gyrus		3.69	-48	-64	-6
L inferior temporal gyrus		3.63	-44	-62	-8
L lateral occipital cortex		3.22	-36	-60	6
L angular gyrus		3.11	-50	-58	10
L lateral occipital cortex		3.1	-48	-72	6
Cluster 2	808				
L lingual gyrus		3.6	-8	-80	-20
Brain stem		3.45	-10	-38	-36
L cerebellum		3.29	-10	-64	-24
Brain stem		3.21	0	-32	-32
L cerebellum		3.12	-28	-52	-28
Cerebellum		3.1	-2	-58	-22
Base to Month - Increase					
Cluster 1	13586				
L lingual gyrus		4.64	-14	56	-8
L putamen		4.51	-22	6	10
R frontal pole		4.41	12	56	-10
L paracingulate gyrus		4.39	-10	28	38
L angular gyrus		4.28	-30	-60	26
L superior parietal lobule		4.28	-34	-42	46
Cluster 2	845				
R lateral occipital cortex		3.96	36	-68	2
R lateral occipital cortex		3.74	50	-70	6
R intracalcerine cortex		3.57	22	-82	6
R lateral occipital cortex		3.55	32	-80	-2
R lateral occipital cortex		3.36	28	-68	24
R occipital pole		3.31	28	-90	-4

Table 6.3: Location and Z statistic of peak voxels. Regions experiencing altered task-based activation following the rehabilitation program when comparing anodal and sham tDCS groups.

6.3.4 STRUCTURAL MRI

tDCS causes structural increase in bilateral motor areas

Given the task-based activation changes produced by the rehabilitation program, we proceeded to investigate structural modifications that may also have occurred. A whole-brain VBM analysis combining both stimulation groups detected

no significant structural changes between any timepoints. When comparing the two stimulation groups to each other, regions that were differentially affected by the two stimulation conditions were detected (anodal versus sham: post intervention – baseline contrast; Figure 6.6A). These regions were largely located in the ipsilesional PMd and M1—particularly the portion representing the hand area, and the contralesional postcentral gyrus. For patients who received anodal tDCS and motor training, grey matter primarily *increased* in these areas; for those receiving sham tDCS and motor training, grey matter *decreased* in these areas (Figure 6.6B). These changes were significantly different than zero in both the anodal ($t(10)=2.678$, $p=0.023$) and sham tDCS groups ($t(10)=3.030$, $p=0.013$). Moreover, these structural changes were positively correlated with improvements on the UE-FM across all patients ($r=0.450$, $p=0.036$, Figure 6.6C). That is, larger increases in these VBM-identified areas were associated with larger behavioural gains as measured by the Fugl-Meyer. Structural changes did not correlate with improvements on the ARAT. The magnitude of the structural changes in these areas also positively correlates with the task-based changes identified by the similar analysis performed on the fMRI data as shown in Figure 6.5A above ($r=0.464$, $p=0.030$, Figure 6.6D).

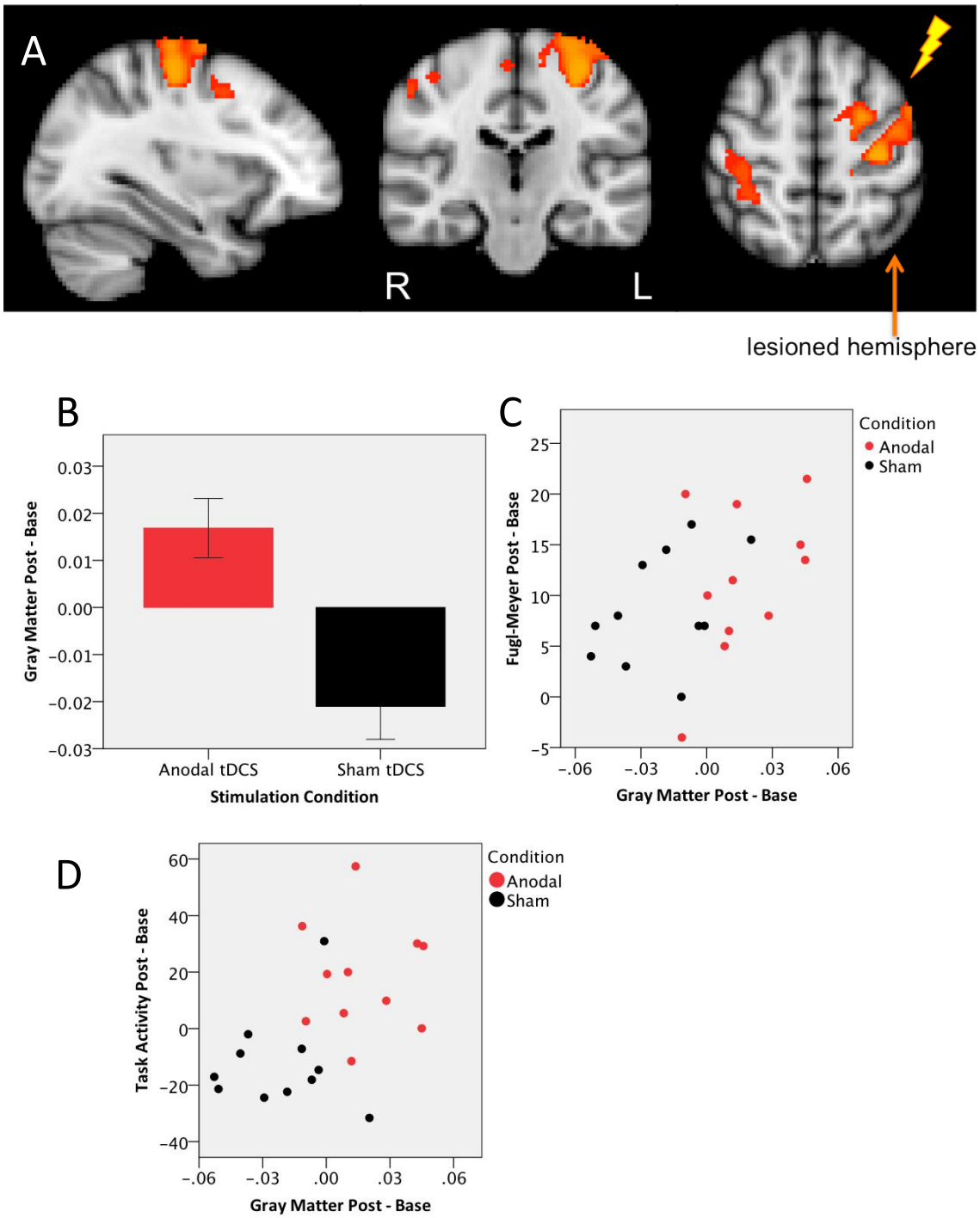

Figure 6.6: Structural increases associated with anodal tDCS. A) Regions that experienced increased grey matter volume from baseline to post-intervention when comparing the anodal and sham tDCS groups. Coordinates are (-32, -22, 56). Significant regions determined using threshold-free cluster enhancement; resulting image thresholded at $p<0.05$. Left hemisphere is lesioned hemisphere. B) Bar graph of the change in grey matter in the areas shown in (A). C) Change in the regions identified in (A) positively correlate with improvements on the UE-FM. D) Changes in the regions identified in (A) positively correlate with changes in task-based fMRI activity in regions shown in Figure 6.5C.

Structural results unlikely to be due to stimulation-induced oedema

Many of the structural changes identified by the VBM analysis were localised to the area underneath the stimulating tDCS electrode. Although we do not expect tDCS to directly cause lasting tissue change, we wished to rule out the possibility that oedema may have occurred under the tDCS electrode, and could have influenced the VBM analysis. This verification was accomplished by performing a voxel-wise analysis of the subjects' T2-weighted structural images: oedema manifests as an increase in brightness, which would be detected with VBM tools. Of the 22 patients included in this study, six had T2-weighted scans at all imaging timepoints (three patients in each stimulation group). A VBM analysis of the T2 images from these subjects showed no regions of significant increases. Given the small group size available for this test, further data exploration was performed. The minimum p-value was located in the ventral cerebellum ($p=0.06$, coordinates are (-18, -50, -58)). The minimum p-value found within the region identified by the initial T1 VBM analysis (see Figure 6.7A) was $p=0.45$. Additionally, using this region as a mask, we extracted COPEs from the contrast of normalised T2-weighted images across time. A t-test comparing the change from baseline to post-intervention yielded no significant differences between groups ($t(4)=2.733$, $p=0.052$); exploratory comparisons between baseline and post-intervention within each group were also not significant (anodal tDCS: $t(2)= 1.1475$, $p= 0.370$; sham tDCS: $t(2)= 2.7188$, $p= 0.113$). If anything, the trend points towards increased brightness in the sham stimulation group.

As this T2 analysis was only performed in six of the 22 patients, we then sought to replicate the initial VBM results in this smaller cohort for whom we could report the absence of tDCS-induced oedema. Replicating the initial VBM analysis for

this group of 6 subjects produced no significant results, as expected in an analysis containing 3 patients per group. However, the areas that most approached significance were indeed found in regions similar to those identified by the initial VBM output. Figure 6.8 shows the results of the analysis of this smaller cohort, achieved using threshold-free cluster enhancement. For display purposes, the image has been thresholded at a significance level of $p<0.30$.

Figure 6.7: VBM analysis of 6 subjects. Note the similarity to the areas presented in Figure 6.6A. Coordinates are (-32, -22, 56). Significant regions determined using threshold-free cluster enhancement; resulting image thresholded at $p<0.30$.

Although T2 images provide the most robust measure of oedema, we sought to investigate an additional imaging modality—present in all 22 patients, which might provide complementary results. To this end, we examined mean diffusivity (MD) across the brain. MD values would be higher in oedemic tissue than in healthy tissue. A VBM analysis of the MD images comparing changes from baseline to post-intervention between the two groups (anodal tDCS versus sham tDCS) found no areas of significant differences. The minimum p-value was located in the right cerebellum ($p=0.32$, coordinates are (42, -74, -36)). The minimum p-value found within the region identified by the initial T1 VBM analysis (see Figure 6.7A) was $p=0.12$. Taken together, the results from the T2 and MD analyses suggest that there

was no evidence for oedema in the anodal tDCS group compared to sham tDCS group that could account for the previous T1 structural results.

6.4 DISCUSSION

Our double-blind, sham-controlled tDCS and motor training program resulted in behavioural improvements in all of the chronic stroke patients, both those receiving anodal tDCS and those in the placebo condition of sham tDCS. These clinical gains as measured by the ARAT and Fugl-Meyer were accompanied by MR-based functional and structural neuroimaging changes. In particular, fMRI analysis revealed that patients in both stimulation groups experienced more task-based deactivation of medial parietal-occipital areas immediately following the intervention as compared to baseline. Relative to those patients receiving motor training and sham tDCS, patients in the anodal tDCS group displayed increased activation of primarily ipsilesional motor areas during task performance, a development that persisted through the one month follow-up. Such functional differences between groups were accompanied by structural changes: grey matter density in the ipsilesional M1 and PMC and contralesional somatosensory cortex increased in the anodal tDCS group and decreased in the sham tDCS group. These brain changes appear to be behaviourally relevant as well: functional changes correlated with improvements on the ARAT, while structural changes correlated with improvements on the Fugl-Meyer.

Task-based fMRI activity

When collapsed across groups and comparing post-intervention to baseline, the fMRI analysis found increased deactivation of posterior parietal and occipital

areas during task performance. Although not apparent during the whole-brain analysis, this result showed a trend toward enduring through the one month follow-up, perhaps supporting the long-term retention of behavioural improvements. Many of these regions, namely those within the inferior parietal lobule at the medial occipito-parietal junction, are key components of the default mode network (DMN) (Beckmann et al., 2005). The DMN is a task-negative network that is normally deactivated during task performance (Kawashima et al., 2000; Raichle et al., 2001). Studies have demonstrated that the degree of deactivation of these posterior regions of the DMN positively correlates with performance during working memory tasks (Esposito et al., 2009). Although this result is based in the cognitive, rather than the motor, domain, it suggests that the increase in deactivation seen here in the stroke patients may reflect—and potentially promote, improved motor ability. That these changes were found when considering the entire group of stroke patients, irrespective of tDCS condition, implies that they were a result of a feature common to all patients: in this case, motor training.

A between-group comparison of changes in task-based activity from baseline to post-intervention revealed increased activity in the anodal tDCS group relative to the sham tDCS group. These changes were primarily ipsilesional and occurred in both cortical and subcortical motor areas such as M1, PMC, caudate, and putamen, a development that remained relatively unchanged through the one month follow-up. Closer analysis of activity levels within these regions for each stimulation group showed that, on average, patients in the anodal tDCS group exhibited increased activity, while those in the sham tDCS group exhibited decreased activity. The upregulation of ipsilesional motor activity present in the anodal tDCS group is in accord with the underlying theory behind using tDCS to improve motor ability:

rectifying interhemispheric imbalance. The results are also in line with previous studies of repeated sessions of tDCS in chronic stroke patients, with the exception that the regions presented here are more broadly distributed than in previous studies (Lindenberg et al., 2010; Nair et al., 2011). This may be due to a variety of reasons, including different motor training protocols, and the use of contralesional cathodal (Nair et al., 2011) and bihemispheric (Lindenberg et al., 2010), rather than anodal, tDCS. Moreover, these studies reported contrasts from only within group comparisons (e.g., post-intervention versus baseline), and not between groups (i.e., tDCS versus placebo). They were also performed in well-recovered patients who retained enough motor function to independently move their wrist or elbow. In contrast, the task used in the present study was researcher-mediated wrist flexion-extension, as most of the patients in the study could not perform such movements independently. This disparity in baseline motor function may have affected the ability to detect changes in activation, as better recovered patients tend to have a more ipsilesional activation pattern to begin with (Cramer, 2008; Wu, et al., 2008).

As a normalising return to contralateral, ipsilesional task-related activity is beneficial (Tombari et al., 2004), the question arises as to how the patients in the sham tDCS group exhibited *decreased* activation in these motor areas, and yet still experienced behavioural improvements. Previous work (Johansen-Berg et al., 2002; O'Shea et al., 2007) has argued for the importance of the contralesional hemisphere in adaptive plasticity, particularly in much impaired patients (Lotze et al., 2006). As many of our patients exhibited a relatively high degree of motor disability, it is possible, then, that they had begun to rely more on the contralesional hemisphere to accomplish tasks, and progressively less on the ipsilesional hemisphere. Thus, without tDCS to externally increase ipsilesional activity, motor training relied on

previously established processes to improve motor behaviour: those in the contralesional hemisphere. A combined TMS-fMRI study found that as clinical disability increases, the influence of contralesional PMd on the ipsilesional becomes less inhibitory and more facilitory at rest, even as fMRI activity during a hand-grip task was increased in the contralesional side (Bestmann et al., 2010). This raises the possibility that, even though the ipsilesional hemisphere may on its own be less active, the contralesional hemisphere is working on a subtle level to facilitate the function of these areas.

Structural grey matter

When comparing the two stimulation groups to each other, we found structural modifications in the ipsilesional M1 and PMC, and in the contralesional somatosensory cortex. Within these areas, patients in the anodal tDCS group experienced increased grey matter, while the sham tDCS exhibited a decrease in grey matter. These changes were apparent immediately post-intervention, and had resolved by the one-month followup. Such rapid, bidirectional structural changes following motor training—appearing here after 2 weeks, have been documented previously, both in healthy adults (Gryga et al., 2012) and in patients (Gauthier et al., 2008). The magnitude of the change in grey matter reported in the present study is similar to that reported in a study by Gauthier and colleagues (Gauthier et al., 2008). In that study, patients underwent 2 weeks of intensive CIMT or comparison motor training. Diffuse structural changes were found after CIMT, but not after simple training, suggesting that the intensity of the training is important (Gauthier et al., 2008). Thus, one potential explanation for structural increases occurring in the anodal, but not sham, tDCS group is that anodal tDCS effectively increased the

intensity of the training from the brain's perspective. It has been shown previously that stimulation alone can modulate grey matter: 5 days of rTMS to superior temporal cortex increased grey matter in the auditory cortex (May et al., 2007). Decreases in grey matter following training. analogous to those found in the sham tDCS group here, have been noted in previous studies (Gauthier et al., 2008; Gryga et al., 2012). It is unclear what mechanism would support a decline in grey matter while promoting concurrent behavioural increases.

As the structural changes presented here correlate with behavioural improvements on the Fugl-Meyer, it is unlikely that they are spurious. Although we did not expect tDCS to cause oedema, because the structural changes were partially localized to the area underneath the anode, we investigated whether these results might be reflective of stimulation-induced oedema. An analysis of T2-structural images and MD images found no evidence of oedema in the anodal tDCS group. It is unclear what mechanism could cause such rapid changes in grey matter, as the timescale for neurogenesis is too slow to account for structural changes on the order of days and weeks (Draganski & May, 2008). Previous studies have postulated that it may be due to dendritic arborization, axonal sprouting, and the formation of synapses (Schaechter et al., 2006; Trachtenberg et al., 2002; Xu et al., 2009), or changes in supporting structures such as glial cells and the surrounding vasculature (Johansen-Berg, 2012). The extent of such modifications may reflect the differing metabolic demands required during motor learning and performance between stimulation groups and subjects, potentially underlying the bidirectional alterations (Black et al., 1990; Gryga et al., 2012; Isaacs et al., 1992). It is possible for stroke patients to experience declining grey matter while simultaneously recovering from their neurological deficit (Kraemer et al., 2004), suggesting that the apparent

decline in grey matter in the sham tDCS group doesn't necessarily preclude concomitant behavioural improvements.

Future Directions

As the functional and structural changes are partially colocalised with each other and correlate in magnitude, it would be interesting to know whether changes within one modality promote modifications in the other (e.g., does increased grey matter provide the substrate necessary for heightened functional activity), or if they are parallel processes that occur in tandem. One proposition is that motor training increases synaptic and capillary density, which contribute to a simultaneous increase in cortical thickness and BOLD response (Schaechter et al., 2006). Both the functional and structural results correlated with changes in clinical score, but on different measures. This serves to highlight the difference between the ARAT and Fugl-Meyer, which are sometimes used interchangeably. Here, we show that they may be attuned to different processes within the brain—structural impairment versus functional disability, a finding that complements previous reports of the specificity of the two tests (Roth et al., 1998). Such a result underscores the importance of accurately matching neuroimaging modalities with the appropriate clinical outcome measure.

Future studies may wish to administer an additional baseline imaging session, two weeks following the initial session. We collected this extra timepoint for some, but not all, of our patients. This additional data would allow for the determination of the stability of structure and function, which could help eliminate the possibility of the results, particularly those found within the sham tDCS group, being due to the passage of time. tDCS carries its own associated issues. Individual

response to tDCS varies, with some people responding positively, negatively, and some not at all (Stagg et al., 2011; personal communication). Prescreening patients to determine elicitability of the desired effect (i.e., improved motor performance after anodal tDCS), could help ensure that positive (or negative) results achieved in the anodal tDCS group are actually due to the stimulation itself, and not to gross variability among patients. We administered anodal tDCS only during the first half of motor training, with the intention that the aftereffects would continue through the latter half of the session. However, the studies that determined the longevity of tDCS aftereffects were performed in healthy adults, and it is not certain whether this would also extend to the patient population. Although it is unclear whether administering anodal tDCS for the entire session is possible from a safety perspective, this may allow for more robust effects. The patients included in this study varied widely in level of motor ability. While performing this experiment in a diversely impaired population allows us to draw conclusions about the population as a whole, it is likely that the effects of our training program are quite varied among the patients, depending on impairment level (Stinear et al., 2006). A larger study that allowed us to stratify patients and look within impairment levels would allow for more focused and tailored results. Lastly, we did not control for patients performing components of the motor training outside of the sessions. It is unlikely, but possible, that this effective variability in motor training duration may have impacted the study's results.

6.5 CONCLUSION

The data presented here suggest that, when combined with motor training, anodal tDCS may promote behavioural improvements by modifying the underlying

structural and functional components of the brain that support motor behaviours. In particular, this chapter has demonstrated that anodal tDCS may help normalise post-stroke interhemispheric imbalance by increasing underlying grey matter and performance-mediated activity in ipsilesional motor regions. Structural increases were associated with improved behavioural scores on the Fugl-Meyer, perhaps indicating a resolution of the physical impairment caused by the infarct. Functional modifications positively correlated with improvements on the ARAT, suggesting that greater ipsilesional functional activity reflects decreases in disability. In addition to finding *correlations* between neuroimaging measures and behavioural improvements, we also sought to determine which baseline neuroimaging measures were *predictive* of behavioural improvements. This is the topic of the final experimental section of this thesis, Chapter 7.

REFERENCES

Allred, R. P., & Jones, T. A. (2008). Maladaptive effects of learning with the less-affected forelimb after focal cortical infarcts in rats. *Experimental neurology*, *210*(1), 172–181.

Allred, R. P., Cappellini, C. H., & Jones, T. A. (2010). The "good" limb makes the “bad” limb worse: experience-dependent interhemispheric disruption of functional outcome after cortical infarcts in rats. *Behavioral neuroscience*, *124*(1), 124–132.

Beckmann, C. F., & Smith, S. M. (2004). Probabilistic independent component analysis for functional magnetic resonance imaging. *IEEE transactions on medical imaging*, *23*(2), 137–152.

Beckmann, C. F., DeLuca, M., Devlin, J. T., & Smith, S. M. (2005). Investigations into resting-state connectivity using independent component analysis. *Philosophical transactions of the Royal Society of London. Series B, Biological sciences*, *360*(1457), 1001–1013.

Bestmann, S., Swayne, O., Blankenburg, F., Ruff, C. C., Teo, J., Weiskopf, N., Driver, J., et al. (2010). The role of contralesional dorsal premotor cortex after stroke as studied with concurrent TMS-fMRI. *Journal of Neuroscience*, *30*(36), 11926–11937.

Black, J. E., Isaacs, K. R., Anderson, B. J., Alcantara, A. A., & Greenough, W. T. (1990). Learning causes synaptogenesis, whereas motor activity causes angiogenesis, in cerebellar cortex of adult rats. *Proceedings of the National Academy of Sciences of the United States of America*, *87*(14), 5568–5572.

Boggio, P. S., Nunes, A., Rigonatti, S. P., Nitsche, M. A., Pascual-Leone, A., & Fregni, F. (2007). Repeated sessions of noninvasive brain DC stimulation is associated with motor function improvement in stroke patients. *Restorative neurology and neuroscience*, *25*(2), 123–129.

Bolognini, N., Vallar, G., Casati, C., Latif, L. A., El-Nazer, R., Williams, J., Banco, E., et al. (2011). Neurophysiological and behavioral effects of tDCS combined with constraint-induced movement therapy in poststroke patients. *Neurorehabilitation and Neural Repair*, *25*(9), 819–829.

Corti, M., Patten, C., & Triggs, W. (2012). Repetitive transcranial magnetic stimulation of motor cortex after stroke: a focused review. *American journal of*

physical medicine & rehabilitation / Association of Academic Physiatrists, *91*(3), 254–270.

Cramer, S. C. (2008). Repairing the human brain after stroke. II. Restorative therapies. *Annals of Neurology*, *63*(5), 549–560.

Douaud, G., Smith, S., Jenkinson, M., Behrens, T., Johansen-Berg, H., Vickers, J., James, S., et al. (2007). Anatomically related grey and white matter abnormalities in adolescent-onset schizophrenia. *Brain*, *130*(Pt 9), 2375–2386.

Draganski, B., & May, A. (2008). Training-induced structural changes in the adult human brain. *Behavioural brain research*, *192*(1), 137–142.

Duque, J., Murase, N., Celnik, P., Hummel, F., Harris-Love, M., Mazzocchio, R., Olivier, E., et al. (2007). Intermanual Differences in movement-related interhemispheric inhibition. *Journal of cognitive neuroscience*, *19*(2), 204–213.

Fan, F., Zhu, C., Chen, H., Qin, W., Ji, X., Wang, L., Zhang, Y., et al. (2012). Dynamic brain structural changes after left hemisphere subcortical stroke. *Human brain mapping*.

Feydy, A., Carlier, R., Roby-Brami, A., Bussel, B., Cazalis, F., Pierot, L., Burnod, Y., et al. (2002). Longitudinal study of motor recovery after stroke: recruitment and focusing of brain activation. *Stroke*, *33*(6), 1610–1617.

Fregni, F., Boggio, P. S., Mansur, C. G., Wagner, T., Ferreira, M. J. L., Lima, M. C., Rigonatti, S. P., et al. (2005). Transcranial direct current stimulation of the unaffected hemisphere in stroke patients. *Neuroreport*, *16*(14), 1551–1555.

Gandiga, P. C., Hummel, F. C., & Cohen, L. G. (2006). Transcranial DC stimulation (tDCS): a tool for double-blind sham-controlled clinical studies in brain stimulation. *Clinical neurophysiology : official journal of the International Federation of Clinical Neurophysiology*, *117*(4), 845–850.

Gauthier, L. V., Taub, E., Perkins, C., Ortmann, M., Mark, V. W., & Uswatte, G. (2008). Remodeling the Brain: Plastic Structural Brain Changes Produced by Different Motor Therapies After Stroke * Supplemental Material. *Stroke*, *39*(5), 1520–1525.

Gryga, M., Taubert, M., Dukart, J., Vollmann, H., Conde, V., Sehm, B., Villringer, A., et al. (2012). Bidirectional gray matter changes after complex motor skill learning. *Frontiers in Systems Neuroscience*, *6*, 37.

Halsband, U., & Lange, R. K. (2006). Motor learning in man: a review of functional

and clinical studies. *Journal of physiology, Paris*, *99*(4-6), 414–424.

Hikosaka, O., Nakamura, K., Sakai, K., & Nakahara, H. (2002). Central mechanisms of motor skill learning. *Current opinion in neurobiology*, *12*(2), 217–222.

Hubbard, I. J., Parsons, M. W., Neilson, C., & Carey, L. M. (2009). Task-specific training: evidence for and translation to clinical practice. *Occupational therapy international*, *16*(3-4), 175–189.

Hummel, F. (2005). Effects of non-invasive cortical stimulation on skilled motor function in chronic stroke. *Brain*, *128*(3), 490–499.

Hummel, F. C., & Cohen, L. G. (2005). Drivers of brain plasticity. *Current opinion in neurology*, *18*(6), 667–674.

Isaacs, K. R., Anderson, B. J., Alcantara, A. A., Black, J. E., & Greenough, W. T. (1992). Exercise and the brain: angiogenesis in the adult rat cerebellum after vigorous physical activity and motor skill learning. *Journal of cerebral blood flow and metabolism : official journal of the International Society of Cerebral Blood Flow and Metabolism*, *12*(1), 110–119.

Jenkinson, M., Bannister, P., Brady, M., & Smith, S. (2002). Improved optimization for the robust and accurate linear registration and motion correction of brain images. *NeuroImage*, *17*(2), 825–841.

Johansen-Berg, H., Baptista C.S., Thomas, A.G. (2012). Human structural plasticity at record speed. *Neuron, 73*(6),1058-1060.

Johansen-Berg, H., Rushworth, M. F. S., Bogdanovic, M. D., Kischka, U., Wimalaratna, S., & Matthews, P. M. (2002). The role of ipsilateral premotor cortex in hand movement after stroke. *Proceedings of the National Academy of Sciences of the United States of America*, *99*(22), 14518–14523.

Kawashima, R., Okuda, J., Umetsu, A., Sugiura, M., Inoue, K., Suzuki, K., Tabuchi, M., et al. (2000). Human cerebellum plays an important role in memory-timed finger movement: an fMRI study. *Journal of Neurophysiology*, *83*(2), 1079–1087.

Kraemer, M., Schormann, T., Hagemann, G., Qi, B., Witte, O. W., & Seitz, R. J. (2004). Delayed shrinkage of the brain after ischemic stroke: preliminary observations with voxel-guided morphometry. *Journal of neuroimaging : official journal of the American Society of Neuroimaging*, *14*(3), 265–272.

Leonard, C. T. (1997). *The Neuroscience Of Human Movement, 1e*. (M. Sasser, Ed.) (1st ed.). Mosby.

Levin, M. F., Kleim, J. A., & Wolf, S. L. (2009). What do motor "recovery" and “compensation” mean in patients following stroke? *Neurorehabilitation and Neural Repair*, *23*(4), 313–319.

Liepert, J., Restemeyer, C., Kucinski, T., Zittel, S., & Weiller, C. (2005). Motor strokes: the lesion location determines motor excitability changes. *Stroke*, *36*(12), 2648–2653.

Lindenberg, R., Renga, V., Zhu, L. L., Nair, D., & Schlaug, G. (2010). Bihemispheric brain stimulation facilitates motor recovery in chronic stroke patients. *Neurology*, *75*(24), 2176–2184.

Lotze, M., Markert, J., Sauseng, P., Hoppe, J., Plewnia, C., & Gerloff, C. (2006). The role of multiple contralesional motor areas for complex hand movements after internal capsular lesion. *Journal of Neuroscience*, *26*(22), 6096–6102.

May, A., Hajak, G., Gänssbauer, S., Steffens, T., Langguth, B., Kleinjung, T., & Eichhammer, P. (2007). Structural brain alterations following 5 days of intervention: dynamic aspects of neuroplasticity. *Cerebral cortex (New York, N.Y. : 1991)*, *17*(1), 205–210.

Murase, N., Duque, J., Mazzocchio, R., & Cohen, L. G. (2004). Influence of interhemispheric interactions on motor function in chronic stroke. *Annals of Neurology*, *55*(3), 400–409.

Nachev, P., Kennard, C., & Husain, M. (2008). Functional role of the supplementary and pre-supplementary motor areas. *Nature Reviews Neuroscience*, *9*(11), 856–869.

Nair, D. G., Renga, V., Lindenberg, R., Zhu, L., & Schlaug, G. (2011). Optimizing recovery potential through simultaneous occupational therapy and non-invasive brain-stimulation using tDCS. *Restorative neurology and neuroscience*, *29*(6), 411–420.

Nowak, D. A., Grefkes, C., Ameli, M., & Fink, G. R. (2009). Interhemispheric Competition After Stroke: Brain Stimulation to Enhance Recovery of Function of the Affected Hand. *Neurorehabilitation and Neural Repair*, *23*(7), 641–656.

O'Shea, J., Johansen-Berg, H., Trief, D., Göbel, S., & Rushworth, M. F. S. (2007). Functionally specific reorganization in human premotor cortex. *Neuron*, *54*(3), 479–490.

Pang, M. Y., Harris, J. E., & Eng, J. J. (2006). A community-based upper-extremity

group exercise program improves motor function and performance of functional activities in chronic stroke: a randomized controlled trial. *Archives of physical medicine and rehabilitation*, *87*(1), 1–9.

Raichle, M. E., MacLeod, A. M., Snyder, A. Z., Powers, W. J., Gusnard, D. A., & Shulman, G. L. (2001). A default mode of brain function. *Proceedings of the National Academy of Sciences of the United States of America*, *98*(2), 676–682.

Reis, J., Schambra, H. M., Cohen, L. G., Buch, E. R., Fritsch, B., Zarahn, E., Celnik, P. A., et al. (2009). Noninvasive cortical stimulation enhances motor skill acquisition over multiple days through an effect on consolidation. *Proceedings of the National Academy of Sciences of the United States of America*, *106*(5), 1590–1595.

Roth, E. J., Heinemann, A. W., Lovell, L. L., Harvey, R. L., McGuire, J. R., & Diaz, S. (1998). Impairment and disability: their relation during stroke rehabilitation. *Archives of physical medicine and rehabilitation*, *79*(3), 329–335.

Schaechter, J. D., Moore, C. I., Connell, B. D., Rosen, B. R., & Dijkhuizen, R. M. (2006). Structural and functional plasticity in the somatosensory cortex of chronic stroke patients. *Brain*, *129*(Pt 10), 2722–2733.

Stagg, C.J., Bachtiar, V., Johansen-Berg, H. (2011). The role of GABA in human motor learning. *Curr Biol, 21*(6), 480-484.

Stagg, C. J., Bachtiar, V., O'Shea, J., Allman, C., Bosnell, R. A., Kischka, U., Matthews, P. M., et al. (2012). Cortical activation changes underlying stimulation-induced behavioural gains in chronic stroke. *Brain*, *135*(Pt 1), 276–284.

Stinear, C. M., Barber, P. A., Smale, P. R., Coxon, J. P., Fleming, M. K., & Byblow, W. D. (2006). Functional potential in chronic stroke patients depends on corticospinal tract integrity. *Brain*, *130*(1), 170–180.

Studenski, S. A., Wallace, D., Duncan, P. W., Rymer, M., & Lai, S. M. (2001). Predicting stroke recovery: three- and six-month rates of patient-centered functional outcomes based on the orpington prognostic scale. *Journal of the American Geriatrics Society*, *49*(3), 308–312.

Synofzik, M., Lindner, A., & Thier, P. (2008). The cerebellum updates predictions about the visual consequences of one's behavior. *Current Biology*, *18*(11), 814–818.

Takeuchi, N., & Izumi, S.-I. (2012). Maladaptive plasticity for motor recovery after

stroke: mechanisms and approaches. *Neural plasticity*, *2012*, 359728.

Tombari, D., Loubinoux, I., Pariente, J., Gerdelat, A., Albucher, J.-F., Tardy, J., Cassol, E., et al. (2004). A longitudinal fMRI study: in recovering and then in clinically stable sub-cortical stroke patients. *NeuroImage*, *23*(3), 827–839.

Trachtenberg, J. T., Chen, B. E., Knott, G. W., Feng, G., Sanes, J. R., Welker, E., & Svoboda, K. (2002). Long-term in vivo imaging of experience-dependent synaptic plasticity in adult cortex. *Nature*, *420*(6917), 788–794.

van der Lee, J. H., Beckerman, H., Lankhorst, G. J., & Bouter, L. M. (2001). The responsiveness of the Action Research Arm test and the Fugl-Meyer Assessment scale in chronic stroke patients. *Journal of rehabilitation medicine : official journal of the UEMS European Board of Physical and Rehabilitation Medicine*, *33*(3), 110–113.

Ward, N. S., Brown, M. M., Thompson, A. J., & Frackowiak, R. S. J. (2003). Neural correlates of motor recovery after stroke: a longitudinal fMRI study. *Brain*, *126*(Pt 11), 2476–2496.

Ward, N. S., Newton, J. M., Swayne, O. B. C., Lee, L., Thompson, A. J., Greenwood, R. J., Rothwell, J. C., et al. (2006). Motor system activation after subcortical stroke depends on corticospinal system integrity. *Brain*, *129*(Pt 3), 809–819.

Wolf, S. L., Winstein, C. J., Miller, J. P., Taub, E., Uswatte, G., Morris, D., Giuliani, C., et al. (2006). Effect of constraint-induced movement therapy on upper extremity function 3 to 9 months after stroke: the EXCITE randomized clinical trial. *JAMA : the journal of the American Medical Association*, *296*(17), 2095–2104.

Woolrich, M. W., Ripley, B. D., Brady, M., & Smith, S. M. (2001). Temporal autocorrelation in univariate linear modeling of FMRI data. *NeuroImage*, *14*(6), 1370–1386.

International Classification of Impairments, Disabilities, and Handicaps. Geneva, Switzerland: World Health Organization; 1980.

Wu, T., Chan, P., & Hallett, M. (2008). Modifications of the interactions in the motor networks when a movement becomes automatic. *The Journal of Physiology*, *586*(Pt 17), 4295–4304.

Xu, T., Yu, X., Perlik, A. J., Tobin, W. F., Zweig, J. A., Tennant, K., Jones, T., et al. (2009). Rapid formation and selective stabilization of synapses for enduring motor memories. *Nature*, *462*(7275), 915–919.

Zimerman, M., Heise, K. F., Hoppe, J., Cohen, L. G., Gerloff, C., & Hummel, F. C. (2012). Modulation of training by single-session transcranial direct current stimulation to the intact motor cortex enhances motor skill acquisition of the paretic hand. *Stroke*, *43*(8), 2185–2191.

Chapter 7: Asymmetry of Hemispheric Connectivity Predicts Response to Rehabilitation

Chapter 6 described the functional and structural brain changes that occur following a combined rehabilitation program of motor training and tDCS in chronic stroke patients. A pattern emerged in which increases in both grey matter and task-related fMRI activity were found primarily in ipsilesional motor-related areas. This final experimental chapter further explores the relative importance of each hemisphere to rehabilitation-mediated improvements. We investigate whether baseline measures reflective of lateralized hemispheric connectivity predict subsequent behavioural gains.

7.1 INTRODUCTION

Recently, work regarding motor recovery after stroke has moved toward anticipating the extent to which patients will regain function of their affected limb, both spontaneously and in response to rehabilitation programs. It has been shown that the degree of spared motor ability two months post-stroke correlates with motor ability at one year (F. D. Shelton et al., 2001). Sometimes referred to as "functional potential" (Stinear et al., 2006), prospective behavioural improvements are also predicted by lesion size and location. While both of these lesion characteristics correlate with motor deficit, lesion location in terms of cross-sectional damage to the corticospinal tract (CST) has been shown to be more strongly predictive of reduced grip strength and performance on the 9 Hole Peg Test (Pineiro et al., 2000). Subsequent studies determined that, within the CST, damage to the posterior limb of the internal capsule (PLIC) was more predictive of a

poorer recovery than damage to the anterior portion (Schiemanck et al., 2008), both of which predicted poorer improvement more strongly than did damage to the corona radiata, subcortex, and cortex (Schiemanck et al., 2008; Shelton & Reding, 2001).

In addition to these measures of CST damage caused directly by the lesion, more subtle indicators of CST functional and structural integrity have been investigated, such as motor evoked potentials (MEPs) and fractional anisotropy values (FA). Eliciting MEPs via stimulation of M1 of the lesioned hemisphere requires that the connections from the cortex to the spinal cord are preserved, particularly those through the CST (Talelli et al., 2006), and is therefore commonly thought of as a marker of residual functional connectivity. FA measures the directional dependence of diffusion of water, which depends on presence of structured barriers to diffusion, and therefore, within white matter, FA can give a marker of structural integrity of fibre pathways. Following a stroke, unilateral reductions in CST integrity in the lesioned cortex cause interhemispheric asymmetries in FA values (Werring et al., 2000). When assessed in these terms, measures of CST integrity are just as effective—if not more so, as baseline motor deficit at predicting behavioural recovery (Coupar et al., 2012). For patients in whom MEPs could be elicited, smaller MEPs are associated with reduced grip strength at that timepoint, as was asymmetry of FA values in the PLIC (Lotze et al., 2012). FA asymmetry in the PLIC has also been shown to predict motor deficits as measured by the Upper Extremity Fugl-Meyer and Wolf Motor Function Test (Lindenberg et al., 2010). A 2012 study by Schulz fractionated the PLIC into components originating from the hand area of M1, the dorsal and ventral premotor cortices, and the SMA. FA was reduced in all four tracts, but only CST from the hand

area and PMd correlated with current grip strength levels (Schulz et al., 2012). Moreover, the extent of injury to tracts originating in M1 and PMd were the strongest predictors of therapy-induced behavioural improvements on the the FM, but not the ARAT, in chronic stroke patients undergoing robotic therapy (Riley et al., 2011).

The different measures of CST integrity interact with each other: the relevance of CST FA in predicting therapy-induced behavioural improvements is modulated by the presence or absence of MEPs. Stinear and colleagues found that if MEPs are present, FA has no added predictive value; if MEPs can not be elicited, then PLIC FA strongly predicted the effects of a 30 day motor training program (Stinear et al., 2006). This and similar work has focused on determining who will benefit from standalone therapy, not who will benefit from a combined brain stimulation and motor training program. A study by Cramer and others investigated predictors of response to a 6-week combined epidural motor stimulation and motor training program. They found that gains were predicted by smaller lesion volume, greater baseline motor ability, and less fMRI task-related activation in the lesioned hemisphere (Cramer et al., 2007).

We followed a similar approach to investigate predictors of response to our training program, both for those patients receiving anodal tDCS, and for those receiving the placebo condition. Because the basis of stimulation is to increase ipsilesional activity and thereby rectify interhemispheric imbalance (see Section 1.3.3.3), we were particularly interested in determining whether the extent of this imbalance predicted disability and improvements. A 2009 systematic review by Chen and colleagues examining the factors that best predict post-stroke motor improvement concluded that “measures that capture the integrity of neural

connections … were the best predictors of functional arm recovery at follow-up" (Chen & Winstein, 2009). Given this finding, we specifically investigated CST integrity and resting fMRI motor activity as potential predictors of recovery. This is because, in a way analogous to the CST FA representing intrinsic *structural* connectivity between areas, analyses of resting state fMRI data reflect intrinsic *functional* connectivity between areas (van den Heuvel & Hulshoff Pol, 2010). Moreover, both animal models of stroke and patient studies have demonstrated that declining motor ability occurs simultaneously with a loss of coherence in interhemipsheric resting motor activity (Carter et al., 2010; van Meer et al., 2010), suggesting that hemispheric asymmetry as a correlate of stroke-related motor function may extend to resting state activity as well.

By examining absolute and relative CST integrity and resting state activity, this chapter investigated the predictive power of each hemisphere in determining which stroke patients will respond the rehabilitation program, and in what manner.

7.2 METHODS

7.2.1 OVERVIEW

The methods contained here are a continuation from the previous chapter, as the topic of both chapters is the same clinical trial. In brief, 22 chronic stroke patients were enrolled in a combined motor training and tDCS rehabilitation program. All patients received 10 days of motor training based on the GRASP program (Krakauer, 2006; Pang et al., 2006). Half of the patients also received anodal tDCS to the ipsilesional M1 during the first half of the motor training; the remaining patients received the placebo condition, sham tDCS, for the same time period. Patients were assessed at three timepoints: baseline, the day following the

end of the intervention, and at a one-month followup. These assessments consisted of neuroimaging sessions and clinical tests evaluating their motor abilities. The primary clinical measures were the Action Reaction Arm Test (ARAT), which is sensitive to behavioural disability, and the Upper Extremity Fugl-Meyer (UE-FM), which is more attuned to physical impairments (van der Lee et al., 2001). For this chapter, measures of baseline clinical scores, and of improvement in clinical scores (percentage change in score from baseline to post-intervention or to follow-up) were considered.

7.2.2 IMAGE ACQUISITION AND ANALYSIS

All scans were performed on a 3T Siemens scanner (Siemens, Erlangen, Germany). Chapter 6 detailed the acquisition, analysis, and results of the task fMRI and structural MRI data. Here, we focus on two additional modalities: resting fMRI and diffusion MRI. Additionally, T1-weighted axial anatomical images were used during the registration processes (voxel size= 1mm isotropic, TR=2040ms, TE=4.7ms, flip angle=8°). For analysis purposes, images from patients with right hemispheric strokes were flipped about the midline after registration to standard space so that lesions appeared on the left side. All analysis was performed using tools from FSL (www.fmrib.ox.ac.uk/fsl).

7.2.2.1 Diffusion MRI

ACQUISITION. Two sets of diffusion weighted volumes were acquired (voxel size= 2mm isotropic; TR=9600ms; TE= 87ms; 60 directions with a b-value 1000 s/mm^2; and 8 volumes without diffusion weighting, b-value=0 s/mm^2). Diffusion data was analysed using FMRIB's Diffusion Toolbox (FDT).

PREPROCESSING. For each subject, the two sets of diffusion images were merged into a single 4D file. Eddy current correction was then run to reduce the distortions induced by the gradient coils, and to correct for head motion by affine registering all images within the file to one another.

TRACT GENERATION. Data from 10 healthy, controls with a similar age range as the patients was used to generate the corticospinal tracts (7F, age range: 44-69 years, mean age: 55.9 years). Bayesian Estimation of Diffusion Parameters Obtained using Sampling Techniques (BedpostX) was used to generate a probabilistic distribution of local diffusion directions for each voxel (Behrens et al., 2003; Behrens et al., 2007). This model allows for multiple fiber populations to be estimated at each voxel. Finally, by repeatedly sampling from these distributions, specified tracts were created probablisitically, utilising probtrackx as implemented within FSL (REF). A mask of the left M1, right M1, and a single slice of the pons (at the level of z=-32) were drawn on a standard space brain. For each subject, probtrackx was then used to generate tracts for the left and right corticospinal tract (CST) separately. The pons was entered as the seed from which the fibers originated; M1 as a waypoint through which the fibers had to pass. A midline exclusion mask was also used to maintain hemispheric independence. Each subject's probtrackx-generated left and right CST were thresholded at 1% of the maximum value to remove implausible tracts. Individual subject masks of the CST were binarised, then combined across all subjects. These group images were then thresholded such that the remaining voxels were common to at least 7 of the 10 subjects.

PATIENT ANALYSIS. The diffusion-weighted images from the stroke patients were preprocessed as detailed above. DTIfit then calculated a diffusion tensor for

each voxel within these images, which were subsequently used to generate fractional anisotropy (FA) values for each voxel. These FA maps were then moved into standard space. Using as masks the control-generated left and right CST, mean FA values were extracted from each patient's processed DTI data. Asymmetry of the corticospinal tracts was calculated as (Contralesional CST FA – Ipsilesional CST FA) / (Contralesional CST FA + Ipsilesional CST FA), with larger asymmetry reflecting relatively higher FA values, i.e., structural integrity, in the contralesional CST.

7.2.2.2 Resting fMRI

Axial echo-planar volumes were acquired (TR=2410ms, TE=30ms, flip angle=90°, voxel size=3mm isotropic). During this time, subjects were instructed to relax with their eyes open; no task was performed. The following preprocessing steps were performed on the reconstructed images: Motion correction using MCFLIRT (Hosp & Luft, 2011; Jenkinson et al., 2002); B_0 unwarping with fieldmaps using FUGUE; spatial smoothing with a Gaussian kernel of 6mm; and highpass temporal filtering at 100 seconds to remove low frequency artefacts. Registration to individual T1-weighted structural images and standard MNI space was performed using BBR.

RESTING STATE NETWORK GENERATION. The preprocessed scans were analysed using independent component analysis (ICA) from within MELODIC (Beckmann & Smith, 2004; Subramanian et al., 2010). Resting state scans from all patients at all timepoints were entered into a group temporal concatenation ICA, constrained to output 25 components. To identify the resting state networks generated from this group of patients, the individual components were visually inspected, then spatially correlated with standard masks of the 8 established resting

state networks, as described previously (Beckmann et al., 2005). A dual-regression was then performed to create subject-specific component maps (Filippini et al., 2009; van Vliet & Wulf, 2006). A dual-regression approach involves first utilising the group-defined RSNs as a regressor in separate GLM analyses for each subject. These analyses produced timeseries of the resting BOLD signal for each patient and each session. Each individual timeseries for each patient and session was then used in a second GLM to extract the spatial maps that corresponsed to each RSN timecourse.

REGION OF INTEREST ANALYSIS. Initial motor regions of interest were defined on a standard-space brain using previously published coordinates as the ROI centre (Haller et al., 2009), which were dilated to generate an 8 mm spherical ROI. As these coordinates were established in healthy volunteers, and cortical regions may have shifted in our patient population due to the effects of the stroke, we sought to tailor these coordinates to our cohort of subjects. To this end, the mean functional activity of the patients was established using data from the task fMRI analysis (see Chapter 6). The voxel of maximum functional activity within each 8 mm ROI was found, and a new 8 mm spherical ROI was recreated around these locations, listed below:

-Hand area of M1: (-28, -24, 58)

-Dorsal premotor cortex: (-26, -10, 58)

-Ventral premotor cortex: (-56, 6, 18)

-Supplementary motor area: (0, -10, 52)

For all regions except the SMA which was located on the midline, these ROIs were then flipped about the midline to create right hemispheric ROIs. The mean contrast of parameter estimate (COPE) for each ROI was extracted from the motor RSN. As

before, asymmetry was defined as (Contralesional COPE – Ipsilesional COPE) / (Contralesional COPE + Ipsilesional COPE), with larger asymmetry values reflecting relatively higher contralesional resting activity.

7.3 RESULTS

7.3.1 TASK FMRI AND STRUCTURAL MRI

No significant predictors of baseline clinical scores or improvement were found within the task fMRI or the structural MRI data.

7.3.2 TRACTOGRAPHY

Corticospinal tract generation

To generate the corticospinal tract from the diffusion-weighted images, data from 10 healthy, older adults was used (7F, age range: 44-69 years, mean age: 55.9 years), as the CST could not be reliably delineated in the stroke patients. Figure 7.1 illustrates the tracts created by Probtrackx.

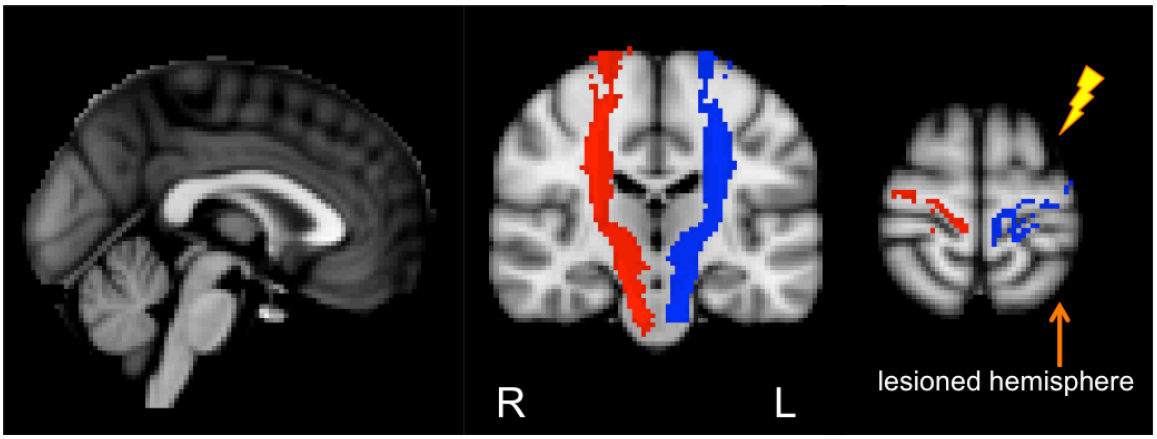

Figure 7.1: Corticospinal tract. Healthy, older control-derived corticospinal tracts. Fibers began in M1 and passed through the pons. Tracts thresholded such that voxels were common to at least 7 of the 10 controls. Right CST (red), Left CST (blue). Coordinates are (0, -20, 68)

Integrity of the ispilesional corticospinal tract correlates with baseline impairment

Integrity of the CST in the patients was assessed using measures of fractional anisotropy (FA). Using as a mask the left and right CST derived from healthy older controls, FA values were extracted from the stroke patients' standard-space registered FA maps at the baseline, post-intervention, and one-month follow up timepoints. These FA values did not change significantly over time (RM-ANOVA, main effect of time: $F(2)=1.705$, $p=0.195$), reflecting relative stability of CST integrity throughout the intervention. Asymmetry between the tracts was calculated as (Contralesional CST FA – Ipsilesional CST FA)/ (Contralesional CST FA + Ipsilesional CST FA), such that larger values reflect a bias toward the contralesional hemisphere, and therefore would be associated with greater damage to the tract. These values were also stable over time (RM-ANOVA, main effect of time: $F(2)=0.435$, $p=0.650$).

We then asked whether these values were associated with functional ability at baseline. Baseline FA values of the ipsilesional CST correlated with baseline scores on the ARAT ($r= 0.743$, $p< 0.001$, Figure 7.2A) and UE-FM ($r= 0.709$, $p< 0.001$,

Figure 7.2B). FA values of the contralesional CST were not associated with baseline performance on either clinical score (ARAT: r= 0.007, p= 0.974; UE-FM: r= -0.057, p= 0.802). FA asymmetry correlated with baseline scores on both the ARAT (r=-0.719, p< 0.001, Figure 7.3A) and UE-FM (r=-0.725, p<0.001, Figure 7.3B).

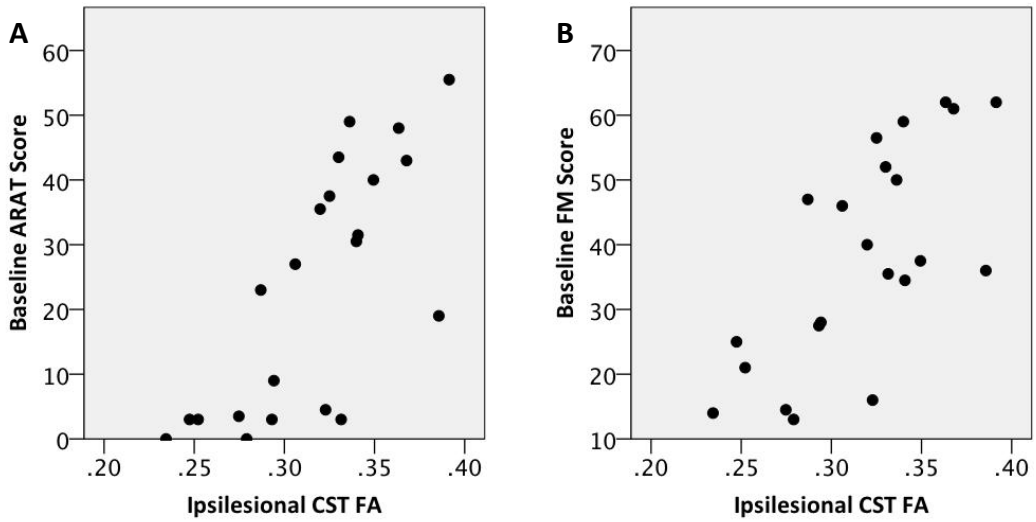

Figure 7.2: Baseline ipsilesional FA predicts baseline clinical measures. Baseline FA in the ipsilesional corticospinal tract correlates with baseline scores on the A) ARAT B) Fugl-Meyer.

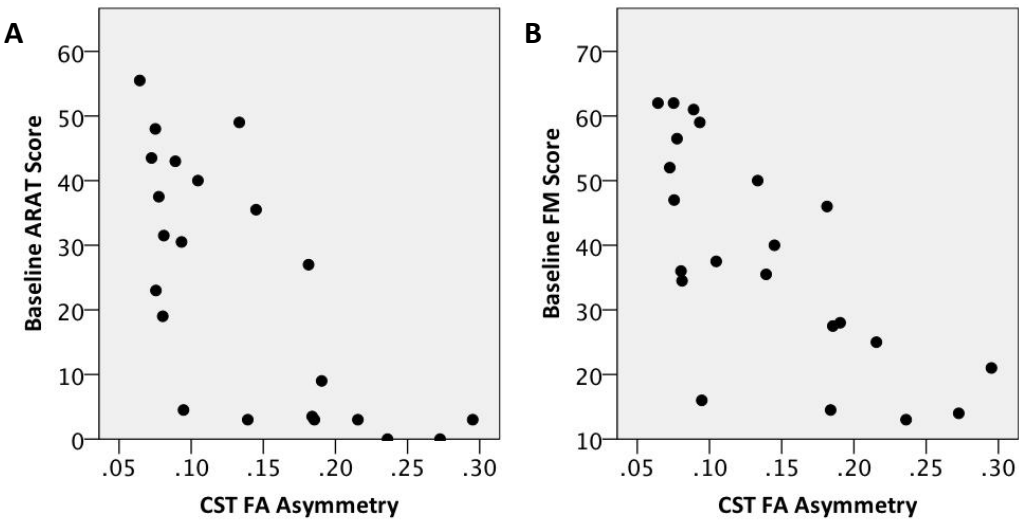

Figure 7.3: Baseline FA asymmetry correlates with baseline clinical measures. Baseline FA asymmetry of corticospinal tract correlated with baseline scores on the A) ARAT B) Fugl-Meyer. Greater asymmetry reflects higher FA in the contralesional CST relative to the ipsilesional CST, and therefore can be thought of as a marker of greater ipsilesional CST damage.

CST asymmetry predicts response to combined stimulation and motor training

Additionally, we investigated the ability of these measures of CST integrity to predict response to the two rehabilitation programs: motor training alone (sham tDCS) or simultaneous motor training and stimulation (anodal tDCS). For those patients receiving motor training alone, ipsilesional CST FA predicted percent increase from baseline to post-intervention on the ARAT and UE-FM (ARAT: r=-0.635, p=0.049; UE-FM: r=-0.684, p=0.020, Figure 7.4). Similar results were found in patients receiving anodal tDCS (ARAT: r=-0.733, p=0.016; UE-FM: r=-0.674, p=0.023, Figure 7.4).

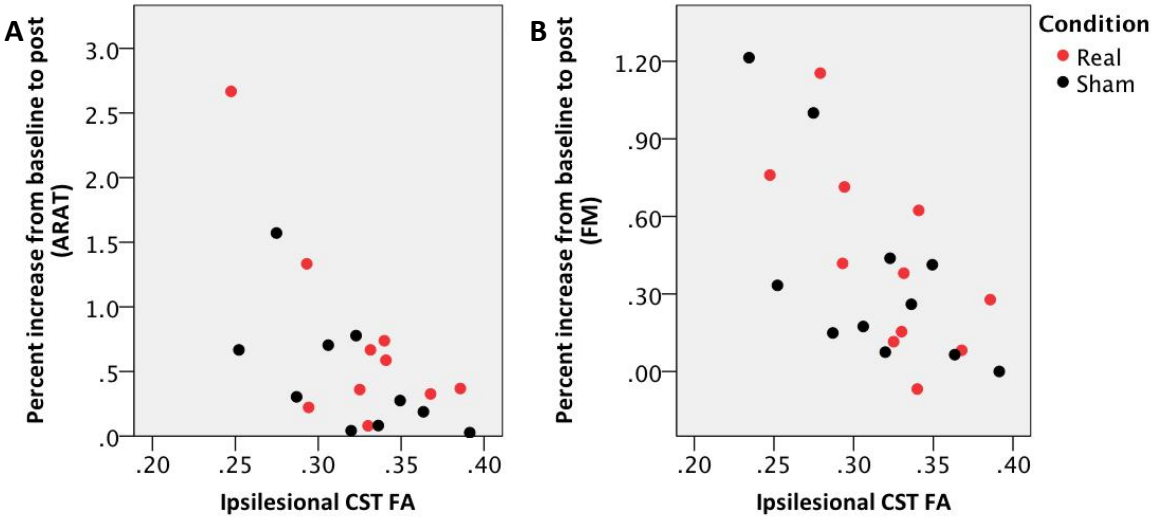

Figure 7.4: Ipsilesional FA predicts behavioural improvements. Ipsilesional CST FA predicted percent increase in scores A) ARAT and B) Fugl-Meyer scores from baseline to post-intervention.

Moreover, for patients receiving anodal tDCS, ipsilesional CST FA also predicted retention of these improvements on the ARAT, illustrated by percent increase in scores from baseline to one-month followup (r=-0.640, p=0.046, Figure 7.5). This relationship was not significant for the sham group (r=-0.375, p=0.286), but the strength of the relationship did not differ significantly between the two groups (Two-tailed Fisher's r to z: z=0.73, p=0.4654).

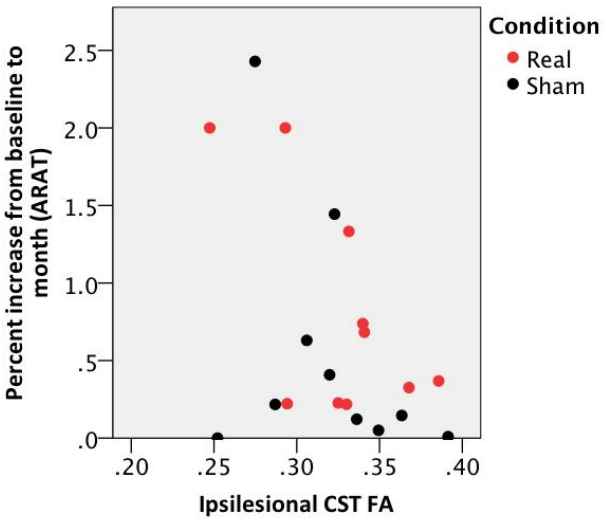

Figure 7.5: Ipsilesional FA predicts retention of behavioural improvements. For patients receiving anodal tDCS, ipsilesional CST FA predicted percent increase in ARAT score from baseline to one-month followup. This relationship was not significant for the sham group.

FA asymmetry predicted behavioural improvements in patients who received motor training in conjunction with anodal tDCS. FA asymmetry predicted percent change from baseline to post-intervention and one-month followup on both the ARAT (post-intervention: r=0.700, p=0.024; month followup: r=0.710, p=0.021, Figure 7.6A,B) and UE-FM (post-intervention: r=0.810, p=0.002; month followup: r=0.645, p=0.032, Figure 7.6C,D). Thus, in the anodal tDCS group, CST FA asymmetry favouring the contralesional hemisphere was associated with greater intervention-mediated behavioural improvements and retention. For the sham group, none of these relationships were statistically significant, but the strength of the relationship was not significantly different between the anodal and sham groups.

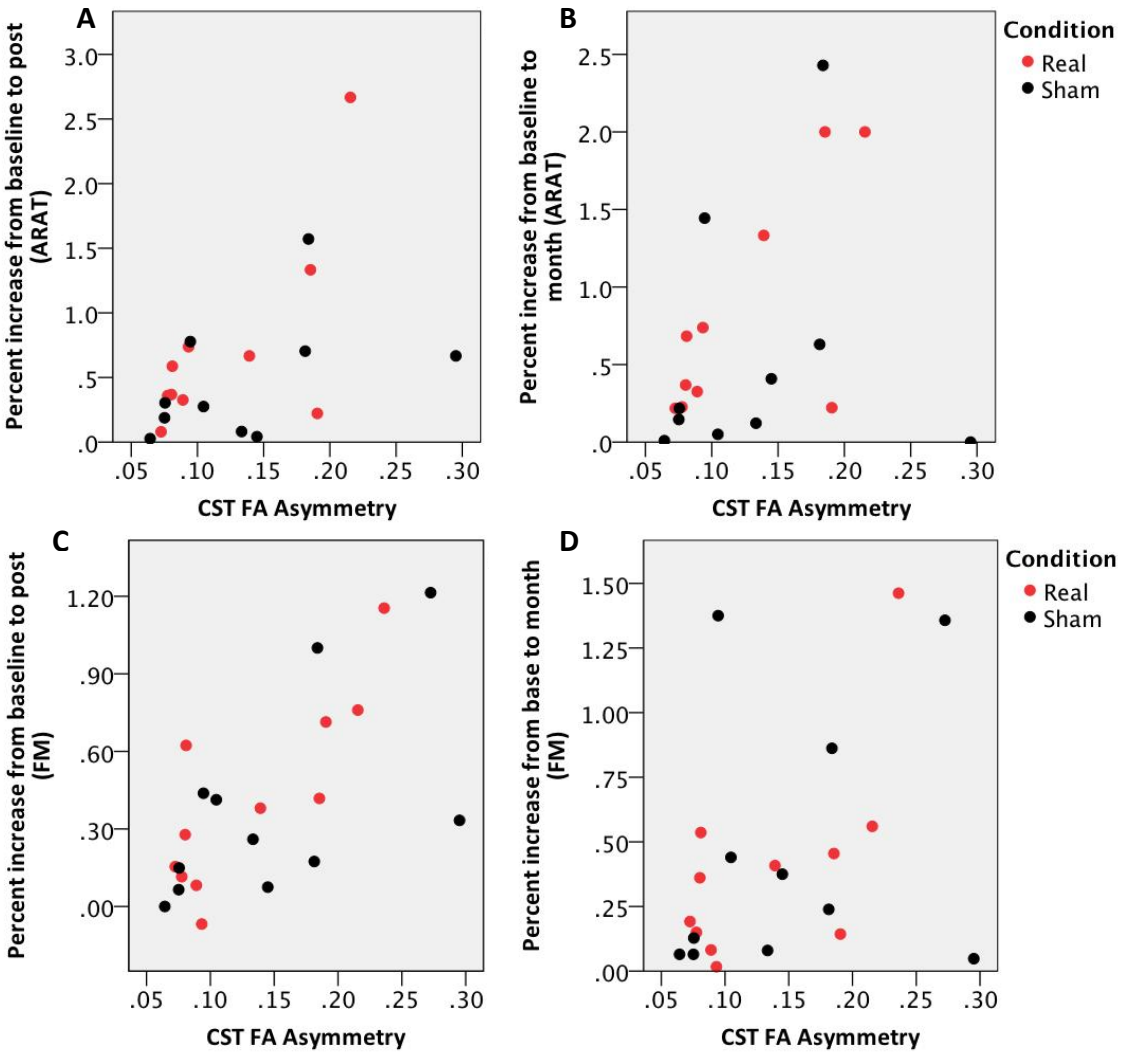

Figure 7.6: FA asymmetry predicts extent and retention of behavioural improvements. For patients receiving anodal CST FA asymmetry predicted percent increase in ARAT score from baseline to A) post-intervention and B) one-month followup, and percent increase in Fugl-Meyer score from baseline to C) post-intervention and D) one-month followup. These relationships were not significant for the sham group. Greater positive asymmetry reflects larger FA in the contralesional CST.

7.3.3 RESTING FMRI

Mean resting motor activity was extracted from predefined regions of interest (left and right hand area of M1, PMd, PMv, and SMA, Figure 7.7).

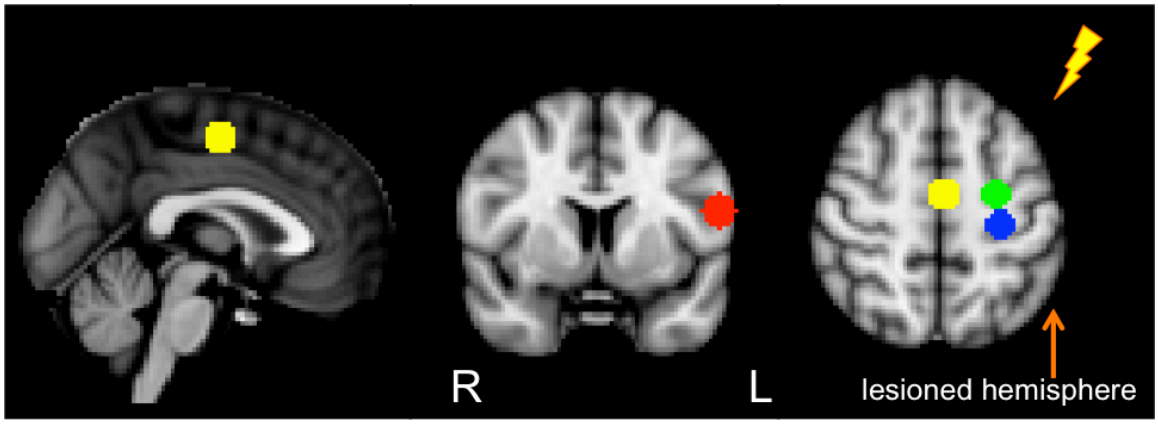

Figure 7.7: Motor region masks. SMA (yellow), left PMd (green), left Hand area of M1 (blue), left PMv (red). Coordinates are (0, 6, 54).

Resting motor activity within these regions was stable over time (RM-ANOVA, main effect of time: $F(2)=1.135$, $p=0.332$), as was the asymmetry between the left and right hemispheres of the regions (RM-ANOVA, main effect of time: $F(2)=0.232$, $p=0.794$). At baseline, asymmetry of activity within the hand area of M1 correlated with baseline clinical scores on both the ARAT ($r=-0.583$, $p=0.004$, Figure 7.8A) and UE-FM ($r=-0.716$, $p<0.001$, Figure 7.8B), such that patients who exhibited greater ipsilesional activity had higher clinical scores.

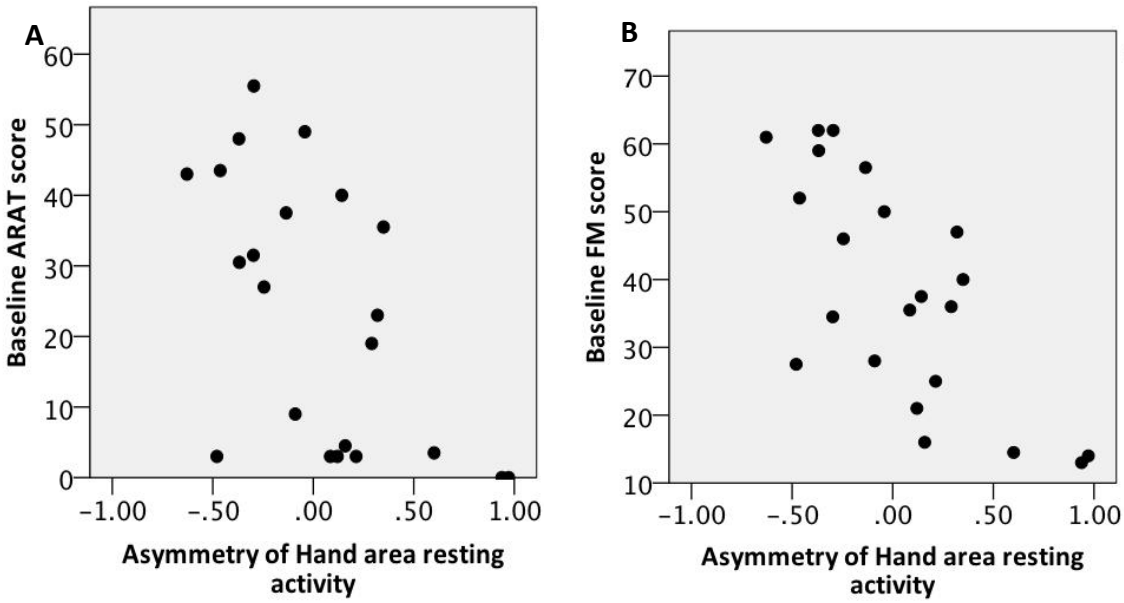

Figure 7.8: Asymmetry of resting activity correlates with baseline impairment. Asymmetry of activity within the hand area of M1 predicts baseline A) ARAT and B) Fugl-Meyer scores. Greater positive asymmetry reflects larger resting activity in the contralesional hand area.

Moreover, this asymmetry of resting activity is predictive of percent increase of UE-FM score for both groups, both from baseline to post-intervention (anodal: r=0.725, p=0.012; sham: r=0.831, p=0.002, Figure 7.9A) and baseline to one-month followup (anodal: r=0.802, p=0.003; sham: r=0.689, p=0.019, Figure 7.9B). Improvement as measured by the ARAT was not predicted by any measure of resting activity.

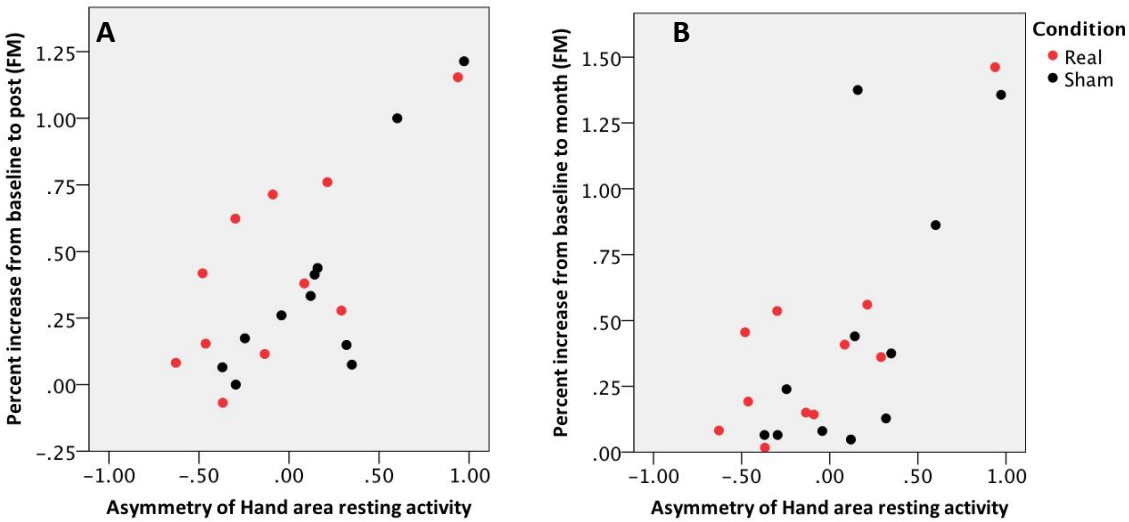

Figure 7.9: Asymmetry of resting activity at baseline predicts extent and retention of behavioural improvement. Asymmetry of activity within the hand area of M1 predicts percent increase in scores on the Fugl-Meyer from baseline to A) post-intervention and B) one-month followup, for both stimulation groups. Greater positive asymmetry reflects larger resting activity in the contralesional Hand area.

7.3.4 Multiple Regression on Asymmetry Values

Given the results of the preceding analyses, we then investigated whether these imaging measures provided additional predictive value beyond traditional clinical scores. Multiple regressions were performed for the Fugl-Meyer and ARAT using as regressors baseline score on the specific clinical test and asymmetry values of: resting motor activity in the hand area and CST FA. These three variables significantly predicted percent improvement on the UE-FM from baseline to post-intervention in both the anodal (R^2=0.873, F(3,7)=16.076, p=0.002) and sham tDCS groups (R^2=0.757, F(3,7)=7.259, p=0.015). For the anodal tDCS group, baseline UE-FM score significantly predicted behavioural improvements (β=-0.696, p=0.039), but asymmetry values did not (resting hand activity: β =0.149, p=0.458; CST FA: β =0.151, p=0.548). Improvement in the sham tDCS group was not predicted by any of the three variables alone (baseline UE-FM: β=-0.379, p=0.278; resting hand activity: β=0.512, p=0.126; CST FA: β=0.045, p=0.857). Similar multiple regressions on the

ARAT did not produce models that significantly predicted behavioural gains (anodal tDCS: R^2=0.520, F(3,7)=2.169, p=0.193; sham tDCS: R^2=0.659, F(3,7)=3.867, p=0.075). These results suggest that the imaging measures presented here do not increase predictive ability over and above that provided by baseline clinical measures.

7.4 DISCUSSION

The results of the analyses presented in this chapter show that measures reflective of integrity of the motor system can predict response to motor training and tDCS in chronic stroke patients. FA of the ipsilesional, but not contralesional, CST correlates with baseline motor ability and predicts response to the training program. Moreover, asymmetry values of CST FA and resting motor activity also correlate with and predict change in motor ability, particularly for those patients receiving anodal tDCS. Results from both modalities demonstrate that the greater the level of ipsilesional impairment (as reflected by smaller FA values and larger asymmetry values, which positively correlate with lower behavioural scores), the greater the rehabilitation-mediated improvement. This suggests that it may be the most disabled patients who can most benefit from a training program such as the one employed here.

Corticospinal tract FA

Here, we report that ipsilesional FA and asymmetry of FA within the CST predicts both baseline motor ability and increase in motor ability mediated by the rehabilitation program. Ipsilesional CST FA predicted improvements in all patients, while CST FA asymmetry only predicted improvements within the anodal tDCS

group. In both of these cases, decreased FA in the ipsilesional hemisphere (i.e., larger asymmetry scores) was correlated with worse baseline ability, and greater improvements. These results suggest that the greater the behavioural deficit at baseline, the greater the benefit gained from the program. This is in line with studies positively correlating FA asymmetries with a lower level of recovery (Lindenberg et al., 2010; Thomalla et al., 2004), but contrary to previous studies regarding CST FA, which have reported that decreased FA/increased asymmetry is found in patients who do *not* respond well to recovery (Stinear et al., 2006).

That FA asymmetry was significantly predictive only in patients receiving anodal tDCS is in line with the idea that tDCS can help alleviate interhemispheric imbalance. If tDCS aides improvement by actively resolving the imbalance between hemispheres, then it follows that those patients who stand the most to gain are those with the greatest imbalance to start with. The processes underlying the behavioural gains resulting from this has been partially investigated in rodents. Carmel and colleagues lesioned the CST of rats, and subsequently stimulated the motor cortex of half of them. Those rats receiving stimulation showed a robust growth of CST axon terminals within the ipsilesional hemisphere. Moreover, though the overall speed with which rats in both groups performed the task was equivalent at the end of the recovery period, only the stimulated rats decreased their error rates back to normal levels (Carmel et al., 2010). This suggests that, both groups of patients exhibited behavioural improvements, anodal tDCS may also have modified motor ability in a way too subtle for our tests to identify.

Resting fMRI results

While task-based analyses of functional activity are useful, the disparity between activity levels in each hemisphere may confounded by the effects of mirror movements and increased effort (Westlake & Nagarajan, 2011). Analysing patterns of resting activity in stroke patients resolves these issues, and can provide insights of their own: following a stroke, resting functional connectivity is disrupted, and correlated with motor impairments (Golestani et al., 2012; Westlake & Nagarajan, 2011). Our study found that asymmetry of resting activity in the hand area can be used to predict behavioural improvements on the Fugl-Meyer. Complementary to the results produced by the CST FA analysis, greater resting asymmetry favouring the contralesional hemisphere predicts greater behavioural gains. It has been shown previously that resting asymmetry that favours the *ipsilesional* M1 is found in more recovered stroke patients (Wang et al., 2010). Thus, our results suggest that it may be the least recovered patients that benefit the most from this type of motor training.

That both resting motor activity and CST FA predict behavioural improvements in similar ways is not entirely surprising, as the extent of damage to the CST has been shown to positively correlate with a decrease in interhemispheric resting connectivity between the left and right central sulci (Carter et al., 2012). Although studies such as those mentioned here document how resting activity evolves post stroke, no study to date has used this imaging modality to predict response to a rehabilitation program in stroke patients. However, such an approach has been used in tinnitus patients: Vanneste and colleagues used patterns of resting

activity to differentiate between responders and nonresponders to a tDCS-mediated rehabilitation program for tinnitus suppression (Vanneste et al., 2011).

Negative task fMRI and structural MRI results

Although the previous chapter reported significant changes in task fMRI and structural MRI measures with therapy, we did not find any markers from these modalities that correlated with baseline motor ability or predicted behavioural gains following the program. Similar conclusions were reached by Stinear and colleagues, who noted that task fMRI activity did not predict behavioural improvement, regardless of the integrity of the CST (as measured by MEPs) (Stinear et al., 2006). Likewise, although our measure of CST integrity, FA, did predict improvement, task fMRI activity did not. In general, the asymmetry of CST integrity has been found to be a more robust predictor of recovery than task fMRI activity (Qiu et al., 2011), potentially because functional activity is dependant on an intact CST (Lotze et al., 2012). In light of this, our lack of positive results from the task fMRI data, but the presence of CST derived positive results, may be because the structural integrity of the CST is a more primary, and therefore sensitive, measure. It is also possible that, because our patients are in the chronic stages of recovery, the imbalance of task-induced activation has resolved to a point where it is difficult to distinguish between disability levels.

Previous studies have also found that various measures of grey matter density predict behavioural changes (Gauthier et al., 2012; Nouri & Cramer, 2011), in that the more preserved grey matter, the more the improvement. In Chapter 6, we showed that change in grey matter in the ipsilesional M1 and PMd, and contralesional somatosenory cortex correlated with change on the Fugl-Meyer.

However, we did not find that grey matter volume in these or other areas predicted baseline or change in motor ability.

Future directions

Although CST FA and resting motor activity were found to predict behavioural improvements, the multiple regression showed that neither imaging modality significantly increased predictive power above those gleaned from baseline motor ability. This could be due to the relatively small number (11) of patients in each group, or because the patients in our study are very heterogeneous in terms of degree of disability. A larger sample might be able to address both of these questions by increasing the statistical sensitivity of the results, and allowing for analysis of improvements within disability levels.

Overall, the results presented in this chapter are promising for chronic stroke rehabilitation, as they show that even severely impaired patients, with significantly compromised motor systems, can benefit from motor training and tDCS; indeed, they may benefit the most.

7.5 CONCLUSION

A striking feature of post-stroke neurological dysfunction, and the tenet upon which stimulation-mediated rehabilitation programs are based, is the presence of an altered balance between the lesioned and contralesional hemispheres. The results of this chapter show that the degree of this imbalance or asymmetry prior to intervention is predictive of subsequent behavioural improvements: the greater the baseline asymmetry, the larger the gains. This is true in patients receiving motor training alone, but occurs in a more robust manner in

those receiving anodal tDCS in conjunction. By analysing both DTI of the corticospinal tract and resting activity across the cortex, we showed that the predictive power extends to both the structural and functional domains.

REFERENCES

Beckmann, C. F., & Smith, S. M. (2004). Probabilistic independent component analysis for functional magnetic resonance imaging. *IEEE transactions on medical imaging*, *23*(2), 137–152.

Behrens, T.E., Johansen-Berg, H., Jbabdi, S., Rushworth, M.F., & Woolrich, M.W. (2007). Probabilistic diffusion tractography with multiple fibre orientations: What can we gain? *Neuroimage, 34*(1), 144-155.

Behrens, T.E., Woolrich, M.W., Jenkinson M., Johansen-Berg, H., Nunes, R.G., Clare S., Matthews P.M., Brady, J.M., & Smith, S.M. (2003). Characterization and propagation of uncertainty in diffusion-weighted MR imaging. *Magnetic Resonance in Medicine, 50*(5), 1077-1088.

Carmel, J. B., Berrol, L. J., Brus-Ramer, M., & Martin, J. H. (2010). Chronic electrical stimulation of the intact corticospinal system after unilateral injury restores skilled locomotor control and promotes spinal axon outgrowth. *Journal of Neuroscience*, *30*(32), 10918–10926.

Carter, A. R., Astafiev, S. V., Lang, C. E., Connor, L. T., Rengachary, J., Strube, M. J., Pope, D. L. W., et al. (2010). Resting interhemispheric functional magnetic resonance imaging connectivity predicts performance after stroke. *Annals of Neurology*, *67*(3), 365–375.

Carter, A. R., Patel, K. R., Astafiev, S. V., Snyder, A. Z., Rengachary, J., Strube, M. J., Pope, A., et al. (2012). Upstream dysfunction of somatomotor functional connectivity after corticospinal damage in stroke. *Neurorehabilitation and Neural Repair*, *26*(1), 7–19.

Chen, S.-Y., & Winstein, C. J. (2009). A systematic review of voluntary arm recovery in hemiparetic stroke: critical predictors for meaningful outcomes using the international classification of functioning, disability, and health. *Journal of neurologic physical therapy : JNPT*, *33*(1), 2–13.

Coupar, F., Pollock, A., Rowe, P., Weir, C., & Langhorne, P. (2012). Predictors of upper limb recovery after stroke: a systematic review and meta-analysis. *Clinical rehabilitation*, *26*(4), 291–313.

Cramer, S. C., Parrish, T. B., Levy, R. M., Stebbins, G. T., Ruland, S. D., Lowry, D. W., Trouard, T. P., et al. (2007). Predicting Functional Gains in a Stroke Trial. *Stroke*,

38(7), 2108–2114.

Filippini, N., MacIntosh, B. J., Hough, M. G., Goodwin, G. M., Frisoni, G. B., Smith, S. M., Matthews, P. M., et al. (2009). Distinct patterns of brain activity in young carriers of the APOE-epsilon4 allele. *Proceedings of the National Academy of Sciences of the United States of America*, *106*(17), 7209–7214.

Gauthier, L. V., Taub, E., Mark, V. W., Barghi, A., & Uswatte, G. (2012). Atrophy of spared gray matter tissue predicts poorer motor recovery and rehabilitation response in chronic stroke. *Stroke*, *43*(2), 453–457.

Golestani, A.-M., Tymchuk, S., Demchuk, A., Goodyear, B. G., VISION-2 Study Group. (2012). Longitudinal Evaluation of Resting-State fMRI After Acute Stroke With Hemiparesis. *Neurorehabilitation and Neural Repair*.

Haller, S., Chapuis, D., Gassert, R., Burdet, E., & Klarhöfer, M. (2009). Supplementary motor area and anterior intraparietal area integrate fine-graded timing and force control during precision grip. *European Journal of Neuroscience*, *30*(12), 2401–2406.

Hosp, J. A., & Luft, A. R. (2011). Cortical plasticity during motor learning and recovery after ischemic stroke. *Neural plasticity*, *2011*, 871296.

Jenkinson, M., Bannister, P., Brady, M., & Smith, S. (2002). Improved optimization for the robust and accurate linear registration and motion correction of brain images. *NeuroImage*, *17*(2), 825–841.

Krakauer, J. W. (2006). Motor learning: its relevance to stroke recovery and neurorehabilitation. *Current opinion in neurology*, *19*(1), 84–90.

Lindenberg, R., Renga, V., Zhu, L. L., Betzler, F., Alsop, D., & Schlaug, G. (2010). Structural integrity of corticospinal motor fibers predicts motor impairment in chronic stroke. *Neurology*, *74*(4), 280–287.

Lotze, M., Beutling, W., Loibl, M., Domin, M., Platz, T., Schminke, U., & Byblow, W. D. (2012). Contralesional motor cortex activation depends on ipsilesional corticospinal tract integrity in well-recovered subcortical stroke patients. *Neurorehabilitation and Neural Repair*, *26*(6), 594–603.

Nouri, S., & Cramer, S. C. (2011). Anatomy and physiology predict response to motor cortex stimulation after stroke. *Neurology*, *77*(11), 1076–1083.

Pang, M. Y., Harris, J. E., & Eng, J. J. (2006). A community-based upper-extremity group exercise program improves motor function and performance of

functional activities in chronic stroke: a randomized controlled trial. *Archives of physical medicine and rehabilitation*, *87*(1), 1–9.

Pineiro, R., Pendlebury, S. T., Smith, S., Flitney, D., Blamire, A. M., Styles, P., & Matthews, P. M. (2000). Relating MRI changes to motor deficit after ischemic stroke by segmentation of functional motor pathways. *Stroke*, *31*(3), 672–679.

Qiu, M., Darling, W. G., Morecraft, R. J., Ni, C. C., Rajendra, J., & Butler, A. J. (2011). White Matter Integrity Is a Stronger Predictor of Motor Function Than BOLD Response in Patients With Stroke. *Neurorehabilitation and Neural Repair*, *25*(3), 275–284.

Riley, J. D., Le, V., Der-Yeghiaian, L., See, J., Newton, J. M., Ward, N. S., & Cramer, S. C. (2011). Anatomy of Stroke Injury Predicts Gains From Therapy. *Stroke*, *42*(2), 421–426.

Schiemanck, S. K., Kwakkel, G., Post, M. W. M., Kappelle, L. J., & Prevo, A. J. H. (2008). Impact of internal capsule lesions on outcome of motor hand function at one year post-stroke. *Journal of rehabilitation medicine : official journal of the UEMS European Board of Physical and Rehabilitation Medicine*, *40*(2), 96–101.

Schulz, R., Park, C.-H., Boudrias, M.-H., Gerloff, C., Hummel, F. C., & Ward, N. S. (2012). Assessing the integrity of corticospinal pathways from primary and secondary cortical motor areas after stroke. *Stroke*, *43*(8), 2248–2251.

Shelton, F. D., Volpe, B. T., & Reding, M. (2001). Motor impairment as a predictor of functional recovery and guide to rehabilitation treatment after stroke. *Neurorehabilitation and Neural Repair*, *15*(3), 229–237.

Shelton, F. N., & Reding, M. J. (2001). Effect of lesion location on upper limb motor recovery after stroke. *Stroke*, *32*(1), 107–112.

Stinear, C. M., Barber, P. A., Smale, P. R., Coxon, J. P., Fleming, M. K., & Byblow, W. D. (2006). Functional potential in chronic stroke patients depends on corticospinal tract integrity. *Brain*, *130*(1), 170–180.

Subramanian, S. K., Massie, C. L., Malcolm, M. P., & Levin, M. F. (2010). Does provision of extrinsic feedback result in improved motor learning in the upper limb poststroke? A systematic review of the evidence. *Neurorehabilitation and Neural Repair*, *24*(2), 113–124.

Talelli, P., Greenwood, R. J., & Rothwell, J. C. (2006). Arm function after stroke: neurophysiological correlates and recovery mechanisms assessed by

transcranial magnetic stimulation. *Clinical neurophysiology : official journal of the International Federation of Clinical Neurophysiology*, *117*(8), 1641–1659.

Thomalla, G., Glauche, V., Koch, M. A., Beaulieu, C., Weiller, C., & Röther, J. (2004). Diffusion tensor imaging detects early Wallerian degeneration of the pyramidal tract after ischemic stroke. *NeuroImage*, *22*(4), 1767–1774.

van den Heuvel, M. P., & Hulshoff Pol, H. E. (2010). Exploring the brain network: a review on resting-state fMRI functional connectivity. *European neuropsychopharmacology : the journal of the European College of Neuropsychopharmacology*, *20*(8), 519–534.

van der Lee, J. H., Beckerman, H., Lankhorst, G. J., & Bouter, L. M. (2001). The responsiveness of the Action Research Arm test and the Fugl-Meyer Assessment scale in chronic stroke patients. *Journal of rehabilitation medicine : official journal of the UEMS European Board of Physical and Rehabilitation Medicine*, *33*(3), 110–113.

van Meer, M. P. A., van der Marel, K., Wang, K., Otte, W. M., Bouazati, El, S., Roeling, T. A. P., Viergever, M. A., et al. (2010). Recovery of sensorimotor function after experimental stroke correlates with restoration of resting-state interhemispheric functional connectivity. *Journal of Neuroscience*, *30*(11), 3964–3972.

van Vliet, P. M., & Wulf, G. (2006). Extrinsic feedback for motor learning after stroke: what is the evidence? *Disability and rehabilitation*, *28*(13-14), 831–840.

Vanneste, S., Focquaert, F., Van de Heyning, P., & De Ridder, D. (2011). Different resting state brain activity and functional connectivity in patients who respond and not respond to bifrontal tDCS for tinnitus suppression. *Experimental Brain Research*, *210*(2), 217–227.

Wang, L., Yu, C., Chen, H., Qin, W., He, Y., Fan, F., Zhang, Y., et al. (2010). Dynamic functional reorganization of the motor execution network after stroke. *Brain*, *133*(Pt 4), 1224–1238.

Werring, D. J., Toosy, A. T., Clark, C. A., Parker, G. J., Barker, G. J., Miller, D. H., & Thompson, A. J. (2000). Diffusion tensor imaging can detect and quantify corticospinal tract degeneration after stroke. *Journal of neurology, neurosurgery, and psychiatry*, *69*(2), 269–272.

Westlake, K. P., & Nagarajan, S. S. (2011). Functional connectivity in relation to

motor performance and recovery after stroke. *Frontiers in Systems Neuroscience*, *5*, 8.

Chapter 8: General Conclusions

The preceding experimental chapters in this thesis investigated tDCS as a tool to modify motor function in healthy controls and stroke patients. Here, the main findings of those studies are summarized, and general conclusions drawn. To close, future directions and applications stemming from the work presented in this thesis are discussed.

8.1 THESIS OVERVIEW

The research chapters of this thesis used transcranial direct current stimulation (tDCS) to perturb motor functioning, ultimately aiming to further elucidate the neurological processes underlying certain motor behaviours. A variety of techniques including MRI measures and transcranial magnetic stimulation (TMS) were employed in both healthy controls and chronic stroke patients, to investigate and document these results.

Chapter 4 tested the effects of tDCS on network connectivity. By considering both anodal and cathodal tDCS, and examining resting BOLD activity in a model-free manner, this first experimental chapter provided an introduction to the interaction between tDCS and the brain as a whole, and focused on the effects of tDCS on the motor system in particular. We chose to study both anodal and cathodal tDCS to distinguish polarity specific effects from those due to tDCS in general.

Chapter 5 then focused on one tDCS polarity and one brain region: the effects of anodal tDCS on circuits within M1. We chose anodal tDCS as this has been

previously shown to modulate motor learning in healthy controls (REF) and, when applied to the ipsilesional hemisphere in stroke patients, to improve function in a single session (REF). In this chapter, we investigated how the relative timing of tDCS application and motor performance affects behavioural and neurophysiological outcomes in healthy controls.

Chapter 6 extended the work introduced in the previous chapters to a patient population. A clinical trial assessed the utility of anodal tDCS applied to the ipsilesional hemisphere as a supplement to motor training in a group of heterogeneously impaired chronic stroke patients.

Chapter 7 drew upon the results from the clinical trial described above, and tested whether baseline imaging measures reflective of hemispheric imbalance predicted baseline motor ability and ensuing rehabilitation-mediated recovery.

8.2 SUMMARY OF RESULTS

8.2.1 WHOLE-BRAIN RESTING NETWORK CONNECTIVITY (CHAPTER 4)

The general aim of this thesis was to investigate how tDCS affects the brain with regard to modifying the performance of motor tasks. We first determined how tDCS affects the brain at rest, independent of a task, with the understanding that such changes in intrinsic connectivity may be one of the substrates by which motor performance may be modified. The results of Chapter 4 demonstrated that cathodal tDCS increased the strength of the default mode network (DMN). A strong trend toward anodal tDCS increasing the strength of the motor network was also noted.

These findings regarding changes in connectivity within specific networks complement previously established behavioural findings. Separately, both increased DMN activity (Peña-Gómez et al., 2011) and cathodal tDCS (Stagg et al., 2011) have been shown to worsen performance of behavioural tasks. Thus, the findings in Chapter 4 imply that these two previously independent findings may be related. Likewise, components of the motor network are activated during motor performance, and the present study suggests that anodal tDCS may increase motor network activity. Accordingly, anodal tDCS generally improves motor performance (Stagg et al., 2011).

8.2.2 TIMING AND CORTICAL NETWORKS WITHIN M1 (CHAPTER 5)

Although the change in resting state strength due to anodal tDCS was relatively subtle, it is known to produce robust improvements in behaviour, but typically only if stimulation is delivered at the same time as motor performance. The next series of experiments, presented in Chapter 5, delved deeper into the neurophysiological processes that may be underlying this phenomenon. Using TMS measures and EMG recordings, a series of experiments found that, when anodal tDCS is applied before the motor task, subsequent learning was impaired and inhibition levels increased. This latter finding was particular to a type of inhibition thought to rely on synaptic $GABA_A$ (Kujirai et al., 1993). These results suggest that the interaction between tDCS and motor performance may conform to the rules of homeostatic plasticity.

An incidental finding of this experiment was the potential specificity of the results with regard to particular muscles. Though often used as a surrogate for the muscle directly involved in sequence tapping, the FDI is actually adjacent to it. In

line with the center-surround hypothesis, activity in this surround muscle was inhibited (Beck et al., 2009; Tamburin et al., 2005), potentially to allow the center muscle, from which we were unable to directly record, to be fully activated.

8.2.3 tDCS AS A TOOL IN STROKE REHABILITATION (CHAPTERS 6, 7)

The final two experimental chapters of the thesis concerned motor function in chronic stroke patients. A 10 day clinical trial of repeated sessions of motor therapy resulted in behavioural improvements in all patients, including those patients receiving the placebo condition, sham tDCS. Patients who received anodal tDCS to the ipsilesional M1 during motor training experienced increased task-based functional activity in ipsilesional motor areas, and increased grey matter in the ipsilesional M1 and PMd, and the contralesional somatosensory cortex. These changes were correlated with improvements on the ARAT and Fugl-Meyer, respectively.

Moreover, it was found that baseline measures of asymmetry between the hemispheres correlated with baseline motor ability. They also predicted behavioural gains: resting M1 activity predicted gains in both groups of patients; integrity of the CST predicted gains in the anodal tDCS group. The more the asymmetry favoured the contralesional hemisphere, the worse the baseline motor ability, and the greater the behavioural improvements. This suggests that better recovered patients have resolved their post-stroke hemispheric imbalance to a greater extent. Moreover, our clinical trial suggests that it may be the most impaired, least recovered patients who stand to gain the most from this type of rehabilitation.

8.3 FUTURE DIRECTIONS

The work in this thesis lends itself to both direct extensions of the current studies, as well as new lines of inquiry arising from particular findings. The following sections touch upon some of these possibilities.

8.3.1 EXTENSION OF CURRENT STUDIES

A handful of questions naturally arise from the results of the experiments performed for this thesis, as detailed in the discussion sections of the relevant chapters. In brief: With regard to the resting state experiment (Chapter 4), a logical next step would be to determine if and how these changes in connectivity correlate with and predict motor performance. This could be accomplished with an experimental protocol identical to the one employed here, with the addition of motor tasks administered at baseline and following the resting state scans.

Two follow-up experiments to the study testing the effect of the timing of tDCS application on motor performance and excitability (Chapter 5) present themselves. First, one might re-perform the online tDCS condition (anodal tDCS during task performance), with the intention of ensuring that the established behavioural augmentation is found. This could, for example, be done in a post-hoc manner in which data was only included from subjects in whom the effect was found. Secondly, a more in-depth appraisal of the center-surround theory may be warranted. This could be achieved by performing a more precise analysis of the involvement of the muscles of the hand in the motor task, and re-running all four conditions while measuring excitability/inhibition within these muscles.

Two protocol related amendments arise as possibilities when considering the stroke clinical trial. Our study applied 1mA tDCS during the first half of each motor training session, i.e., for 20 minutes. Two variations on this procedure are

readily apparent: the first is to administer tDCS for the entirety of the motor training; the second is to increase the intensity to 2 mA. A study investigating whether these two simple modifications increase behavioural gains would be helpful, though would need to first be performed at the single session level before being extended to the full 10 day program.

8.3.2 Future Studies Involving Healthy Controls

8.3.2.1 Exploring the behavioural effects of cathodal tDCS

The resting state experiment in Chapter 4 showed that cathodal tDCS works in such a way as to increase the strength of the DMN, which may negatively affect behaviour. As noted above, an experiment directly linking such changes to behavourial modifications could be beneficial. Moreover, the remaining experiments in this thesis focused on anodal tDCS, as it has been shown to improve behaviour more reliably. However, cathodal tDCS to the contralesional hemisphere has been used to improve motor ability in stroke patients, among other populations (Fregni et al., 2005), although significant improvements have not been seen in all studies (Stagg et al., 2012). Thus, continued investigation into the neurological correlates of cathodal tDCS application is required, particularly as it relates to cross-hemispheric interactions (Vines et al., 2008). A TMS study similar to that presented in Chapter 5, with the addition of measures of interhemispheric changes (e.g., interhemispheric inhibition (IHI) and facilitation (IHF)) could provide initial steps to understanding how this tool could best be harnessed to facilitate performance in both healthy and patient populations (Di Lazzaro et al., 2012).

8.3.2.2 Combined TMS-fMRI to correlate neurophysiological and imaging findings

The results of Chapter 5 showed changes in inhibition and task performance following offline anodal tDCS application. We posited that these changes were due to modifications in $GABA_A$ levels. A combined tDCS-TMS-fMRI experiment documenting changes both in inhibition as measured by MEP levels and by fMRI related measures (potentially resting BOLD response or spectroscopy measures) would further clarify these results. A recent study by Kriváneková and others following a similar design found that the changes in TMS-derived MEP measures accompanied, but did not correlate with, BOLD signal changes, suggesting that they were distinct physiological mechanisms (Kriváneková et al., 2012). Other concurrent TMS-fMRI studies have applied bursts of TMS while scans are being acquired (Bestmann et al., 2008; Leitão et al., 2012; Sack et al., 2007). Modifying paradigms used such as this to deliver single or paired-pulse TMS measures that were recorded with EMG while simultaneously, for example, acquiring resting state data would allow for parallel information and conclusion drawing.

8.3.3 FUTURE STUDIES INVOLVING PATIENT POPULATIONS

8.3.3.1 Comparing tDCS-mediated changes in controls and patients

Studies performed in healthy controls allow researchers to probe the processes occurring in the normally-functioning brain. At times, these results are used as a surrogate for what may be occurring in a brain affected by pathology, or may serve as a template upon which to base conjecture and future experiments to explore those affected brains. As a first pass, it would be interesting to repeat the studies in Chapters 4 and 5 to see if and how they translate to a patient population. This would be fairly straightforward for the resting state study, and slightly more

challenging for the study in Chapter 5, as not all patients have recordable MEPs. To circumvent this, the study could be performed in well-recovered patients. Ultimately, this might lead to a dual control-patient study similar to that performed in healthy subjects in 2009 by Reis (Reis et al., 2009).

8.3.3.2 Comparing the long-term efficacy of tDCS polarities in stroke rehabilitation

Previous studies investigating the use of tDCS in stroke rehabilitation have used cathodal tDCS (Boggio et al., 2007) or bilateral tDCS (Lindenberg et al., 2010b). The study presented in chapters 6 and 7 of this thesis used anodal tDCS. While single session studies have compared the utility of the four stimulation types (anodal, cathodal, bilateral, and sham) in stroke patients, none have been done over the long term (Fregni et al., 2005; Stagg et al., 2012). Such a study would allow for the elucidation of how well the different polarities work, and would also help to begin tailoring therapies for particular patients. Studies have already suggested that upregulation of the ipsilesional hemisphere may be more beneficial for better recovered patients (Lindenberg et al., 2010a; Stinear et al., 2012; Stinear et al., 2006), even suggesting that upregulation of the contralesional would be best for the most impaired (Stinear et al., 2006). A study such as the one proposed here, on a large enough scale, perhaps multi-center, would allow one to see whether this was true.

8.4 OVERALL CONCLUSIONS

tDCS continues to gain popularity as a tool used to explore motor behaviour. Generally, cathodal tDCS to the dominant hemisphere worsens performance; anodal tDCS improves it. The experiments contained within this thesis help clarify and

broaden our understanding of the potential processes behind these behavioural modifications. On the whole-brain level, cathodal tDCS may worsen motor performance by increasing activity in the DMN, a network that should be deactivated in order to facilitate task performance. Anodal tDCS, on the other hand, may improve motor performance by increasing activity in the motor network itself (Chapter 4).

Coupled with the information gleaned from the MEP analysis, this result may help explain the differential effects of online and offline anodal tDCS. Using tDCS to increase motor activity prior to task performance (quantified in this thesis as greater activity in the motor network (Chapter 4) and increased MEP size (Chapter 5)) exhausts the motor system and increases the likelihood of subsequent inhibition. This inhibition, in turn, worsens motor behaviour. Both of these results—inhibition and worsened performance, were documented following offline tDCS (Chapter 5). As such, the studies in this thesis concerning healthy adults support the theory of homeostatic plasticity as it relates to tDCS and motor behaviour.

The results of this thesis also provide support for an additional theory: the relevance of altered interhemispheric interactions in stroke patients. Anodal tDCS paired with motor training resulted in increased ipsilesional activity and grey matter (Chapter 6), and baseline measures of asymmetry were predictive of response to the rehabilitation program (Chapter 7). Taken together, these two chapters reveal that the balance of function between the hemispheres plays a central role in stroke pathology and recovery.

REFERENCES

Beck, S., Schubert, M., Richardson, S. P., & Hallett, M. (2009). Surround inhibition depends on the force exerted and is abnormal in focal hand dystonia. *Journal of applied physiology (Bethesda, Md. : 1985)*, *107*(5), 1513–1518.

Bestmann, S., Swayne, O., Blankenburg, F., Ruff, C. C., Haggard, P., Weiskopf, N., Josephs, O., et al. (2008). Dorsal premotor cortex exerts state-dependent causal influences on activity in contralateral primary motor and dorsal premotor cortex. *Cerebral cortex (New York, N.Y. : 1991)*, *18*(6), 1281–1291.

Boggio, P. S., Nunes, A., Rigonatti, S. P., Nitsche, M. A., Pascual-Leone, A., & Fregni, F. (2007). Repeated sessions of noninvasive brain DC stimulation is associated with motor function improvement in stroke patients. *Restorative neurology and neuroscience*, *25*(2), 123–129.

Di Lazzaro, V., Manganelli, F., Dileone, M., Notturno, F., Esposito, M., Capasso, M., Dubbioso, R., et al. (2012). The effects of prolonged cathodal direct current stimulation on the excitatory and inhibitory circuits of the ipsilateral and contralateral motor cortex. *Journal of neural transmission (Vienna: 1996)*.

Fregni, F., Boggio, P. S., Mansur, C. G., Wagner, T., Ferreira, M. J. L., Lima, M. C., Rigonatti, S. P., et al. (2005). Transcranial direct current stimulation of the unaffected hemisphere in stroke patients. *Neuroreport*, *16*(14), 1551–1555.

Kriváneková, L., Baudrexel, S., Bliem, B., & Ziemann, U. (2012). Relation of brain stimulation induced changes in MEP amplitude and BOLD signal. *Brain Stimulation*.

Kujirai, T., Caramia, M. D., Rothwell, J. C., Day, B. L., Thompson, P. D., Ferbert, A., Wroe, S., et al. (1993). Corticocortical inhibition in human motor cortex. *The Journal of Physiology*, *471*, 501–519.

Leitão, J., Thielscher, A., Werner, S., Pohmann, R., & Noppeney, U. (2012). Effects of Parietal TMS on Visual and Auditory Processing at the Primary Cortical Level - A Concurrent TMS-fMRI Study. *Cerebral cortex (New York, N.Y. : 1991)*.

Lindenberg, R., Renga, V., Zhu, L. L., Betzler, F., Alsop, D., & Schlaug, G. (2010a). Structural integrity of corticospinal motor fibers predicts motor impairment in chronic stroke. *Neurology*, *74*(4), 280–287.

Lindenberg, R., Renga, V., Zhu, L. L., Nair, D., & Schlaug, G. (2010b). Bihemispheric

brain stimulation facilitates motor recovery in chronic stroke patients. *Neurology*, *75*(24), 2176–2184.

Peña-Gómez, C., Sala-Lonch, R., Junqué, C., Clemente, I. C., Vidal, D., Bargalló, N., Falcón, C., et al. (2011). Modulation of large-scale brain networks by transcranial direct current stimulation evidenced by resting-state functional MRI. *Brain Stimulation*.

Reis, J., Schambra, H. M., Cohen, L. G., Buch, E. R., Fritsch, B., Zarahn, E., Celnik, P. A., et al. (2009). Noninvasive cortical stimulation enhances motor skill acquisition over multiple days through an effect on consolidation. *Proceedings of the National Academy of Sciences of the United States of America*, *106*(5), 1590–1595.

Sack, A. T., Kohler, A., Bestmann, S., Linden, D. E. J., Dechent, P., Goebel, R., & Baudewig, J. (2007). Imaging the brain activity changes underlying impaired visuospatial judgments: simultaneous FMRI, TMS, and behavioral studies. *Cerebral cortex (New York, N.Y. : 1991)*, *17*(12), 2841–2852.

Stagg, C. J., Bachtiar, V., O'Shea, J., Allman, C., Bosnell, R. A., Kischka, U., Matthews, P. M., et al. (2012). Cortical activation changes underlying stimulation-induced behavioural gains in chronic stroke. *Brain*, *135*(Pt 1), 276–284.

Stagg, C. J., Jayaram, G., Pastor, D., Kincses, Z. T., Matthews, P. M., & Johansen-Berg, H. (2011). Polarity and timing-dependent effects of transcranial direct current stimulation in explicit motor learning. *Neuropsychologia*, *49*(5), 800–804.

Stinear, C. M., Barber, P. A., Petoe, M., Anwar, S., & Byblow, W. D. (2012). The PREP algorithm predicts potential for upper limb recovery after stroke. *Brain*, *135*(Pt 8), 2527–2535.

Stinear, C. M., Barber, P. A., Smale, P. R., Coxon, J. P., Fleming, M. K., & Byblow, W. D. (2006). Functional potential in chronic stroke patients depends on corticospinal tract integrity. *Brain*, *130*(1), 170–180.

Tamburin, S., Fiaschi, A., Andreoli, A., Marani, S., & Zanette, G. (2005). Sensorimotor integration to cutaneous afferents in humans: the effect of the size of the receptive field. *Experimental Brain Research*, *167*(3), 362–369.

Vines, B. W., Nair, D., & Schlaug, G. (2008). Modulating activity in the motor cortex affects performance for the two hands differently depending upon which hemisphere is stimulated. *European Journal of Neuroscience*, *28*(8), 1667–1673.